

To the Graduate Council:

I am submitting herewith a dissertation written by Çağdaş Devrim Son entitled “Identification of Ligand-Receptor Interactions between *Saccharomyces cerevisiae* α -factor Pheromone Receptor (Ste2p) and its tridecapeptide Ligand” I have examined the final electronic copy of this dissertation for form and content and recommend that it be accepted in partial fulfillment of the requirements for the degree of Doctor of Philosophy, with a major in Biochemistry, Cellular and Molecular Biology.

Jeffrey M. Becker
Major Professor

We have read this dissertation
and recommend its acceptance:

Elizabeth E. Howell

Engin Serpersu

John W. Koontz

Salil K. Niyogi

Accepted for the Council:
Anne Mayhew

Vice Chancellor and
Dean of Graduate Studies

(Original signatures are on file with official student record)

**Identification of Ligand-Receptor Interactions between
Saccharomyces cerevisiae α -factor Pheromone Receptor
(Ste2p) and its tridecapeptide Ligand**

A Dissertation

Presented for the

Doctor of Philosophy Degree

The University of Tennessee, Knoxville

Çağdaş Devrim Son

December 2004

Copyright © 2004 by Çağdaş Devrim Son,

All rights reserved

Dedication

I would like to dedicate this dissertation to my parents, Adil Baki Son and İffet Son, and to my parents in-law, Dr. Yusuf Aydın and Sevil Aydın. It was very hard to be far away from the loved ones while pursuing this lofty goal. I know I would not be able to achieve any of this without the sacrifices you made in order for me to receive the best education possible.

I would also like to dedicate this work to my wife, Yeşim Aydın Son, for all the support she gave me. Thank you for all the help to overcome the difficulties I experienced during this time and rest of our lives. I could not be able to do it without you.

Acknowledgments

I would like to thank several people who helped me throughout my studies and be a guide in this tough path. I would first like to thank to my committee members: Dr. Elizabeth E. Howell, Dr. Engin Serpersu, Dr. John W. Koontz, and Dr. Salil K. Niyogi for their suggestions, critical reviews, and guidance during my studies.

I want to thank my mentor and teacher Dr. Jeffrey Becker, it was really a great pleasure to work for such an enthusiastic scientist. Dr. Becker has provided me with strength, support and directions. I am thankful that he was so patient during the times I was struggling with problems. His critical suggestions and guidance helped me overcome lots of problems that I wouldn't even try without him. I am honored to work for you.

I also would like to thank to Dr. Naider for his support and valuable ideas on critical decisions throughout these studies. Furthermore I want to thank all the Dr. Naider laboratory members for the peptide syntheses that made this study possible.

In addition I wish to thank all the friends in Dr. Becker's laboratory, who kept me sane during the four years I was with them. I want to thank Dr. Melinda Hauser, Dr. Keith Henry, Dr. Ayca Akal-Strader and Dr. Byung-Kwon Lee for their help on Ste2p experiments. I would like to thank to Dr. Tom Masi, Dr. Agnieszka Janiak and Dr. Kyeong-Man Kim for their wise criticism and insightful thoughts. I want to thank all the laboratory citizens: Yong Lee, Amy Wiles, Houjian Cai, Sarah Kauffman, Steve Minkin, Heejung Kim, and Gagan Rajpal for making the work, fun!

I also want to acknowledge Network Ma. for their computer support, and scientific discussions. I want to thank Gokhan Tolun, Serdar Turkarslan, and Secil Acar

for all their helps. I want to thank the software companies including Valve, Crytech, Id and Blizzard for the production of software used during these studies.

Finally I want to thank to my family in Turkey and my wife for all the support that they gave me during all these years.

Abstract

G protein-coupled receptors (GPCRs) are a class of integral membrane receptor proteins that are characterized by a signature seven-transmembrane (7TM) configuration. These receptors comprise a large and diverse gene family found in fungi, plants, and the animal kingdom. Recent studies with GPCRs have begun to elucidate their importance in many physiological processes, thus various human diseases are associated with GPCR pathology. Although the overall 3D structure of these receptors carry similar features, binding of an extraordinarily diverse array of ligands trigger many different biological pathways.

The α -factor receptor (Ste2p) of *Saccharomyces cerevisiae* belongs to the GPCR family. Upon the α -factor binding to Ste2p, a signal is transduced via an associated guanine-nucleotide binding protein initiating a cascade of events that leads to the mating of haploid yeast cells. As only two GPCRs and two G proteins are encoded in the *S. cerevisiae* genome, this yeast presents a relatively simple system to study GPCR signal transduction in comparison to mammalian cells that possess hundreds of GPCRs and tens of G proteins. Part I of this dissertation is an overview of GPCRs in general with specific emphasis on the peptide pheromone α -factor and its receptor Ste2p.

Part II of this dissertation details the design and characterization of a number of iodinated α -factor pheromone analogs containing the photo-cross-linkable 4-benzoyl-L-phenylalanine (Bpa) group. One of these analogs [Bpa¹, Y³, R⁷, Nle¹², F¹³] was radioiodinated for detection and used as a probe for cross-linking studies with Ste2p.

Chemical (with CNBr & BNPS-skatole) and enzymatic (with Trypsin) cleavage of the receptor/analog complex after the cross-linking was examined to determine the interaction between the α -factor probe and a fragment of the receptor. Data from these digestions indicated that the position one of the α -factor interacts with residues 251 to 294 in the receptor.

Similarly Part III of this dissertation describes the design and synthesis of five photoactivatable α -factor analogs that carry Bpa at positions one, three, five, eight, or thirteen. All of these analogs were biotinylated at the ϵ -amine of the Lys⁷ for detection and purification purposes. The biological activity (growth arrest assay) and binding affinities of all analogs for Ste2p were determined. Two of the analogs tested, Bpa¹ and Bpa⁵, showed three- to four-fold lower affinity compared to α -factor, whereas Bpa³ and Bpa¹³ had seven- to twelve-fold lower affinities, respectively. Bpa⁸ competed poorly with [³H] α -factor for Ste2p. All of the analogs tested had detectable halos in the growth arrest assay indicating that these analogs are α -factor agonists. Cross-linking studies demonstrated that [Bpa¹] α -factor, [Bpa³] α -factor, [Bpa⁵] α -factor and [Bpa¹³] α -factor were cross-linked to Ste2p; the biotin tag on the pheromone was detected by a NeutrAvidin-HRP conjugate on Western blots. Digestion of Bpa¹, Bpa³, and Bpa¹³ cross-linked receptors with chemical and enzymatic reagents suggested that the N-terminus of the pheromone interacts with a binding domain consisting of residues from the extracellular ends of TM5, TM6, and TM7 and portions of EL2 and EL3 close to these TMs. Additionally it was concluded that there is a direct interaction between the position 13 side chain and a region of Ste2p (F55-R58) at the extracellular end of TM1. Parts II

and III of this dissertation indicate that Bpa-containing α -factor probes are useful in determining contacts between α -factor and Ste2p and initiating mapping of the ligand binding site of the GPCR for its peptide ligand.

This dissertation (Part IV) also presents the application of different purification methods and the use of two mass spectrometry instruments for identification of ligand-receptor interactions at the molecular level. Results presented in this part showed that although a single step purification was enough for western blot analyses of the cross-linked receptor fragments, at least a two-step purification and enrichment of the biotinylated peptide fragments were necessary for mass spectrometric studies. MALDI-TOF experiments showed that the affinity purification of the biotinylated fragments by monomeric avidin beads was successful. Data obtained from CNBr fragments of Bpa1 cross-linked membranes were in agreement with the previous results discussed in Parts II and III of this dissertation suggesting the cross-linking between position one of α -factor and a region of Ste2p covering residues 251 to 294. This part also illustrated that the analyses of the MS/MS data from the cross-linked fragments were more complex than the fragmentation data obtained from biotinylated α -factor; the presence of multiple charge states of fragment ions and unusual fragmentation of branched peptides indicated the necessity of using an instrument with higher resolution. In addition, analyses of the MS/MS data with a customized algorithm would be required to deconvolute the sequence of the cross-linked fragment(s) to identify the cross-linked residue(s) on Ste2p.

The final part of this dissertation reviews the overall conclusions and discussion. This part also contains suggestions for future experiments that could help identification of

contact points between Ste2p and its peptide ligand α -factor. Additional studies on this GPCR system employing high-resolution mass spectral characterization of fragments should allow identification of residue-to-residue interactions between the analogs used in this study and Ste2p. Such information will aid the mapping of the ligand-binding site of the pheromone receptor and has the potential to provide key insights into peptide ligand mediated activation of GPCRs. This and similar studies may ultimately lead to the discovery of how peptide ligands initiate signal transduction through GPCRs.

TABLE OF CONTENTS

CHAPTER		PAGE
	PART I: General Introduction	1
1	G Protein-coupled Receptors: An overview	2
2	α -factor Pheromone and its G Protein-coupled Receptor (Ste2p) in <i>Saccharomyces cerevisiae</i>	17
	List of References for Part I	28
	 PART II: Identification of a Contact Region between the Tridecapeptide α-Factor Mating Pheromone of <i>Saccharomyces cerevisiae</i> and its G Protein-Coupled Receptor by Photoaffinity Labeling	 45
1	Introduction	47
2	Materials and Methods	50
3	Results	60
4	Discussion	88
	List of References for Part II	95
	 PART III: Identification of Ligand Binding Regions of the <i>Saccharomyces cerevisiae</i> α-factor Pheromone Receptor (Ste2p) by Photo-affinity Cross-linking	 100
1	Introduction	102
2	Materials and Methods	105
3	Results	115
4	Discussion	144
	List of References for Part III	153
	 PART IV: Purification of Cross-linked Receptor Fragments and Mass Spectrometry Analysis	 161
1	Introduction	162
2	Materials and Methods	166
3	Results	176
4	Discussion	206
	List of References for Part IV	214
	 PART V: General Conclusions and Future Studies	 221
1	General Conclusions and Discussion	222
2	Future Studies	232
	List of References for Part V	238
	 VITA	 242

LIST OF TABLES

TABLE		PAGE
	PART I: General Introduction	
1	GPCR-based drugs among the 200 best-selling prescriptions in 2000 and their GPCR targets	4
2	Sequence-based groupings within the G-protein-coupled receptors	6
	PART II: Identification of a Contact Region between the Tridecapeptide α-Factor Mating Pheromone of <i>Saccharomyces cerevisiae</i> and its G Protein-Coupled Receptor by Photoaffinity Labeling	
1	Physicochemical properties of photoactivatable peptides	61
2	Biological activity of α -factor analogs	65
3	Peptides of CNBr-digested Ste2p	83
	PART III: Identification of Ligand Binding Regions of the <i>Saccharomyces cerevisiae</i> α-factor Pheromone Receptor (Ste2p) by Photo-affinity Cross-linking	
1	Biotinylation yield for α -factor analogs	116
2	Summary of receptor affinities and biological activities for Bpa-scanned biotinylated α -factor analogs	122
3	Summary of the cross-linking optimization with Bpa-scanned α -factor analogs	126
4	Summary of the binding affinities and biological activities of Ala mutants	140
5	Summary of the binding affinities and biological activities of position 13 α -factor analogs	142

LIST OF FIGURES

FIGURE		PAGE
	PART I: General Introduction	
1	A model for the structure of inactive rhodopsin (dark) and light-dependent changes (activated) in the relative positions	13
2	Pheromone mediated mating in <i>Saccharomyces cerevisiae</i>	19
3	<i>Saccharomyces cerevisiae</i> mating pathway	20
4	Functional domains of α -factor ligand	23
	PART II: Identification of a Contact Region between the Tridecapeptide α-Factor Mating Pheromone of <i>Saccharomyces cerevisiae</i> and its G Protein-Coupled Receptor by Photoaffinity Labeling	
1	Binding affinity of Bpa-substituted α -factor analogs	63
2	Competition binding assay for various analogs vs. [^{125}I Tyr ¹ , Arg ⁷ , Phe ¹³] α -factor	67
3	HPLC analysis of products from iodination of tyrosine-substituted α -factor analogs	69
4	Competition binding of [Bpa ¹ , (^{125}I)Tyr ³ , Arg ⁷ , Phe ¹³] α -factor by nonradiolabeled α -factor	70
5	Total radioactive counts of [Bpa ¹ , (^{125}I)Tyr ³ , Arg ⁷ , Phe ¹³] α -factor bound to membranes following cross-linking in the presence and absence of nonradiolabeled α -factor	72
6	Autoradiograph of SDS-PAGE analysis of UV-irradiated DK102pNED membranes in the presence of [Bpa ¹ , (^{125}I)Tyr ³ , Arg ⁷ , Phe ¹³] α -factor	73
7	Schematic representation of chemical and enzymatic cleavage of Ste2p	76
8	Western blot analysis of BNPS-skatole digested membranes	78
9	Autoradiograph of SDS-PAGE 10-20% tricine gel analysis of	79

	membranes photolabeled with [Bpa ¹ , (¹²⁵ I)Tyr ³ , Arg ⁷ , Phe ¹³] α -factor	
10	Autoradiographs of membranes photo-cross-linked with [Bpa ¹ , (¹²⁵ I)Tyr ³ , Arg ⁷ , Phe ¹³] α -factor and treated with CNBr	81
11	Autoradiograph of membranes photo-cross-linked with [Bpa ¹ , (¹²⁵ I)Tyr ³ , Arg ⁷ , Phe ¹³] α -factor and treated with trypsin	85
12	Western blot analysis of [Bpa ¹ , Lys ⁷ (ϵ -biotinyl- β -alanyl)] α -factor cross-linked membranes	86
 PART III: Identification of Ligand Binding Regions of the <i>Saccharomyces cerevisiae</i> α-factor Pheromone Receptor (Ste2p) by Photo-affinity Cross-linking		
1	Competition binding assay of various α -factor analogs vs. tritiated α -factor	118
2	Halo assay with Bpa-scanned biotinylated α -factor analogs	120
3	Optimization of the [Bpa ¹] α -factor analog concentration and time for cross-linking	124
4	Western blot analysis of BJS21pNED (expresses Ste2p), and BJS21(Δ Ste2p) photo-cross-linked membranes	127
5	Western blot analysis of BJS21pNED photo-cross-linked membranes in the presence or absence of excess α -factor	130
6	Western blot analysis of Trypsin digested BJS21pNED photo-cross-linked membranes	132
7	Schematic representation of receptor fragments after chemical or enzymatic cleavage of Ste2p	133
8	Western blot analysis of CNBr digested BJS21pNED photo-cross-linked membranes	136
9	Western blot analysis of BNPS-skatole digested BJS21pNED photo-cross-linked membranes	137
10	Saturation binding assay with R58 mutants	141

11	Western blot analysis of photo-cross-linked Ala mutant BJS21pGA314.Cys-less.STE2.FT.HT membranes	143
12	Working model for the fitting of α -factor pheromone into the ligand binding site on its GPCR, Ste2p	151
PART IV: Purification of Cross-linked Receptor Fragments and Mass Spectrometry Analysis		
1	Schematic representation of the MALDI procedure with avidin beads	173
2	Elution of Ste2p.FT.HT from HiTrap column	177
3	Silver stained SDS-PAGE gel loaded with HiTrap elutions	178
4	Elution of cross-linked Ste2p.FT.HT from HiTrap column	180
5	Western blot analysis of the fractions from Ni-NTA column	182
6	Silver stained SDS-PAGE gel loaded with Ni-NTA column elutions	183
7	Partial purification of cross-linked Ste2p by gel extraction	185
8	Total ion spectrum of CNBr digested HiTrap elution from LCQ-DECA	186
9	MS/MS spectrums of CNBr digested HiTrap elution from LCQ-DECA	187
10	Capture of biotinylated peptides from a simple mixture with monomeric avidin beads	189
11	Capture of biotinylated peptides from a simple mixture with streptavidin beads	192
12	Capture of biotinylated peptides from a complex mixture with monomeric avidin beads	194
13	Capture of cross-linked fragments with monomeric avidin beads	197
14	Analysis of elutions from monomeric avidin column with LCQ-DECA	199

15	MS/MS analysis of the 1080.79 m/z ion at 53 rd minute	201
16	Analysis of monomeric avidin column purified CNBr digested cross-linked membranes with LCQ-DECA	203
17	Comparison of the interaction of different metal chelating matrices with nickel ion	208
PART V: General Conclusions and Future Studies		
1	Working model for the fitting of α -factor pheromone into the ligand binding site o its GPCR, Ste2p	229
2	Total ion spectrum of two [Bpa ¹] α -analogs obtained by LCQ-DECA	236

PART I

General Introduction

CHAPTER 1

G Protein-coupled Receptors: An overview

A class of integral membrane receptor proteins that are characterized by a signature seven-transmembrane (7TM) configuration consists of large and diverse gene families found in fungi, plants, and the animal kingdom. Members of this class of receptors are coupled to heterotrimeric guanine nucleotide-binding proteins (G proteins); thus they are called G protein-coupled receptors (GPCRs) [1]. GPCRs are located at the cell surface and are responsible for the transduction of an extracellular signal into an intracellular response [2]. The natural ligands of this receptor superfamily are extraordinarily diverse, embracing biogenic amines (for example, adrenaline, dopamine, histamine, and serotonin), peptide and protein hormones (such as angiotensin, bradykinin, endothelin, and melanocortin), peptide pheromones (i.e. α -factor, **a**-factor of various fungi species), nucleosides and nucleotides (adenosine, adenosine triphosphate, uridine triphosphate), and lipids and eicosanoids (cannabinoids, leukotrienes, prostaglandins, and thromboxanes) [3]. Furthermore, the awareness of exogenous stimuli, such as light, odor, and taste, is also mediated via this class of receptors [3-5].

Heterotrimeric G proteins transduce ligand binding to GPCRs into intracellular responses. These proteins are composed of three subunits (α , $\beta\gamma$ -dimer) and each subunit plays important roles in determining the specificity and temporal characteristics of the cellular responses to signals [6]. Activation of GPCRs by agonists induces a conformational change in the associated G protein α -subunit leading to release of GDP

followed by binding of GTP [7]. This change initiates the dissociation of the α -subunit from the receptor and the $\beta\gamma$ -dimer. Both the GTP bound α -subunit and the released $\beta\gamma$ -dimer can mediate the stimulation or inhibition of a diverse collection of effector enzymes and ion channels, including adenylate cyclase, guanylyl cyclase, phospholipase C, mitogen-activated protein kinases (MAPKs), Ca^{+2} , and K^{+} channels. Thus, stimulation of different cell-surface GPCRs with specific agonists results in changes in levels of a wide variety of second-messenger molecules [8, 9]. G protein deactivation is rate-limiting for turnoff of the cellular response and occurs when the G_α subunit hydrolyzes GTP to GDP.

Considering the wide variety of biological pathways regulated by GPCRs it is not surprising that irregularities of signaling by these receptors are at the root of disorders that affect tissues and organs in the human body [10]. So widespread are the physiological processes controlled by GPCRs that it has been estimated approximately 50% of all modern prescription drugs and 25% of the top-selling drugs directly or indirectly affect GPCRs [2, 11] (Table 1). In contrast, only a very small portion of the known GPCRs represent targets of currently marketed drugs. With the completion of the human genome it has been estimated that hundreds of genes code for the GPCR family [12] of which only approximately 30 represent targets of currently marketed drugs. Hundreds of so-called 'orphan receptors' have been identified within the human genome, for which the ligand and the (patho)physiological function is unknown [13], and the GPCR target family represents approximately a quarter of the portfolio of many pharmaceutical companies [14]. It is thus clear that future studies of GPCRs should make a dramatic impact on understanding and treatment of a variety of diseases.

Table 1: GPCR-based drugs among the 200 best-selling prescriptions in 2000 and their GPCR targets*.

GPCR target	Drug	Disease	Company	2000 sales (US \$m)
Histamine receptors	Zantac	Ulcers	GlaxoSmithKline	870
	Pepcid	Ulcers	Merck	850
	Claritin	Allergies	Schering-Plough	3,000
	Allegra	Allergies	Aventis	1,100
5-HT receptors	Risperdal	Psychosis	Johnson & Johnson	1,600
	Imitrex	Migraine	GlaxoSmithKline	1,100
	BuSpar	Anxiety	Bristol-Myers Squibb	714
	Zyprexa	Schizophrenia	Eli Lilly	2,400
Angiotensin receptors	Cozaar	Hypertension	Merck	1,700
Adrenoceptors	Toprol-XL	Hypertension	AstraZeneca	580
	Coreg	Congestive heart failure	GlaxoSmithKline	250
	Serevent	Asthma	GlaxoSmithKline	940
Muscarinic acetylcholine receptors	Atrovent	COPD	Boehringer Ingelheim	600
GnRH receptors	Zoladex	Cancer	AstraZeneca	740
Dopamine receptors	Requip	Parkinson's diseases	GlaxoSmithKline	90
Prostaglandin (PGE1) receptors	Cytotec	Ulcers	Pharmacia	100
ADP receptors	Plavix	Stroke	Bristol-Myers Squibb	900

*Source: McKinsey Analysis "http://www.predixpharm.com/market_table.htm".

Abbreviations: COPD, chronic obstructive pulmonary disease; 5HT, 5-hydroxytryptamine (serotonin); GnRH, Gonadotrophin-releasing-hormone

Classification of GPCRs:

Despite the wide variety of agonists that stimulate the diverse secondary-messenger pathways activated by the GPCR family, these receptors share structure similarities [8]. All members of the superfamily contains seven transmembrane-spanning α -helical segments connected by alternating intracellular and extracellular loops (IL and EL, respectively), with the amino terminus located on the extracellular side of the cytoplasmic membrane and the carboxy terminus on the intracellular side. Although GPCRs share common membrane topological features, they are diverse in sequence and vary especially in size of the extracellular amino-terminal tails, extracellular and intracellular loops, and carboxy-terminal tails. Currently several classification systems based on these differences have been used to sort out the GPCR superfamily. Some systems group the receptors by their ligand, and others have used both physiological and structural features. Today one of the most commonly used systems classifies GPCRs into six distinct families (A to F clans). This A-F system is designed to cover all GPCRs, in both vertebrates and invertebrates with regard to their sequence similarity. According to this classification a 'Superfamily' is a collection of proteins with structural and functional characteristics in common, but which lack obvious sequence similarity. A GPCR 'Clan' is a collection of receptors, within a superfamily, whose protein sequences share greater than 20% sequence identity in their transmembrane regions, and is presumed to have evolved from a common ancestor. A 'Family' within a clan shares obvious common biochemical properties [15, 16] (Table 2).

Table 2: Sequence-based groupings within the G-protein-coupled receptors.

Clan A: Rhodopsin-like receptors	
<i>Family I</i>	Olfactory receptors, adenosine receptors, melanocortin receptors, and others
<i>Family II</i>	Biogenic amine receptors
<i>Family III</i>	Vertebrate opsins and neuropeptide receptors
<i>Family IV</i>	Invertebrate opsins
<i>Family V</i>	Chemokine, chemotactic, somatostatin, opioids and others
<i>Family VI</i>	Melatonin receptors and others
Clan B: Calcitonin and related receptors	
<i>Family I</i>	Calcitonin, calcitonin-like, and CRF receptors
<i>Family II</i>	PTH/PTHrP receptors
<i>Family III</i>	Glucagon, secretin receptors and others
<i>Family IV</i>	Latrotoxin receptors and others
Clan C: Metabotropic glutamate and related receptors	
<i>Family I</i>	Metabotropic glutamate receptors
<i>Family II</i>	Calcium receptors
<i>Family II</i>	GABA-B receptors
<i>Family IV</i>	Putative pheromone receptors
Clan D: STE2 pheromone receptors	
Clan E: STE3 pheromone receptors	
Clan F: cAMP and archaebacterial opsin receptors	

Table adapted from Flower *et al.* [17]

According to A-F classification the rhodopsin-like family (Clan A) has the largest number of receptors and is by far the most studied. This group contains receptors for odorants, small molecules such as the catecholamines and amines, some peptides and glycoprotein hormones [18]. The overall sequence identity among all type A receptors is low compared to the sequence identity among the members of other clans, and restricted to a number of highly conserved motifs such as NSxxNPxxY motif in transmembrane domain seven (TMVII) and the DRY motif or D(E)-R-Y(F) at the border between TMIII and IL2[19]. Clan B is presently the next largest family, with around 25 distinct members, including receptors for a variety of gastrointestinal peptide hormones (secretin, glucagons, vasoactive intestinal peptide, and growth-hormone-releasing hormone), calcitonin, corticotrophin-releasing hormone and parathyroid hormone [1]. Receptors in this clan do not contain any of the structural features characterizing Clan A receptors except the presence of a disulfide bridge between the second (EL2) and third extracellular loops (EL3). The most noticeable characteristic of this clan is that the amino terminus contains several cysteines, presumably forming a network of disulfide bridges [20]. Clan C on the other hand is relatively a smaller group, containing the metabotropic glutamate and γ -amino-butyric acid receptors, the calcium receptors, the vomeronasal, mammalian pheromone receptors, as well as some taste receptors [5]. All receptors in this clan have a very large extracellular amino terminus (500-600 amino acids) that seems to be crucial for ligand binding and activation [21, 22]. Clan D is the STE2 yeast pheromone receptors, and clan E is the STE3 yeast pheromone receptors. These two groups will be discussed in the next section (Chapter 2). Finally Clan F comprises the receptors that are

related to slime mold cyclic adenosine monophosphate (cAMP) receptors and archaeobacterial opsins.

The tertiary structure of GPCRs:

Information about the tertiary structure of a GPCR is crucial for the understanding of its function and for the design of drugs to correct possible problems caused by failure of this function. Currently methods used to understand the interactions between the ligand and its receptor at the atomic level include X-ray crystallography, electron microscopy or diffraction, NMR spectroscopy and molecular modeling. One of the advantages for NMR spectroscopy compared to the other methods is that dynamic information can be obtained. However, for solving structures by this method, high concentrations of dissolved protein (fairly pure) are needed; unfortunately at these high concentrations GPCRs are mostly insoluble. Except for several studies where single helices were measured in a membrane, using solid state NMR, technical problems have precluded NMR studies from giving structural information on GPCRs [23]. Electron diffraction has so far been successful in obtaining information on structure of one GPCR-like molecule (bacterio-rhodopsin) at medium high resolution (3.5 Å) [24], and one GPCR (rhodopsin) at low resolution (9.0 Å) [25, 26]. These studies with the addition of further biochemical and theoretical studies led to structural information about other members of the superfamily through homology-modeling studies [27-34].

Similar to NMR studies, X-ray studies of GPCRs are hampered by poor solubility and suboptimal purification methods of integral membrane proteins. Thus, so far there is only one high-resolution 3D GPCR structure determined by X-ray crystallography. The

3D structural determination of the dark-adapted bovine rhodopsin by X-ray crystallography provides deep insight into the structure of the rhodopsin family of GPCRs and related GPCRs in general [35, 36](see review [37]). Remarkably, the X-ray structure of rhodopsin was generally in good agreement with the models of various GPCRs derived from low-resolution structures of rhodopsin.

The crystal structure of rhodopsin revealed a highly organized heptahelical transmembrane bundle with 11-cis-retinal as a key cofactor involved in maintaining rhodopsin in the ground state. The EL2 is connected to TM3 via a disulfide bridge and fits tightly into this helix bundle [38]. A significant feature, from the crystal structure, is that the transmembrane helices in rhodopsin are not regular α -helices [39]. The helices are bent and contain segments with 3_{10} - or π -helical conformation. One of the strongest distortions is in TM6 induced by the presence of Pro 267 (a highly conserved residue among GPCRs). It has been shown that mutations at this residue can have long range effects such as conformational changes on IL3 [27]. In addition a pronounced kink is observed in TM2, caused by flexibility in the Gly-Gly sequence in the middle of this helix. The crystal structure also revealed a short 8th helix, which runs parallel to the cytoplasmic membrane. This helix and the generated fourth cytoplasmic loop cover part of the binding site for the C-terminus of the G_{α} subunit and plays a role in G_{γ} binding. A set of residues including portions of IL3 and the 8th helix likely undergoes a conformational change upon photoactivation of the chromophore that leads to the receptor activation and signal transduction (see review[40]).

It is generally agreed that 3D models of rhodopsin guided by the crystal structure will provide a general picture of the other GPCR classes, especially rhodopsin-like

GPCRs (Clan A) (see review[41]). Comparisons of the tertiary structures of homologous proteins have shown that three-dimensional structures have been better conserved in evolution than primary structures, indicating the feasibility of model-building by homology. However differences between 3D structures increase with decreasing sequence identity and accordingly the accuracy of models built by homology decreases. Unfortunately the sequence similarity between different clans of GPCRs is very low, thus homology modeling is difficult for GPCRs in non-rhodopsin like families. In case of low homology ($\leq 25\%$ sequence identity) the alignment of the sequences is the main bottleneck for model building, and large errors are often generated. To overcome this problem development of secondary structure predictions and *ab initio* 3D modeling techniques with experimental constraints are being used [42, 43].

Ligand binding and receptor activation:

The family of G protein-coupled receptors binds and is activated by a wide variety of ligands, ranging in size from small molecules to large glycoproteins. Much of the current emphasis on receptor research is focused on identification of the binding domains for these structurally divergent ligands, using genetic, biochemical, and biophysical approaches [8]. Receptor mutagenesis (site-directed or random), domain swapping, and use of fluorescence probes are the most commonly used methods for elucidating structure-function relationship between GPCRs and their ligands. The binding sites of endogenous “small-molecule” ligands in family A receptors, such as for the retinal chromophore in rhodopsin and for catecholamines in the adrenergic receptors are the most widely studied and well characterized of these receptor-binding domains

(see reviews [44-46]). Recent studies on several peptide receptors such as the receptors for angiotensin [47-49], parathyroid hormone [50, 51], secretin [52], bradykinin B2 [53, 54], gonadotropin-releasing hormone [55], opioids [56, 57], neurokinin (NK) [58, 59], vasopressin/oxytocin [60-62], cholecystokinin/gastrin [63, 64], and neurotensin 1 [65] supplied valuable information on the binding domains for other classes of GPCRs.

Although the specific ligand receptor interactions vary, certain similarities are observed in ligand GPCR interactions. Large ligands, such as proteins, bind to extracellular loops, while small molecules, including pharmacological agents, bind within the transmembrane region of receptor. Peptides on the other hand can exhibit a combined binding mode whereby they bind primarily to the extracellular loops while part of the structure penetrates the transmembrane region and interacts with residues buried in lipids [66-69].

Photo-affinity cross-linking is one of the few direct methods applied to identify the contact regions between the peptide ligands and their GPCRs, thus providing information on how the ligand interacts with its receptor. Benzophenones have been used extensively as photophysical probes to identify and map peptide-protein interactions [70]. In contrast to other cross-linkers, like aryl azides, diazoesters, and diazaarenes, they are chemically stable under ambient light and could be activated by low energy UV (at 350-360 nm) minimizing protein damage. They preferentially react with carbon-hydrogen bonds resulting in a covalent adduct, which would be stable to chemical and enzymatic peptide cleavage [71]. Furthermore, relative to other photo cross-linkers, benzophenones do not photo-dissociate and their photo-excited state readily relaxes in the absence of a suitable C-H bond. This relaxed state could be excited again which will result in higher cross-linking yields upon repeated excitation by long-wavelength UV light [72]. This

dissertation will mainly focus on the use of photoactivatable analogs carrying 4-benzoyl-*L*-phenylalanine (Bpa), for cross-linking the pheromone to its GPCR, and analysis of the results by the aid of other techniques such as site-directed mutagenesis, use of analogs and mass spectrometry. The discussions of these methodologies are expanded in parts 2, 3, and 4 of this dissertation.

Conformational Changes Involved in Agonist Induced GPCR Activation:

Several studies on GPCR activation by agonist binding suggested that relative movements of the transmembrane domains are the key to transfer the extracellular signal to the heterotrimeric G protein. Spin-labeling studies on cysteine-substituted mutants of rhodopsin showed that a rigid body motion of TM6 relative to TM3 accompanied by anti-clockwise rotation (as viewed from the extracellular side) (Figure 1) [73]. Disulfide cross-linking of these helices prevented activation of transducin, thus suggesting the importance of this movement for activation of rhodopsin. More detailed analysis of conformational changes in TM6 of the β_2 -adrenergic receptor (β_2 AR) provides evidence for a rigid body motion similar to that observed upon activation of rhodopsin [74, 75]. Additional support for movement of TM3 and TM6 in the β_2 AR comes from zinc cross-linking studies [76] and chemical reactivity measurements in constitutively active β_2 AR mutants [77, 78]. Cysteine cross-linking studies in the muscarinic acetylcholine M3 receptor provided evidence for the movement of the cytoplasmic ends of TM5 and TM6. These results indicated that there are intermolecular interactions allowing the receptor to undergo conversion between its inactive and active state.

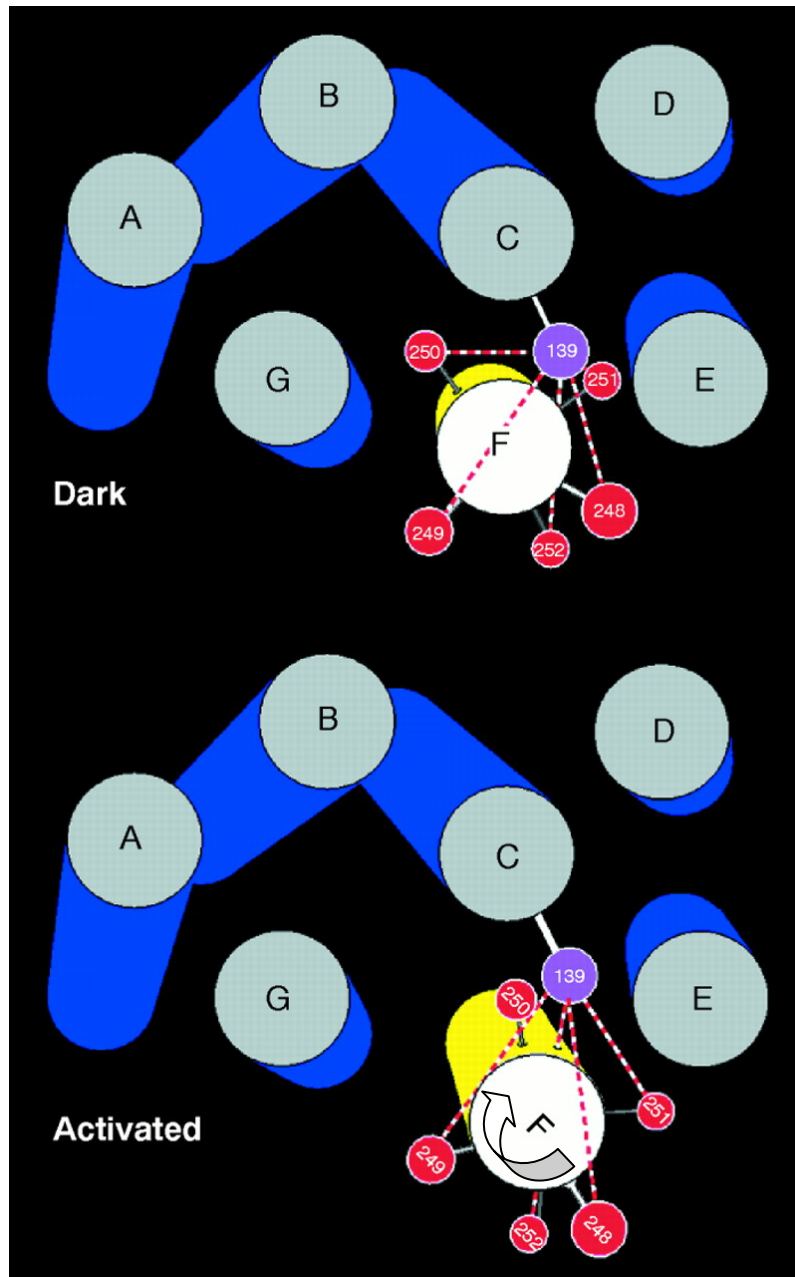


Figure 1: A model for the structure of inactive rhodopsin (dark) and light-dependent changes (activated) in the relative positions. Figure adapted from Farrens *et al.* [73].

There are currently two widely accepted models for GPCR activation. One of these models is the extended ternary complex model (often referred to simply as two-state model) [79]. According to this model the receptor exists in an equilibrium between an inactive conformation (R) and an active conformation (R*). In the absence of agonist, the inactive R state is predominant; however, the energy required to convert R to R* is sufficiently low, allowing a certain fraction of the receptors spontaneously to assume the R* state. In 1994, it was demonstrated that a G protein coupled receptor can be spontaneously active in the absence of agonists and that ligands, which were previously considered as neutral antagonists, can act as inverse agonist by inhibiting spontaneous activity[80]. This concept, originally demonstrated for the β_2 AR, was then extended to many GPCRs including the 5-HT_{2c} serotonin [81], δ -opioid [82] and V₂-vasopressin receptors [83]. In fact, spontaneous activity and inverse agonism are now considered to be general properties of GPCRs that may have physiological implications (reviewed in: [84] and [85]). These observations were rationalized by proposing that receptors spontaneously isomerize between inactive (R) and active (R*) conformations and that inverse agonists and agonists function by stabilizing R and R*, respectively. Agonists are predicted to bind with highest affinity to the R* conformation and in this way shift the equilibrium and increase the ratio of receptor in R* (conformational selection). On the other hand, inverse agonists (also called negative antagonists) have higher affinity to the R state, thus bind and stabilize the inactive state shifting the equilibrium away from R*. Neutral antagonists, according to this model, are defined as compounds that bind with the same affinity to both R and R* thus cause no change in the equilibrium. This model can

explain the basal activity of GPCRs in the absence of agonist and the action of inverse agonists that inhibit the activity of constitutively-activated receptors.

The second model for GPCR activation is called multi-state model and suggests that the receptor alternates spontaneously between multiple active and inactive conformations [86]. This model is becoming more popular due to the limitations of the two-state model to explain the complex behavior of GPCRs. Several experiments have provided strong support that GPCRs may exist in multiple conformational states. For example, a two-state model cannot explain how mutation of certain residues of the dopamine D₂ receptor can lead to loss of functional coupling in response to some agonists, but only had modest effect on the others [87]. Likewise, different constitutively-active mutants of the α 1b-receptor are differentially phosphorylated and internalized although they express a similar agonist-independent activity to the receptor, which suggests the existence of more than one active receptor state [88]. Furthermore, direct structural evidence has been obtained by fluorescence spectroscopy analysis of the purified β ₂AR[89]. This study indicated that most ligands promote alterations in receptor structure consistent with the existence of multiple ligand specific conformation states. The most critical point in this model is that the biological response to a given ligand is determined by the conformation to which the ligand binds with highest affinity. Thus this model is considered as an extension of conformational selection in which ligand binding depends on the conformational status of receptor. However, there is evidence suggesting that ligand might have an active role of inducing conformational changes in the receptor ([90-92] for review see [93]).

It has been recently shown that norepinephrine binds to the β_2 AR in a sequential manner and can induce at least two kinetically and functionally distinct conformational states [94]. Similarly studies on μ -opioid receptor demonstrates that different ligands induce distinct conformational states that differ in promoting G protein activation and receptor internalization [95]. Time-resolved peptide binding studies on the neurokinin receptor revealed that an agonist peptide binds with biphasic kinetics. The rapid binding component was associated with a cellular calcium response, whereas the slow component was required for cAMP signaling [96]. More recently it has been shown that compounds which act as inverse agonists on the β -adrenergic-stimulated adenylyl cyclase pathway are partial agonists for the receptor-stimulated MAP-kinase activity [83]. These data, which support a multi-state model of receptor activation, indicate that different receptor conformations lead to the activation of distinct signaling pathways and that ligands can selectively activate one while inhibiting the other. Thus, it is likely that a single agonist can induce or stabilize multiple functionally distinct conformational states will be generalizable to other GPCRs, particularly those activated by peptides and protein hormones where there are a larger number of sites of interaction between receptor and agonist. A better understanding of this conformational heterogeneity will facilitate the design of more effective and selective pharmaceuticals.

CHAPTER 2

α -factor Pheromone and its G Protein-coupled Receptor (Ste2p) in

Saccharomyces cerevisiae

One of the biggest challenges facing GPCR research is the complexity of eukaryotic systems. The presence of receptor subtypes, known and unknown, within the same biological system and cross-talk between different types of receptors regulating many different pathways complicate biochemical and physiological studies. *S. cerevisiae* is a species of budding yeast which is most widely known to mankind both for its use since ancient times in baking and brewing, and for being one of the most intensively studied eukaryotic model organisms in molecular and cell biology. The simplicity of single-celled yeast and widely studied mitogen-activated protein kinase (MAPK) system regulated by the mating pathway made it a perfect model system for the study of GPCRs. After the completion of the sequencing of its genome it is now known that *S. cerevisiae* has only three GPCRs. Two of these are the pheromone receptors (either Ste2p or Ste3p) and the other is the Gpr1p which is a carbohydrate sensor. While the pheromone and carbohydrate-sensing pathways share some down-stream components, there is no cross-talk between the two systems as the pheromone receptors and the Gpr1p couple to two different G-proteins (Gpa1p and Gpa2p, respectively) [97, 98]. Thus *S. cerevisiae* provides an ideal system to study the relation between a peptide ligand and its GPCR in the absence of interfering biological complexities.

Mating in yeast, Saccharomyces cerevisiae:

S. cerevisiae, commonly referred to as Brewer's or Baker's yeast, can grow as a haploid or diploid [99, 100]. Haploid cells exist in two mating cell types *MATa* and *MAT α* . The secretion and reciprocal detection of peptide pheromones (α -factor and **a**-factor) by GPCRs (Ste2p and Ste3p, respectively) initiate mating and eventual fusion of two haploids. **a**-cells secrete **a**-factor, a hydrophobic farnesylated, carboxymethylated, dodecapeptide with the sequence YIIKGVFWD PAC(Farnesyl)-OCH₃ while α -cells secrete α -factor, a tridecapeptide with the sequence WHWLQLKPGQPMY (see Figure 2 for schematic representation).

Pheromone binding to its GPCR and activation of the G protein induces initiation of the downstream MAPK cascade which, in turn, activates the transcription of genes involved in the production of pheromone itself, pheromone receptor and the proteins of the signaling pathway. Also components mediating cellular adhesion (sex-specific agglutinins), arresting the cell cycle in the G1 phase by eliminating the function of G1 cyclin complex and Cdc28 protein kinase, inducing cell and nuclear fusion and also genes reducing the reactivity of the cell to pheromone and those releasing the cell cycle arrest (desensitization) are activated [101, 102] (Figure 3). The activation of cells by pheromone results in morphological changes. First, conjugation projections are formed to facilitate connection of the cells. By the action of agglutinins, the tips of the projections fuse forming a conjugation bridge. Next, the nuclei migrate into the bridge and subsequently fuse to produce a diploid nucleus of the zygote. All these morphological processes occur with an involvement of cytoskeletal components, i.e., microtubules and actin structures, and the cell wall [103].

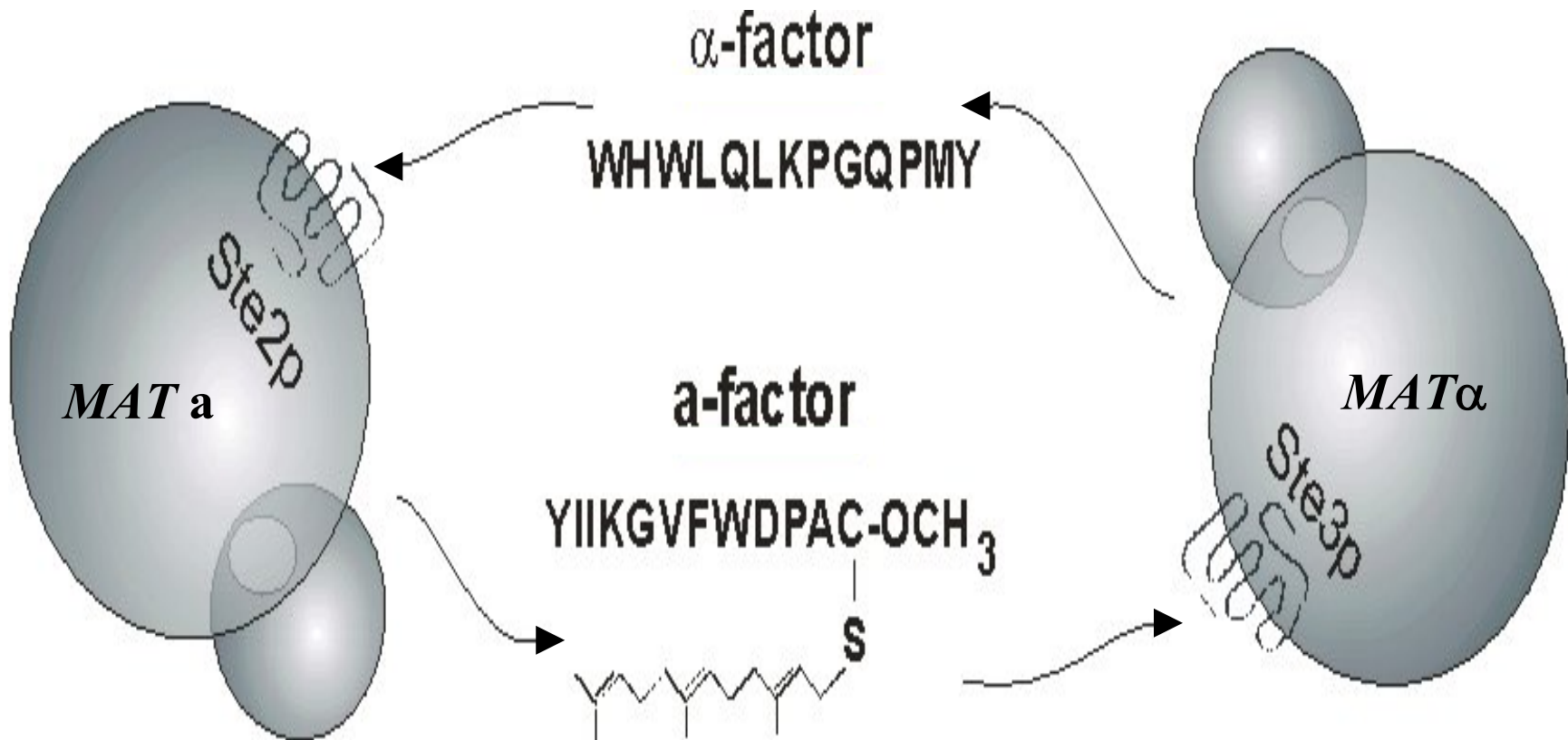
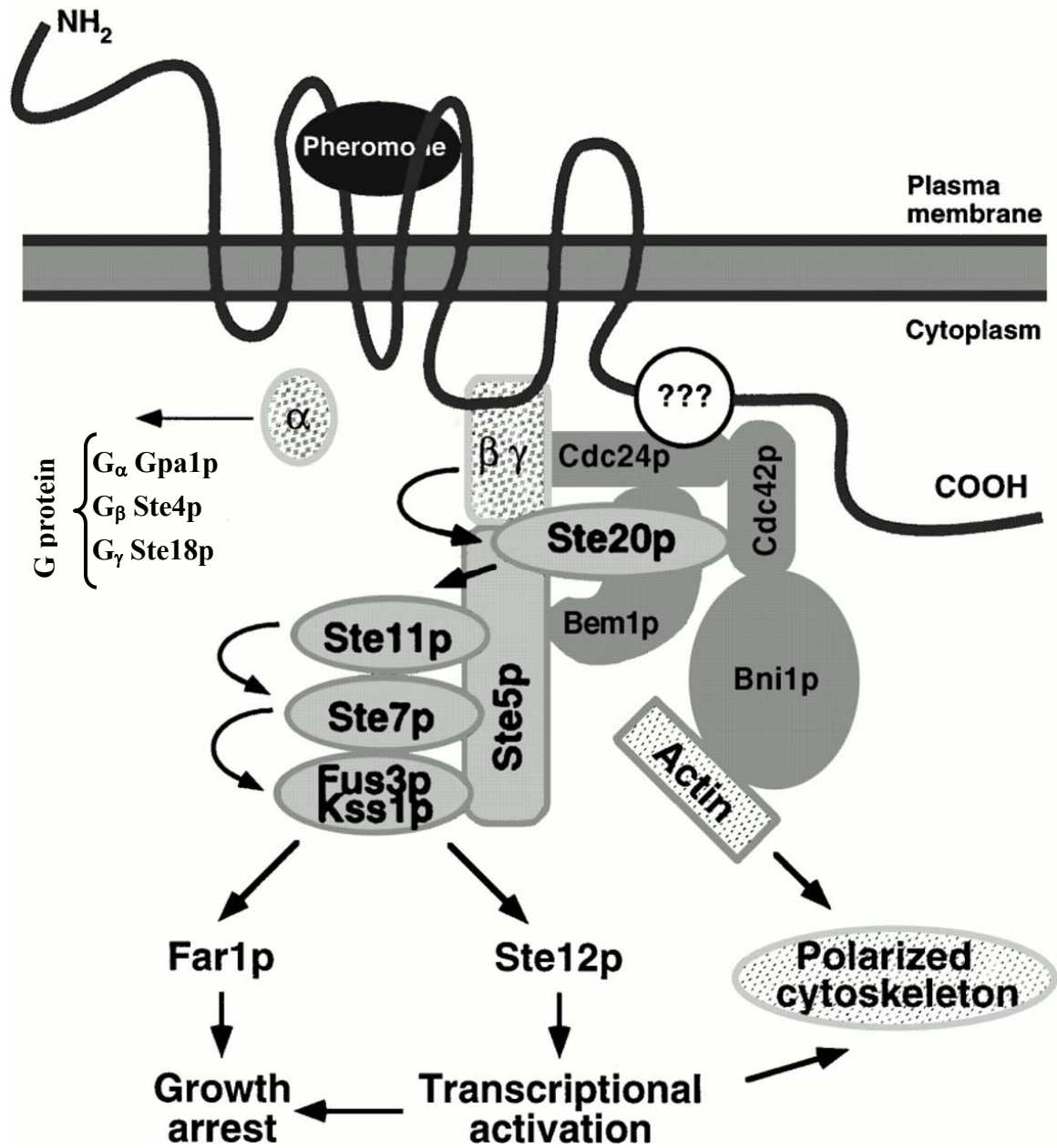


Figure 2: Pheromone mediated mating in *Saccharomyces cerevisiae*. Schematic representation of pheromone/receptor mediated communication between MATa and MAT α haploid cells prior to mating.

Figure 3: *Saccharomyces cerevisiae* mating pathway. Binding of the pheromone to its GPCR stimulates downstream responses such as transcriptional activation of pheromone induced genes, cell cycle arrest, and polarization of the cytoskeleton. (Adapted from Madden and Snyder [103]). Ste5p is the scaffold protein, Ste20p is mitogen-activated quadruple protein kinase (MKKKK), Ste11p is MKKK, Ste7p is MKK, Fus3p and Kss1p are MAPK.

Saccharomyces cerevisiae pheromone receptor (Ste2p or Ste3p)



Structure-function analysis of α -factor pheromone:

The α -factor is a tridecapeptide secreted by *MAT α* cells and has the sequence of WHWLQLKPGQPMY. Extensive analyses of α -factor analogs in combination with receptor mutagenesis have provided insights into the structural basis of α -factor activity [104-108]. These studies aided the discovery of several antagonists, partial agonists and a ligand with novel function which is able to enhance the activity of α -factor but, alone, has no agonistic activity termed a synergist. Additionally biochemical and biophysical analysis of α -factor and its analogs have suggested structural and functional information. Briefly the results of these studies indicated that residues near the amino terminus play an important role in receptor activation, the carboxyl terminus of the peptide contributes mostly to the binding affinity and the central residues of the peptide form a β -turn around the Pro⁸-Gly⁹ bound aiding the orientation of the signaling and the binding domains of the pheromone (Figure 4) [109-111].

Several of the *D*-Ala series analogs, near the N-terminus, specifically [*D*-Ala²] α -factor, [*D*-Ala³] α -factor and [*D*-Ala⁴] α -factor had no measurable biological activity [107]. However, these peptides bound relatively strongly to Ste2p and antagonized the biological activity of wild type ligand (α -factor pheromone). Previous studies from our laboratory showed that most of the antagonists discovered involved changes in residues near the amine terminus. Based on these findings it seems clear that residues near this region play an important role in triggering cell signaling through Ste2p or in stabilizing the activated state of this receptor.

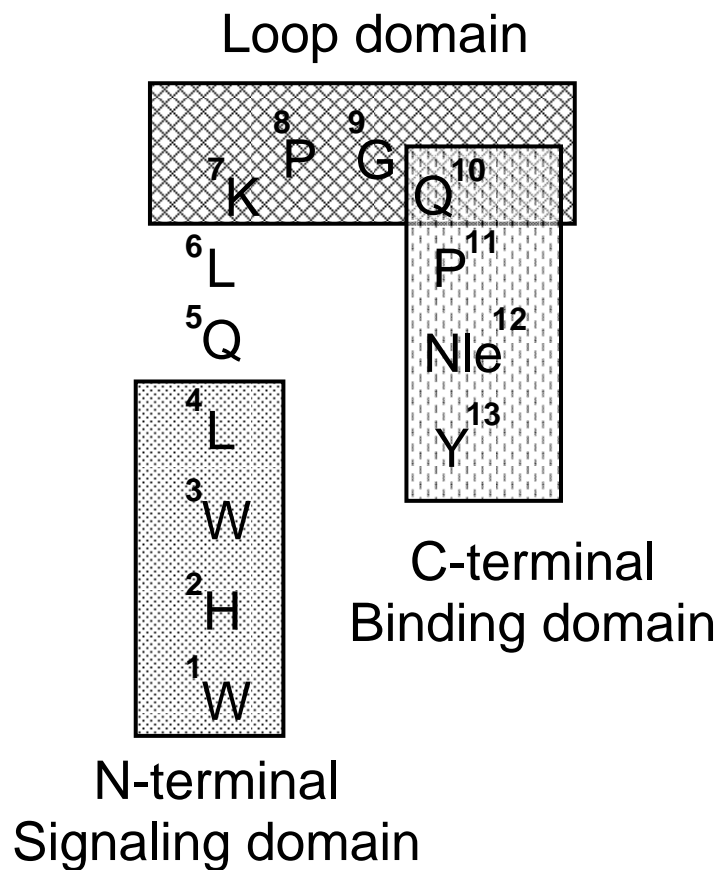


Figure 4: Functional domains of α -factor ligand. Studies of α -factor analogs have revealed two regions according to their major contributions to activity and binding affinity. The residues at the N-terminus appeared to mainly function in activation of the receptor signaling, the residues at the C-terminus strongly contribute to the binding affinity. However the two functions cannot be completely separated. The loop domain corresponds to residues of the peptide which are thought to induce a bend in the ligand structure. (Figure adapted from Abel *et al.* [107])

On the other hand the residues at the carboxyl terminus of α -factor strongly influence the binding. Replacement of these residues by either *L*- or *D*-Ala caused decreases in affinity of up to 3000-fold [107]. Moreover, these carboxy-terminal residues are not sufficient to cause signaling as evidenced by the total absence of agonist activity in [*D*-Ala³] α -factor. Removal of the carboxyl terminal residues result in pheromones with drastically reduced receptor affinity and, in some cases, also with complete loss of affinity. Similar observations for other peptide receptors, where the functional domains for binding and activity are separated, have been reported [112-115].

As mentioned above, the central residues of α -factor contains a Pro-Gly sequence. This sequence has been associated with a high probability of β -turns, in particular Type II β -turns [116, 117]. Studies on desTrp¹- α -factor analogs indicated that a turn at this position was involved in biological activity of the pheromone [118]. Additional studies with *L*- or *D*-Ala α -factor analogs suggested that this region of the peptide may lead to create the proper overall conformation for the pheromone [107].

Interactions between α -factor pheromone and its GPCR, Ste2p:

The yeast α -factor pheromone receptor is one of the most extensively studied GPCRs. While many techniques have been applied to study the structure-function relationship for this receptor, much of our knowledge comes from the characterization of mutant receptors and α -factor analogs. Today several research groups (5 in the United States) are working with Ste2p as a model system. Mutagenesis studies carried out by these groups cover almost 70-80% of all the residues present in this 431 amino acid

receptor. Although it is not possible to summarize all of these mutational analyses in the context of this dissertation, studies relevant to our results will be discussed in parts 2 & 3.

In addition to the mutagenesis studies, chimeric receptors between *S. cerevisiae* and *S. kluyveri* α -factor receptors also supplied important information to understand the ligand receptor interaction(s) [119, 120]. These studies helped the identification of three small regions that are mostly contributing to the specificity of the two receptors to their wild type ligands. A substitution at residues 47-49 (region of N-terminus connected to TM1) affected specificity for pheromone binding but not for pheromone activation of response. Substitution of residues 267-269 (extracellular portion of TM6) affected pheromone specificity for activation of cellular responses, but not for pheromone binding. Finally substitution of residues 104-123 (part of EL1 attached to TM2) modestly affected both types of specificity.

Regulation of Ste2p in Saccharomyces cerevisiae:

The coordination of complex cellular processes, from growth and differentiation to responses of environmental changes, often depend on careful regulation of GPCRs. Like many other GPCRs, Ste2p is highly regulated by several control mechanisms. The most well characterized regulation of Ste2p are: rapid phosphorylation and desensitization [121]; internalization and recycling [122]; and down-regulation and degradation [123, 124]. GPCRs often become less responsive (desensitize) after prolonged agonist exposure. In many eukaryotic systems a highly conserved mechanism involving multiple protein-protein interactions, receptor phosphorylation [by G-protein coupled receptor kinases (GRKs)] and receptor endocytosis (internalization) is

responsible for this desensitization [125]. Phosphorylation by GRKs and trafficking events are usually associated with acute desensitization as the immediate occurrence of these events coincides with the rapid desensitization observed with most receptors. On the other hand receptor down-regulation results in an overall reduction in receptor levels in the cell, which usually has a longer term effect on signaling [126].

The mating process in yeast is further regulated by the control of the expression levels or the activities of the downstream elements in the signaling pathway (i.e. subunits of the G protein or/and MAPK). One of the well characterized regulators is Sst2p, a yeast homologue of regulators of G protein signaling (RGS), which effect the G protein signaling by accelerating the GTP hydrolysis and promoting re-association of the heterotrimer [127, 128]. Additionally, expression of some proteases like Bar1p (Sst1p), which specifically cleaves α -factor pheromone, adds further complexity to the regulation of mating [129]. Furthermore, several different types of post-translational modifications have been described for the heterotrimeric G protein subunits, which may be involved in signal regulation. Details of these modifications are beyond the scope of this study, however a few of the well characterized modifications are: 1) palmitoylation [130], myristoylation [131, 132] and ubiquitination of the G_{α} (Gpa1p) [133]; 2) isoprenylation [134], farnesylation [135] and palmitoylation of the G_{γ} (Ste18p) [136]; and 3) phosphorylation of the G_{β} (Ste4p) [137].

Although the *S. cerevisiae* mating signal transduction pathway is one of the best defined MAPK pathways, the mechanism that triggers this pathway is poorly understood. The lack of information how the peptide pheromone interacts with its GPCR and causes

conformational changes leading to the dissociation of the G protein limits our understanding of α -factor receptor activation. Mapping the α -factor binding region(s) in Ste2p could supply great insights for understanding the overall mechanism of GPCR activation by peptide ligands. This dissertation mainly describes the use of novel α -factor ligand analogs as tools and probes to study receptor binding and activation. Parts II and III detail the construction, characterization and use of α -factor probes that contain the photo-cross-linkable group, 4-benzoyl-*L*-phenylalanine (Bpa), for use in determining ligand-receptor contact sites. Part III also introduces the use of biotin for detection of the ligand as an alternative to radioactive ligand. Part IV describes the methods applied for cross-linked sample preparation for mass spectrometry (MS) analysis. This part also covers some of the preliminary MS results that support our findings presented in part II and III. Finally part IV is an overall evaluation of these studies, contributions to the working model of α -factor-Ste2p interaction and future studies that could be performed to refine this model, thus aiding us to better understand how peptide ligands interact with their GPCRs.

List of References for Part I

1. Pierce, K.L., R.T. Premont, and R.J. Lefkowitz, *Seven-transmembrane receptors*. Nat Rev Mol Cell Biol, 2002. 3(9): p. 639-50.
2. Klabunde, T. and G. Hessler, *Drug design strategies for targeting G-protein-coupled receptors*. Chembiochem, 2002. 3(10): p. 928-44.
3. Watson, S.a.A., S. (eds), *The G Protein Linked Receptor Facts Book*. 1994: Academic Press, London, UK.
4. Horn, F., et al., *GPCRDB information system for G protein-coupled receptors*. Nucleic Acids Res, 2003. 31(1): p. 294-7.
5. Hoon, M.A., et al., *Putative mammalian taste receptors: a class of taste-specific GPCRs with distinct topographic selectivity*. Cell, 1999. 96(4): p. 541-51.
6. Hamm, H.E., *The many faces of G protein signaling*. J Biol Chem, 1998. 273(2): p. 669-72.
7. Bourne, H.R., D.A. Sanders, and F. McCormick, *The GTPase superfamily: conserved structure and molecular mechanism*. Nature, 1991. 349(6305): p. 117-27.
8. Strader, C.D., et al., *Structure and function of G protein-coupled receptors*. Annu Rev Biochem, 1994. 63: p. 101-32.
9. Dolphin, A.C., *G-proteins*, in *Textbook of Receptor Pharmacology*. 1996, CRC Press, Inc. p. 187-196.

10. Karnik, S.S., et al., *Activation of G-protein-coupled receptors: a common molecular mechanism*. Trends Endocrinol Metab, 2003. 14(9): p. 431-7.
11. George, S.R., B.F. O'Dowd, and S.P. Lee, *G-protein-coupled receptor oligomerization and its potential for drug discovery*. Nat Rev Drug Discov, 2002. 1(10): p. 808-20.
12. Venter, J.C., et al., *The sequence of the human genome*. Science, 2001. 291(5507): p. 1304-51.
13. Wise, A., K. Gearing, and S. Rees, *Target validation of G-protein coupled receptors*. Drug Discov Today, 2002. 7(4): p. 235-46.
14. Hopkins, A.L. and C.R. Groom, *The druggable genome*. Nat Rev Drug Discov, 2002. 1(9): p. 727-30.
15. Attwood, T.K. and J.B. Findlay, *Fingerprinting G-protein-coupled receptors*. Protein Eng, 1994. 7(2): p. 195-203.
16. Kolakowski, L.F., Jr., *GCRDb: a G-protein-coupled receptor database*. Receptors Channels, 1994. 2(1): p. 1-7.
17. Flower, D.R., *Modelling G-protein-coupled receptors for drug design*. Biochim Biophys Acta, 1999. 1422(3): p. 207-34.
18. Lee, D.K., S.R. George, and B.F. O'Dowd, *Novel G-protein-coupled receptor genes expressed in the brain: continued discovery of important therapeutic targets*. Expert Opin Ther Targets, 2002. 6(2): p. 185-202.
19. Fredriksson, R., et al., *The G-protein-coupled receptors in the human genome form five main families. Phylogenetic analysis, paralogon groups, and fingerprints*. Mol Pharmacol, 2003. 63(6): p. 1256-72.

20. Ulrich, C.D., 2nd, M. Holtmann, and L.J. Miller, *Secretin and vasoactive intestinal peptide receptors: members of a unique family of G protein-coupled receptors*. *Gastroenterology*, 1998. 114(2): p. 382-97.
21. O'Hara, P.J., et al., *The ligand-binding domain in metabotropic glutamate receptors is related to bacterial periplasmic binding proteins*. *Neuron*, 1993. 11(1): p. 41-52.
22. Conn, P.J. and J.P. Pin, *Pharmacology and functions of metabotropic glutamate receptors*. *Annu Rev Pharmacol Toxicol*, 1997. 37: p. 205-37.
23. Arshava, B., et al., *High resolution NMR analysis of the seven transmembrane domains of a heptahelical receptor in organic-aqueous medium*. *Biopolymers*, 2002. 64(3): p. 161-76.
24. Henderson, R., et al., *Model for the structure of bacteriorhodopsin based on high-resolution electron cryo-microscopy*. *J Mol Biol*, 1990. 213(4): p. 899-929.
25. Schertler, G.F., C. Villa, and R. Henderson, *Projection structure of rhodopsin*. *Nature*, 1993. 362(6422): p. 770-2.
26. Unger, V.M., et al., *Arrangement of rhodopsin transmembrane alpha-helices*. *Nature*, 1997. 389(6647): p. 203-6.
27. Ernst, O.P., et al., *Mutation of the fourth cytoplasmic loop of rhodopsin affects binding of transducin and peptides derived from the carboxyl-terminal sequences of transducin alpha and gamma subunits*. *J Biol Chem*, 2000. 275(3): p. 1937-43.
28. Baldwin, J.M., G.F. Schertler, and V.M. Unger, *An alpha-carbon template for the transmembrane helices in the rhodopsin family of G-protein-coupled receptors*. *J Mol Biol*, 1997. 272(1): p. 144-64.

29. Baldwin, J.M., *The probable arrangement of the helices in G protein-coupled receptors*. Embo J, 1993. 12(4): p. 1693-703.
30. Shieh, T., et al., *The steric trigger in rhodopsin activation*. J Mol Biol, 1997. 269(3): p. 373-84.
31. Pogozheva, I.D., A.L. Lomize, and H.I. Mosberg, *The transmembrane 7-alpha-bundle of rhodopsin: distance geometry calculations with hydrogen bonding constraints*. Biophys J, 1997. 72(5): p. 1963-85.
32. Herzyk, P. and R.E. Hubbard, *Combined biophysical and biochemical information confirms arrangement of transmembrane helices visible from the three-dimensional map of frog rhodopsin*. J Mol Biol, 1998. 281(4): p. 741-54.
33. Farahbakhsh, Z.T., et al., *Mapping light-dependent structural changes in the cytoplasmic loop connecting helices C and D in rhodopsin: a site-directed spin labeling study*. Biochemistry, 1995. 34(27): p. 8812-9.
34. Kim, J.M., et al., *Structure and function in rhodopsin: rhodopsin mutants with a neutral amino acid at E134 have a partially activated conformation in the dark state*. Proc Natl Acad Sci U S A, 1997. 94(26): p. 14273-8.
35. Palczewski, K., et al., *Crystal structure of rhodopsin: A G protein-coupled receptor*. Science, 2000. 289(5480): p. 739-45.
36. Teller, D.C., et al., *Advances in determination of a high-resolution three-dimensional structure of rhodopsin, a model of G-protein-coupled receptors (GPCRs)*. Biochemistry, 2001. 40(26): p. 7761-72.
37. Ridge, K.D., et al., *Phototransduction: crystal clear*. Trends Biochem Sci, 2003. 28(9): p. 479-87.

38. Okada, T., et al., *Activation of rhodopsin: new insights from structural and biochemical studies*. Trends Biochem Sci, 2001. 26(5): p. 318-24.
39. Filipek, S., et al., *The crystallographic model of rhodopsin and its use in studies of other G protein-coupled receptors*. Annu Rev Biophys Biomol Struct, 2003. 32: p. 375-97.
40. Filipek, S., et al., *G protein-coupled receptor rhodopsin: a prospectus*. Annu Rev Physiol, 2003. 65: p. 851-79.
41. Ballesteros, J.A., L. Shi, and J.A. Javitch, *Structural mimicry in G protein-coupled receptors: implications of the high-resolution structure of rhodopsin for structure-function analysis of rhodopsin-like receptors*. Mol Pharmacol, 2001. 60(1): p. 1-19.
42. Nikiforovich, G.V., et al., *Novel approach to computer modeling of seven-helical transmembrane proteins: current progress in the test case of bacteriorhodopsin*. Acta Biochim Pol, 2001. 48(1): p. 53-64.
43. Vaidehi, N., et al., *Prediction of structure and function of G protein-coupled receptors*. Proc Natl Acad Sci U S A, 2002. 99(20): p. 12622-7.
44. Kobilka, B., *Adrenergic receptors as models for G protein-coupled receptors*. Annu Rev Neurosci, 1992. 15: p. 87-114.
45. Strader, C.D., et al., *The family of G-protein-coupled receptors*. Faseb J, 1995. 9(9): p. 745-54.
46. Ji, T.H., M. Grossmann, and I. Ji, *G protein-coupled receptors. I. Diversity of receptor-ligand interactions*. J Biol Chem, 1998. 273(28): p. 17299-302.

47. Bondensgaard, K., et al., *Recognition of privileged structures by G-protein coupled receptors*. J Med Chem, 2004. 47(4): p. 888-99.
48. Hunyady, L., G. Vauquelin, and P. Vanderheyden, *Agonist induction and conformational selection during activation of a G-protein-coupled receptor*. Trends Pharmacol Sci, 2003. 24(2): p. 81-6.
49. Rihakova, L., et al., *Methionine proximity assay, a novel method for exploring peptide ligand-receptor interaction*. J Recept Signal Transduct Res, 2002. 22(1-4): p. 297-313.
50. Chorev, M., *Parathyroid hormone 1 receptor: insights into structure and function*. Receptors Channels, 2002. 8(3-4): p. 219-42.
51. Tsomaia, N., et al., *Cooperative interaction of arginine-19 and the N-terminal signaling domain in the affinity and potency of parathyroid hormone*. Biochemistry, 2004. 43(12): p. 3459-70.
52. Dong, M., et al., *Spatial approximation between the amino terminus of a peptide agonist and the top of the sixth transmembrane segment of the secretin receptor*. J Biol Chem, 2004. 279(4): p. 2894-903.
53. Bellucci, F., et al., *A different molecular interaction of bradykinin and the synthetic agonist FR190997 with the human B2 receptor: evidence from mutational analysis*. Br J Pharmacol, 2003. 140(3): p. 500-6.
54. Schroeder, C., et al., *Changes in amino-terminal portion of human B2 receptor selectively increase efficacy of synthetic ligand HOE 140 but not of cognate ligand bradykinin*. Am J Physiol Heart Circ Physiol, 2003. 284(6): p. H1924-32.

55. Millar, R.P., et al., *Gonadotropin-releasing hormone receptors*. *Endocr Rev*, 2004. 25(2): p. 235-75.
56. Janecka, A., J. Fichna, and T. Janecki, *Opioid receptors and their ligands*. *Curr Top Med Chem*, 2004. 4(1): p. 1-17.
57. Judd, A.K., et al., *N-terminal modifications leading to peptide ORL1 partial agonists and antagonists*. *J Pept Res*, 2003. 62(5): p. 191-8.
58. Sachon, E., et al., *Met174 side chain is the site of photoinsertion of a substance P competitive peptide antagonist photoreactive in position 8*. *FEBS Lett*, 2003. 544(1-3): p. 45-9.
59. Ulfers, A.L., A. Piserchio, and D.F. Mierke, *Extracellular domains of the neurokinin-1 receptor: structural characterization and interactions with substance P*. *Biopolymers*, 2002. 66(5): p. 339-49.
60. Breton, C., et al., *Direct identification of human oxytocin receptor-binding domains using a photoactivatable cyclic peptide antagonist: comparison with the human V1a vasopressin receptor*. *J Biol Chem*, 2001. 276(29): p. 26931-41.
61. Wesley, V.J., et al., *Agonist-specific, high-affinity binding epitopes are contributed by an arginine in the N-terminus of the human oxytocin receptor*. *Biochemistry*, 2002. 41(16): p. 5086-92.
62. Politowska, E., et al., *Docking ligands to vasopressin and oxytocin receptors via genetic algorithm*. *J Recept Signal Transduct Res*, 2002. 22(1-4): p. 393-409.
63. Smith, C.J., et al., *Radiochemical investigations of [188Re(H₂O)(CO)₃-diaminopropionic acid-SSS-bombesin(7-14)NH₂]: syntheses, radiolabeling and in*

- vitro/in vivo GRP receptor targeting studies*. *Anticancer Res*, 2003. 23(1A): p. 63-70.
64. Silvente-Poirot, S., C. Escriuet, and S.A. Wank, *Role of the extracellular domains of the cholecystinin receptor in agonist binding*. *Mol Pharmacol*, 1998. 54(2): p. 364-71.
65. Barroso, S., et al., *Identification of residues involved in neurotensin binding and modeling of the agonist binding site in neurotensin receptor I*. *J Biol Chem*, 2000. 275(1): p. 328-36.
66. Mills, J.S., et al., *Identification of a ligand binding site in the human neutrophil formyl peptide receptor using a site-specific fluorescent photoaffinity label and mass spectrometry*. *J Biol Chem*, 1998. 273(17): p. 10428-35.
67. Fathy, D.B., et al., *A single position in the third transmembrane domains of the human B1 and B2 bradykinin receptors is adjacent to and discriminates between the C-terminal residues of subtype-selective ligands*. *J Biol Chem*, 1998. 273(20): p. 12210-8.
68. Fanelli, F., et al., *Activation mechanism of human oxytocin receptor: a combined study of experimental and computer-simulated mutagenesis*. *Mol Pharmacol*, 1999. 56(1): p. 214-25.
69. Flanagan, C.A., et al., *Multiple interactions of the Asp(2.61(98)) side chain of the gonadotropin-releasing hormone receptor contribute differentially to ligand interaction*. *Biochemistry*, 2000. 39(28): p. 8133-41.
70. Dorman, G. and G.D. Prestwich, *Benzophenone photophores in biochemistry*. *Biochemistry*, 1994. 33(19): p. 5661-73.

71. Galardy, R.E., L.C. Craig, and M.P. Printz, *Benzophenone triplet: a new photochemical probe of biological ligand-receptor interactions*. *Nat New Biol*, 1973. 242(117): p. 127-8.
72. Kauer, J.C., et al., *p-Benzoyl-L-phenylalanine, a new photoreactive amino acid. Photolabeling of calmodulin with a synthetic calmodulin-binding peptide*. *J Biol Chem*, 1986. 261(23): p. 10695-700.
73. Farrens, D.L., et al., *Requirement of rigid-body motion of transmembrane helices for light activation of rhodopsin*. *Science*, 1996. 274(5288): p. 768-70.
74. Ghanouni, P., et al., *Agonist-induced conformational changes in the G-protein-coupling domain of the beta 2 adrenergic receptor*. *Proc Natl Acad Sci U S A*, 2001. 98(11): p. 5997-6002.
75. Jensen, A.D., et al., *Agonist-induced conformational changes at the cytoplasmic side of transmembrane segment 6 in the beta 2 adrenergic receptor mapped by site-selective fluorescent labeling*. *J Biol Chem*, 2001. 276(12): p. 9279-90.
76. Sheikh, S.P., et al., *Similar structures and shared switch mechanisms of the beta2-adrenoceptor and the parathyroid hormone receptor. Zn(II) bridges between helices III and VI block activation*. *J Biol Chem*, 1999. 274(24): p. 17033-41.
77. Javitch, J.A., et al., *Constitutive activation of the beta2 adrenergic receptor alters the orientation of its sixth membrane-spanning segment*. *J Biol Chem*, 1997. 272(30): p. 18546-9.
78. Rasmussen, S.G., et al., *Mutation of a highly conserved aspartic acid in the beta2 adrenergic receptor: constitutive activation, structural instability, and*

- conformational rearrangement of transmembrane segment 6*. Mol Pharmacol, 1999. 56(1): p. 175-84.
79. Leff, P., *The two-state model of receptor activation*. Trends Pharmacol Sci, 1995. 16(3): p. 89-97.
80. Chidiac, P., et al., *Inverse agonist activity of beta-adrenergic antagonists*. Mol Pharmacol, 1994. 45(3): p. 490-9.
81. Labrecque, J., et al., *Serotonergic antagonists differentially inhibit spontaneous activity and decrease ligand binding capacity of the rat 5-hydroxytryptamine type 2C receptor in Sf9 cells*. Mol Pharmacol, 1995. 48(1): p. 150-9.
82. Pineyro, G., et al., *Short-term inverse-agonist treatment induces reciprocal changes in delta-opioid agonist and inverse-agonist binding capacity*. Mol Pharmacol, 2001. 60(4): p. 816-27.
83. Azzi, M., et al., *Beta-arrestin-mediated activation of MAPK by inverse agonists reveals distinct active conformations for G protein-coupled receptors*. Proc Natl Acad Sci U S A, 2003. 100(20): p. 11406-11.
84. Bond, R.A.a.B., M., *Inverse Agonists and G protein-coupled Receptors. Receptor-Based drug design.*, P. Leff, Editor. 1998, Marcel Dekker Inc: New-York. p. chap:16, pp:363-377.
85. Bond, R., Milligan, G. and Bouvier, M, *Inverse agonism*, in *Handbook of Experimental Pharmacology. The pharmacology of functional, biochemical, and recombinant receptor system.*, T.K.a.J.A. Angus., Editor. 2001, Springer-Verlag publisher. p. 167-182.

86. Kobilka, B., *Agonist binding: a multistep process*. Mol Pharmacol, 2004. 65(5): p. 1060-2.
87. Wiens, B.L., C.S. Nelson, and K.A. Neve, *Contribution of serine residues to constitutive and agonist-induced signaling via the D2S dopamine receptor: evidence for multiple, agonist-specific active conformations*. Mol Pharmacol, 1998. 54(2): p. 435-44.
88. Mhaouty-Kodja, S., et al., *Constitutively active alpha-1b adrenergic receptor mutants display different phosphorylation and internalization features*. Mol Pharmacol, 1999. 55(2): p. 339-47.
89. Kobilka, B., et al., *Characterization of ligand-induced conformational states in the beta 2 adrenergic receptor*. J Recept Signal Transduct Res, 1999. 19(1-4): p. 293-300.
90. Gether, U. and B.K. Kobilka, *G protein-coupled receptors. II. Mechanism of agonist activation*. J Biol Chem, 1998. 273(29): p. 17979-82.
91. Jarnagin, K., et al., *Mutations in the B2 bradykinin receptor reveal a different pattern of contacts for peptidic agonists and peptidic antagonists*. J Biol Chem, 1996. 271(45): p. 28277-86.
92. Turner, P.R., et al., *Transmembrane residues together with the amino terminus limit the response of the parathyroid hormone (PTH) 2 receptor to PTH-related peptide*. J Biol Chem, 1998. 273(7): p. 3830-7.
93. Bourne, H.R., *How receptors talk to trimeric G proteins*. Curr Opin Cell Biol, 1997. 9(2): p. 134-42.

94. Swaminath, G., et al., *Sequential binding of agonists to the beta2 adrenoceptor. Kinetic evidence for intermediate conformational states.* J Biol Chem, 2004. 279(1): p. 686-91.
95. Keith, D.E., et al., *Morphine activates opioid receptors without causing their rapid internalization.* J Biol Chem, 1996. 271(32): p. 19021-4.
96. Palanche, T., et al., *The neurokinin A receptor activates calcium and cAMP responses through distinct conformational states.* J Biol Chem, 2001. 276(37): p. 34853-61.
97. Lorenz, M.C., N.S. Cutler, and J. Heitman, *Characterization of alcohol-induced filamentous growth in Saccharomyces cerevisiae.* Mol Biol Cell, 2000. 11(1): p. 183-99.
98. Lorenz, M.C., et al., *The G protein-coupled receptor gpr1 is a nutrient sensor that regulates pseudohyphal differentiation in Saccharomyces cerevisiae.* Genetics, 2000. 154(2): p. 609-22.
99. Sprague, G.F., Jr., R. Jensen, and I. Herskowitz, *Control of yeast cell type by the mating type locus: positive regulation of the alpha-specific STE3 gene by the MAT alpha 1 product.* Cell, 1983. 32(2): p. 409-15.
100. Thorner J., *Pheromonal regulation of development in Saccharomyces cerevisiae,* in *Molecular biology of the yeast Saccharomyces: Life cycle and inheritance*, S. J.N., Editor. 1981, Cold Spring Harbor.
101. Herskowitz, I., *MAP kinase pathways in yeast: for mating and more.* Cell, 1995. 80(2): p. 187-97.

102. Banuett, F., *Signalling in the yeasts: an informational cascade with links to the filamentous fungi*. Microbiol Mol Biol Rev, 1998. 62(2): p. 249-74.
103. Madden, K. and M. Snyder, *Cell polarity and morphogenesis in budding yeast*. Annu Rev Microbiol, 1998. 52: p. 687-744.
104. Eriotou-Bargiota, E., et al., *Antagonistic and synergistic peptide analogues of the tridecapeptide mating pheromone of Saccharomyces cerevisiae*. Biochemistry, 1992. 31(2): p. 551-7.
105. Xue, C.B., et al., *Probing the functional conformation of the tridecapeptide mating pheromone of Saccharomyces cerevisiae through study of disulfide-constrained analogs*. Int J Pept Protein Res, 1996. 47(3): p. 131-41.
106. Yang, W., et al., *Systematic analysis of the Saccharomyces cerevisiae alpha-factor containing lactam constraints of different ring size*. Biochemistry, 1995. 34(4): p. 1308-15.
107. Abel, M.G., et al., *Structure-function analysis of the Saccharomyces cerevisiae tridecapeptide pheromone using alanine-scanned analogs*. J Pept Res, 1998. 52(2): p. 95-106.
108. Liu, S., et al., *Position 13 analogs of the tridecapeptide mating pheromone from Saccharomyces cerevisiae: design of an iodinated ligand for receptor binding*. J Pept Res, 2000. 56(1): p. 24-34.
109. Xue, C.B., et al., *A covalently constrained congener of the Saccharomyces cerevisiae tridecapeptide mating pheromone is an agonist*. J Biol Chem, 1989. 264(32): p. 19161-8.

110. Antohi, O., et al., *Conformational analysis of cyclic analogues of the Saccharomyces cerevisiae alpha-factor pheromone*. Biopolymers, 1998. 45(1): p. 21-34.
111. Zhang, Y.L., et al., *Synthesis, biological activity, and conformational analysis of peptidomimetic analogues of the Saccharomyces cerevisiae alpha-factor tridecapeptide*. Biochemistry, 1998. 37(36): p. 12465-76.
112. Carpenter, K.A., B.C. Wilkes, and P.W. Schiller, *The octapeptide angiotensin II adopts a well-defined structure in a phospholipid environment*. Eur J Biochem, 1998. 251(1-2): p. 448-53.
113. Greenberg, Z., et al., *Mapping the bimolecular interface of the parathyroid hormone (PTH)-PTH1 receptor complex: spatial proximity between Lys(27) (of the hormone principal binding domain) and leu(261) (of the first extracellular loop) of the human PTH1 receptor*. Biochemistry, 2000. 39(28): p. 8142-52.
114. Chauvin, S., et al., *Functional importance of transmembrane helix 6 Trp(279) and exoloop 3 Val(299) of rat gonadotropin-releasing hormone receptor*. Mol Pharmacol, 2000. 57(3): p. 625-33.
115. de Gasparo, M., et al., *International union of pharmacology. XXIII. The angiotensin II receptors*. Pharmacol Rev, 2000. 52(3): p. 415-72.
116. Venkatachalam, C.M., *Stereochemical criteria for polypeptides and proteins. V. Conformation of a system of three linked peptide units*. Biopolymers, 1968. 6(10): p. 1425-36.
117. Chou, P.Y. and G.D. Fasman, *Prediction of beta-turns*. Biophys J, 1979. 26(3): p. 367-73.

118. Shenbagamurthi, P., et al., *Biological activity and conformational isomerism in position 9 analogues of the des-1-tryptophan,3-beta-cyclohexylalanine-alpha-factor from Saccharomyces cerevisiae*. *Biochemistry*, 1985. 24(25): p. 7070-6.
119. Sen, M., A. Shah, and L. Marsh, *Two types of alpha-factor receptor determinants for pheromone specificity in the mating-incompatible yeasts S. cerevisiae and S. kluyveri*. *Curr Genet*, 1997. 31(3): p. 235-40.
120. Sen, M. and L. Marsh, *Novel antagonist to agonist switch in chimeric G protein-coupled alpha-factor peptide receptors*. *Biochem Biophys Res Commun*, 1995. 207(2): p. 559-64.
121. Chen, Q. and J.B. Konopka, *Regulation of the G-protein-coupled alpha-factor pheromone receptor by phosphorylation*. *Mol Cell Biol*, 1996. 16(1): p. 247-57.
122. Hicke, L. and H. Riezman, *Ubiquitination of a yeast plasma membrane receptor signals its ligand-stimulated endocytosis*. *Cell*, 1996. 84(2): p. 277-87.
123. Stefan, C.J. and K.J. Blumer, *A syntaxin homolog encoded by VAM3 mediates down-regulation of a yeast G protein-coupled receptor*. *J Biol Chem*, 1999. 274(3): p. 1835-41.
124. Mulholland, J., et al., *Visualization of receptor-mediated endocytosis in yeast*. *Mol Biol Cell*, 1999. 10(3): p. 799-817.
125. Noble, B., et al., *Development of a yeast bioassay to characterize G protein-coupled receptor kinases. Identification of an NH2-terminal region essential for receptor phosphorylation*. *J Biol Chem*, 2003. 278(48): p. 47466-76.

126. Kallal, L. and J.L. Benovic, *Using green fluorescent proteins to study G-protein-coupled receptor localization and trafficking*. Trends Pharmacol Sci, 2000. 21(5): p. 175-80.
127. Dohlman, H.G. and J. Thorner, *RGS proteins and signaling by heterotrimeric G proteins*. J Biol Chem, 1997. 272(7): p. 3871-4.
128. Dohlman, H.G., *G proteins and pheromone signaling*. Annu Rev Physiol, 2002. 64: p. 129-52.
129. Ballensiefen, W. and H.D. Schmitt, *Periplasmic Bar1 protease of Saccharomyces cerevisiae is active before reaching its extracellular destination*. Eur J Biochem, 1997. 247(1): p. 142-7.
130. Wedegaertner, P.B., *Lipid modifications and membrane targeting of G alpha*. Biol Signals Recept, 1998. 7(2): p. 125-35.
131. Dohlman, H.G., et al., *Pheromone action regulates G-protein alpha-subunit myristoylation in the yeast Saccharomyces cerevisiae*. Proc Natl Acad Sci U S A, 1993. 90(20): p. 9688-92.
132. Casey, P.J., *Protein lipidation in cell signaling*. Science, 1995. 268(5208): p. 221-5.
133. Madura, K. and A. Varshavsky, *Degradation of G alpha by the N-end rule pathway*. Science, 1994. 265(5177): p. 1454-8.
134. Fu, H.W. and P.J. Casey, *Enzymology and biology of CaaX protein prenylation*. Recent Prog Horm Res, 1999. 54: p. 315-42; discussion 342-3.
135. Finegold, A.A., et al., *Common modifications of trimeric G proteins and ras protein: involvement of polyisoprenylation*. Science, 1990. 249(4965): p. 165-9.

136. Hirschman, J.E. and D.D. Jenness, *Dual lipid modification of the yeast ggamma subunit Ste18p determines membrane localization of Gbetagamma*. Mol Cell Biol, 1999. 19(11): p. 7705-11.
137. Cole, G.M. and S.I. Reed, *Pheromone-induced phosphorylation of a G protein beta subunit in S. cerevisiae is associated with an adaptive response to mating pheromone*. Cell, 1991. 64(4): p. 703-16.

PART II

Identification of a Contact Region between the Tridecapeptide α -Factor

Mating Pheromone of *Saccharomyces cerevisiae* and its G Protein-

Coupled Receptor by Photoaffinity Labeling[§]

§Part II was published in its entirety as L. Keith Henry, Sanjay Khare, Cagdas Son, V. V. Suresh Babu, Fred Naider, and Jeffrey M. Becker (2002) *Biochemistry*, 41 (19), pp. 6128-6139. Dr. Naider's laboratory was responsible for synthesis and purification of the peptides used in the study. Dr. Keith Henry was responsible for the characterization of the analogs and carried out the iodination and cross-linking studies. Cagdas D. Son was involved in the characterization of the analogs and carried out iodination, cross-linking studies, and T7 epitope tagged experiments.

CHAPTER 1

Introduction

G protein-coupled receptors (GPCRs) comprise one of the largest super-families of proteins with over 1000 members represented in the human genome alone [1, 2]. One of the key steps in understanding the mechanisms of action of these diverse GPCRs is to elucidate the structure of their ligand binding sites. With this information in hand, the mechanism of activation of the GPCR can begin to be understood.

While there has been considerable data published on the GPCR ligand binding sites for biogenic amines (see [3] for a review), much less information exists concerning the binding sites of peptide-responsive GPCRs. Recently, several reports have addressed this issue with the use of 4-benzoyl-*L*-phenylalanine (Bpa) photoreactive chemical groups [4-10]. Incorporation of Bpa into the first position of parathyroid hormone (PTH) and its use as a cross-linkable probe resulted in evidence that the N-terminal residue of PTH interacts with the extracellular end of transmembrane helix 6 of its receptor PTH1-Rc [11]. A recent study by Mouldous *et al.* [8] investigating the interaction between the heptadecapeptide nociceptin and the opioid receptor-like (ORL1) GPCR made use of [Bpa¹⁰, Tyr¹⁴]nociceptin and found that the photoactivatable Bpa moiety cross-linked to a six amino acid fragment (amino acids 296-302). These studies and others using Bpa-containing peptides have allowed for the identification of interacting receptor fragments and in some cases even specific contact residues [5-7, 9]. Identification of these cross-linked receptor fragments is a first but critical step in the elucidation of direct residue to

residue contacts between ligand and receptor and has the potential to provide significant insight into the mechanism of activation of GPCRs by peptide ligands.

GPCRs can bind a variety of molecules including biogenic amines, peptides, and sugars. The unicellular yeast *Saccharomyces cerevisiae* contains two GPCRs used by haploid cells in the detection and response to peptide pheromones secreted by cells of the opposite mating type during sexual reproduction (see [12, 13] for reviews). One of these receptors, Ste2p, responds to the α -factor peptide pheromone (WHWLQLKPGQPMY) while the other receptor, Ste3p, responds to the post-translationally modified **a**-factor peptide (YIIKGVFWDPA[C[S-farnesyl]-OCH₃).

The study of the pheromone receptors in *S. cerevisiae* has led to many critical findings concerning the biology of GPCRs, such as the discovery of the Regulator of G-protein Signaling (RGS) family of proteins [14, 15]. Additionally, Ste2p serves as a model protein for the study of GPCRs, as (i) its transmembrane domains (TMDs) appear to be arranged similarly to those of other GPCRs, (ii) interactions between the fifth and sixth transmembrane domains appear to be critical for proper signal transduction to the G protein, and (iii) close packing of the fifth and sixth TMDs appears to be structurally similar to that of rhodopsin [16]. All of these factors suggest that while most GPCRs do not share sequence homology, they do have strong structural and functional similarities. Therefore, elucidation of contact residues between receptor and ligand should provide insight into structure-function relationships in binding and activation of peptide-responsive GPCRs.

Part II of this dissertation describes the synthesis, the chemical, and biochemical characterization of iodinated Bpa-containing α -factor analogs. One of the analogs,

[Bpa¹, (¹²⁵I)Tyr³, Arg⁷, Phe¹³] α -factor, was specifically cross-linked into the α -factor binding pocket of Ste2p and used to determine direct contacts between the pheromone and the receptor. Biochemical analysis localized the cross-link site within residues 251-294 of the Ste2p receptor.

CHAPTER 2

Materials and Methods

Organisms:

S. cerevisiae DK102 [*MATa ste2::HIS3 bar1 leu2 ura3 lys2 ade2 his3 trp1*] transformed with pNED1[*STE2*] [17] was used in binding studies and in the growth arrest assays of various α -factor analogs. Strain LM23-3AZ [*MATa FUS1::lacZ bar1-1*] from Lorraine Marsh, Albert Einstein College of Medicine, New York, NY, was used in *FUS1-lacZ* gene induction assays. Strain BJ2168 [*MATa prc1-407 prb1-1122 pep4-3 leu2 trp1 ura3-52*] transformed with pNED1[*STE2*] [17] and BJS21 [*MATa ste2::kan^R prc1-407 prb1-1122 pep4-3 leu2 trp1 ura3-52*] transformed with pJL147 [*STE2-T7*] were used in cross-linking assays. Strain BJS21 was constructed by deleting *STE2* from strain BJ2168 using the kanamycin deletion cassette. pJL147 (a gift from J. Konopka, [16]) encoded Ste2p containing the T7 epitope (Met-Ala-Ser-Met-Thr-Gly-Gly-Gln-Gln-Met-Gly) introduced between Ste2p residues 303 and 304. All strains used had similar binding of α -factor. However, the BJ2168pNED and BJS21 strains lacked several peptidases, so they were used to increase the yield of Ste2p in experiments involving cross-linking.

Chemical Reagents:

All reagents and solvents used for the solid-phase peptide synthesis of the photoactivatable peptides were analytical grade and were purchased from Advanced Chem Tech (Louisville, KY), VWR Scientific (Piscataway, NJ), or Aldrich Chemical Co.

(Milwaukee, WI). High-performance liquid chromatography (HPLC) grade dichloromethane (CH₂Cl₂), acetonitrile (ACN), methanol (MeOH), and water were purchased from VWR Scientific and Fisher Scientific (Springfield, NJ).

Synthesis of Bpa-Containing [Nle¹²]α-Factor Analogs:

Automated syntheses were carried out on an Applied Biosystem 433A peptide synthesizer (Applied Biosystem, Foster City, CA) using preloaded Wang resins (0.70 mmol/g, Advanced ChemTech) for most of the peptides. Two series of peptides were synthesized. In the first series, 4-benzoyl-*L*-phenylalanine (Bpa) was systematically used to replace the wild-type residue in all positions of the tridecapeptide except for Gly⁹. The latter residue was not replaced because previous studies had concluded that substitution of Gly⁹ by an *L*-residue results in a marked decrease in activity and affinity [18, 19]. In the second series of peptides, Tyr¹³ was replaced by Phe, Bpa was substituted at either position 1, 3, or 5, and a Tyr residue was substituted at either position 1 or 3. The goal of the second series of analogs was to prepare a photo-cross-linkable peptide which could also be followed by autoradiography. In most peptides, *L*-norleucine (Nle), which is isosteric with *L*-methionine, was incorporated at position 12 to replace the naturally occurring *L*-methionine to prevent oxidation of the sulfur atom of this amino acid during peptide synthesis and purification. Replacement of Met by Nle was shown previously to result in an analogue with equal activity and receptor affinity to those of the native pheromone [20]. Since all analogs have Nle in place of Met¹², this residue is eliminated from the abbreviated names for simplicity. The 0.1 mmol FastMoc chemistry of Applied

Biosystems was used for the elongation of the peptide chain with an HBTU/HOBt/DIEA-catalyzed, single coupling step using 10 equiv of protected amino acids for 30 min.

Cleavage of Peptide:

The N- α -deprotected peptidyl resin was washed thoroughly with 1-methyl-2-pyrrolidinone and dichloromethane and dried in vacuum for 2 h. The peptide was cleaved from the resin support with simultaneous side chain deprotection using a cleavage cocktail containing trifluoroacetic acid (10 mL), crystalline phenol (0.75 g), thioanisole (0.5 mL), and water (0.5 mL) at room temperature for 1.5 h with the omission of 1,2-ethanedithiol in the cleavage reaction, because it was known to transform Bpa-containing peptides to cyclic dithioketal derivatives [21]. The filtrates from the cleavage reaction were collected, combined with trifluoroacetic acid washes of the resin, concentrated under reduced pressure, and treated with cold ether to precipitate the crude product.

Purification and Characterization:

The crude peptide so obtained was purified by reversed phase HPLC (Hewlett-Packard Series 1050) on a semipreparative Waters μ -Bondapak C₁₈ (19 \times 300 mm) column with detection at 220 nm. The crude product (50 mg) was dissolved in about 4 mL of aqueous acetonitrile (20%) containing 0.025% TFA, applied to the column, and eluted with a linear gradient of water/acetonitrile containing 0.025% TFA (0-70% acetonitrile over 2 h at a flow rate of 5 mL/min). The fractions were collected and analyzed at 220 nm by reversed phase HPLC (Hewlett-Packard Series 1050) on an analytical Waters μ -Bondapak C₁₈ (3.9 \times 300 mm) column. Fractions of over 99%

homogeneity were pooled and subjected to lyophilization. The purity of the final peptide was assessed by analytical HPLC using two different solvent systems (10-55% acetonitrile gradient, 15 min, with 0.025% trifluoroacetic acid; and 50-80% methanol gradient, 30 min, with 0.025% trifluoroacetic acid), amino acid analysis (Biopolymer lab, Brigham and Women's Hospital, Cambridge, MA), and electrospray ionization mass spectrometry (ESI-MS Peptido Genic Inc., Livermore, CA).

Growth Arrest (Halo) Assay:

Solid MLT medium [yeast nitrogen base without amino acids (Difco), 6.7 g/L; casamino acids (Difco), 10 g/L; glucose, 20 g/L; adenine sulfate, 0.058 g/L; arginine, 0.026 g/L; asparagine, 0.058 g/L; aspartic acid, 0.14 g/L; glutamic acid, 0.14 g/L; histidine, 0.028 g/L; isoleucine, 0.058 g/L; leucine, 0.083 g/L; lysine, 0.042 g/L; methionine, 0.028 g/L; phenylalanine, 0.69 g/L; serine, 0.52 g/L; threonine, 0.28 g/L; tyrosine, 0.042 g/L; valine, 0.21 g/L; and uracil, 0.028 g/L] [11] was overlaid with 4 mL of *S. cerevisiae* DK102pNED cell suspension (2.5×10^5 cells/mL of Nobel agar). Filter disks (sterile blanks from Difco), 8 mm in diameter, were impregnated with 10 μ L portions of peptide solutions at various concentrations and placed onto the overlay. The plates were incubated at 30 °C for 24-36 h and then observed for clear zones (halos) around the disks. The data were expressed as the diameter of the halo including the diameter of the disk. A minimum value for growth arrest is 9 mm, which represents the disk diameter (8 mm) and a small zone of inhibition. All assays were carried out at least 3 times with no more than a 2 mm variation in halo size at a particular amount applied for each peptide. The values reported represent the mean of these tests.

Effect of α -Factor Analogs on Gene Induction:

S. cerevisiae LM23-3AZ carries a *FUS1* gene that is inducible by mating pheromone and which is fused to the reporter gene β -galactosidase. Cells were grown overnight in MLT at 30 °C to 5×10^6 cells/mL, washed by centrifugation, and grown for one doubling at 30 °C. Induction was performed by adding 15 μ L of peptide at various concentrations to 135 μ L of concentrated cells (2×10^8 cells/mL) in a 96 well microtiter plate. The mixtures were placed at 30 °C with shaking for 2 h. After this time, cells were harvested by centrifugation, and each pellet was resuspended in Z-Buffer containing β -mercaptoethanol [22] and assayed for β -galactosidase production (expressed as Miller units) in triplicate. Each experiment was carried out at least 3 times with the results similar in each assay. As cells were suspended in liquid medium, any contribution of diffusion through agar potentially present in the halo assay was eliminated in the gene induction assay.

Binding Competition Assay with [3 H] α -Factor:

This assay was performed using strain DK102pNED and tritiated α -factor prepared by reduction of [dehydroproline⁸, Nle¹²] α -factor as described previously [20]. In general, cells were grown at 30 °C overnight and harvested at 1×10^7 cells/mL by centrifugation at 5000g at 4 °C. The pelleted cells were washed 2 times in ice-cold buffer [PPBi: 0.5 M potassium phosphate (pH 6.24) containing 10 mM TAME, 10 mM sodium azide, 10 mM potassium fluoride, 1% BSA (fraction IV)] and resuspended to 4×10^7 cells/mL. The binding assay was started by addition of [3 H] α -factor and various

concentrations of nonlabeled peptide (140 μL) to a 560 μL cell suspension so that the final concentration of radioactive peptide was 6×10^{-9} M (20 Ci/mmol). Analogue concentrations were adjusted using UV absorption at 280 nm and the corresponding extinction coefficients. After 30 min incubation, triplicate samples of 200 μL were filtered and washed over glass fiber filtermats using the Standard Cell Harvester (Skatron Instruments, Sterling, VA) and placed in scintillation vials for counting. Each experiment was carried out at least 3 times with the results similar in each assay. Binding of labeled α -factor to filters in the absence of cells was less than 20 cpm. The K_i values were calculated by using the equation of Cheng and Prusoff, where $K_i = EC_{50}/(1 + [\text{ligand}]/K_d)$ [23].

Synthesis of Iodinated α -Factor Peptides:

Peptides were iodinated with Iodogen tubes from Pierce, Inc., using conditions recommended by the manufacturer. Briefly, Iodogen tubes were pre-wet with 2 \times Tris Iodination Buffer (TIB: 50 mM Tris, pH 7.5, 0.8 M NaCl). The TIB was decanted, 100 μL of fresh TIB was added directly to the bottom of the Iodogen tube, and either 10 μL of Na^{127}I (1.86 mg/mL) or 10 μL of Na^{125}I (100 $\mu\text{Ci}/\mu\text{L}$, pH 10, ICN) was added and incubated for 15 min with gentle swirling every 30 s. Activated iodide was transferred to a siliconized microfuge tube containing 100 μL of the peptide (0.5 mmol/L in TIB) and incubated for 20 min with gentle mixing every 30 sec. Scavenging buffer (50 μL at 10 mg/mL tyrosine in TIB) was added and incubated for 5 min with mixing at minutes 1 and 4. Following incubation, 1 mL of TIB containing 5 mM EDTA was added. The remaining unreacted iodine was separated from peptide using a Waters Sep-Pak C_{18}

minicolumn. The eluted products were separated by HPLC using water/acetonitrile/0.025% TFA with an acetonitrile percentage of 20-35% over 30 min at 1.4 mL/min on a Waters μ Bondapak C₁₈ reversed phase analytical column (3.9 × 300 mm). ¹²⁷I-labeled peptides were quantitated by UV spectrophotometry using their extinction coefficients. Radioiodinated peptides were labeled using carrier-free Na¹²⁵I, and the resulting monoiodinated peptides were quantitated by converting total dpm associated with the HPLC-purified peptide to millimoles of peptide using the specific activity of carrier-free Na¹²⁵I (2159 Ci/mmol).

Synthesis of [Bpa¹, Lys⁷(ϵ -biotinyl- β -alanyl)] α -Factor:

This analogue was synthesized by first adding Boc- β -alanine hydroxysuccinimide ester and then hydroxysuccinimido biotin ester to [α -Fmoc-Bpa¹] α -factor that had been prepared by solid-phase peptide synthesis. After removal of all protecting groups, the final peptide was purified to near-homogeneity by reversed phase HPLC. Its molecular weight was determined by electron spray mass spectrometry to be 2028.0 (theoretical = 2028.35). This compound was a full agonist in the growth arrest assay and exhibited a binding affinity close to that of α -factor.

Binding Assays with ¹²⁵I-Labeled α -Factor:

DK102 pNED1 cells (grown in MLT medium) [17] and DK102 cells (grown in MLT medium supplemented with tryptophan) were harvested at 1×10^7 cells/mL by centrifugation and resuspended to 6.25×10^7 cells/mL in PPBi buffer (pH 6.24) and

placed at 4 °C. In competition binding assays, [Bpa¹, (¹²⁵I)Tyr³, Arg⁷, Phe¹³]α-factor (2.4 × 10⁻⁹ M final concentration) was premixed with various concentrations of cold competitor. In saturation binding assays, radiolabeled α-factor analogs were diluted with cold analogue to obtain the peptide concentrations used in the assay. Cells in PPBi were then added to peptide solutions to a final density of 6.25 × 10⁶ cells/mL and incubated for 45 min at room temperature. Following incubation, the suspension was transferred (3 × 200 μL) to wells of a 0.45 μm MultiScreen-HV, 96 well plate (Millipore MHVBN4510) preblocked with PPBi. Samples were vacuum-filtered, washed with PPBi (2 × 200 μL), and counted on an LKB-Wallac CliniGamma 1272 gamma counter. Using this methodology, nonspecific binding of radiolabeled peptide to the filter was at background levels. Specific binding was determined by subtracting counts associated with the DK102 (*ste2*) strain from counts bound to the DK102pNED1 (*STE2*) strain.

Cross-Linking of [Bpa¹, (¹²⁵I)Tyr³, Arg⁷, Phe¹³]α-Factor to Ste2p:

BJ2168pNED1 membranes (220 μg of protein) [17] were incubated with 975 μL of PPBi buffer (with 0.1%BSA) in siliconized microfuge tubes for 10 min at ambient temperature. [Bpa¹, (¹²⁵I)Tyr³, Arg⁷, Phe¹³]α-factor (10 and 20 million cpm) was added, and the reaction was incubated for 2 h at room temperature with gentle mixing. The reaction mixture was aliquoted into 3 wells of a chilled 24 well plastic culture plate preblocked with PPBi (0.1% BSA). Separation of the reaction mixtures into separate wells kept the depth of the samples minimal (~2 mm) for efficient UV penetration of the sample. The samples were held at 4 °C and irradiated without the culture plate lid at 365

nm for 1 h at a distance of 12 cm in a Stratlinker (Stratagene, La Jolla, CA). Membrane samples were recombined in siliconized microfuge tubes and washed twice by centrifugation (14000g) with PPBi (0.1% BSA). Membrane pellets were dissolved in 2 × sample buffer (0.25 M Tris-HCl, pH 8.8, 0.005% bromphenol blue, 5% glycerol, 1.25% β-mercaptoethanol, 2% SDS). Samples were heated to 37 °C for 10 min and separated by SDS-PAGE (10% gel; 30 mA). In competition cross-linking experiments, cold α-factor was added together with radioiodinated peptide. For subsequent receptor digestion analysis, the gel was exposed to a phosphorimager screen (STORM, Molecular Dynamics), and the band of radioactivity corresponding to Ste2p was excised and placed into dialysis tubing (15 000 molecular weight cutoff) with buffer (0.2 M Tris-acetate, pH 7.4, 1.0% SDS, 100 mM dithiothreitol). Electroelution was performed by placing dialysis tubing containing the gel in a horizontal electrophoresis chamber with running buffer (50 mM Tris-acetate, pH 7.4, 0.1% SDS, 0.5 mM sodium thioglycolate). Elution was carried out at 100 V for 3 h. The buffer in the dialysis tubing was transferred to a Millipore Ultrafree-15 centrifuge filter device (30 000 molecular weight cutoff) and concentrated by centrifugation. Concentrated sample was washed 3 times with 50 mM Tris-HCl, pH 7.5. Half of the sample was further treated with PNGaseF (Glyco) according to the supplier's instructions.

Digestion of Cross-Linked Ste2p:

Cross-linked samples were digested with BNPS-skatole, CNBr, or trypsin. For BNPS-skatole digestions, samples were dissolved in 70% acetic acid, and approximately 10 mg of BNPS-skatole was added. For CNBr digestion, samples were dissolved in 70%

formic acid, and a few crystals of CNBr were added. For trypsin digestion, samples were dissolved in trypsin digestion buffer (Promega), and 20 µg of trypsin (Sequencing Grade modified trypsin, Promega) was added. All digestion reactions took place under nitrogen and complete darkness. After digestion, samples were dried by vacuum centrifugation, resuspended in 50 µL of 0.5 M Tris, pH 8.25, and re-dried. BNPS-skatole and CNBr samples were then dissolved in Tris-tricine sample buffer from Novex (San Diego, CA) and run on 16% and 10-20% tricine gels (Novex). Trypsin-digested samples were dissolved in loading buffer (Invitrogen) and run on 12% Bis-tris gels with MES running buffer (Invitrogen). Gels were dried and exposed to a phosphorimager screen for 1-4 days.

Cross-Linking of Biotinylated α -Factor to Ste2p-T7:

[Bpa¹, Lys⁷(ϵ -biotinyl- β -alanyl)] α -factor was used in cross-linking studies with strain BJS21-pJL147 membranes. Receptors cross-linked with the biotinylated probe as described above were digested with trypsin for 18 h with addition of fresh trypsin after 12 h at 30 °C. Digested samples were run on two separate gels (18% SDS-PAGE), transferred to Immobilon-P, and blocked with 5% milk-TBS for 1 h. One blot was probed with NeurtAvidin-HRP (Pierce Chemical) and detected with Western Lightning Chemiluminescence Reagent plus (WLCR+, PerkinElmer). The second blot was probed with T7-HRP antibody (Novagen) according to manufacturer's instructions, and detected by WLCR+.

CHAPTER 3

Results

Synthesis of α -Factor Analogs:

The automated solid-phase synthesis of most of the α -factor analogs yielded crude peptides which were 60-70% homogeneous. Lower purities (<50%) were observed with the peptides containing diiodoTyr. In previous studies, we obtained better incorporation of diiodotyrosine into α -factor when arginine replaced lysine in the seventh position [24, 25]. Therefore, all α -factor analogs synthesized in this investigation contained Arg⁷. [Arg⁷] α -Factor was previously shown to have the same activity and binding affinity as α -factor [20]. The crude peptides were all purified by reversed phase HPLC to over 99% homogeneity based on analytical HPLC in both an acetonitrile/water/TFA and a methanol/water/TFA gradient system. All peptides were subjected to amino acid analysis and electrospray ionization mass spectrometry. Physicochemical data for peptides containing both Bpa and Tyr substitutions are summarized in Table 1. Similar characterization of the series containing only the Bpa substitution was also carried out (data not shown). Amino acid analysis and mass spectrometry verified the purity and composition of the synthetic α -factor analogs used in this study.

Table 1: Physicochemical properties of photo activatable peptides

#	Peptides	MW ^a	MS ^b	K(a) ^c	K(b) ^c	Amino acid analysis
1	Bpa ¹ Y ³ R ⁷ Nle ¹² F ¹³	1720.03	1721.1	4.74	3.79	Y: 0.92(1); H: 0.93(1); L: 1.99(2); Q: 2.16(2); R: 0.89(1); P: 1.99(2); G: 0.99(1); Nle: 1.21(1); F: 0.98(1)
2	Y ¹ Bpa ³ R ⁷ Nle ¹² F ¹³	1719.09	1720.3	4.61	2.99	Y: 0.91(1); H: 0.94(1); L: 1.98(2); Q: 2.13(2); R: 0.88(1); P: 1.97(2); G: 0.99(1); Nle: 1.23(1); F: 0.99(1)
3	Y ¹ Bpa ⁵ R ⁷ Nle ¹² F ¹³	1779.12	1779.4	4.39	5.04	Y: 0.97(1); H: 0.81(1); L: 2.00(2); Q: 1.08(1); R: 0.96(1); P: 1.97(2); G: 0.99(1); Nle: 1.23(1); F: 0.99(1)
4	Y ¹ R ⁷ Nle ¹² Bpa ¹³	1759.06	1760.0	5.19	3.83	Y: 0.95(1); H: 0.95(1); L: 1.95(2); Q: 2.11(2); R: 0.94(1); P: 1.92(2); G: 0.99(1); Nle: 1.19(1)
5	Bpa ¹ (I ₂)Y ³ R ⁷ Nle ¹² F ¹³	1972.05	1973.0	4.15	4.92	Y: 0.82(1); H: 0.99(1); L: 2.01(2); Q: 2.18(2); R: 0.86(1); P: 1.94(2); G: 0.99(1); Nle: 1.23(1); F: 0.99(1)
6	(I ₂)Y ¹ Bpa ³ R ⁷ Nle ¹² F ¹³	1972.21	1972.7	2.66	3.19	Y: 0.93(1); H: 0.97(1); L: 1.99(2); Q: 2.13(2); R: 0.92(1); P: 1.91(2); G: 0.96(1); Nle: 1.22(1); F: 0.98(1)
7	(I ₂)Y ¹ Bpa ⁵ R ⁷ Nle ¹² F ¹³	2030.13	2030.7	2.92	5.56	Y: 0.91(1); H: 0.96(1); L: 1.99(2); Q: 1.08(2); R: 0.96(1); P: 1.93(2); G: 0.97(1); Nle: 1.21(1); F: 0.98(1)
8	(I ₂)Y ¹ R ⁷ Nle ¹² Bpa ¹³	2011.08	2011.7	5.50	6.42	Y: 0.92(1); H: 0.89(1); L: 1.96(2); Q: 2.13(2); R: 0.89(1); P: 2.02(2); G: 0.97(1); Nle: 1.21(1)

^a Calculated monoisotopic molecular weight.

^b Molecular mass determined using electron ionization mass spectroscopy (ESI-MS).

^c *K* is defined as $(V_p - V_f)/V_f$ where V_p = the elution volume for the peptide and V_f = the breakthrough volume.

K-values (a) were determined on a C₁₈ μ -Bondpack column using a 10-55% acetonitrile gradient (0.025% trifluoroacetic acid) over 15 min and (b) were determined using 50-80% methanol gradient (0.025% trifluoroacetic acid) over 30 min.

Receptor Affinities of Bpa-Scanned α -Factor Analogs:

To attain efficient cross-linking of a ligand into a receptor binding site, it is necessary to employ ligands that bind tightly to the receptor. To ascertain the positions at which Bpa replacements would be tolerated, introduction of this residue throughout the peptide backbone was tested. As seen in Figure 1, Bpa replacements at positions 1 (Trp), 3 (Trp), 5 (Gln), 7 (Lys), 8 (Pro), 12 (Met), and 13 (Tyr) were well tolerated, exhibiting decreases in K_i from 4-fold to 45-fold in comparison to α -factor (Figure 1). In contrast, substitutions at positions 2, 4, 6, 10, and 11 resulted in 100-fold to greater than 1500-fold decreases in affinity. Based on these data and our working model for pheromone binding to receptor [26], analogs with Bpa at positions 1, 3, 5, and 13 were chosen for further evaluation as photo-cross-linkable α -factors.

Bioactivities of Iodinatable Bpa Analogs of α -Factor:

To determine cross-link points between a ligand and its binding protein, tags are useful to reveal the covalent linkage point of the ligand. The most powerful tag available in terms of sensitivity is ^{125}I [26, 27]. Previous studies showed that iodination of the C-terminal residue (Tyr¹³) resulted in biological inactivation of α -factor [28]. Another report by Masui *et al.* [29] suggested that Tyr¹³ in α -factor was essential and could not be substituted by other amino acids without loss of activity. However, it was recently demonstrated that Tyr¹³ was replaceable by Phe with little to no effect on biological activity or binding affinity of α -factor [25, 30]. Therefore, α -factor analogs [Bpa^x, Phe¹³]

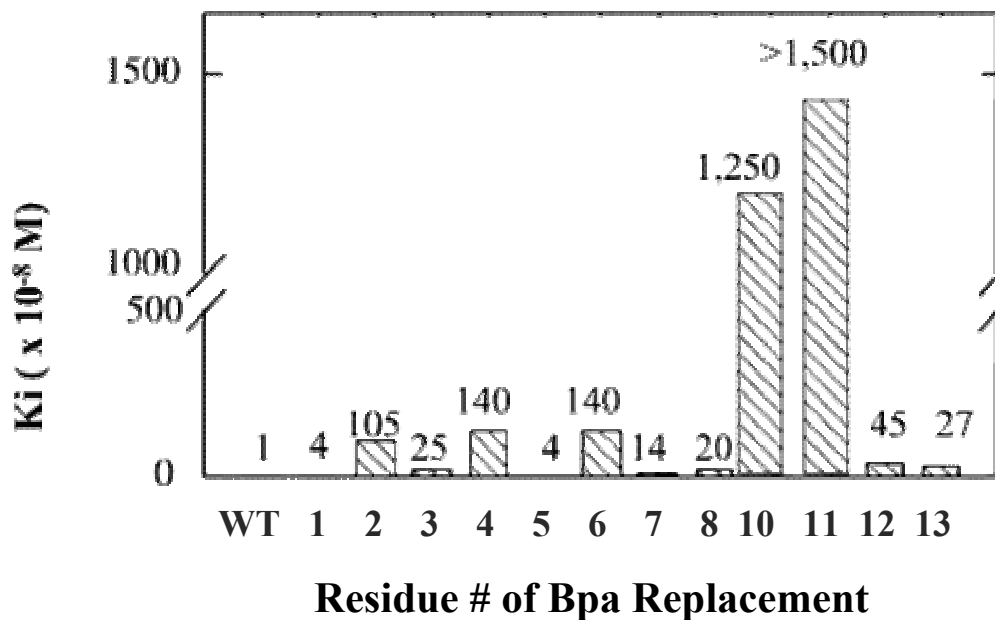


Figure 1: Binding affinity of Bpa-substituted α -factor analogs. The binding affinities of Bpa-scanned α -factor analogs were measured using [^3H] α -factor and the binding competition assay described under Materials and Methods. The figure shows the calculated K_i (23) for each analogue. The numbers on the abscissa represent the position of the Bpa replacement. Each measurement was carried out at least 3 times with an error of not more than 10% for each value shown. The number above each bar represents the K_i value ($\times 10^8$) of that analogue.

(where $x = 1, 3, \text{ or } 5$) and [Bpa¹³] α -factor analogs in which Tyr residues were substituted at other positions were evaluated. Based on the occurrence of Trp in positions 1 and 3 of the native α -factor structure, analogs **1-8** were synthesized (Table 1).

Growth arrest assays and *FUS1* gene induction assays were performed to determine the biological activity of these analogs (Table 2). Semi-logarithmic plots of halo diameter versus amount of peptide applied to the disk were all linear and exhibited similar slopes (data not shown). All analogs used in this assay were stable to enzymatic cleavage under the conditions tested as strains used in this analysis lacked the Bar1p protease that cleaves α -factor. Therefore, the growth arrest data were indicative of the relative agonist activity of each peptide. The data show that peptides containing Bpa¹ with either Tyr³ (compound **1**) or (I₂)Tyr³ (compound **5**) retain good agonist activity, requiring about 2.3-fold and 4-fold more of the pheromone derivative, respectively, to trigger the receptor. In contrast, tyrosine substituted analogs with Bpa³ (**2** and **6**), with Bpa⁵ (**3** and **7**), or with Bpa¹³ (**4** and **8**) had little or no activity in the growth arrest assay. In the solution-phase, gene induction assay, compound **1** caused 50% of the maximal gene induction at only 33% higher concentration than α -factor, and compound **5** required a 4-fold higher concentration. These results correlated with those of the growth arrest assay. Several of the peptides that were not active at the highest tested amount (10 $\mu\text{g/disk}$) in the halo assay were agonists in the gene induction assay. In fact, all four iodinated compounds (**5-8**) had comparable activities in this assay. None of the α -factor analogs

Table 2: Biological activity of α -factor analogs

Peptide (compound no.)	Growth arrest^a (μg of peptide)	<i>FUSI-lacZ</i>^b induction potency (nM)	Binding affinity,^c K_i (nM)
α -factor	0.4	3.1	9
Bpa ¹ Y ³ R ⁷ F ¹³ (1)	1.0	4.4	127
Y ¹ Bpa ³ R ⁷ F ¹³ (2)	inactive	149	157
Y ¹ Bpa ⁵ R ⁷ F ¹³ (3)	>10	184	150
Y ¹ R ⁷ Bpa ¹³ (4)	inactive	inactive	132
Bpa ¹ (I ₂)Y ³ R ⁷ F ¹³ (5)	1.5	14	199
(I ₂)Y ¹ Bpa ³ R ⁷ F ¹³ (6)	7.3 ^d	19	216
(I ₂)Y ¹ Bpa ⁵ R ⁷ F ¹³ (7)	>10	26	22
(I ₂)Y ¹ R ⁷ Bpa ¹³ (8)	inactive	33	315

^a Values represent micrograms of peptide necessary to produce a halo with a diameter of 15 mm. Each assay was done in duplicate at least 3 times with a standard error of ± 0.1 .

^b Values represent nanomolar concentration of ligand to give 50% maximal activity in a *FUSI-lacZ* gene induction assay. Each assay was done in duplicate 3 times with a standard error of about 10% for each value shown.

^c Binding affinities were determined by calculation of K_i in competition binding assays using [¹²⁵I]Y¹R⁷F¹³] α -factor. Each assay was done in duplicate 3 times with a standard error of about 10% for each value shown.

^d The zone of growth inhibition was partially filled in, giving the halo a fuzzy appearance.

induced growth arrest or *FUS1-lacZ* activation in a mutant lacking Ste2p, confirming that the α -factor receptor was required for the biological activity of these peptides. Overall, the bioassays demonstrate that α -factor analogs containing both Bpa and iodotyrosine can induce Ste2p-dependent signaling.

Binding Affinities of α -Factor Analogs:

Binding affinities of the peptides were determined by competition and saturation binding assays as described under Materials and Methods. Representative competition binding data for α -factor, and **1**, **3**, and **5** are presented in Figure 2. For most analogs, substitution of Bpa at positions 1, 3, 5, and 13 resulted in only 15-17-fold reduction in binding affinity versus native α -factor (Table 2). With the exception of [(I₂)Tyr¹, Bpa⁵, Arg⁷, Phe¹³] α -factor which showed increased binding, di-iodination of the Bpa analogs resulted in a slight reduction (1.5-2.4-fold) in binding compared to the noniodinated peptides.

Iodination and Purification of α -Factor Analogs:

Several of the Bpa-containing analogs were chosen for radioiodination based on the criteria that they had relatively good biological activity and binding affinities in the submicromolar range. [Bpa¹, Tyr³, Arg⁷, Phe¹³] α -Factor, [Tyr¹, Bpa⁵, Arg⁷, Phe¹³] α -factor, and [Tyr¹, Arg⁷, Bpa¹³] α -factor were successfully iodinated, but the iodination of

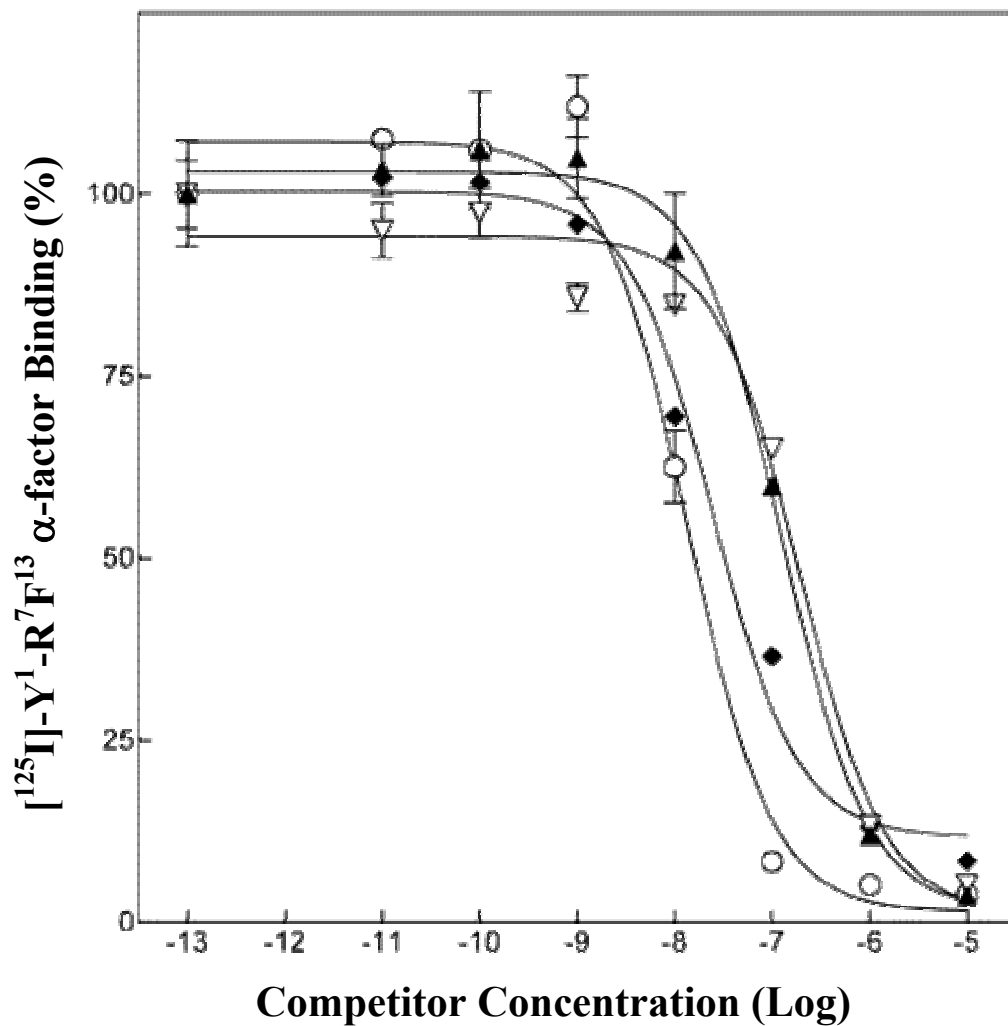


Figure 2: Competition binding assay of various α -factor analogs vs. [125 I]Tyr¹, Arg⁷, Phe¹³] α -factor. Competitors were α -factor (○), compound 1 (▲), compound 5 (▽), and compound 7 (◆).

[Tyr¹, Bpa³, Arg⁷, Phe¹³] α -factor led to an unresolvable mixture (Figure 3B). This latter result was consistent with the recent observation that certain α -factor analogs are resistant to iodination [25]. As seen in Figure 3A, iodination of [Bpa¹, Tyr³, Arg⁷, Phe¹³] α -factor resulted in both the mono- and di-iodinated derivatives. The masses of the iodinated peptides were verified by electrospray mass spectrometry (data not shown). Based on the relatively high biological activity of [Bpa¹, Tyr³, Arg⁷, Phe¹³] α -factor (**1**) and its diiodinated homologue (**5**), the radio-iodinated form of this peptide was chosen for photolabeling of Ste2p.

Competition of α -Factor for [Bpa¹, (¹²⁵I)Tyr³, Arg⁷, Phe¹³] α -Factor Binding to Ste2p:

[Bpa¹, (¹²⁵I)Tyr³, Arg⁷, Phe¹³] α -Factor was shown to be displaced from Ste2p by α -factor in a competition binding assay (Figure 4). The amount of bound peptide was expressed in dpm and plotted against the amount of cold competitor added. The binding competition was greater than 90%. The shape of the curve is consistent with competitive binding inhibition, indicating the radioligand is specific for Ste2p. Similar results were also obtained with [Bpa¹, (¹²⁵I₂)Tyr³, Arg⁷, Phe¹³] α -factor, the di-iodinated form of this photoactivatable peptide (data not shown).

Cross-Linking of [Bpa¹, (¹²⁵I)Tyr³, Arg⁷, Phe¹³] α -Factor to Ste2p:

Membranes were incubated with [Bpa¹, (¹²⁵I)Tyr³, Arg⁷, Phe¹³] α -factor, and cross-linking was carried out using light at 365 nm. A portion (20 μ L) of the reaction mixture was removed following irradiation and tested for incorporation of radioactivity

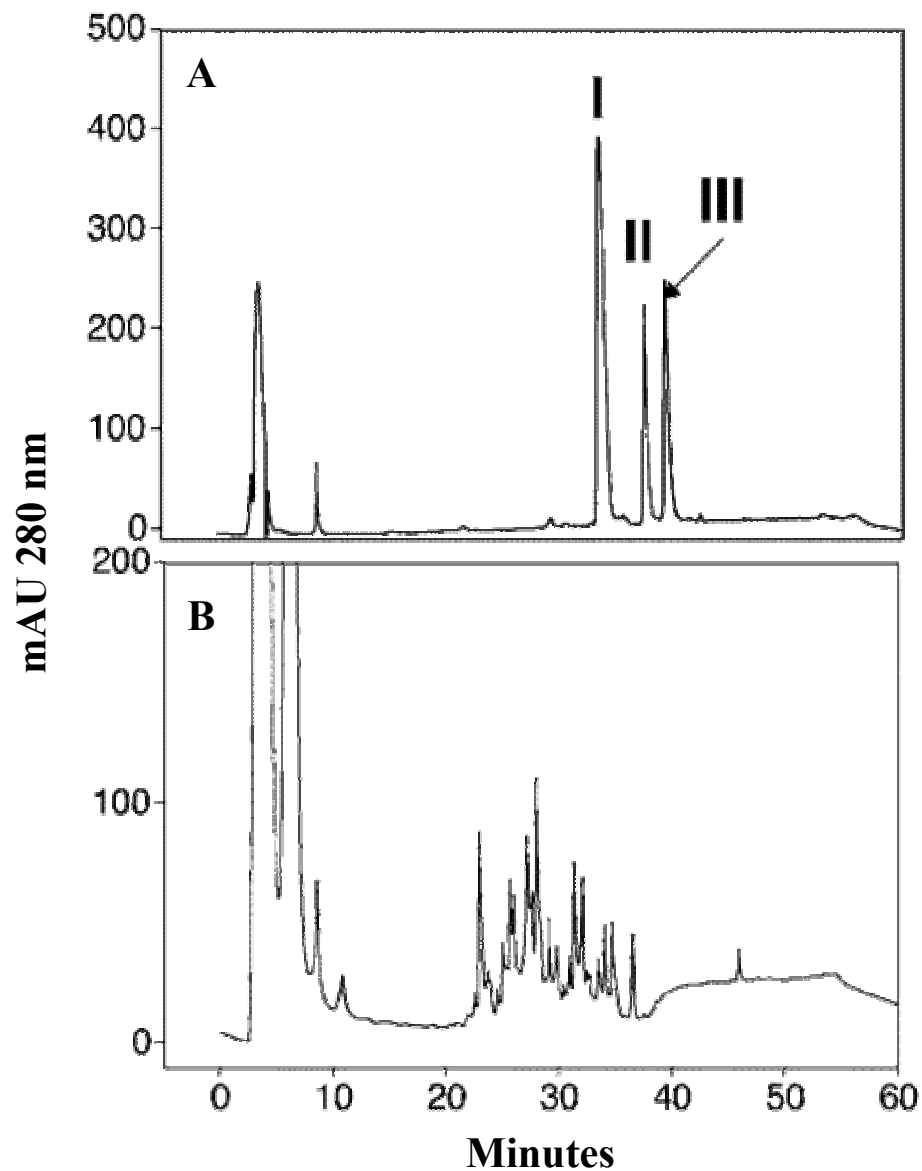


Figure 3: HPLC analysis of products from iodination of tyrosine-substituted α -factor analogs. α -Factor analogs were chemically iodinated using Iodogen reagent and products separated by HPLC. (Panel A) Iodination of $[\text{Bpa}^1, \text{Tyr}^3, \text{Arg}^7, \text{Phe}^{13}]\alpha$ -factor: I, noniodinated peptide; II, mono-iodinated peptide; III, di-iodinated peptide. (Panel B) Iodination of $[\text{Tyr}^1, \text{Bpa}^3, \text{Arg}^7, \text{Phe}^{13}]\alpha$ -factor.

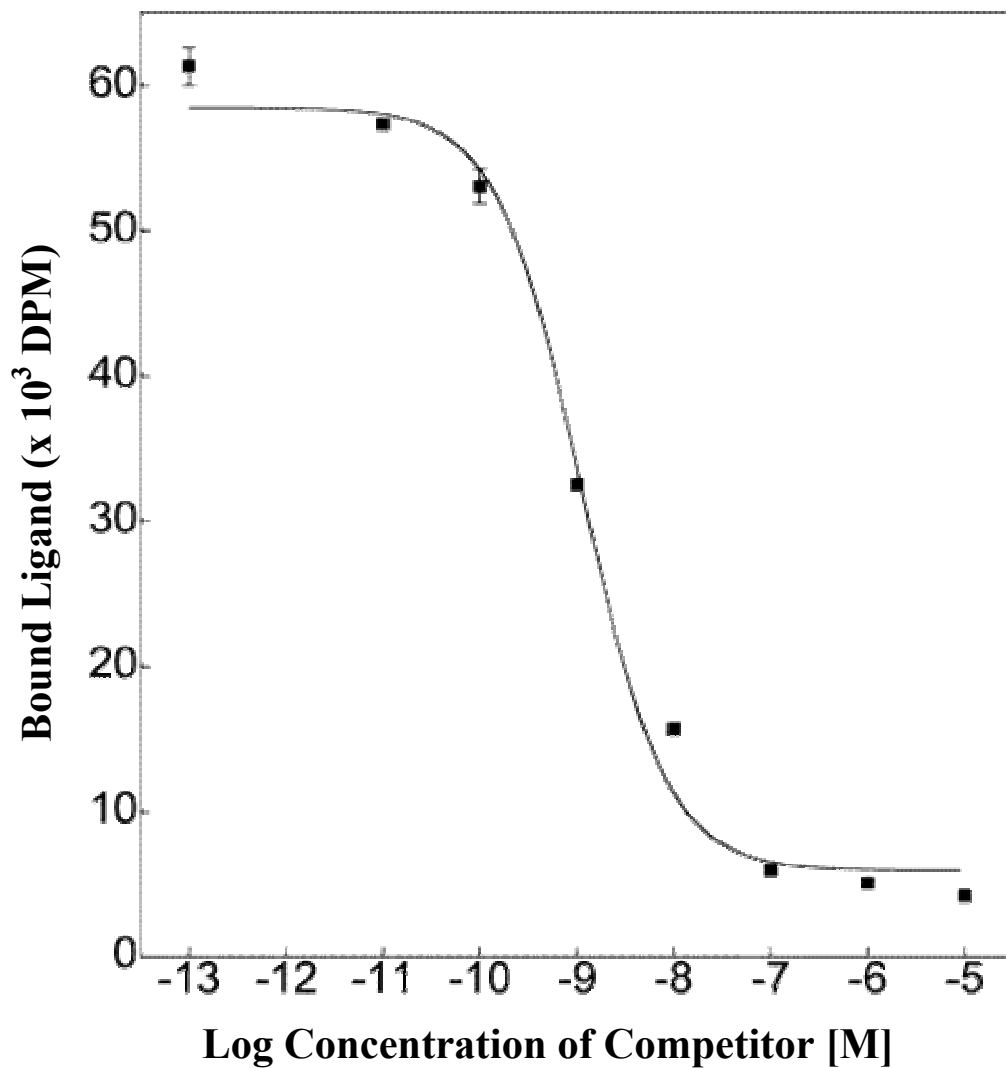


Figure 4: Competition binding of [Bpa¹, (¹²⁵I)Tyr³, Arg⁷, Phe¹³]α-factor by nonradiolabeled α-factor. Data were analyzed using a single-site competition binding equation. Error bars on some points were contained within the symbol and cannot be seen.

by processing over Multiscreen durapore membranes [26]. The radioactive counts of the samples with and without competitor reveal a 76% reduction in cross-linked product in the presence of 100-fold excess α -factor (Figure 5). The remainder of the reaction mixture was analyzed by SDS-PAGE, and a cross-linked product (54 kDa) which migrated to the expected size of Ste2p (52 kDa) + probe (2 kDa) was detected by autoradiography (Figure 6). No cross-linked products were observed with samples that were not UV-irradiated (Figure 6, lanes 3 and 4). Co-incubation of membranes with radiolabeled probe and cold α -factor resulted in a decrease in cross-linked product, showing that the cross-linking to Ste2p was specific (Figure 6, lane 1 vs. lane 2). Western analysis using anti-Flag antibodies to detect Ste2p showed that all lanes had equivalent amounts of the receptor (data not shown).

Fragmentation Analysis of Cross-Linked Ste2p:

Based on the specific cross-linking of [Bpa¹, (¹²⁵I)Tyr³, Arg⁷, Phe¹³] α -factor to Ste2p, digestion of the receptor was initiated to identify the cross-linked fragment(s) of the receptor. Chemical cleavage with CNBr and BNPS-skatole was performed. These methods take place under strongly acidic conditions, which should result in unfolding of the receptor, thereby making it more accessible to cleavage [17]. Chemical digestion of the receptor was carried out on native and deglycosylated Ste2p prepared by treatment of Ste2p with PNGaseF. Deglycosylation of the receptor was verified by SDS-PAGE with the deglycosylated receptor migrating with a molecular mass that was approximately 2 kDa smaller than the native receptor (data not shown). Similar results of deglycosylation

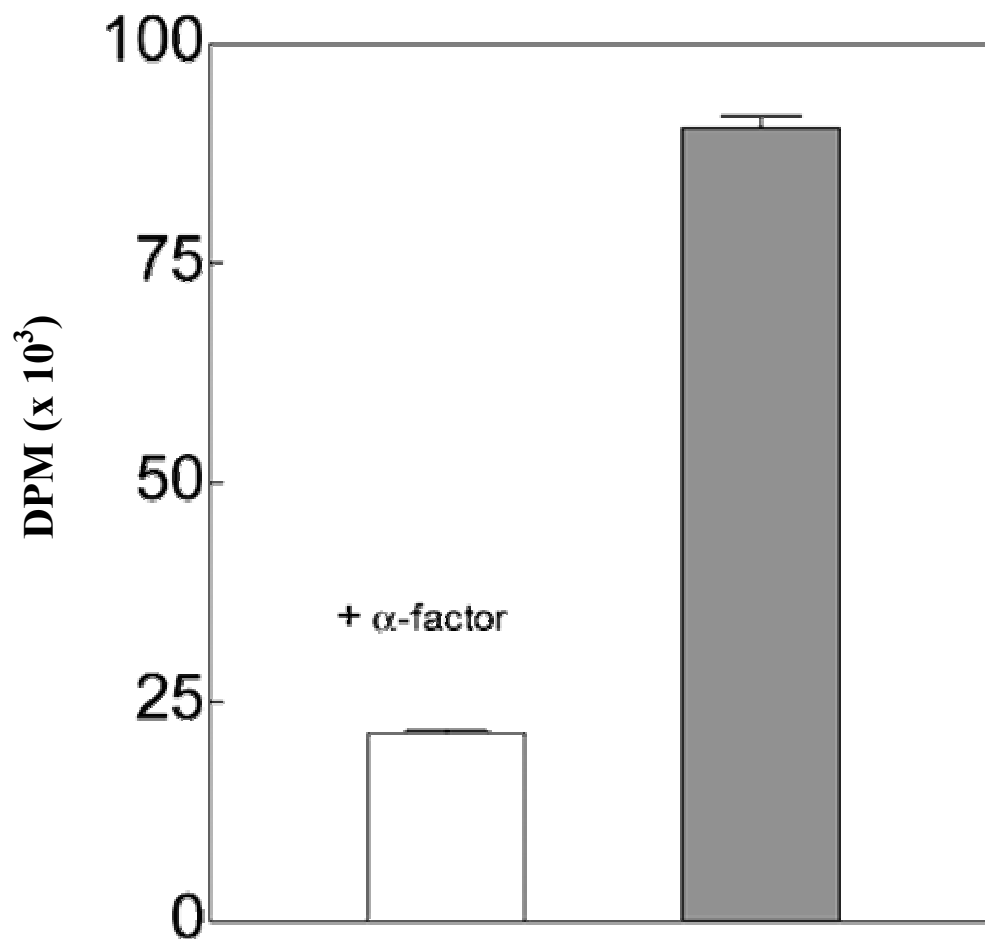
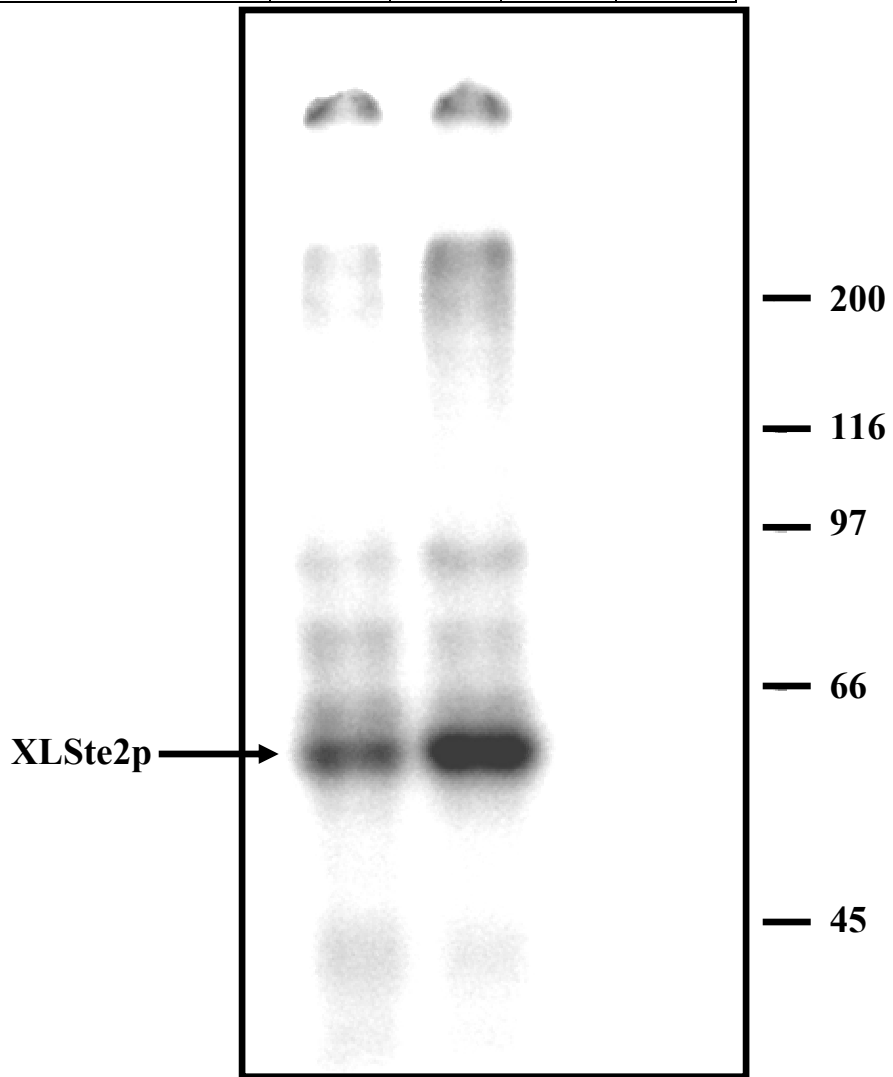


Figure 5: Total radioactive counts of [Bpa¹, (¹²⁵I)Tyr³, Arg⁷, Phe¹³]α-factor bound to membranes following cross-linking in the presence and absence of nonradiolabeled α-factor. Bars represent amount of ligand associated with membranes. Cross-linking was carried out in the presence (open bar) or absence (shaded bar) of nonlabeled α-factor. The experiment was performed 3 times, and the error bars represent the variance observed.

Figure 6: Autoradiograph of SDS-PAGE analysis of UV-irradiated DK102pNED membranes in the presence of [Bpa¹, (¹²⁵I)Tyr³, Arg⁷, Phe¹³] α -factor. Membranes containing Ste2p were incubated with [Bpa¹, (¹²⁵I)Tyr³, Arg⁷, Phe¹³] α -factor and irradiated at 365 nm as described under Materials and Methods. Control samples either were not irradiated or contained α -factor as a competitor. Lane 1, UV irradiated plus 100-fold excess nonradiolabeled α -factor; lane 2, UV irradiated; lane 3, 100-fold excess nonradiolabeled α -factor without UV irradiation; lane 4, without excess nonradiolabeled α -factor and without UV irradiation; lane 5, molecular weight markers.

Lane	1	2	3	4
α -factor	+	-	+	-
UV irradiation	+	+	-	-



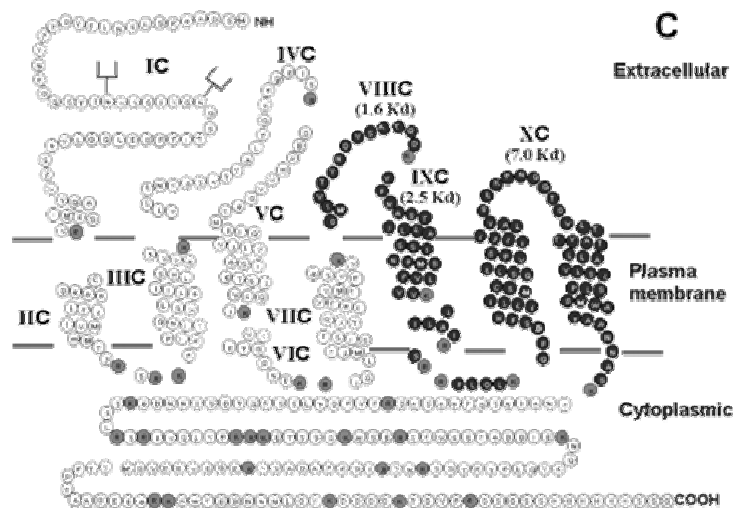
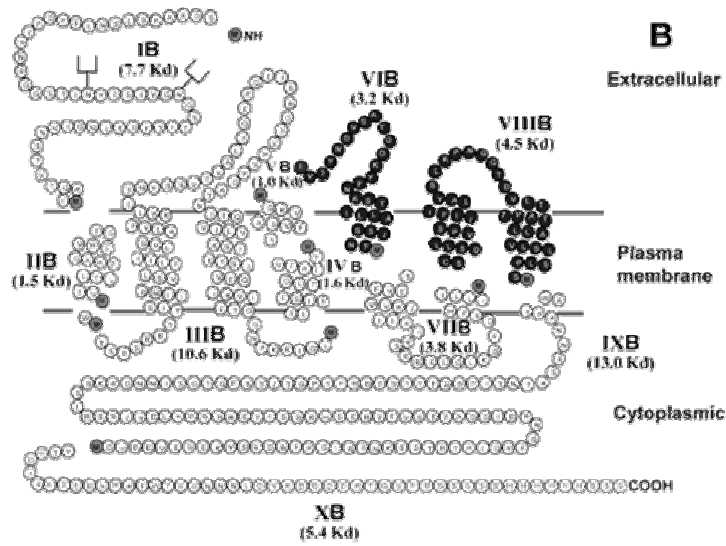
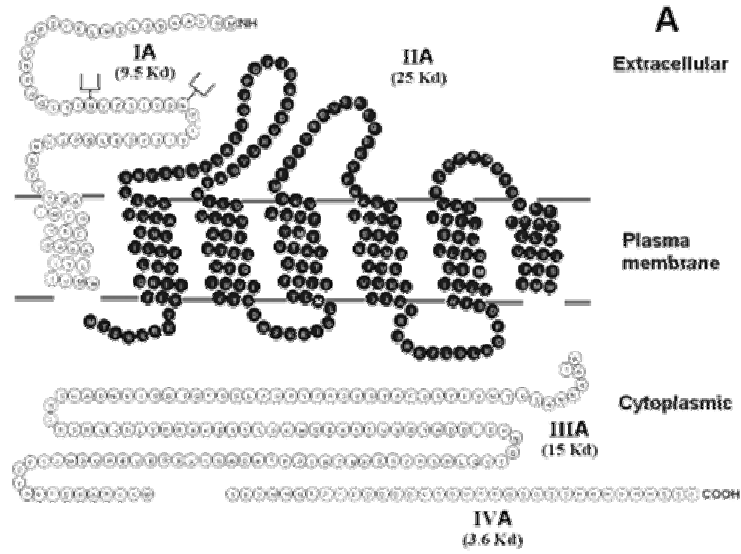
of Ste2p were obtained previously by others [31, 32]. In certain gels, Ste2p appeared as a diffuse band and sometimes appeared as a doublet. This is most likely due to the fact that strain BJ2168pNED1 expresses both a native chromosomal copy of *STE2* which codes for a 50 kDa protein when glycosylated, and an epitope-tagged, episomally expressed *STE2* which contains two epitope tags and codes for a 52 kDa protein when glycosylated.

BNPS-skatole, which cleaves at tryptophan residues, theoretically fragments the receptor into four pieces [**IA**: 9.5 kDa (7.5 kDa for residues 1-70 of Ste2p plus glycosyl groups of 2.5 kDa), **IIA**: 25 kDa (71-295), **IIIA**: 15 kDa (296-424), and **IVA**: 3.6 kDa (425-457)] (Figure 7A). Western analysis of native receptor with polyclonal antibodies against residues 1-60 revealed that, after 2 min incubation with the BNPS-skatole reagent, a broad band at approximately 35 kDa began to appear (Figure 8, lane B). The size of this band contains glycosylated and deglycosylated forms of a fragment consisting of residues 1-295 (fragments **IA** + **IIA**). After 24 h incubation with the BNPS-skatole reagent, two fragments of 7.5 and 9.5 kDa, corresponding to glycosylated and deglycosylated forms of fragment **IA**, were detectable (Figure 8, lane D) by a similar Western analysis. Thus, 24 h incubation was required to ensure complete digestion of the Ste2p under the conditions used.

Ste2p containing cross-linked [Bpa¹, (¹²⁵I)Tyr³, Arg⁷, Phe¹³]α-factor was digested for 24 h with BNPS-skatole, dissolved in tricine sample buffer, and run on gradient tricine gels. Phosphorimaging of the gels revealed two fragments of approximately 27 and 6 kDa (Figure 9, panel B). The 27 kDa fragment corresponds to that expected for complete BNPS-skatole cleavage of Ste2p (25 kDa fragment **IIA**, Figure 7A), plus 2 kDa for the probe. The 6 kDa fragment appears to be anomalous (see Discussion). In this

Figure 7: Schematic representation of chemical and enzymatic cleavage of Ste2p.

These figures represent the BNPS-skatole, CNBr, and trypsin cleavage sites for the Ste2p receptor. Ste2p receptor is shown here using snake diagrams to represent the putative transmembrane domains. (Panel A) Cleavage of the receptor by BNPS-skatole results in four fragments labeled **IA** (residues 1-70 of Ste2p), **IIA** (71-295), **IIIA** (296-424), and **IVA** (425-458) with their respective molecular masses given in parentheses. Fragment **IA** contains the putative N-linked glycosylation sites as represented by the goalpost symbols. The oligosaccharides add 2 kDa of mass to fragment **IA**. Panel B represents the peptides resulting from a complete CNBr cleavage of Ste2p. Panel C represents the peptides resulting from a complete trypsin cleavage of Ste2p.



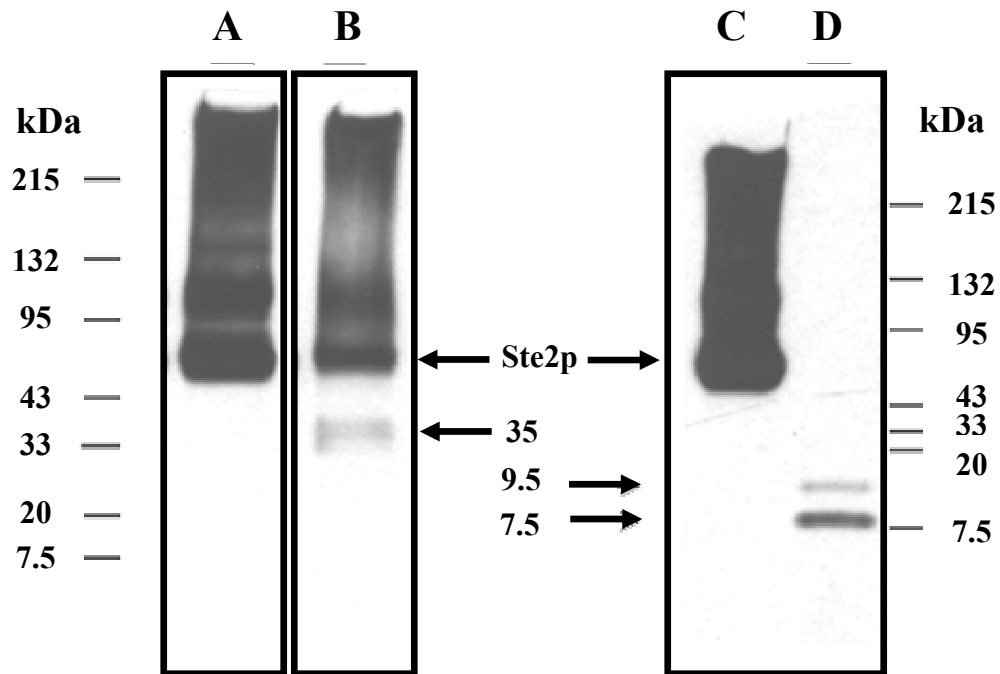


Figure 8: Western blot analysis of BNPS-skatole-digested membranes. Membranes were digested with BNPS-skatole, and at various time points, portions of the reaction mixture were removed and dried under vacuum centrifugation. Samples were then dissolved in tricine sample buffer and run on gradient tricine gels. Protein was transferred to Immobilon P membranes and probed with polyclonal antibodies specific for the first 60 amino acids of Ste2p. Lanes A and C were loaded with undigested membrane protein with intact Ste2p indicated in the figure. Lane B represents a 2 min digestion, and lane D shows a 24 h digestion with BNPS-skatole. The sizes of the detected fragments were indicated by arrows. Detected bands above 52 kDa are routinely observed in Western blot analysis of Ste2p and are widely believed to represent multimeric or aggregate structures of Step2 [32].

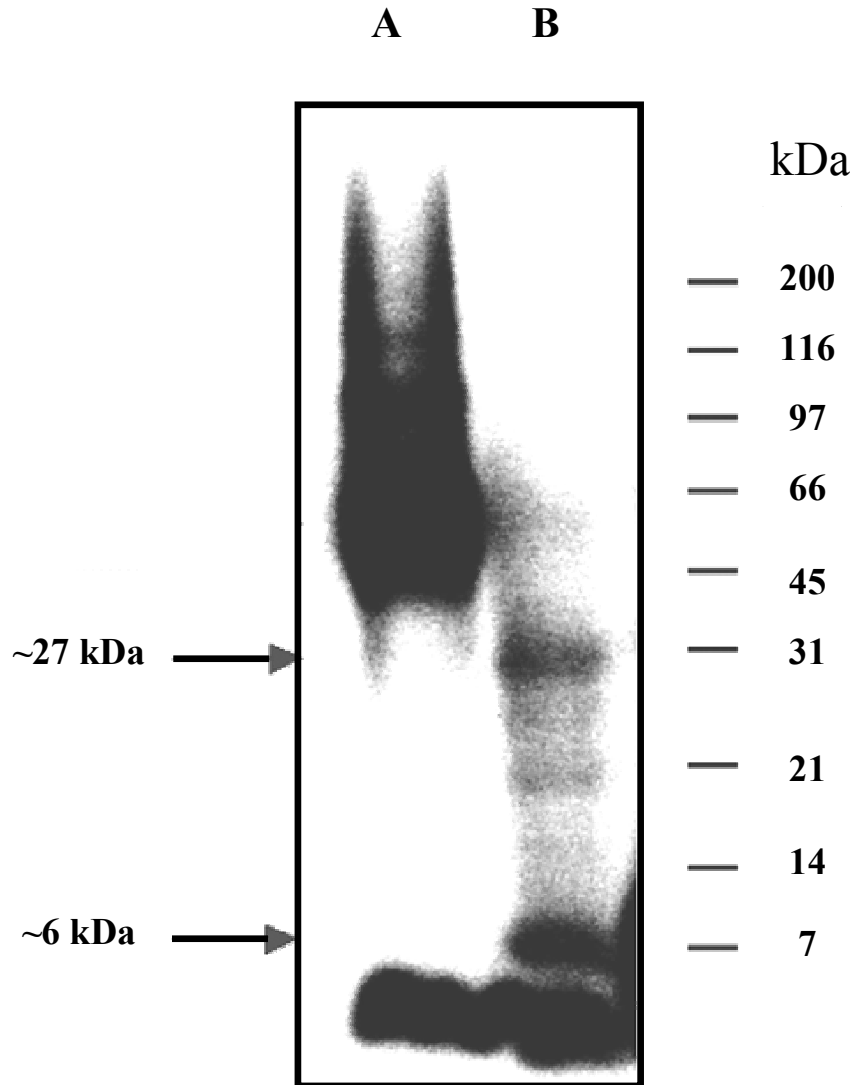


Figure 9: Autoradiograph of SDS-PAGE 10-20% tricine gel analysis of membranes photolabeled with [Bpa¹, (¹²⁵I)Tyr³, Arg⁷, Phe¹³]α-factor. (A) Photo-cross-linked membranes, untreated, and (B) photo-cross-linked membranes treated with BNPS-skatole and PNGaseF to remove N-linked oligosaccharides. Arrows denote cross-linked Ste2p receptor (lane A) and receptor fragments (lane B). Detected bands above 52 kDa are routinely observed in Western blot analysis of Ste2p and are widely believed to represent multimeric or aggregate structures of Step2 [32].

gel and subsequent ones, an unidentified, low molecular weight form of radioactive iodine was readily discernible in the portion of the gel corresponding to a molecular size less than 4 kDa.

Complete cleavage of the cross-linked receptor with CNBr yielded one labeled fragment of ~6 kDa (Figure 10, panel I, lane B). Total cleavage of Ste2p labeled with [Bpa¹, (¹²⁵I)Tyr³, Arg⁷, Phe¹³]α-factor could result in several possible radioactive fragments with a molecular mass of 6 kDa. Therefore, a partial CNBr digestion of cross-linked Ste2p was performed. This resulted in fragments of 35, 22, 9, and 6 kDa (Figure 10, panel II, lane B). All of these fragments can be rationalized in terms of theoretical CNBr cleavage points in Ste2p (Table 3). For example, the 35 kDa band (Figure 7B) could correspond to fragments **IVB** through **XB** (32.5 kDa) plus ligand (2 kDa). The smaller bands [23 (fragments **VIIB-IXB** plus ligand), 10 (fragments **VIIB-VIIIB** plus ligand), and 6 kDa (fragment **VIIIB** plus ligand)] could all result from cleavages at Met residues within the 35 kDa peptide (Table 3). PNGaseF treatment of the mixture of fragments obtained by partial CNBr degradation did not result in any shifts in the band sizes (Figure 10, lane C). This was interpreted as ruling out fragment **IB** (glycosylated) in any of the cross-linked fragments detected.

Digestion of the cross-linked receptor with trypsin revealed one band of approximately 9 kDa corresponding to fragment **XC** (Figure 7C). It should be noted that cleavage at the Arg residue within the α-factor analogue does not occur because Arg is followed by a Pro residue. Cross-linking of ligand into **VIIIC** or **IXC** (Figure 7), two fragments of trypsin-hydrolyzed Ste2p that could correspond to fragments of CNBr-

Figure 10: Autoradiographs of membranes photo-cross-linked with [Bpa¹, (¹²⁵I)Tyr³, Arg⁷, Phe¹³]α-factor and treated with CNBr. Samples run on an SDS-PAGE 10-20% tricine gel. I: lane A, photo-cross-linked membranes; lane B, complete digestion of photo-cross-linked membranes with CNBr. Arrows indicate photolabeled Ste2p and 6.7 kDa cleavage fragment of Ste2p. II: lane A, photo-cross-linked membranes; lane B, incomplete digestion of photo-cross-linked membranes; lane C, PNGaseF treatment of membranes from lane B.

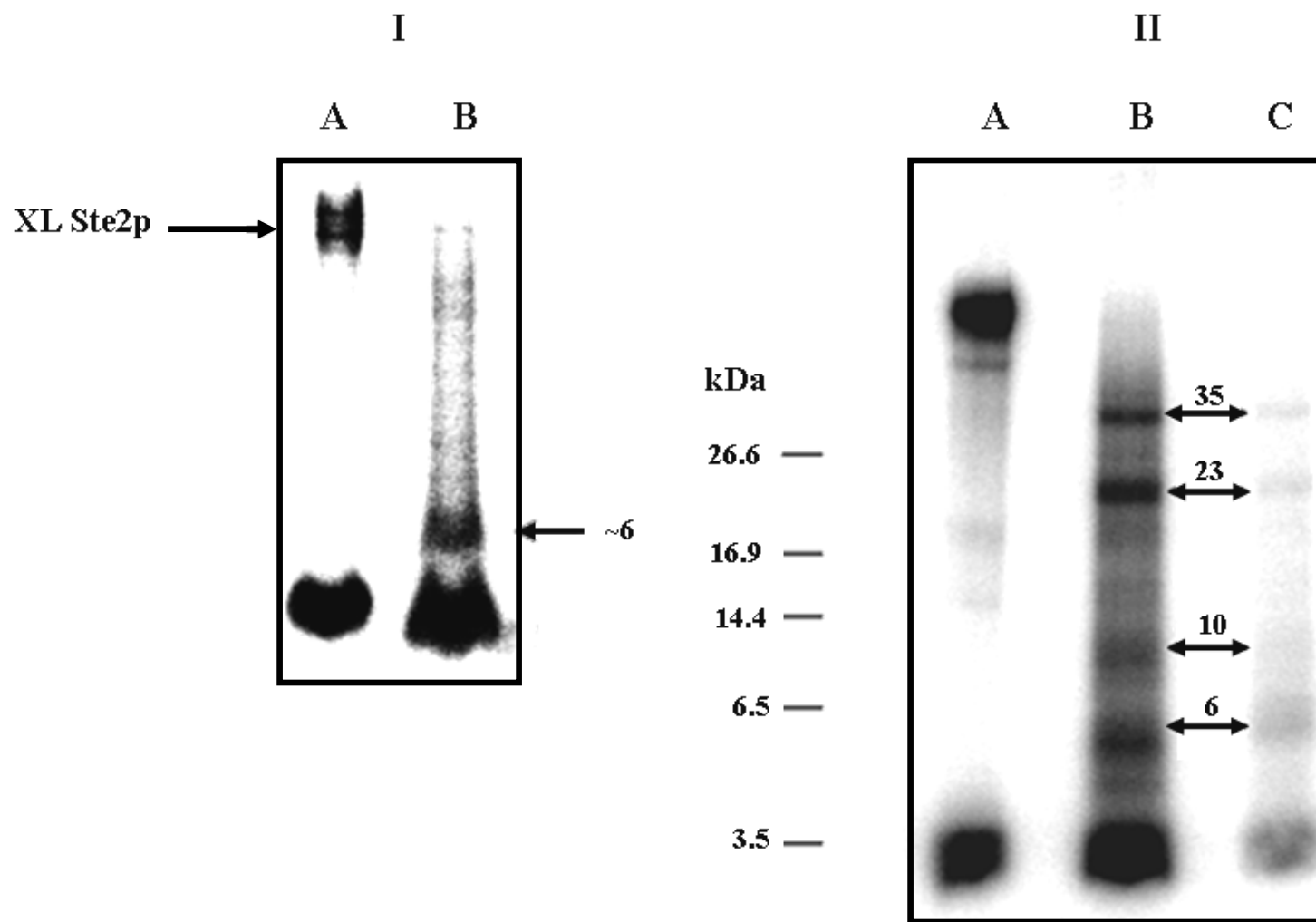


Table 3: Peptides of CNBr-digested Ste2p

Peptide designation ^a	Starting residue no. ^b	Ending residue no. ^c	Total no. of residues	Molecular mass (kDa)	Accumulated molecular mass (kDa) ^d			
IB	2	54	53	5679	5.7	-	-	-
IIB	55	69	15	1521	7.2	1.5	-	-
IIIB	72	165	94	10621	17.8	12.1	10.6	-
IVB	166	180	15	1554	19.4	13.6	12.1	1.5
VB	181	189	9	1000	20.4	14.6	13.1	2.5
VIB	190	218	29	3227	23.6	17.8	16.3	5.7
VIIB	219	250	32	3774	27.4	21.6	20.1	9.5
VIIIB	251	294	44	4619	32	26.2	24.7	14.1
IXB	295	409	115	12962	45	39.2	37.7	27.1
XB^e	410	end	48	5407	50.4	44.6	43.1	32.5

^a Peptides are named in order from the N-terminus to the C-terminus of Ste2p. Peptides of only one or two amino acids resulting from CNBr cleavage are not included in the table.

^b The residue within Ste2p of the first amino acid of this CNBr fragment.

^c The residue within Ste2p of the last amino acid of this CNBr fragment.

^d The total molecular mass of all fragments within a possible partial digest. For example, in the first column, fragments **IB** through **IIIB** have a molecular mass of 17.8 kDa.

^e The carboxyl terminus of Ste2p used in this study contained a His-tag and a FLAG tag (see Materials and Methods).

digested Ste2p, would have led to a much smaller band of radioactivity (approximately 3.5-4.5 kDa). Taken together, examination of all the digestion maps [BNPS-skatole (Figure 7A), CNBr (Figure 7B), and trypsin (Figure 7C)] indicated that the cyanogen bromide fragment **VIIIB** (Figure 7B, residues 251-294) was the smallest common cross-linked fragment. This portion of Ste2p corresponds to transmembrane domain 6, the extracellular loop between transmembrane domains 6 and 7, and transmembrane domain 7.

The position of cross-linking on Ste2p and the probe was further examined using an epitope-tagged Ste2p (Ste2p-T7) and biotinylated, photoactivatable [Bpa¹, Lys⁷(ϵ -biotinyl- β -alanyl)] α -factor. The T7 epitope, introduced between residues 303 and 304 at the C-terminal end of the tryptic fragment that spans TMD6 and TMD7, was fully tolerated by Ste2p [16]. Trypsin digestion of Ste2p-T7 results in fragments similar to the wild-type Ste2p receptor (Figure 11), but fragment **XC** (Figure 7C) is tagged with the T7 epitope (1.1 kDa), allowing identification of this receptor fragment by western blotting with anti-T7 antibodies. Ste2p-T7 was cross-linked with [Bpa¹, Lys⁷(ϵ -biotinyl- β -alanyl)] α -factor, digested with trypsin (18 h, 30 °C), run on SDS-PAGE, and probed with T7 antibodies to detect the epitope or probed with NeutrAvidin to detect biotin of the cross-linked α -factor analogue (Figure 12). The 14 kDa band corresponds to a partial trypsin digestion product containing **IXC**, **IL3**, and **XC** (Figure 7C) covering TMD5-TMD7 plus the cross-linked ligand (2.0 kDa) and the T7 epitope (1.1 kDa), and the 11 kDa band corresponds to fragment **XC** (Figure 7C) plus the cross-linked ligand and the T7 epitope. These fragments of cross-linked Ste2p-T7 were detected in lanes probed with either anti-T7 antibody or NeutrAvidin. In a parallel experiment (data not shown), the

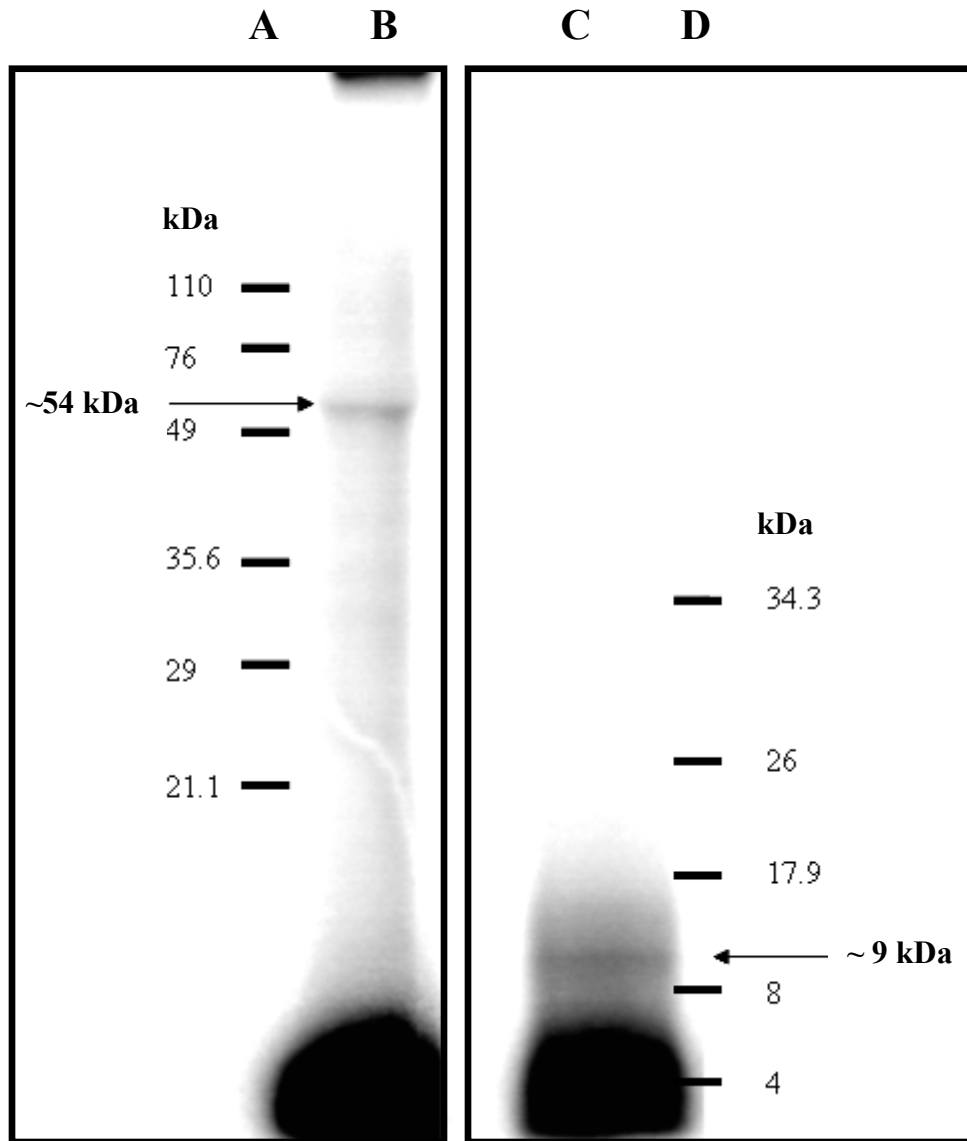


Figure 11: Autoradiograph of membranes photo-cross-linked with $[Bpa^1, (^{125}I)Tyr^3, Arg^7, Phe^{13}]α\text{-factor}$ and treated with trypsin. Samples run on SDS-PAGE 12% Bis-Tris with MES buffer. Lane B, cross-linked receptor before trypsin digestion; lane D, after trypsin digestion; lanes A and C, molecular mass markers with sizes indicated in the left and right margins.

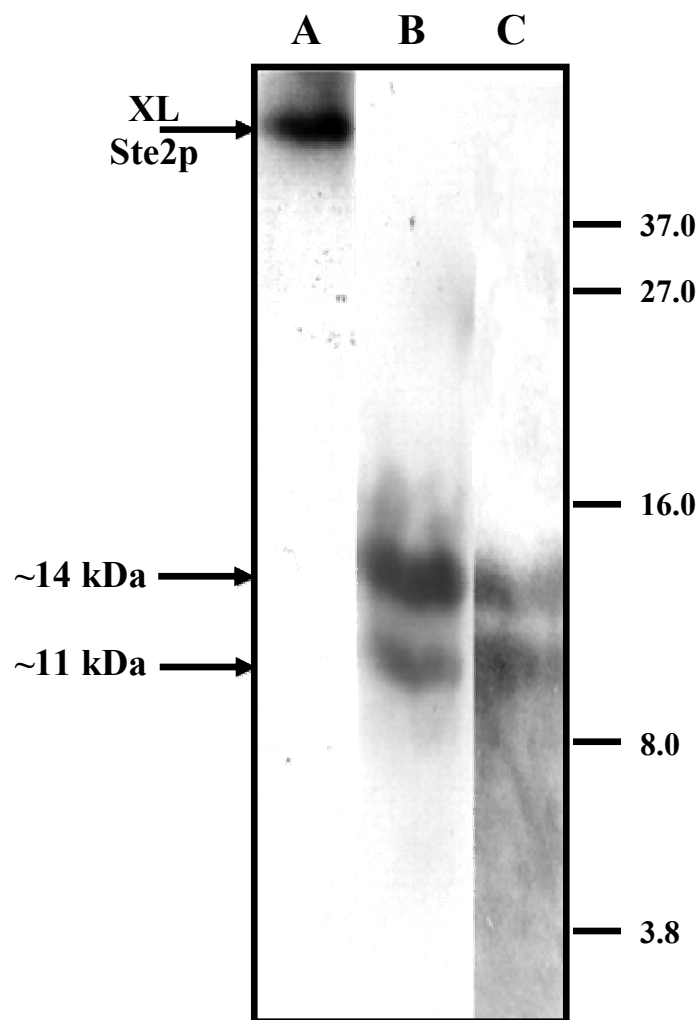


Figure 12: Western blot analysis of [Bpa¹, Lys⁷(ϵ -biotinyl- β -alanyl)] α -factor cross-linked membranes. [Bpa¹, K⁷(ϵ -biotinyl- β -alanyl)] α -factor was cross-linked into Ste2p-T7, treated with trypsin, and run on 18% SDS-PAGE. Lane A, before trypsin digestion probed with NeutrAvidin-horseradish peroxidase (NA-HRP); lane B, after trypsin digestion probed with NA-HRP; lane C, after trypsin digestion probed with anti-T7-HRP conjugate.

same two bands at 11 and 14 kDa were detected when a single gel blot was probed with anti-T7 antibody and then stripped and reprobed with NeutrAvidin. These results indicate that one fragment corresponding to **XC** contained the T7 epitope and the cross-linked [Bpa¹, Lys⁷(ϵ -biotinyl- β -alanyl)] α -factor.

CHAPTER 4

Discussion

Photoaffinity labeling with Bpa has been shown to be a useful tool in elucidating direct contacts between ligands and their cognate receptors [4-11]. These photoaffinity studies, which include work on the parathyroid, secretin, and nociceptin receptors, have used receptor digestion analysis to elucidate fragments of the receptor that were cross-linked to the photo-activatable ligand probe. It should be noted, however, that receptor fragments may move anomalously on polyacrylamide gels and that molecular weights of small fragments are difficult to determine accurately. In favorable cases, specific residues involved in cross-linking were identified [5-7, 9]. Site-directed mutagenesis studies can then be used to corroborate the importance of such residues in the binding of the ligand to the receptor.

This part (Part II) of the dissertation detailed the synthesis and testing of α -factor analogs containing Bpa for use as photoprobes to elucidate binding sites on the Ste2p receptor. Results from the Bpa-scanned α -factor series (Figure 1) allowed the conclusion that residues at positions 1, 3, 5, and 13 could be replaced with the photoactivatable amino acid without severe decreases in binding affinity. Based on previous structure-activity analyses [18-20, 24, 27-29], analogs containing iodinated tyrosine residues at positions 1 or 3 with phenylalanine at position 13 were designed. Bioassay and receptor binding studies indicated that these analogs triggered biological responses characteristic

of Ste2p activation, and retained Ste2p-specific submicromolar binding affinities for this receptor (Table 2).

One of the analogs tested, [Bpa¹, Tyr³, Arg⁷, Phe¹³] α -factor, was iodinated and exhibited relatively good agonistic activity in two standard pheromone response assays (growth arrest and *FUS1*-lacZ). Binding of [Bpa¹, (¹²⁵I)Tyr³, Arg⁷, Phe¹³] α -factor was found to be specific for the Ste2p receptor based on the ability of native α -factor to displace [Bpa¹, (¹²⁵I)Tyr³, Arg⁷, Phe¹³] α -factor in a competition binding assay (Figure 4). SDS-PAGE analysis of photolabeling experiments with [Bpa¹, (¹²⁵I)Tyr³, Arg⁷, Phe¹³] α -factor resulted in detection of one major radiolabeled product which migrated at the expected size of Ste2p covalently attached to the probe (54 kDa). The amount of 54 kDa product was reduced by >70% in the presence of excess cold α -factor, indicating that cross-linking was occurring at the pheromone binding site of Ste2p. These findings showed that the radioiodinated probe had biological and binding characteristics similar to native α -factor and cross-linked specifically to Ste2p. Thus [Bpa¹, (¹²⁵I)Tyr³, Arg⁷, Phe¹³] α -factor can be used to determine the binding site contacts between α -factor and its receptor.

Receptor cross-linked with the radiolabeled probe was purified by SDS-PAGE, eluted from the gel, and treated with various cleavage agents to identify a fragment(s) that covalently attached to the radioprobe. It was expected that cleavage at the Trp residues of Ste2p with BNPS-skatole would break the receptor into four fragments (Figure 8A: fragments **IA**, **IIA**, **IIIA**, and **IVA**). Previous studies by others have shown that the intracellular C-terminal tail of Ste2p has no effect on binding of α -factor and can

actually be removed without loss of α -factor binding to Ste2p [31, 32]. Based on this information, fragments **III A** and **IV A** were eliminated as possible sites for cross-linking as they make up the intracellular C-terminal tail of the receptor and are not accessible to α -factor. SDS-PAGE analysis with high percentage tricine gels resulted in identification of two major radiolabeled products of 27 and 6 kDa in size. The 27 kDa fragment corresponded to fragment **II A** (25 kDa) plus the probe (2 kDa). The 6 kDa fragment was unexpected in that it does not correspond to a cross-linked form of fragment **I A** which would have an expected size of approximately 11 kDa (7.5 kDa + 2 kDa for the probe + 2 kDa for the polysaccharides = 11.5 kDa). The unexpected 6 kDa fragment most likely corresponds to cleavage of receptor fragment **II A** at methionines and/or cysteines due to reagent contamination. It has been reported that slight impurities in BNPS-skatole can result in cleavage at methionines and cysteines [33]. These impurities can arise from incomplete removal of *N*-bromosuccinimide (NBS) substrate during the synthesis of BNPS-skatole. However, NBS contamination is usually only a small fraction of the total reagent. As a result, Trp residues were cleaved fast by BNPS-skatole while the Met and Cys residues were cleaved at a slower rate. Based on this information, it is believed that the 6 kDa fragment was generated by cleavage at sites other than Trp in the 27 kDa fragment and would explain why the fragment was not detected in Western analysis by anti-N-terminal Ste2p antibodies following BNPS cleavage. This argument is strengthened by the observation that complete cleavage of Ste2p by CNBr at methionines also resulted in a 6 kDa fragment.

Complete cleavage of the cross-linked receptor with cyanogen bromide resulted in the identification of a single labeled band ~6 kDa in size. Based on the BNPS-skatole

results, the band should be part of fragment **IIA** (Figure 7A). Complete CNBr cleavage of Fragment **IIA** should yield six fragments [**IIIB**: 10.6 kDa (residues 72-165 of Ste2p), **IVB**: 1.6 kDa (166-180), **VB**: 1.0 kDa (181-189), **VIB**: 3.2 kDa (190-218), **VIIB**: 3.8 kDa (219-250), and **VIIIB**: 4.5 kDa (251-294)] (Figure 7B). Of these, fragments **VIB**, **VIIB**, and **VIIIB** when cross-linked to the probe would give sizes similar to the identified radiolabeled fragment. Incomplete digestion of the cross-linked receptor with CNBr yielded four fragments (Figure 10, panel II, lane B). Digestion of the cross-linked receptor with trypsin revealed one band (Figure 11) of approximately 9 kDa corresponding to fragment **XC** (Figure 7C). Taken together, the results of the two chemical cleavages and trypsin cleavage indicated the receptor was labeled between residues 251 and 294. This portion of Ste2p corresponds to transmembrane domain 6, the extracellular loop between transmembrane domains 6 and 7, and transmembrane domain 7.

To verify that the 9 kDa fragment in Figure 11 was composed of a portion of Ste2p and the cross-linked α -factor analogue, a receptor containing an epitope tag was utilized. This receptor, Ste2p-T7, carried the T7 epitope (Met-Ala-Ser-Met-Thr-Gly-Gly-Gln-Gln-Met-Gly) introduced between Ste2p residues 303 and 304. The epitope is thus N-terminal to a trypsin-sensitive Lys residue at position 304. In this manner, the **XC** fragment (Figure 7C) and any fragments resulting from partial digestion of Ste2p-T7 containing this portion of the receptor could be detected by antibody to T7. The Ste2p-T7 receptor was utilized successfully by Dube, DeConstanzo, and Konopka [16] previously to determine interactions between TMD5 and TMD6. Using Ste2p-T7 and a biotinylated, photoactivatable α -factor analog, [Bpa¹K⁷(ϵ -biotinyl- β -alanyl)] α -factor, detection of the

cross-linked fragment was carried out by anti-T7 antibody and a biotin probe. Two bands at 11 and 14 kDa, corresponding respectively to **XC** with the T7 epitope plus the α -factor and to **IXC-IL3-XC** with the T7 epitope and the α -factor were observed. The detection of both bands by the two probing methods indicated that the bands contained cross-linked [Bpa¹K⁷(ϵ -biotinyl- β -alanyl)] α -factor and a portion of Ste2p-T7. The increase in size from 9 kDa (Figure 11, Ste2p cross-linked to iodinated, photoaffinity probe) to 11 kDa (Figure 12, Ste2p-T7 cross-linked with biotinylated, photoaffinity probe) is consistent with the extra mass due to the ϵ -biotinyl- β -alanyl modification and the T7 epitope. These results strongly indicate that the region of the receptor cross-linked by a Bpa¹-photoactivatable probe, either iodinated or biotinylated, corresponded to residues 251-294 of Ste2p. The fact that the only two bands found on the protein blots were revealed by both epitope and biotin probes was strong evidence for the position of the cross-linking in the receptor. Although other 11 and 14 kDa fragments might occur during trypsin cleavage, they would not react with the anti-T7 antibodies.

The determination of a contact between the position 1 side chain of α -factor and residues of Ste2p allows us to refine our current working model for the placement of α -factor into the active site of this receptor. Based on site-directed mutagenesis and synthetic analogs, evidence was recently presented for a contact between the side chain of residue 10 (Gln) of α -factor and residues 47 and/or 48 at the extracellular interface of the first transmembrane domain of the receptor [26]. Fluorescence spectroscopy studies indicate that the side chain of Lys⁷ most likely faces toward a pocket formed by the extracellular loops and that this pocket has both apolar and polar character [34]. In

addition, the side chain of Trp³ is in a hydrophobic cavity based on fluorescence analyses (Ding, Becker, and Naider, unpublished results), and previous studies with position 1 analogs also indicate a strong preference for a large hydrophobic residue at the amino-terminal position of the pheromone [35]. This latter result taken together with the present photolabeling analysis suggests that cross-linking occurs with residues that are at, or slightly below, the extracellular interface of transmembrane helices 6 and/or 7 of Ste2p. Finally, biophysical evidence exists supporting a bend around the Pro-Gly center of α -factor as the biologically relevant conformation of the pheromone. In total, these results allow us to develop a crude two-dimensional model for fitting the tridecapeptide into the pheromone binding site. The working model has a contact of Gln¹⁰ with residues S47 and/or T48, a contact of residues 1 and 3 with F262 and/or Y266, and a β -turn around the Pro-Gly sequence in the center of α -factor. Recent studies indicate that F262 and Y266 are important for α -factor binding and activity [36]. Additional features of the bound structure should be forthcoming as further refinements of side chain contacts using the other photoactivatable analogs and site-directed mutagenesis studies currently carried out in our laboratory progresses.

The results presented in this part represent the first direct evidence of contact between the α -factor ligand and a domain of the Ste2p receptor. Additionally, this is the first study to use Bpa photo-cross-linkable probes to study ligand-receptor interaction in class IV GPCRs. Future studies should allow for identification of a residue or residues that cross-link to the α -factor probe used in this study. These results along with planned studies to use a series of α -factor probes that will place cross-linkable moieties at various

positions in the pheromone should allow for mapping of the ligand binding site of the Ste2p receptor. Results from such studies have the potential to provide key insight into peptide ligand mediated activation of GPCRs by identifying contact residues.

Identification of the contact residues would be useful in assigning structure-function relationships between the α -factor pheromone and Ste2p and compare the results to information gained from other classes of GPCRs.

List of References for Part II

1. Venter, J.C., et al., *The sequence of the human genome*. Science, 2001. 291(5507): p. 1304-51.
2. Lander, E.S., et al., *Initial sequencing and analysis of the human genome*. Nature, 2001. 409(6822): p. 860-921.
3. Fong, T.M. and C.D. Strader, *Functional mapping of the ligand binding sites of G-protein coupled receptors*. Med Res Rev, 1994. 14(4): p. 387-99.
4. Dorman, G. and G.D. Prestwich, *Using photolabile ligands in drug discovery and development*. Trends Biotechnol, 2000. 18(2): p. 64-77.
5. Dong, M., et al., *Identification of an interaction between residue 6 of the natural peptide ligand and a distinct residue within the amino-terminal tail of the secretin receptor*. J Biol Chem, 1999. 274(27): p. 19161-7.
6. Behar, V., et al., *Direct identification of two contact sites for parathyroid hormone (PTH) in the novel PTH-2 receptor using photoaffinity cross-linking*. Endocrinology, 1999. 140(9): p. 4251-61.
7. Hadac, E.M., et al., *Direct identification of a second distinct site of contact between cholecystokinin and its receptor*. J Biol Chem, 1998. 273(21): p. 12988-93.
8. Mouldous, L., et al., *Direct identification of a peptide binding region in the opioid receptor-like 1 receptor by photoaffinity labeling with [Bpa(10),Tyr(14)]nociceptin*. J Biol Chem, 2000. 275(38): p. 29268-74.

9. Boucard, A.A., et al., *Photolabeling identifies position 172 of the human AT(1) receptor as a ligand contact point: receptor-bound angiotensin II adopts an extended structure*. *Biochemistry*, 2000. 39(32): p. 9662-70.
10. Shoelson, S.E., et al., *BpaB25 insulins. Photoactivatable analogues that quantitatively cross-link, radiolabel, and activate the insulin receptor*. *J Biol Chem*, 1993. 268(6): p. 4085-91.
11. Bitan, G., et al., *Mapping the integrin alpha V beta 3-ligand interface by photoaffinity cross-linking*. *Biochemistry*, 1999. 38(11): p. 3414-20.
12. Blumer, K.J. and J. Thorner, *Receptor-G protein signaling in yeast*. *Annu Rev Physiol*, 1991. 53: p. 37-57.
13. Dohlman, H.G., et al., *Model systems for the study of seven-transmembrane-segment receptors*. *Annu Rev Biochem*, 1991. 60: p. 653-88.
14. Koelle, M.R., *A new family of G-protein regulators - the RGS proteins*. *Curr Opin Cell Biol*, 1997. 9(2): p. 143-7.
15. Dohlman, H.G., et al., *Sst2, a negative regulator of pheromone signaling in the yeast *Saccharomyces cerevisiae*: expression, localization, and genetic interaction and physical association with Gpa1 (the G-protein alpha subunit)*. *Mol Cell Biol*, 1996. 16(9): p. 5194-209.
16. Dube, P., A. DeCostanzo, and J.B. Konopka, *Interaction between transmembrane domains five and six of the alpha -factor receptor*. *J Biol Chem*, 2000. 275(34): p. 26492-9.

17. David, N.E., et al., *Expression and purification of the Saccharomyces cerevisiae alpha-factor receptor (Ste2p), a 7-transmembrane-segment G protein-coupled receptor*. J Biol Chem, 1997. 272(24): p. 15553-61.
18. Shenbagamurthi, P., et al., *Biological activity and conformational isomerism in position 9 analogues of the des-1-tryptophan,3-beta-cyclohexylalanine-alpha-factor from Saccharomyces cerevisiae*. Biochemistry, 1985. 24(25): p. 7070-6.
19. Abel, M.G., et al., *Structure-function analysis of the Saccharomyces cerevisiae tridecapeptide pheromone using alanine-scanned analogs*. J Pept Res, 1998. 52(2): p. 95-106.
20. Raths, S.K., F. Naider, and J.M. Becker, *Peptide analogues compete with the binding of alpha-factor to its receptor in Saccharomyces cerevisiae*. J Biol Chem, 1988. 263(33): p. 17333-41.
21. Aletras, A., et al., *Preparation of the very acid-sensitive Fmoc-Lys(Mtt)-OH. Application in the synthesis of side-chain to side-chain cyclic peptides and oligolysine cores suitable for the solid-phase assembly of MAPs and TASP s*. Int J Pept Protein Res, 1995. 45(5): p. 488-96.
22. Kippert, F., *A rapid permeabilization procedure for accurate quantitative determination of beta-galactosidase activity in yeast cells*. FEMS Microbiol Lett, 1995. 128(2): p. 201-6.
23. Cheng, Y. and W.H. Prusoff, *Relationship between the inhibition constant (K_I) and the concentration of inhibitor which causes 50 per cent inhibition (I₅₀) of an enzymatic reaction*. Biochem Pharmacol, 1973. 22(23): p. 3099-108.

24. Jiang, Y., et al., *Synthesis of alpha-factor analogues containing photoactivatable and labeling groups*. Int J Pept Protein Res, 1995. 45(2): p. 106-15.
25. Liu, S., et al., *Position 13 analogs of the tridecapeptide mating pheromone from Saccharomyces cerevisiae: design of an iodinated ligand for receptor binding*. J Pept Res, 2000. 56(1): p. 24-34.
26. Lee, B.K., et al., *Identification of residues of the Saccharomyces cerevisiae G protein-coupled receptor contributing to alpha-factor pheromone binding*. J Biol Chem, 2001. 276(41): p. 37950-61.
27. Elliott, J.T., et al., *Tritiated photoactivatable analogs of the native human thrombin receptor (PAR-1) agonist peptide, SFLLRN-NH2*. J Pept Res, 2001. 57(6): p. 494-506.
28. Naider, F. and J.M. Becker, *Structure-activity relationships of the yeast alpha-factor*. CRC Crit Rev Biochem, 1986. 21(3): p. 225-48.
29. Masui, Y., et al., *Amino acid substitution of mating factor of Saccharomyces cerevisiae structure-activity relationship*. Biochem Biophys Res Commun, 1979. 86(4): p. 982-7.
30. Siegel, E.G., et al., *Characterization of novel peptide agonists of the alpha mating factor of Saccharomyces cerevisiae*. Anal Biochem, 1999. 275(1): p. 109-15.
31. Konopka, J.B., D.D. Jenness, and L.H. Hartwell, *The C-terminus of the S. cerevisiae alpha-pheromone receptor mediates an adaptive response to pheromone*. Cell, 1988. 54(5): p. 609-20.
32. Bukusoglu, G. and D.D. Jenness, *Agonist-specific conformational changes in the yeast alpha-factor pheromone receptor*. Mol Cell Biol, 1996. 16(9): p. 4818-23.

33. Fontana, A., *Modification of tryptophan with BNPS-skatole (2-(2-nitrophenylsulfenyl)-3-methyl-3-bromoindolenine)*. Meth Enzymol, 1972. 25: p. 419-423.
34. Ding, F.X., et al., *Probing the binding domain of the Saccharomyces cerevisiae alpha-mating factor receptor with fluorescent ligands*. Biochemistry, 2001. 40(4): p. 1102-8.
35. Zhang, Y.L., et al., *Position one analogs of the Saccharomyces cerevisiae tridecapeptide pheromone*. J Pept Res, 1997. 50(5): p. 319-28.
36. Lee, B.K., et al., *Tyr266 in the sixth transmembrane domain of the yeast alpha-factor receptor plays key roles in receptor activation and ligand specificity*. Biochemistry, 2002. 41(46): p. 13681-9.

PART III

Identification of Ligand Binding Regions of the *Saccharomyces cerevisiae* α -factor Pheromone Receptor (Ste2p) by Photo-affinity

Cross-linking

Part III presents collaborative work with Dr. Fred Naider's laboratory at the City University of New York, Staten Island. Cagdas D. Son performed all the studies in this part with the exception of synthesis of the peptides used in this study. The peptide syntheses were carried out by Hasmik Sargsyan in Dr. Naider's laboratory. This part, excluding the portions describing optimization of cross-linking and site-directed mutagenesis of Ste2p residues 54-58, has been submitted for publication in Biochemistry.

CHAPTER 1

Introduction

The yeast *Saccharomyces cerevisiae* is a sexual organism that manifests a conjugative response when opposite mating type cells, *MATa* and *MAT α* , are mixed together (For Reviews see [1-5]). The mating reaction is initiated by stimulation of cell surface receptors on each cell type by a polypeptide pheromone secreted from cells of the opposite mating type. Ste2p is a G protein-coupled receptor (GPCR) expressed on the surface of haploid cells of mating type *MATa*, which is involved in this initiation event. Binding of the α -factor tridecapeptide mating pheromone (Trp-His-Trp-Leu-Gln-Leu-Lys-Pro-Gly-Gln-Pro-Met-Tyr), secreted by the mating type *MAT α* , to Ste2p activates the pheromone-signaling pathway by promoting dissociation of a coupled heterotrimeric G protein into its constituent α subunit and $\beta\gamma$ subunit complex on the cytoplasmic side of the plasma membrane. The activation of the receptor leads to a series of events including G₁ growth arrest, cellular elongation, gene induction, agglutinin biosynthesis and ultimately cell fusion with the opposite mating type *MAT α* cells.

GPCRs constitute a major family of human proteins [6]. To date more than 1,000 GPCRs have been identified, and these proteins recognize diverse signaling molecules including neurotransmitters, sensory molecules and chemotactic agents [7]. The ubiquitous nature of GPCRs together with their highly specific ligand recognition makes them an important target for therapeutic agents [8, 9]. Among the most important GPCR ligands are peptides including hormones, growth factors, and pheromones.

Understanding the molecular mechanism of peptide recognition by their cognate GPCRs may lead to design of novel peptide analogs for treatment of disorders involving defective ligands and/or mutant receptors.

Although there has been considerable literature on the GPCR ligand binding sites for small molecules like biogenic amines [10], relatively less information exists concerning the binding sites of peptide-responsive GPCRs. Photoreactive cross-linking studies, using 4-benzoyl-*L*-phenylalanine (Bpa)-containing peptide ligands, are a powerful complement to site-directed mutagenesis studies for mapping peptide-receptor interaction(s). Studies reported on parathyroid hormone (PTH), opioid receptor (ORL1) [11-17], substance P [18-20], cholecystokinin [21], and vasopressin [22] showed that Bpa-containing peptides can be successfully used for identification of receptor fragments that are interacting with photoactivatable peptide analogs. Recent work on human PTH receptor [23, 24], the secretin receptor [25], the ORL1 receptor [26] and human angiotensin type I receptor [27], showed that specific contact residues can be mapped after photoaffinity labeling by sequencing of the cross-linked fragment and site-directed mutagenesis in the region of cross-linking. A new method called the methionine proximity assay took advantage of modified analogs of Bpa, e.g. *p*-nitro-benzoyl-phenylalanine (NO₂Bpa), that have selectivity for methionine residues [28]. This unique property allowed the identification of a contact site by methionine scanning of the putative contact residues of three GPCRs, followed by analysis of the cross-linked receptor. All of these studies using Bpa-analogs revealed that generation of covalently linked ligand-receptor conjugates has become a valuable tool for the identification of the

cross-linked domains allowing mapping of the interface between a peptide ligand and its GPCR [29].

In part II of this dissertation, a general approach to directly identify the interaction between position 1 of α -factor and a region between residues 251-294 of the receptor Ste2p was reported [30]. However, this study was limited to the use of only one Bpa- α -factor analog. Similarly in this part (part III) the evaluation of a series of biotinylated photoactivatable analogs containing Bpa at various positions throughout the α -factor pheromone was described. An important aspect of the present part is the use of biotin as a tag allowing detection of cross-linking using avidin based chromophores and eliminating problems previously encountered with radioactive iodine [30]. Four analogs studied were selectively cross-linked into the α -factor binding site of Ste2p. Chemical and enzymatic fragmentation of the cross-linked receptor allowed the identification of contacts between the position 3 and 13 side chains of the pheromone and Ste2p residues in the EL2-TM5 and/or TM6-EL3-TM7 region and first transmembrane domain, respectively. In addition, interaction of position 1 of α -factor with a region of Ste2p covering residues 251-294 was confirmed.

CHAPTER 2

Materials and Methods

Organisms:

S. cerevisiae DK102 [MATa *ste2::HIS3 bar1 leu2 ura3 lys2 ade2 his3 trp1*] transformed with pNED1[*STE2*] [31] was used in binding studies and in the growth arrest assays of various α -factor analogs. Strain BJ2168 was used as parental strain to construct BJS21 by deleting *STE2* using the kanamycin deletion cassette according to a standard protocol [32]. BJS21 [MATa *ste2::Kan^R, prc1-407, prb 1-1122, pep4-3, Leu2, trp1, ura 3-52*] strain transformed with pNED1 [*STE2*] was used in cross-linking studies. Strain LM102 [33] [MATa *ste2::HIS3 bar1 leu2 ura3 lys2 ade2 his3 trp1*] transformed with pGA314.Cys-less.STE2.FT.HT [34] was used for generating site directed Ala mutations between residues M54 and R58 of Ste2p. All strains used had similar binding of α -factor. However, the BJS21 pNED strain lacked several peptidases, so it was used to increase the yield of Ste2p in experiments involving cross-linking.

Chemical Reagents:

All reagents and solvents used for the solid-phase peptide synthesis of the photoactivatable peptides were analytical grade and were purchased from Advanced Chem. Tech. (Louisville, KY), VWR Scientific (Piscataway, NJ), or Aldrich Chemical Co. (Milwaukee, WI). High-performance liquid chromatography (HPLC) grade

dichloromethane (CH₂Cl₂), acetonitrile (ACN), methanol (MeOH), and water were purchased from VWR Scientific and Fisher Scientific (Springfield, NJ).

Synthesis of N- α -Fmoc-Protected α -factor Analogs:

N- α -Fmoc-protected α -factor analogs needed for the preparation of their biotinylated derivatives were synthesized by solid-phase peptide synthesis on an Applied Biosystems 433A peptide synthesizer (Applied Biosystems, Foster City, CA) starting with N- α -Fmoc-Tyr(OBu^t) - or N- α -Fmoc-Bpa-Wang resin (0.7 mmol/g substitution, Advanced ChemTech, Louisville, KY). In all of the peptides, *L*-norleucine (Nle), which is isosteric with *L*-methionine, was incorporated at position 12 to replace the naturally occurring *L*-methionine to prevent oxidation of the sulfur atom of this amino acid during peptide synthesis and purification. Replacement of Met by Nle was shown previously to result in an analog with equal activity and receptor affinity to that of the native pheromone [35]. Since all analogs have Nle in place of Met¹², this residue is eliminated from the abbreviated names for simplicity. The 0.1 mmol FastMoc chemistry of Applied Biosystems was used for the elongation of the peptide chain with an HBTU/HOBt/DIEA-catalyzed, single coupling step using 10 equiv of protected amino acids for 30 min. Upon completion of chain assembly the N- α -Fmoc group was not removed from the peptide chain.

Cleavage, Purification and Characterization of Peptides:

Cleavage, purification and characterization of the peptides were carried out as detailed in material methods chapter, Part II of this dissertation. Briefly, the N- α -Fmoc-protected peptidyl resin was washed thoroughly with 1-methyl-2-pyrrolidinone and dichloromethane and dried in vacuum. The peptide was cleaved from the resin support with simultaneous side chain deprotection using a cleavage cocktail at room temperature for 1.5 hour with the omission of 1,2-ethanedithiol in the cleavage reaction, to transform Bpa-containing peptides to cyclic dithioketal derivatives [36]. The filtrates from the cleavage reaction were collected, combined with trifluoroacetic acid washes of the resin, concentrated under reduced pressure, and treated with cold ether to precipitate the crude product.

The crude peptide so obtained was purified by reversed phase HPLC (Hewlett-Packard Series 1050) on a semi-preparative Waters μ -Bondapack C₁₈ (19 x 300 mm) column with detection at 220 nm. The fractions were collected and analyzed at 220 nm by reversed phase HPLC (Hewlett-Packard Series 1050) on an analytical Waters μ -Bondapack C₁₈ (3.9 x 300 mm) column. Fractions of over 99% homogeneity were pooled and subjected to lyophilization. The purity of the final peptide was assessed by analytical HPLC using two different solvent systems (10- 55% acetonitrile gradient, 15 min, with 0.025% trifluoroacetic acid; and 50-80% methanol gradient, 30 min, with 0.025% trifluoroacetic acid) and ESI-MS (Hunter College, CUNY).

Biotinylation of N- α -Fmoc-protected α -factor analogs:

Biotinylation of N- α -Fmoc-protected α -factor analogs was carried out using biotinylamidocaproate-N-hydroxysuccinimide ester (Sigma). The N- α -Fmoc-protected α -factor analog (10.0 mg, 5 μ mol) was dissolved in 0.5 ml of cold (0 °C) DMF, then the same volume (0.5 ml) of cold buffer (Na₂B₄O₇, pH 9.5, 50mM) was added. The solution was stirred at 0 °C (ice bath) for 2 min., and 10.0 mg (20 μ mol) of biotinylamidocaproate-N-hydroxysuccinimide ester (Sigma) dissolved in 0.5 ml of cold DMF (0 °C) was added very slowly. Reaction was monitored by analytical reversed phase HPLC using a linear gradient of 20-70 % ACN in 30 min and when the starting peptide disappeared (20-40 min) 0.5ml of a 20% solution of piperidine in DMF was added, and the reaction mixture was stirred at room temperature for 30 min until the Fmoc-group was fully deprotected, as monitored by analytical HPLC. The reaction mixture was neutralized with acidified buffer (0.2 M HCl), and injected immediately onto a preparative HPLC column (conditions for preparative HPLC: 20-70% ACN in 150 min, column; Waters μ -Bondopack C₁₈, 19x300 mm). The main fraction was collected and lyophilized. The purity of the biotinylated peptide was > 99 % by analytical HPLC and the molecular weight of peptide was confirmed by mass spectral analysis. The overall recovery of purified biotinylated peptide was 85-90%.

Site-directed mutagenesis:

Oligonucleotide-directed mutagenesis of single-stranded phagemid DNA of pGA314.Cys-less.STE2.FT.HT [*STE2* gene with the wild-type cysteine residues (Cys59

and Cys292) replaced by alanine and containing the FLAG[®] and 6xHis tags on the C-terminus] was constructed as described previously [37, 38]. This construct was shown to have full wild-type Ste2p activity as determined by binding and biological activities. Briefly, single-stranded DNA was prepared by infecting *E. coli* strain CJ236 (*ung⁻, dut⁻*) carrying the pGA314.Cys-less.STE2.FT.HT with the helper phage M13KO7 [39]. *In vitro* mutagenesis was performed on the single-stranded DNA using mutagenic oligonucleotides according to standard protocols. The product of the mutagenesis reaction mixture was transformed into DH5 α (Invitrogen) *E. coli* strain, and transformants were selected on ampicillin-containing plates. Plasmids were then isolated from transformants using the Wizard Miniprep kit (Promega). After sequencing of the isolated plasmids to confirm correct incorporation of the intended mutations, constructs were transformed into yeast strain LM102 (*ste2* deletion strain), and transformants were selected by their growth on medium lacking tryptophan.

Growth Arrest (Halo) Assay:

Solid MLT medium[40] as detailed in material and methods of Part II was overlaid with 4 mL of *S. cerevisiae* DK102pNED cell suspension (2.5×10^5 cells/mL of Nobel agar). Filter disks (sterile blanks from Difco), 8 mm in diameter, were presoaked with 10 μ L portions of peptide solutions at various concentrations and placed onto the overlay. The plates were incubated at 30 °C for 24-36 h and then observed for clear zones (halos) around the disks. The data were expressed as the diameter of the halo including the diameter of the disk. A minimum value for growth arrest is 9 mm, which represents the disk diameter (8 mm) and a small zone of inhibition. All assays were carried out at

least 3 times with no more than a 2 mm variation in halo size at a particular amount applied for each peptide. The values reported represent the mean of these tests.

Binding Competition Assay with [³H]α-Factor:

Competition binding assay was performed using strains DK102pNED and tritiated α-factor prepared by reduction of [dehydroproline⁸, Nle¹²]α-factor as described previously [35]. In general, cells were grown at 30 °C overnight and harvested at 1 x 10⁷ cells/mL by centrifugation at 5000g at 4 °C. The pelleted cells were washed 2 times in ice-cold buffer [PPBi: 0.5 M potassium phosphate (pH 6.24) containing 10 mM TAME, 10 mM sodium azide, 10 mM potassium fluoride, 1% BSA (fraction IV)] and resuspended to 4 x 10⁷ cells/mL. The binding assay was started by addition of [³H]α-factor (6 nM) and various concentrations of non-labeled peptide (140 μL) to a 560 μL cell suspension. Analog concentrations were adjusted using UV absorption at 280 nm and the corresponding extinction coefficients (Table 1). After 30 min incubation, triplicate samples of 200 μL were filtered and washed over glass fiber filtermats using the Standard Cell Harvester (Skatron Instruments, Sterling, VA) and placed in scintillation vials for counting. Each experiment was carried out at least 3 times with the results similar in each assay. The Ki values were calculated by using the equation of Cheng and Prusoff, where $K_i = IC_{50}/(1 + [ligand]/K_m)$ [41].

Binding Saturation Assay with [³H]α-Factor:

LM102 pGA314.Cys-less.STE2.FT.HT and various Ala mutants in this background strain were used in the saturation binding assay. In these assays, various concentrations of [³H]α-factor were added to the cell suspension prepared as described in competition binding assay part. Specific binding was determined by subtracting counts associated with the LM102 (*STE2* deletion) strain from counts bound to the strains harboring WT or mutant receptors. Each experiment was carried out at least three times with similar results. Nonspecific binding of labeled α-factor to filters in the absence of cells was less than 20 counts/min. Data curves for competition and saturation binding assays were fitted from at least eight triplicate data points using PrismTM software (GraphPad) with nonlinear regression one site saturation hyperbola equation.

Optimization of Cross-linking conditions:

10 μl of membranes (22 mg/ml of total protein, prepared according to protocols previously described, see PART II of this dissertation) derived from cells with a deletion in the α-factor receptor encoding gene *STE2* (BJS21) and membranes from these same cells transformed with a plasmid (pNED) encoding Ste2p (BJS21 pNED) were incubated with 975 μL of PPBi buffer (with 0.1%BSA) in siliconized microfuge tubes for 10 min at ambient temperature. Various concentrations (0, 0.3, 5.0, 10.0, and 20 μg/ml) of Bpa-scanned biotinylated α-factor analogs were added, and the reaction was incubated for 30 min at room temperature with gentle mixing. The reaction mixture was aliquoted into 3 wells of a chilled 24 well plastic culture plate preblocked with PPBi (0.1% BSA).

Division of the reaction mixtures into separate wells kept the depth of the samples minimal for efficient UV penetration of the sample. The samples were held at 4 °C and irradiated without the culture plate lid at 365 nm for 5, 15, 20, 25, 45, 60, and 90 min at a distance of 12 cm in a Stratlinker (Stratagene, La Jolla, CA). Membrane samples were recombined in siliconized microfuge tubes and washed twice by centrifugation (14000g) with PPBi (0.1% BSA). Membrane pellets were dissolved in 5µl sample buffer (0.25 M Tris-HCl, pH 8.8, 0.005% bromphenol blue, 5% glycerol, 1.25% β-mercaptoethanol, 2% SDS). Samples were heated to 37 °C for 10 min and separated by SDS-PAGE (10% gel; 30 mA). After transfer to a PVDF membrane blots were analyzed with NA-HRP conjugate (from Pierce).

Cross-Linking of α-factor analogs to Ste2p:

Membranes (220 µg/ml of total protein) from BJS21, BJS21 pNED strains [31], and LM102 pGA314.Cys-less.STE2.FT.HT strains carrying various Ala mutants were incubated with 975 µL of PPBi buffer (with 0.1%BSA) in siliconized microfuge tubes for 10 min at ambient temperature. Bpa scanned biotinylated α-factor analogs (10 to 20 nM) were added, and the reaction was incubated for 30 min at room temperature with gentle mixing. The reaction mixture was aliquoted into 3 wells of a chilled 24 well plastic culture plate preblocked with PPBi (0.1% BSA). Division of the reaction mixtures into separate wells kept the depth of the samples minimal for efficient UV penetration of the sample. The samples were held at 4 °C and irradiated without the culture plate lid at 365 nm for 1 h at a distance of 12 cm in a Stratlinker (Stratagene, La Jolla, CA). Membrane

samples were recombined in siliconized microfuge tubes and washed twice by centrifugation (14000g) with PPBi (0.1% BSA). Membrane pellets were dissolved in 5 μ l sample buffer (0.25 M Tris-HCl, pH 8.8, 0.005% bromphenol blue, 5% glycerol, 1.25% β -mercaptoethanol, 2% SDS). Samples were heated to 37 °C for 10 min and separated by SDS-PAGE (10% gel; 30 mA). In competition cross-linking experiments, 100x cold α -factor was added together with biotinylated peptide. For subsequent receptor digestion analysis, the band between 45 and 60 kDa covering cross-linked Ste2p mass was excised and placed into dialysis tubing (30000 molecular weight cutoff) with buffer (0.2 M Tris-acetate, pH 7.4, 1.0% SDS, 100 mM dithiothreitol). Electro-elution was performed by placing dialysis tubing that contains the gel in a horizontal electrophoresis chamber with running buffer (50 mM Tris-acetate, pH 7.4, 0.1% SDS, 0.5 mM sodium thioglycolate). Elution was carried out at 100 V for 3 h. The buffer in the dialysis tubing was transferred to a Millipore Ultrafree-15 centrifuge filter device (30 000 molecular weight cutoff) and concentrated by centrifugation. Concentrated sample was washed 3 times with 50 mM Tris-HCl, pH 7.5. The cross-linked samples were resolved with SDS-PAGE, transferred to a PVDF membrane and assayed for the detection of proteins that are covalently linked with biotinylated analogs with NeutrAvidin-HRP conjugate (NA-HRP) (Pierce). All the gels used in these blots were analyzed by staining with coomassie blue to ensure efficient transfer of the protein to the membrane.

Digestion of Cross-Linked Ste2p:

Cross-linked samples were digested with CNBr, trypsin, or BNPS-skatole. For CNBr digestion, samples were dissolved in 70% formic acid, and 200 mg/ml of CNBr

were added. For trypsin digestion, samples were dissolved in trypsin digestion buffer (100 mM Tris-HCl, pH 8.5), and 6.25 μ g of trypsin (Sequencing Grade modified trypsin, Roche) was added to 250 μ g of total proteins. After 6 hr of incubation a second batch of trypsin (6.25 μ g) is added to achieve complete digestion. Ste2p contains a lysine residue (K269) followed by a proline residue (P270) in the extracellular loop 3, which makes it less likely to be digested by trypsin. Nevertheless, we found that this region is reproducibly susceptible to trypsin digestion under the conditions described above. For BNPS-skatole digestion, samples were dissolved in 50% acetic acid with addition of 10mg/ml BNPS-skatole. To prevent anomalous cleavage of Ste2p at histidine and tyrosine residues, tyrosine at 100-fold molar excess was added to the reaction mixture during BNPS-skatole digestion [42]. Deglycosylated samples for BNPS-skatole digestion were prepared by treatment with PNGaseF (500 units/ μ l, BioLabs). Briefly, \sim 10 μ l of partially purified Ste2p-containing membrane proteins (1 μ g/ μ l) was incubated with 5 μ l of 10x glycoprotein denaturing buffer (5% SDS, 10% β -mercaptoethanol) at 100 °C for 10 min. After 10 min, 5 μ l of 10x G7 buffer (0.5M sodium phosphate, pH=7.5) and 5 μ l of 10% NP-40 were added. Finally, 5 μ l PNGase F and 20 μ l of water was added (total volume, 50 μ l) and incubated at room temperature overnight. All digestion reactions took place under nitrogen and complete darkness at 37°C. After digestion, samples were dried by vacuum centrifugation, resuspended in 50 μ L of 0.5 M Tris, pH 8.25, and re-dried. The digested samples were dissolved in loading buffer (Bio-Rad) and resolved on 12% NuPAGE Bis-tris gels with MES running buffer (Invitrogen).

CHAPTER 3

Results

Synthesis of α -factor analogs:

N- α -Fmoc protected α -factor analogs containing Bpa¹, Bpa³, Bpa⁵, Bpa⁸, or Bpa¹³ were prepared by automated solid phase synthesis using standard coupling and deprotection protocols. During several of the syntheses we noted partial Fmoc removal occurred using the “complete wash protocol” of the Applied Biosystems 433A synthesizer. This problem was eliminated by washing only with DCM. N- α -Fmoc-protected Bpa-containing α -factor analogs were purified by semi-preparative HPLC (Waters μ -Bondopack C₁₈, 125Å, 19x300mm, gradient 20-60% acetonitrile in 150 min). After lyophilization they were used in the synthesis of the corresponding biotinyl-amidocaproate (BioACA) derivatives. Thus all biotinylated analogs used in this part of the dissertation were biotinylated at the epsilon amine of Lys⁷ and a spacer was used to ensure that the biotin group was available to the avidin detection protein. The final products containing both Bpa and biotin were more than 99% pure as determined by analytical reversed-phase HPLC and had the expected molecular weight (Table 1).

Receptor Affinities of Bpa-Scanned Biotinylated α -factor analogs:

α -factor analogs that bind tightly to the pheromone receptor (Ste2p) were essential to achieve an efficient cross-linking. Studies detailed in part II showed that Bpa

Table 1: Biotinylation yield for α -factor analogs. Table represents yields of biotinylation and results of mass spectral analysis

Bpa^x, Lys⁷(biotinylamidocaproate)α-factor-analogs	Yield of biotinylated product (%)	Purity (%) by HPLC	E₂₈₀^a	M.W. (Calculated)	ESI-MS^b
Bpa¹, K⁷(biotinylamidocaproate), Nle¹², Y¹³-α-factor [Bpa¹]	51.0% ^c	>99%	14000	2070	2070.2
Bpa³, K⁷(biotinylamidocaproate), Nle¹², Y¹³-α-factor [Bpa³]	89.9%	>99(%)	14000	2070	2070.2
Bpa⁵, K⁷(biotinylamidocaproate), Nle¹², Y¹³-α-factor [Bpa⁵]	90.2%	>99(%)	19500	2128	2127.7
Bpa⁸, K⁷(biotinylamidocaproate), Nle¹², Y¹³-α-factor [Bpa⁸]	86.2%	>99(%)	19500	2159	2159.0
Bpa¹³, K⁷(biotinylamidocaproate), Nle¹²-α-factor [Bpa¹³]	84.1%	>99(%)	18000	2093	2093.0

^a The extinction coefficients were calculated by the DNASTAR™ program (Lasergene, Madison, WI) on the basis of the peptide sequence.

^b Mass-spectral analysis of biotinylated analogs were performed by Dr.Cliff Soll, Hunter College,CUNY

^c This synthesis was not optimized.

replacements were well tolerated at positions 1(Trp), 3(Trp), 5(Gln), 7(Lys), 8(Pro), 12(Met), and 13(Tyr) of α -factor pheromone with K_i values indicating poorer binding from 4-fold to 45-fold in comparison to α -factor [30]. Based on these data and our current working model for pheromone binding to receptor [43], we chose photo-cross-linkable analogs with Bpa at positions 1, 3, 5, 8, and 13 to determine contact points between the peptide and its receptor. This placed potential crosslink sites in side chains throughout the pheromone. The position seven side-chain was used for the biotin tag for detection purposes [44].

Binding affinities of the Bpa-scanned biotinylated α -factor analogs were determined by measuring their ability to compete with [^3H] α -factor as described under Experimental Details. Analogs containing Bpa¹ and Bpa⁵ exhibited only a 3- to 4-fold reduction in binding affinity compared to native α -factor (Figure 1). The binding affinity for Bpa¹³ was relatively poor (~12 fold lower than wild type). [Bpa⁸] α -factor showed very poor competition and did not compete fully at the highest concentration tested making the binding affinity for this analog only an estimate. [Bpa³] α -factor exhibited a comparatively intermediate binding of ~40 nM, although this is also only an estimate as full competition did not occur at the highest concentration tested.

Bioactivities of Bpa-Scanned Biotinylated α -factor analogs:

For the cross-linking studies to relate to a biologically relevant receptor-ligand interaction it is important to determine whether the ligand has biological activity. Therefore, the ability of the Bpa-scanned biotinylated α -factor analogs, used in this part

Competiton binding Assay

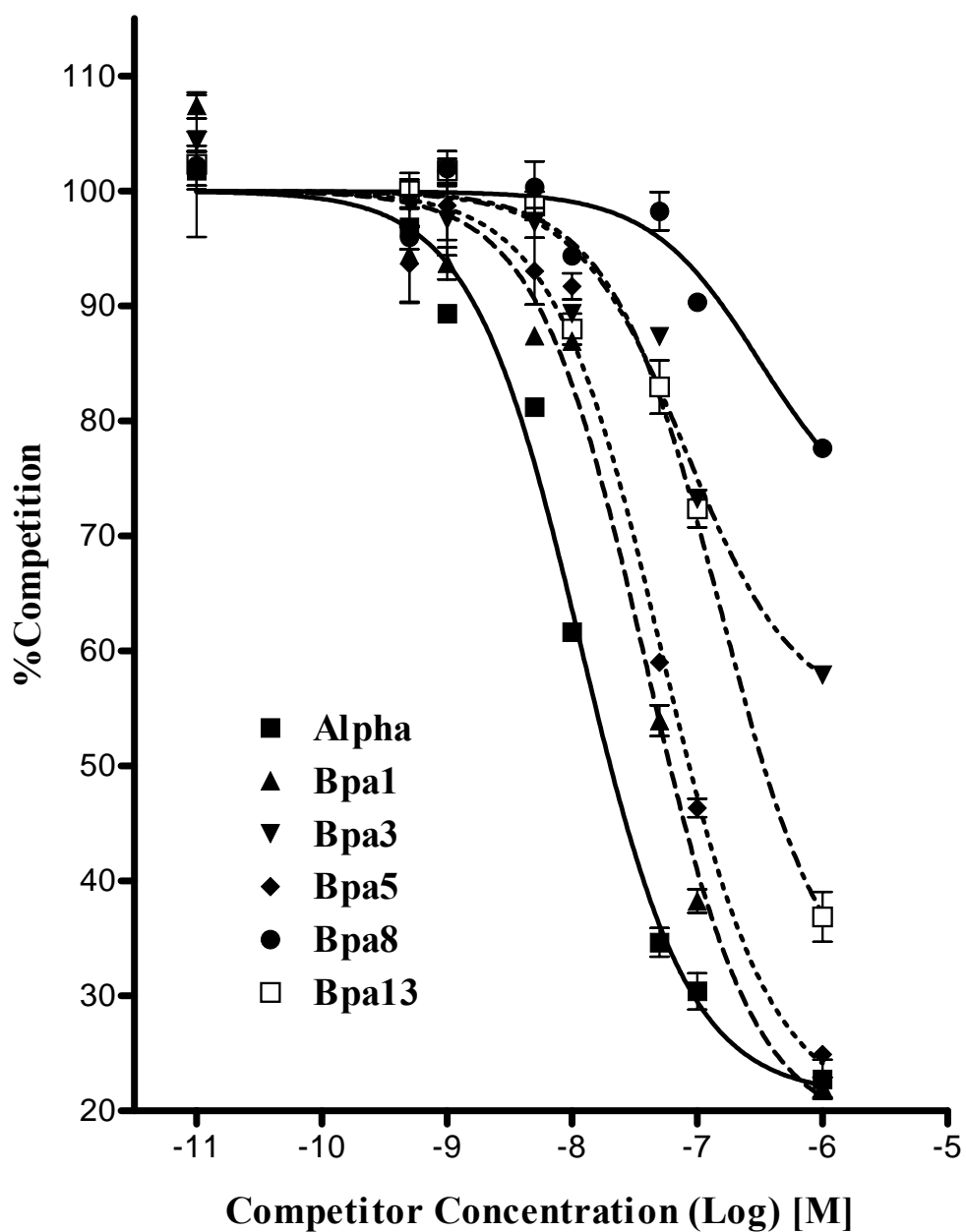


Figure 1: Competition binding assay of various α -factor analogs vs. tritiated α -factor. Competitors were cold α -factor (■), Bpa1 (▲), Bpa3 (▼), Bpa5 (◆), Bpa8 (●), and Bpa13 (□).

of the dissertation, to cause growth arrest in *MATa* as tested by growth arrest assay (Figure 2, Table 2). Semi-logarithmic plots of halo diameter versus amount of peptide applied to the disk were all linear and exhibited similar slopes (data not shown). All analogs used in this assay were stable to enzymatic cleavage under the conditions tested as strains used in this analysis lacked the Bar1p protease that cleaves α -factor. Therefore, the growth arrest data are indicative of the relative agonist activity of each peptide. The data show that the biotinylated peptides, where Bpa is at position 1, 3, 5, and 13 retained detectable agonistic activity, although the Bpa³, Bpa⁵, and Bpa¹³ pheromones had relatively low ability to trigger signal transduction (Table 2). On the other hand biotinylated [Bpa⁸] α -factor did result in a small halo (~2 mm around the filter disk) at the highest concentration (20 μ g/disk) used in this assay. None of the α -factor analogs induced growth arrest in a mutant lacking Ste2p (BJS21), confirming that the α -factor receptor was required for the biological activity of these peptides.

Optimization of Cross-linking of Bpa-Scanned Biotinylated α -factor analogs:

The cross-linking reaction between the photoactivatable Bpa group and the receptor is affected by the concentration of the reactants, temperature, and time. Throughout this study, temperature and the concentration of the receptor were kept constant, while the concentrations of Bpa-containing α -factor analogs and the time of UV irradiation varied. Following cross-linking under these various conditions, the yield was determined by the comparison of the signal intensities detected by NA-HRP blots.

Figure 2: Halo assay with Bpa-scanned biotinylated α -factor analogs. Various amounts (labeled on the disks [μg]) of α -factor analog were spotted on sterile filter disks placed on solid agar media and the growth arrest was quantified by measuring the diameter of the halo formed after 48 hr incubation at 30 °C.

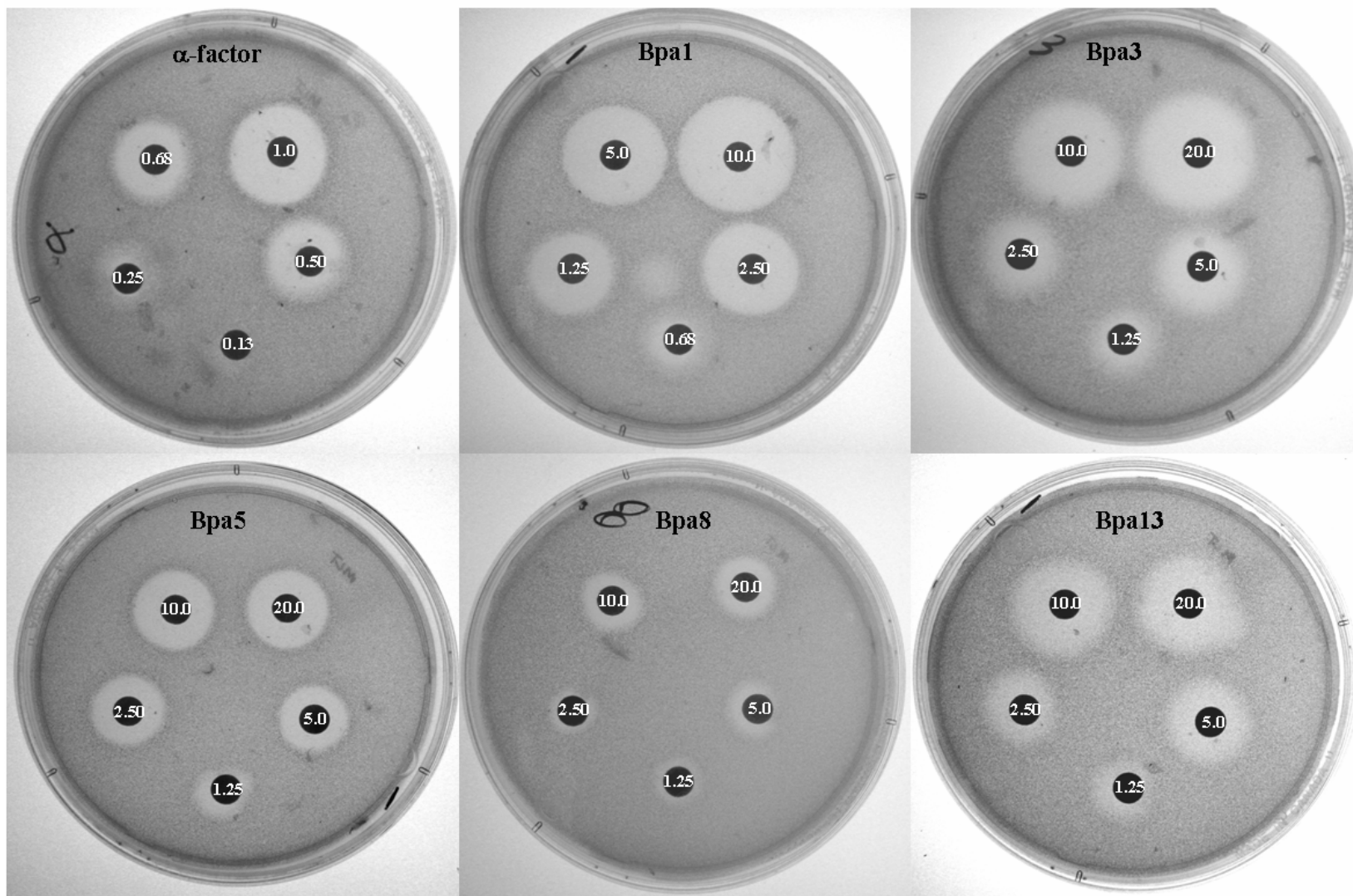


Table 2: Summary of receptor affinities and biological activities for Bpa-scanned biotinylated α -factor analogs.

Position of Bpa	WT	Bpa1	Bpa3	Bpa5	Bpa8	Bpa13
Ki [nM]	6	20	~40	25	~160	75
Biological Activity^a	0.4	1.5	3.5	9.4	~50 ^b	9
% affinity	100	30	15	24	~4	8
% activity	100	23	10	4	<1	5

^a Amount of analog (μg) needed to form 15 mm halo of growth arrest.

^b Out of linear range the highest amount (20 μg) tested in this assay gave only 13mm halo.

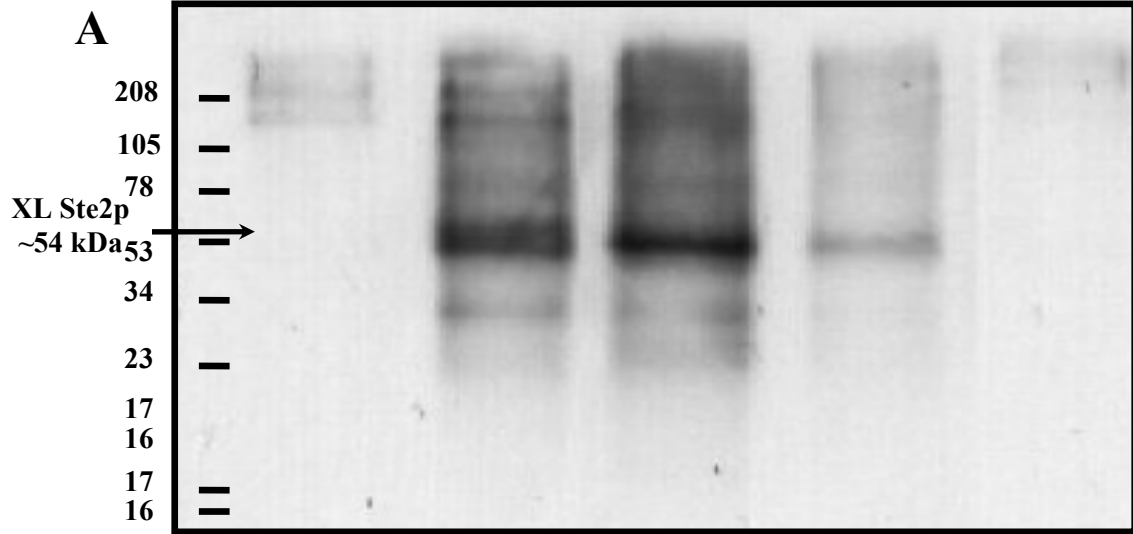
Figure 3a and 3b show representations of these studies carried out with the [Bpa¹] α -factor analog. Results for all the Bpa-containing analogs are summarized in table 3.

Cross-linking of Bpa-Scanned Biotinylated α -factor analogs to Ste2p:

The membranes derived from cells with a deletion in the α -factor receptor encoding gene *STE2* (BJS21) and membranes from these same cells transformed with a plasmid (pNED) encoding Ste2p (BJS21 pNED) were incubated with Bpa-scanned biotinylated α -factor analogs, and cross-linking was carried out using UV light (365 nm). BJS21 membranes were used as control in this experiment to check the possible interference from endogenous biotin signal and/or non-specific cross-linking products. Aliquots from each reaction mixture were removed following cross-linking and tested for incorporation of the biotinylated ligand to Ste2p by western blot analysis probed with NA-HRP (Figure 4). The cross-linked product (54 kDa), which migrated to the expected size of Ste2p (52 kDa) + α -factor analog (2 kDa) was detected in all lanes that contain cross-linked BJS21 pNED membranes, although the [Bpa⁸] α -factor analog exhibited a low degree of cross-linking consistent with its low biological activity and poor binding data. During the scanning of the film for preparation of the figure, a doublet seen for Ste2p on the original gels faded into the broader single band seen at ~54 kDa. No detectable signal was present on lanes loaded with BJS21 membranes (that lack Ste2p). In addition no cross-linked products were visible with samples that were not UV-irradiated (data not shown).

Figure 3: Optimization of the [Bpa¹]α-factor analog concentration and time for cross-linking. A) Different concentrations of [Bpa¹]α-factor analog were incubated with the membranes from BJS21 pNED strain (45 min. UV irradiation). B) Duration of UV irradiation was varied at constant concentration (10μg/ml) of [Bpa¹]α-factor analog. After cross-linking the samples were solubilized in sample buffer and resolved by 10% SDS-PAGE. Following the transfer of proteins to PVDF membranes cross-linking was identified by NA-HRP conjugate, which detected the biotin tag on the ligands.

[Bpa1]µg/ml	0	20	10	5	0.3
-------------	---	----	----	---	-----



Time (min)	90	60	45	25	20	15	5
------------	----	----	----	----	----	----	---

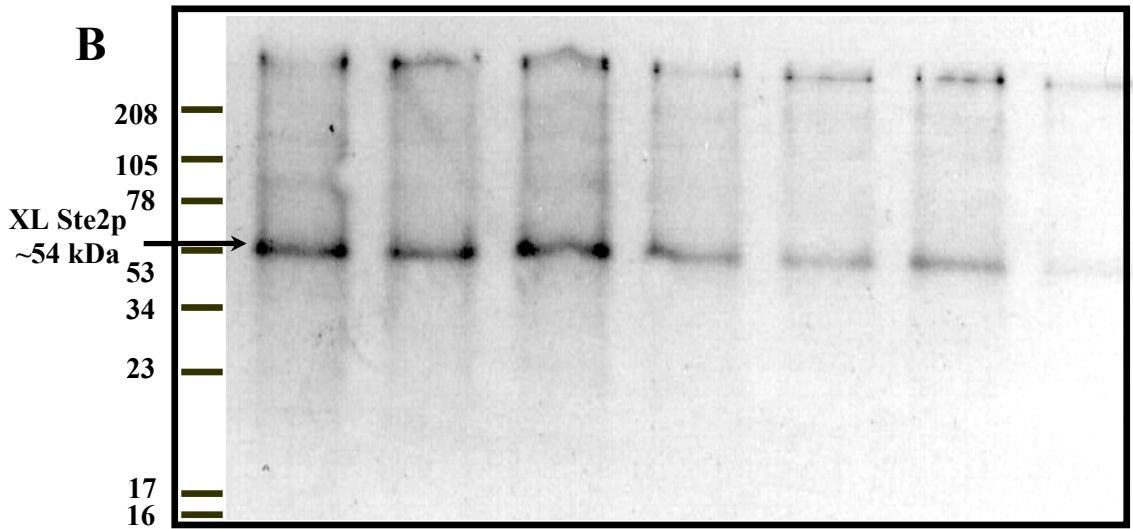


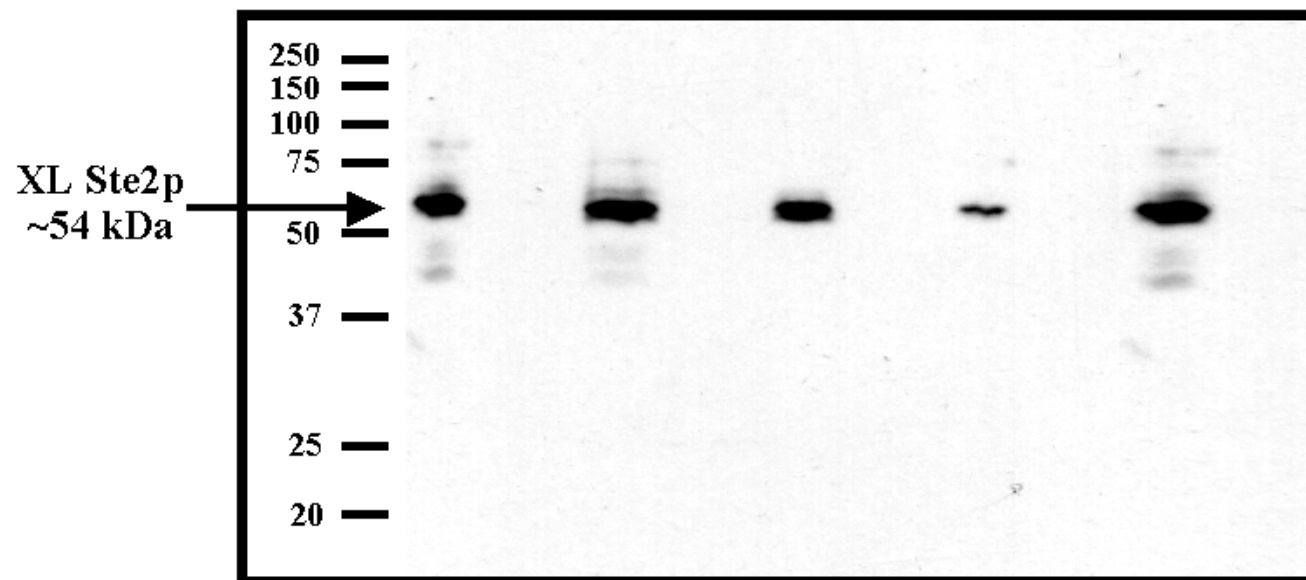
Table 3: Summary of the cross-linking optimization with Bpa scanned α -factor analogs.

Position of Bpa	Bpa1	Bpa3	Bpa5	Bpa8	Bpa13
Time for XL (min)	45	45	60	ND	30
Amount of Bpa Analog ($\mu\text{g/ml}$)	5	5	10	ND	3

ND: Due to the low binding affinity and poor biological activity this analog was not used in the optimization studies.

Figure 4: Western blot analysis of BJS21 pNED (expresses Ste2p), and BJS21 (Δ Ste2p) photo-cross-linked membranes. Membranes photo-cross-linked with various Bpa containing α -factor analogs were dissolved in Tricine sample buffer and resolved by Nu-PAGE 12% Bis-Tris gel. Proteins were transferred to a PVDF membrane and probed with NA-HRP to detect the biotin signal on the analog.

Bpa position	Bpa1		Bpa3		Bpa5		Bpa8		Bpa13	
Presence of Ste2p	+	-	+	-	+	-	+	-	+	-



In a follow up experiment, the BJS21 pNED membranes were co-incubated with Bpa-scanned biotinylated α -factor analogs and 100-fold molar excess of wild type α -factor pheromone (Figure 5). Results indicated that in the presence of excess α -factor pheromone the cross-linking of the biotinylated analogs was greatly diminished indicating that the cross-linking to Ste2p with the Bpa-scanned biotinylated α -factor analogs occurs at the α -factor binding site. Cross-linking of [Bpa⁸] α -factor was not blocked by addition of 100-fold molar excess of α -factor (data not shown). We concluded that the low amount of cross-linking observed with the Bpa⁸ analog (Figure 4) may not reflect interaction with the α -factor binding site. This conclusion is supported by the relatively poor competition of this analog for α -factor binding (Figure 1) and the poor biological activity of this analog (Table 2). Therefore, further investigations with this probe were discontinued. Cross-linking of [Bpa⁵] α -factor was blocked by excess α -factor, however, the amount of cross-linked product was very low in comparison to the amount of cross-linked product using Bpa¹, Bpa³, and Bpa¹³ analogs (Figure 5). Therefore, experiments using this analog were also discontinued. Cross-linking efficiency for Bpa¹, Bpa³, and Bpa¹³ analogs was estimated to be around 50% by comparison of the chemiluminescence signals from two different blots, one probed with NA-HRP (to detect cross-linked Ste2p by the reaction with the biotinylated analog) and the other probed with a FLAG[®] antibody detected by anti-mouse IgG HRP (Promega, to detect the total FLAG-tagged Ste2p; data not shown).

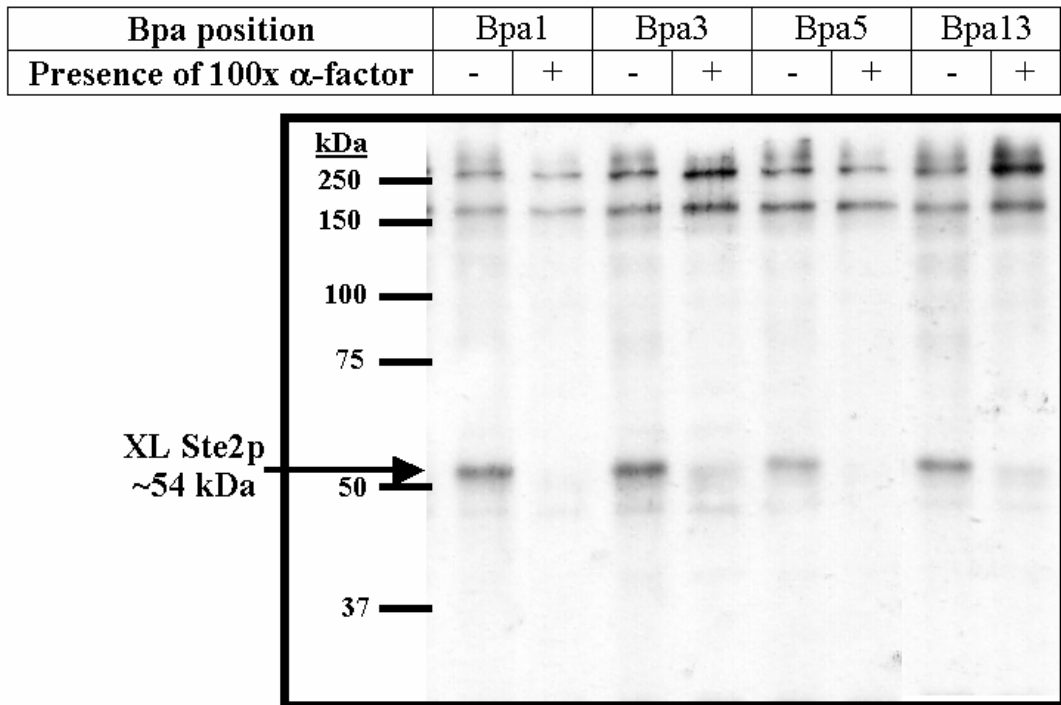


Figure 5: Western blot analysis of BJS21 pNED photo-cross-linked membranes in the presence or absence of excess α -factor. Membranes photo-cross-linked with various Bpa containing α -factor analogs either in the presence or in the absence of 100x excess wt. ligand and resolved by Nu-PAGE 12% Bis-Tris gel. Proteins were transferred to a PVDF membrane and probed with NA-HRP to detect the biotin signal on the analog.

Fragmentation Analysis of Cross-linked Ste2p:

Membranes containing Ste2p (BJS21 pNED) cross-linked with various Bpa-scanned analogs described in this part were resolved by preparative SDS-PAGE. Cross-linked Ste2p was electro-eluted from the gel and was treated with various cleavage agents to identify a fragment that covalently attached to the biotinylated ligand. Fragments of the cross-linked receptor were analyzed after Trypsin, CNBr and BNPS-skatole digestion to identify a putative Bpa¹, Bpa³, and Bpa¹³ cross-linked fragment(s). Trypsin digestion of the cross-linked receptor was carried out with sequencing grade trypsin at 37 °C for 16 hr. To monitor trypsin digestion, we used a T7 epitope-tagged Ste2p [45] and detected a ~4 kDa band (residues 270-303 +T7 tag) by T7 antibody instead of a ~8kDa band (residues 240-303 + T7-tag), indicating that the Lys-Pro site in the 3rd extracellular loop was susceptible to complete trypsin digestion under current digestion conditions (data not shown). A similar unexpected trypsin digestion at a Lys-Pro bond was observed by others [46]. Chemical cleavage was performed by CNBr or BNPS-skatole under strongly acidic conditions. BNPS-skatole digestion was carried out on native and deglycosylated Ste2p prepared by treatment of Ste2p with PNGase-F. These methods were previously used in our laboratory and applied by other groups in studies on Ste2p [30, 47, 48].

Trypsin digestion resulted in fragments around 5 kDa for both Bpa¹ and Bpa³ α -factor analogs whereas ~10 and ~8 kDa bands for Bpa¹³ α -factor were detected on the same blot (Figure 6). The theoretical digestion of Ste2p by trypsin shows multiple possible fragments that might correspond to 5 kDa after cross-linking with Bpa¹ or Bpa³ (Figure 7A). CNBr digestion of the cross-linked receptor was carried out to narrow down the putative cross-linked regions. Following CNBr digestion a band approximately 6 kDa

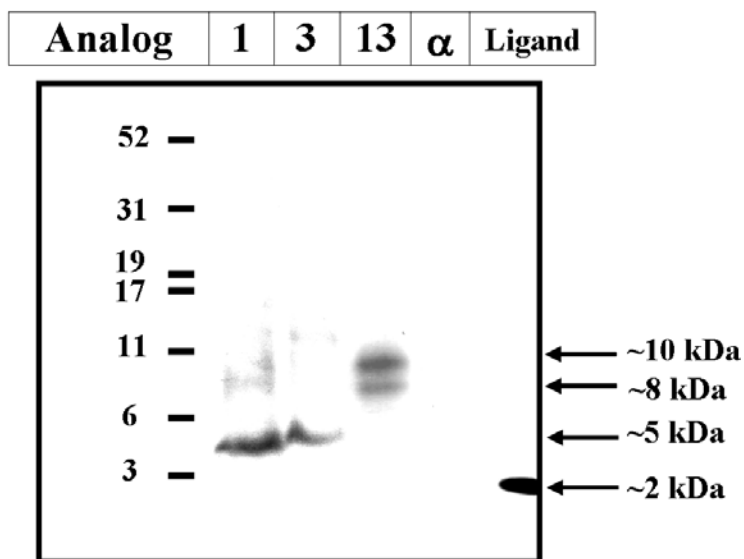
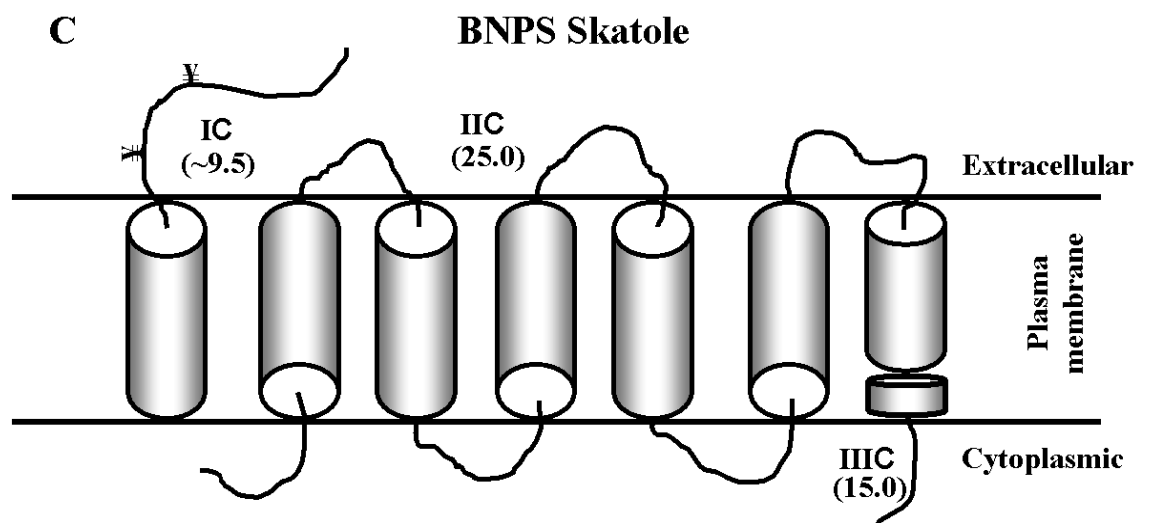
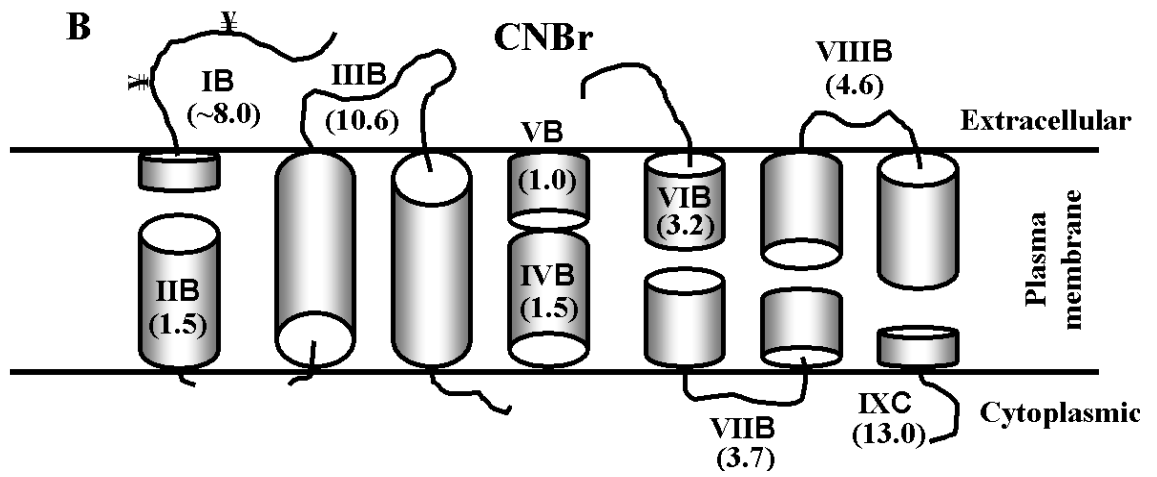
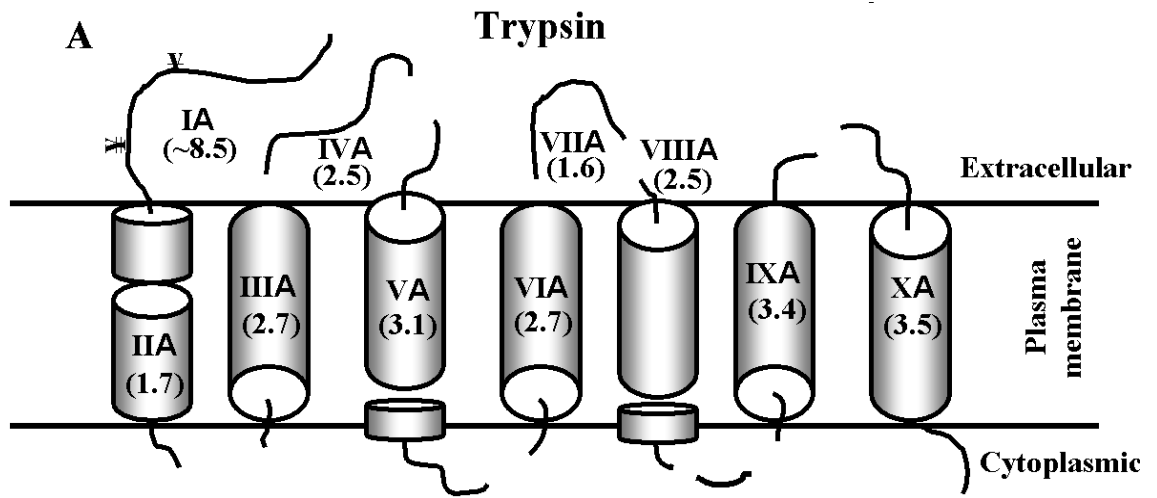


Figure 6: Western blot analysis of Trypsin digested BJS21 pNED photo-cross-linked membranes. Membranes photo-cross-linked with various Bpa containing α -factor analogs were digested with Trypsin and resolved by Nu-PAGE 12% Bis-Tris gel. Proteins were transferred to a PVDF membrane and probed with NA-HRP to detect the biotin signal on the analogs. Membranes, cross-linked with α -factor, were used as negative control, and ligand alone was used for positive control.

Figure 7: Schematic representation of receptor fragments after chemical or enzymatic cleavage of Ste2p. These figures represent the theoretical BNPS-skatole, Trypsin, and CNBr cleavage sites for the Ste2p receptor. For simplicity purposes the cytoplasmic tail is not represented in these cartoons. (Panel A) Represents the peptides resulting from a complete Trypsin digestion of Ste2p. (Panel B) Represents the receptor fragments generated after a complete CNBr cleavage of the receptor. (Panel C) Cleavage of the receptor by BNPS-skatole results in four fragments three of which represented IC (residues 1-70 of Ste2p), IIC (71-295), and IIIC (296-424). Molecular weights are represented on the figure in kDa. N-terminus fragments IA, IB, and IC contains two known N-linked glycosylation sites which adds ~2 kDa to these fragments thus the molecular weights for these fragments indicated as approximations.



was detected for both Bpa¹ and Bpa³ (Figure 8). This result in combination with the trypsin digestion narrows the possible cross-linking to two regions: VIB (190-218), or VIIIB (251-294) (Figure 7B), where the latter is in agreement with our previous findings for Bpa¹ [30]. CNBr digestion of Bpa¹³ cross-linked Ste2p resulted in a ~3 kDa band (Figure 8). The overlapping region of the two digestions (Trypsin and CNBr) corresponded to the region of Ste2p between residues F55 to R58 for Bpa¹³ cross-linking. Further analysis of Bpa¹³ cross-linked Ste2p with BNPS-skatole was carried out. Digestion of the cross-linked native receptor resulted in two detectable bands around 12 and 10 kDa (Figure 9). Similar digestion with the deglycosylated receptor resulted in a single band around 10 kDa indicating that Bpa¹³ cross-linked to a glycosylated region of Ste2p represented by IC (region 1 to 70 of Ste2p) (Figure 9, Figure 7C). As a control to determine whether anomalous cleavage occurred with the BNPS-skatole reagent, we subjected the Bpa¹-cross-linked receptor to fragmentation under similar conditions. In this case only one band (~27 kDa) was observed (Figure 9). Although one might predict that the BNPS-skatole reagent would cleave inside the peptide ligand thus releasing this ligand, we believe that the proximity of the cross-linked site (position one) to Trp3 in the analog might significantly slow down this reaction.

Site-directed Ala mutations between residues M54 and R58 of Ste2p:

After assignment of a region of interaction for [Bpa¹³] α -factor analog by cross-linking studies, site-directed Ala mutations in this region were carried out to identify a possible contact point. Five individual alanine mutations were introduced in the region of Ste2p between M54 and R58. Additionally two mutants (R58D and R58E) generated by

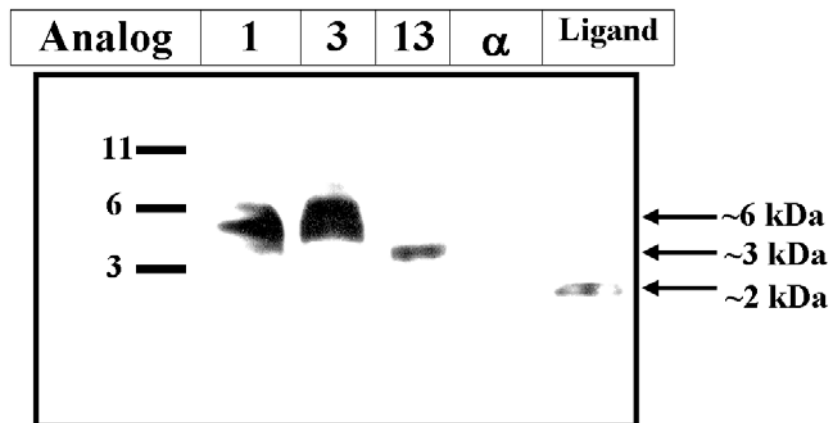
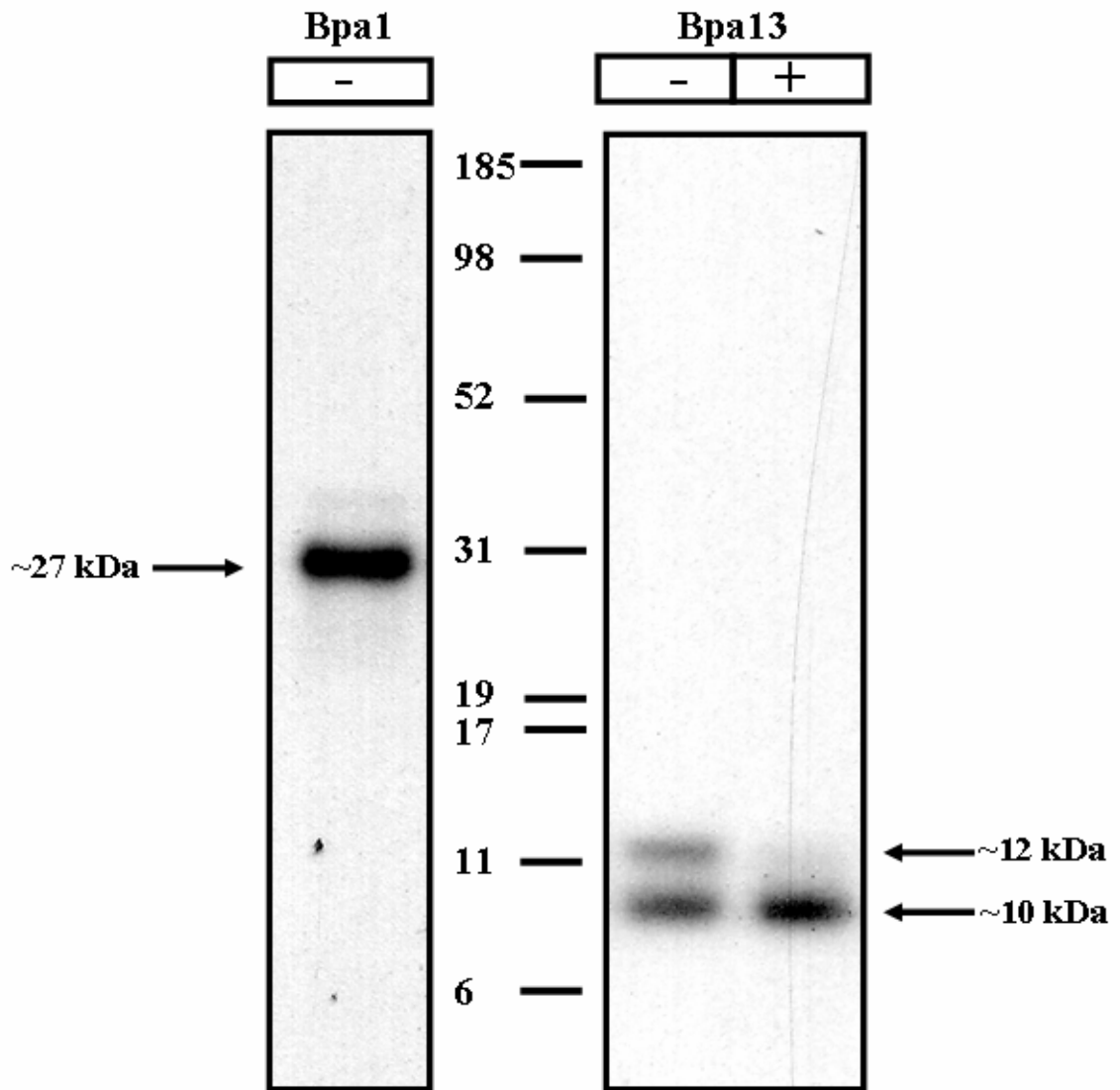


Figure 8: Western blot analysis of CNBr digested BJS21 pNED photo-cross-linked membranes. Membranes photo-cross-linked with various Bpa containing α -factor analogs were digested with CNBr and resolved by Nu-PAGE 12% Bis-Tris gel. Proteins were transferred to a PVDF membrane and probed with NA-HRP to detect the biotin signal on the analogs. Membranes, cross-linked with α -factor, were used as negative control, and ligand alone was used for positive control.

Figure 9: Western blot analysis of BNPS-skatole digested BJS21 pNED photo-cross-linked membranes. Bpa1 and Bpa13 cross-linked BJS21 pNED membranes [native (-) or deglycosylated (+)] were digested with BNPS-skatole (Pierce) for 16 hr @ 37 °C, then resolved by 12% Bis-Tris gel (Invitrogen) and transferred to PVDF membrane. Membranes were probed with NA-HRP conjugate to detect the biotin signal on the Bpa1 and Bpa13 analogs. A) ~27 kDa band corresponding to a region of Ste2p between residues 71 to 295 (25 kDa) plus the ligand (2 kDa) B) Left lane is the BNPS-skatole digest of the native (-) membranes and generates two bands (~12 and ~10 kDa), right lane is the BNPS-skatole digest of the PNGaseF treated [deglycosylated (+)] membranes.



Ayca Akal-Strader and a double mutant F55A-R58A were used in these experiments. Halo assays indicated that the biological activity for the mutant receptors, except F55A-R58A double mutant and G56A mutant, were similar or slightly reduced as compared to the wild type receptor (Table 4). The G56A mutant was previously characterized by Blumer *et al.* with similar results [49]. This study concluded that G56 residue was involved in receptor dimerization forming a GXXXG motif like that found in glycoporphin A; mutation at this residue resulted a 3-5 fold lower response to α -factor induced growth arrest as detected by the halo assay.

Binding affinities for the mutant receptors, detected by saturation binding assay, showed that receptors carrying a mutation at the R58 position had poor binding to the α -factor indicated by a large decrease in the K_i (Figure 10, Table 4). Other mutant receptors had similar or slightly lower binding affinities to α -factor. The combination of our previous results for position 13 α -factor analogs [50] (Table 5) and the current findings by cross-linking and site-directed mutagenesis suggested that position 13 of α -factor might be interacting with R58 of Ste2p. In order to further validate this hypothesis cross-linking experiments were carried out with the five Ala mutants generated in this study. Western blot analysis detecting the FLAG tag on Ste2p showed that all of the mutants were expressed in the membrane (data not shown). Detection of biotin tag on the [Bpa¹³] α -factor analog by NA-HRP showed that cross-linking of [Bpa¹³] α -factor analog to the R58A mutant was highly diminished. Similarly a lower amount of cross-linking was observed to the M54A mutant (Figure 11). Unlike R58A and M54A, the remaining Ala mutants (F55A, G56A, and V57A) showed relatively equal amounts of biotin signal.

Table 4: Summary of the binding affinities and biological activities of Ala mutants.

Receptor	Binding affinity (K_i, nM)	% Biological activity (Halo assay)
Wild type	2.7 ±0.5	100
M54A	3.6 ±0.3	~80
F55A	7.6 ±1.4	~70
F55A & R58A	>100 ^a	~50
G56A	3.7 ±1.1	~20
V57A	2.7 ±0.5	~70
R58A	20.4 ±5.5	~80
R58D	>100 ^a	~70
R58E	20.9 ±6.7	~70

^a Saturation curve was linear under the tested concentrations, thus the K_i is only an estimation.

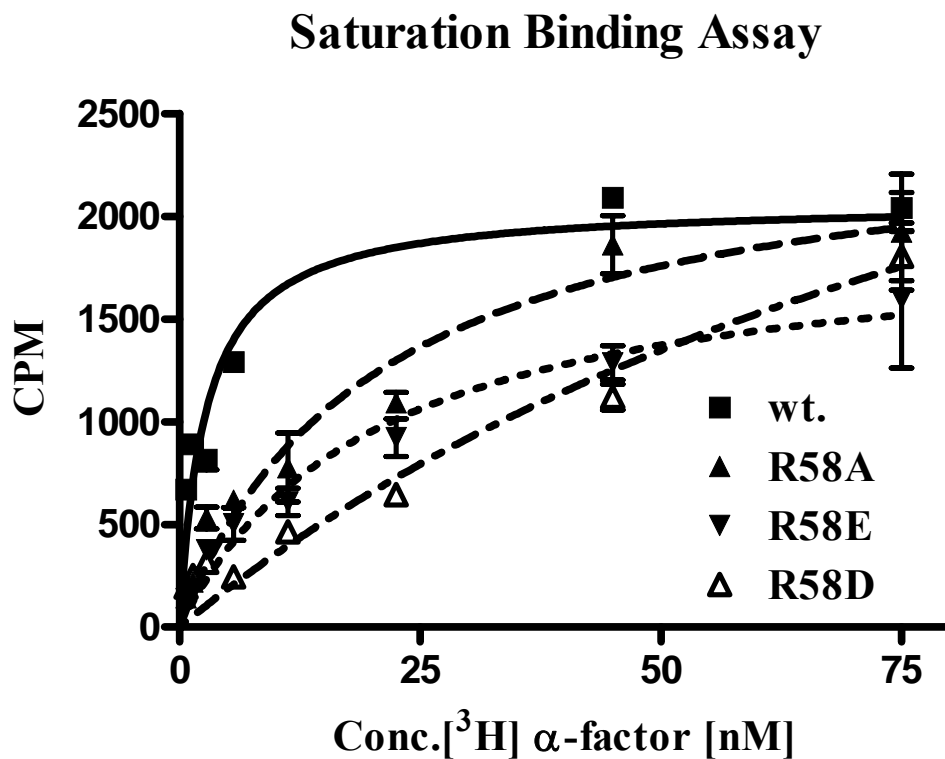


Figure 10: Saturation binding assay with R58 mutants. Site-directed mutagenesis of the R58 residue in Ste2p (to Ala, Glu, and Asp) was carried out and the binding affinities of the mutants were determined by a saturation binding assay. (■) Wild type receptor, (▲) R58A mutant, (▼) R58E mutant, and (△) R58D mutant.

Table 5: Summary of the binding affinities and biological activities of position 13 α -factor analogs.

Peptide	Binding affinity (K_i, nM)	% Biological activity (Halo assay)
α-factor	11 \pm 3	100
Phe13	22 \pm 3	120
<i>p</i>-F-Phe13	16 \pm 3	110
<i>m</i>-F-Phe13	59 \pm 6	86
<i>p</i>-NO₂-Phe13	58 \pm 7	94
Ala13	>1000	40
Ser13	>1000	55

Table adapted from S. Liu *et al.* [50]

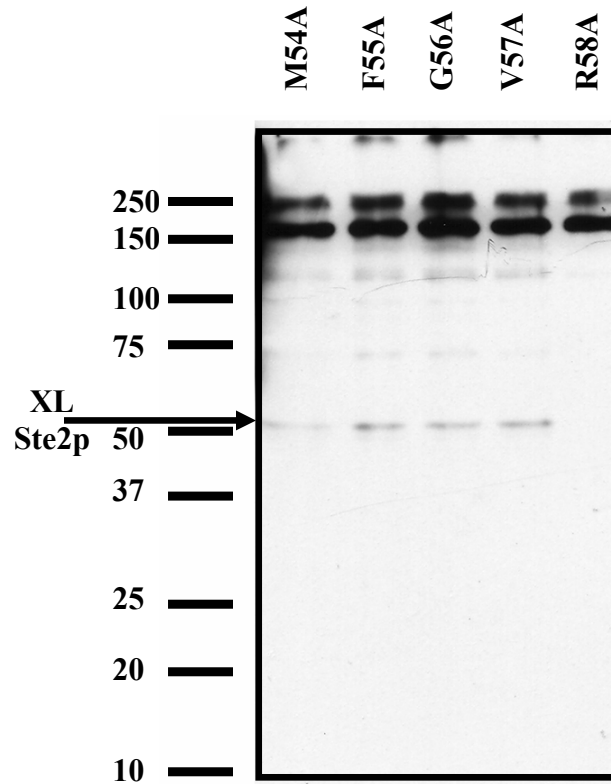


Figure 11: Western blot analysis of photo-cross-linked Ala mutant BJS21

pGA314.Cys-less.STE2.FT.HT membranes. Membranes carrying five individual Ala mutants of Ste2p (M54A, F55A, G56A, V57A and R58A) were photo-cross-linked with biotinylated [Bpa¹³]α-factor analog and resolved by 10% SDS-PAGE. Proteins were transferred to a PVDF membrane and probed with NA-HRP to detect the biotin signal on the analog.

CHAPTER 4

Discussion

This part of the dissertation details the synthesis and characterization of a new set of α -factor analogs containing Bpa as a photoactivatable cross-linker and biotin as a tag for detection. Photoaffinity labeling of receptor residues with Bpa has been used as a powerful tool to obtain constraints to better understand the molecular basis of ligand binding and activation of receptors [11-13, 15-17, 25, 26, 29, 51]. Most of these studies used ^{125}I as a tag to track the cross-linking efficiency and detect the resulting cross-linked fragment after various chemical and enzymatic digestions for mapping the contact region. Previous studies described in part II showed that iodination of Bpa-scanned α -factor analogs except Bpa at position 1, resulted in either loss of function due to multiple iodination or drastic decrease in binding affinity, which made it impractical for cross-linking studies [30]. Although biotin detection uses an indirect method that includes transfer to membrane, probing with NA-HRP and detection by a colorimetric enzymatic reaction compared to direct detection of radioiodine, the relatively unstable nature and high hydrophobicity of the ^{125}I tagged ligand raised additional problems during comparison of consecutive experiments. Furthermore, in future investigations biotinylated peptide fragments generated by chemical or enzymatic degradation can be isolated by affinity purification procedures and subjected to mass spectrometry. Therefore, in this part (part III) of the dissertation the use of biotin instead of ^{125}I as a reporting tag with a series of Bpa scanned α -factor analogs was summarized.

Early studies on angiotensin II receptor [52] and recent work on chemotactic peptide analogs [53] and the integrin receptor [54] showed that biotin can be used as a reporting tag instead of radioactive isotopes. However, most of these studies were hampered by the low affinity of the ligand analogs due to incorporation of biotin as a reporter tag. Results presented in this part (part III) indicated that all of the Bpa/biotinylated analogs tested except Bpa⁸ retained binding affinities within approximately one order of magnitude of that of α -factor and were agonists (Table 2). Detection of the biotin tag was achieved by NeutrAvidin-horse radish peroxidase conjugate, which takes advantage of the strong interaction between the biotin and NeutrAvidin and a powerful reporting signal from the product of the peroxidase reaction thus avoiding the use of iodine at any point in the detection protocol.

Cross-linking experiments done with the membranes from a Ste2p knock-out strain (BJS21) showed that under the conditions tested no nonspecific cross-linking or endogenous biotin signal in the region of Ste2p was detected (Figure 4), although some higher molecular weight bands were detected (Figure 5). In addition cross-linking of the biotinylated Bpa analogs to Ste2p was prevented by mixing 100-fold molar excess of wild type pheromone into the reaction mixture prior to UV irradiation (Figure 5). Thus, in principle these α -factor analogs can be used to determine contacts between ligand side chains and receptor residues involved in binding interactions between α -factor and its GPCR Ste2p.

The [Bpa⁵] α -factor had good binding affinity but was a weak agonist (Table 2). Using an excess of ligand we obtained reasonable cross-linking of this analog (Figure 4). However, only limited amounts of cross-linked product were recovered from preparative

gels and digestion with both chemical and enzymatic reagents resulted in loss of signal (data not shown). Considering our current working model for ligand-receptor interactions, residue 5 of α -factor might be exposed to solvent or involved in interactions with the extracellular loops. Relative to the trans-membrane (TM) domains, the loops are more mobile which might cause the environment around Bpa⁵ to be more dynamic. Such mobility around Bpa⁵ might influence cross-linking efficiency and thus hinder Bpa⁵- α -factor incorporation compared to the other analogs that seem to be interacting with the TMs. Supporting the lack of importance of the position 5 side chain in tight interactions with the binding site was our observation that the [L-Ala⁵] α -factor had the highest receptor affinity of any of the alanine scanned α -factors [55]. Thus, further analysis was not carried out with [Bpa⁵] α -factor although we plan to revisit this issue if we can optimize cross-linking efficiencies in future studies. Due to lack of detectable biological activity and poor competition between the [Bpa⁸] α -factor analog and α -factor for receptor binding (Figure 1, Table 2), fragmentation analysis for the receptor cross-linked with this analog was not carried out.

Trypsin digestion of the cross-linked receptor resulted in a band ~5 kDa for both [Bpa¹] α -factor and [Bpa³] α -factor analogs (Figure 6). The presence of multiple possible trypsin digestion fragments that could give a band around 5 kDa (IIIA, IVA, VA, VIA, VIIIA, IXA, and XA, Figure 5A, when cross-linked to the 2 kDa Bpa¹ or Bpa³ analogs would give a ~5 kDa fragment) made it very difficult to assign a cross-link region for Bpa¹ and Bpa³ with only these results. On the other hand, when these results were combined with the CNBr digestion data, the region of the Ste2p interacting with [Bpa¹] α -

factor and [Bpa³] α -factor analogs was narrowed down to two possibilities: a region covering part of EL2 and an extracellular portion of TM5 (Figure 7B, VIB) or part of TM6, EL3 and part of TM7 (Figure 7B, VIIIB). In part II, it has been determined that [Bpa¹] α -factor cross-linked to a portion of Ste2p comprising TM6-EL3-TM7 [30] in agreement with the second possibility mentioned above. If both N-terminal tryptophan residues of α -factor interact with the same portion of Ste2p, then [Bpa³] α -factor might interact as well with the TM6-EL3-TM7 region. However, based on the present experimental results, we can not rule out the interaction of [Bpa³] α -factor with EL2-TM5.

Trypsin digestion of the Bpa¹³-cross-linked receptor resulted in bands of ~8 and ~10 kDa (Figure 6). After complete trypsin digestion of cross-linked Ste2p there is only one theoretical Ste2p region that could give these bands with the cross-linked ligand: the glycosylated and unglycosylated N-terminus of the receptor (residues 1-58; Figure 7A, fragment IA) [56]. Additional digestions with CNBr and BNPS-skatole were carried out to further probe the cross-linking. Detection of a ~3 kDa band after CNBr digestion (Figure 8) in combination with two bands, ~12 kDa (presumably the glycosylated N-terminal ~10 kDa fragment plus ligand) and ~10 kDa (the unglycosylated N-terminal plus ligand) after BNPS-skatole digestion (Figure 9), strongly indicated that the N-terminus of the receptor was the region cross-linked with [Bpa¹³] α -analog. The higher intensity of the lower molecular weight band observed in figure 9 (middle lane) suggests one of two explanations: glycosylation may interfere with either cross-linking efficiency or detection by NA-HRP. To further test whether the ~12 kDa, BNPS-skatole fragment, was

glycosylated, deglycosylation of the cross-linked receptor followed by BNPS-skatole digestion was carried out. Results showed that upon deglycosylation only a single band ~10 kDa was detected (Figure 9). Thus, we conclude that the [Bpa¹³] α -analog interacts with the junction between the N-terminus of Ste2p and the start of TM1. The smallest overlapping region between the three different digestions (trypsin, CNBr, and BNPS-skatole) carried with Ste2p cross-linked with [Bpa¹³] α -analog indicated that cross-linking occurs at a region between residues F55 to R58. Although the [Bpa¹³]-analog had a relatively higher loss in affinity and efficacy, almost complete competition with the wild type ligand in a receptor binding assay, detection of biological activity by the halo assay, and prevention of cross-linking by an excess of α -factor indicated that this analog interacted with the receptor in a similar manner as the wild type ligand. Thus information gathered from this ligand will be helpful to interpret the possible contact(s) of position 13 of α -factor with its receptor Ste2p. Nevertheless, it is conceivable that the presence of the large diphenylketone group in the position 13 side-chain does result in a reorientation of the peptide in the binding site. The identification of contacts between the position 1, 3 and 13 side chains of α -factor and specific regions of Ste2p leads refinement of the current working model [30] for the placement of the pheromone into its binding pocket on the receptor. Results presented herein indicate that the [Bpa¹] α -factor analog and the [Bpa³] α -factor analog interact with a region of Ste2p covering EL2-TM5 or TM6-EL3-TM7. Results reported in part II using an iodinated [Bpa¹] α -analog showed a contact between position one of the ligand and TM6-EL3-TM7 [30]. Taken together, the present and previous results suggested that the N-terminus of the pheromone interacts with a

binding domain consisting of residues from the extracellular ends of TM5, TM6, and TM7 and portions of EL2 and EL3 close to these TMs. These conclusions are consistent with a previously proposed model [57] for α -factor bound to Ste2p. Nevertheless, it is important to emphasize that the cross-linking results do not preclude other portions of Ste2p participating in the binding domain for the N-terminus of α -factor.

This part also presented a direct interaction between the [Bpa¹³] α -analog and a region of Ste2p at the extracellular end of TM1. Supporting this interaction are studies from our laboratory demonstrating that changes at both residue 58 in TM1 and position 13 of the ligand exhibit a similar phenotype (Tables 3 and 4). Site-directed mutagenesis studies in TM1 showed that mutation of the R58 residue (R58A, R58D, or R58E) results in a 25-100 fold decrease in binding affinity of the wild type pheromone (Figure 10) and only 20-30% decrease in the biological activity determined by halo assay (Table 4). Similarly, previous work reported by Liu *et al.* [50] showed that position 13 analogs of α -factor, where Tyr was replaced by Ala or Ser had very poor binding affinities, but showed relatively good biological activity (Table 5). Thus, data from pheromone-receptor cross-linking studies, receptor mutagenesis analysis, and the structure-activity relationships of α -factor analogs would be consistent with an interaction between position 13 of the pheromone and TM1. However, this conclusion conflicts with a previously reported hypothesis on a possible interaction between position 13 of α -factor and F204 (located at the extracellular end of TM5) of Ste2p [57]. This hypothesis was mainly based on site-directed mutagenesis (F204C) resulting in a receptor defective in α -factor binding, and previous studies from our laboratory [55] showing defective binding

of position 13 α -factor analogs. Considering the current working model and results presented in this part (part III) of the dissertation, an interaction between position 13 of α -factor and TM5 of Ste2p is unlikely.

Cross-linking analyses, presented in this part of the dissertation, suggested that Trp¹, Trp³ and Tyr¹³ of the pheromone interact with TM6-EL3-TM7, EL2-TM5 or TM6-EL3-TM7, and TM1 regions of Ste2p, respectively. These findings have led the refinement of the working model for fitting the tridecapeptide into the pheromone binding site (Figure 12). This model has a contact of Tyr¹³ of the pheromone with Ste2p residues between F55 to R58, an interaction between pheromone residue Gln¹⁰ with receptor residues S47 and/or T48, contacts of residues Trp¹ and Trp³ of α -factor with Y266 and F204 of Ste2p, and a β -turn around the Pro-Gly sequence in the center of α -factor allowing the middle of the pheromone to interact with extracellular loops. Additional constraints of the bound structure should be forthcoming as further refinements achieved by cross-linking studies with Bpa³ and Bpa⁵ analogs and sequencing analysis of the cross-linked fragments by mass spectrometry currently in progress in our laboratory.

Understanding how G protein-coupled receptors are activated by ligand binding is an important goal of workers in the GPCR field. A *de novo* computer model of Ste2p in the resting state (G. Nikiforovich, unpublished data) suggests that R58 and Y98 are in close enough proximity to be involved in a cation- π interaction. An interaction between the Tyr¹³ of the pheromone and R58 of Ste2p, as described in the binding model presented herein, would disturb this cation- π interaction leading to a conformational change that might facilitate a receptor shift to a more active state. Mutational studies on

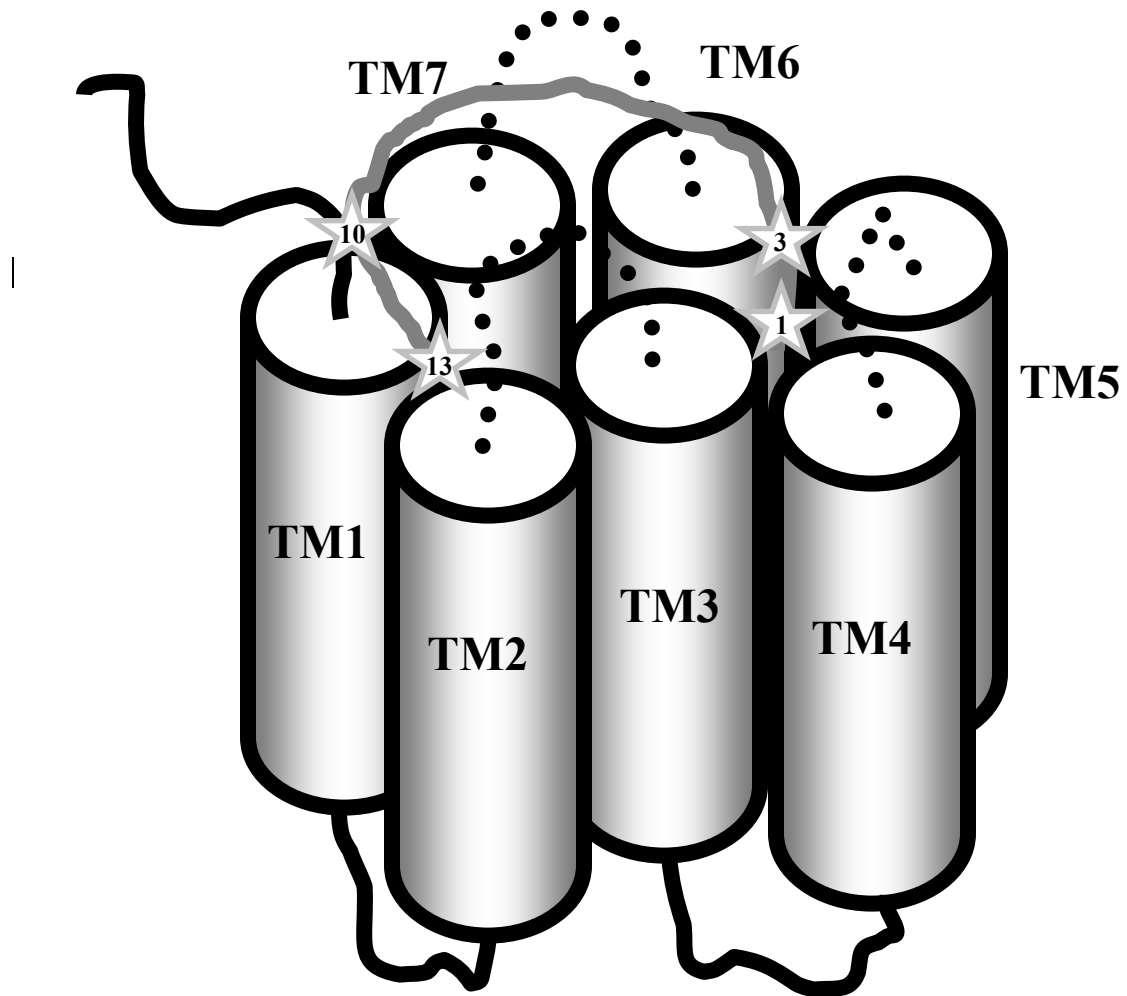


Figure 12: Working model for the fitting of α -factor pheromone into the ligand binding site on its GPCR, Ste2p. α -factor and the loops are represented by the grey curve and dotted lines respectively. Contact residues determined in this study and previous studies indicated by a star symbol with the residue number of the pheromone.

Y98 showed that replacing this residue with a histidine resulted in a receptor that was weakly constitutive and supersensitive to pheromone [59], which supports the idea that Y98 is important for stabilizing the inactive state of Ste2p, perhaps by interacting with R58. Additional studies on this GPCR system should lead to valuable insights into the mechanism of GPCR activation by a peptide ligand.

List of References for Part III

1. Dohlman, H.G., *G proteins and pheromone signaling*. Annu Rev Physiol, 2002. 64: p. 129-52.
2. Dohlman, H.G., et al., *Model systems for the study of seven-transmembrane-segment receptors*. Annu Rev Biochem, 1991. 60: p. 653-88.
3. Elion, E.A., *Pheromone response, mating and cell biology*. Curr Opin Microbiol, 2000. 3(6): p. 573-81.
4. Konopka, J.B. and S. Fields, *The pheromone signal pathway in Saccharomyces cerevisiae*. Antonie Van Leeuwenhoek, 1992. 62(1-2): p. 95-108.
5. Sprague, G.F., Jr., *Signal transduction in yeast mating: receptors, transcription factors, and the kinase connection*. Trends Genet, 1991. 7(11-12): p. 393-8.
6. Fredriksson, R., et al., *The G-protein-coupled receptors in the human genome form five main families. Phylogenetic analysis, paralogon groups, and fingerprints*. Mol Pharmacol, 2003. 63(6): p. 1256-72.
7. Lefkowitz, R.J., *G protein-coupled receptors and receptor kinases: from molecular biology to potential therapeutic applications*. Nat Biotechnol, 1996. 14(3): p. 283-6.
8. Balakin, K.V., et al., *Property-based design of GPCR-targeted library*. J Chem Inf Comput Sci, 2002. 42(6): p. 1332-42.
9. Klabunde, T. and G. Hessler, *Drug design strategies for targeting G-protein-coupled receptors*. Chembiochem, 2002. 3(10): p. 928-44.

10. Fong, T.M. and C.D. Strader, *Functional mapping of the ligand binding sites of G-protein coupled receptors*. Med Res Rev, 1994. 14(4): p. 387-99.
11. Hadac, E.M., et al., *Direct identification of a second distinct site of contact between cholecystinin and its receptor*. J Biol Chem, 1998. 273(21): p. 12988-93.
12. Dorman, G. and G.D. Prestwich, *Using photolabile ligands in drug discovery and development*. Trends Biotechnol, 2000. 18(2): p. 64-77.
13. Dong, M., et al., *Identification of an interaction between residue 6 of the natural peptide ligand and a distinct residue within the amino-terminal tail of the secretin receptor*. J Biol Chem, 1999. 274(27): p. 19161-7.
14. Behar, V., et al., *Direct identification of two contact sites for parathyroid hormone (PTH) in the novel PTH-2 receptor using photoaffinity cross-linking*. Endocrinology, 1999. 140(9): p. 4251-61.
15. Shoelson, S.E., et al., *BpaB25 insulins. Photoactivatable analogues that quantitatively cross-link, radiolabel, and activate the insulin receptor*. J Biol Chem, 1993. 268(6): p. 4085-91.
16. Mouldous, L., et al., *Direct identification of a peptide binding region in the opioid receptor-like 1 receptor by photoaffinity labeling with [Bpa(10),Tyr(14)]nociceptin*. J Biol Chem, 2000. 275(38): p. 29268-74.
17. Boucard, A.A., et al., *Photolabeling identifies position 172 of the human AT(1) receptor as a ligand contact point: receptor-bound angiotensin II adopts an extended structure*. Biochemistry, 2000. 39(32): p. 9662-70.

18. Girault, S., et al., *The use of photolabelled peptides to localize the substance-P-binding site in the human neurokinin-1 tachykinin receptor*. Eur J Biochem, 1996. 240(1): p. 215-22.
19. Li, Y.M., et al., *Mapping peptide-binding domains of the substance P (NK-1) receptor from P388D1 cells with photolabile agonists*. J Biol Chem, 1995. 270(3): p. 1213-20.
20. Kage, R., et al., *Identification of methionine as the site of covalent attachment of a p-benzoyl-phenylalanine-containing analogue of substance P on the substance P (NK-1) receptor*. J Biol Chem, 1996. 271(42): p. 25797-800.
21. Ji, Z., et al., *Direct identification of a distinct site of interaction between the carboxyl-terminal residue of cholecystinin and the type A cholecystinin receptor using photoaffinity labeling*. J Biol Chem, 1997. 272(39): p. 24393-401.
22. Kojro, E., et al., *Direct identification of an extracellular agonist binding site in the renal V2 vasopressin receptor*. Biochemistry, 1993. 32(49): p. 13537-44.
23. Schievano, E., et al., *Conformational and biological characterization of human parathyroid hormone hPTH(1-34) analogues containing beta-amino acid residues in positions 17-19*. Biopolymers, 2003. 70(4): p. 534-47.
24. Gensure, R.C., et al., *Identification of a Contact Site for Residue 19 of Parathyroid Hormone (PTH) and PTH-Related Protein Analogs in Transmembrane Domain Two of the Type 1 PTH Receptor*. Mol Endocrinol, 2003. 17(12): p. 2647-58.

25. Zang, M., et al., *Spatial approximation between a photolabile residue in position 13 of secretin and the amino terminus of the secretin receptor*. Mol Pharmacol, 2003. 63(5): p. 993-1001.
26. Bes, B. and J.C. Meunier, *Identification of a hexapeptide binding region in the nociceptin (ORL1) receptor by photo-affinity labelling with Ac-Arg-Bpa-Tyr-Arg-Trp-Arg-NH₂*. Biochem Biophys Res Commun, 2003. 310(3): p. 992-1001.
27. Perodin, J., et al., *Residues 293 and 294 are ligand contact points of the human angiotensin type 1 receptor*. Biochemistry, 2002. 41(48): p. 14348-56.
28. Rihakova, L., et al., *Methionine proximity assay, a novel method for exploring peptide ligand-receptor interaction*. J Recept Signal Transduct Res, 2002. 22(1-4): p. 297-313.
29. Bisello, A., et al., *Parathyroid hormone-receptor interactions identified directly by photocross-linking and molecular modeling studies*. J Biol Chem, 1998. 273(35): p. 22498-505.
30. Henry, L.K., et al., *Identification of a contact region between the tridecapeptide alpha-factor mating pheromone of Saccharomyces cerevisiae and its G protein-coupled receptor by photoaffinity labeling*. Biochemistry, 2002. 41(19): p. 6128-39.
31. David, N.E., et al., *Expression and purification of the Saccharomyces cerevisiae alpha-factor receptor (Ste2p), a 7-transmembrane-segment G protein-coupled receptor*. J Biol Chem, 1997. 272(24): p. 15553-61.
32. Guldener, U., et al., *A new efficient gene disruption cassette for repeated use in budding yeast*. Nucleic Acids Res, 1996. 24(13): p. 2519-24.

33. Marsh, L., *Substitutions in the hydrophobic core of the alpha-factor receptor of Saccharomyces cerevisiae permit response to Saccharomyces kluyveri alpha-factor and to antagonist.* Mol Cell Biol, 1992. 12(9): p. 3959-66.
34. Akal-Strader, A., et al., *Residues in the first extracellular loop of a G protein-coupled receptor play a role in signal transduction.* J Biol Chem, 2002. 277(34): p. 30581-90.
35. Raths, S.K., F. Naider, and J.M. Becker, *Peptide analogues compete with the binding of alpha-factor to its receptor in Saccharomyces cerevisiae.* J Biol Chem, 1988. 263(33): p. 17333-41.
36. Aletras, A., et al., *Preparation of the very acid-sensitive Fmoc-Lys(Mtt)-OH. Application in the synthesis of side-chain to side-chain cyclic peptides and oligolysine cores suitable for the solid-phase assembly of MAPs and TASPs.* Int J Pept Protein Res, 1995. 45(5): p. 488-96.
37. Kunkel, T.A., J.D. Roberts, and R.A. Zakour, *Rapid and efficient site-specific mutagenesis without phenotypic selection.* Methods Enzymol, 1987. 154: p. 367-82.
38. Kunkel, T.A., *Rapid and efficient site-specific mutagenesis without phenotypic selection.* Proc Natl Acad Sci U S A, 1985. 82(2): p. 488-92.
39. Vieira, J. and J. Messing, *Production of single-stranded plasmid DNA.* Methods Enzymol, 1987. 153: p. 3-11.
40. Bitan, G., et al., *Mapping the integrin alpha V beta 3-ligand interface by photoaffinity cross-linking.* Biochemistry, 1999. 38(11): p. 3414-20.

41. Cheng, Y. and W.H. Prusoff, *Relationship between the inhibition constant (K_I) and the concentration of inhibitor which causes 50 per cent inhibition (I₅₀) of an enzymatic reaction*. *Biochem Pharmacol*, 1973. 22(23): p. 3099-108.
42. Durrer, P., et al., *H⁺-induced membrane insertion of influenza virus hemagglutinin involves the HA2 amino-terminal fusion peptide but not the coiled coil region*. *J Biol Chem*, 1996. 271(23): p. 13417-21.
43. Lee, B.K., et al., *Identification of residues of the Saccharomyces cerevisiae G protein-coupled receptor contributing to alpha-factor pheromone binding*. *J Biol Chem*, 2001. 276(41): p. 37950-61.
44. Ding, F.X., et al., *Study of the binding environment of alpha-factor in its G protein-coupled receptor using fluorescence spectroscopy*. *J Pept Res*, 2002. 60(1): p. 65-74.
45. Dube, P., A. DeCostanzo, and J.B. Konopka, *Interaction between transmembrane domains five and six of the alpha -factor receptor*. *J Biol Chem*, 2000. 275(34): p. 26492-9.
46. Kieliszewski, M.J., J.F. Leykam, and D.T. Lamport, *Trypsin cleaves lysylproline in a hydroxyproline-rich glycoprotein from Zea mays*. *Pept Res*, 1989. 2(3): p. 246-8.
47. Bukusoglu, G. and D.D. Jenness, *Agonist-specific conformational changes in the yeast alpha-factor pheromone receptor*. *Mol Cell Biol*, 1996. 16(9): p. 4818-23.
48. Konopka, J.B., D.D. Jenness, and L.H. Hartwell, *The C-terminus of the S. cerevisiae alpha-pheromone receptor mediates an adaptive response to pheromone*. *Cell*, 1988. 54(5): p. 609-20.

49. Overton, M.C., S.L. Chinault, and K.J. Blumer, *Oligomerization, biogenesis, and signaling is promoted by a glycoporphin A-like dimerization motif in transmembrane domain 1 of a yeast G protein-coupled receptor*. J Biol Chem, 2003. 278(49): p. 49369-77.
50. Liu, S., et al., *Position 13 analogs of the tridecapeptide mating pheromone from Saccharomyces cerevisiae: design of an iodinated ligand for receptor binding*. J Pept Res, 2000. 56(1): p. 24-34.
51. Tan, Y.V., et al., *Photoaffinity labeling demonstrates physical contact between vasoactive intestinal peptide and the N-terminal ectodomain of the human VPAC1 receptor*. J Biol Chem, 2003. 278(38): p. 36531-6.
52. Bonnafous, J.C., et al., *New probes for angiotensin II receptors. Synthesis, radioiodination and biological properties of biotinylated and haptened angiotensin derivatives*. Biochem J, 1988. 251(3): p. 873-80.
53. Shibue, M., et al., *Synthesis of chemotactic peptide analogs with a photoaffinity cross-linker as new probes for analysis of receptor-ligand interaction*. Protein Pept Lett, 2003. 10(2): p. 147-53.
54. Bitan, G., et al., *Design and evaluation of benzophenone-containing conformationally constrained ligands as tools for photoaffinity scanning of the integrin α V β 3-ligand bimolecular interaction*. J Pept Res, 2000. 55(3): p. 181-94.
55. Abel, M.G., et al., *Structure-function analysis of the Saccharomyces cerevisiae tridecapeptide pheromone using alanine-scanned analogs*. J Pept Res, 1998. 52(2): p. 95-106.

56. Montesana, P.E. and J.B. Konopka, *Mutational analysis of the role of N-glycosylation in alpha-factor receptor function*. *Biochemistry*, 2001. 40(32): p. 9685-94.
57. Lin, J.C., et al., *Aromatic residues at the extracellular ends of transmembrane domains 5 and 6 promote ligand activation of the G protein-coupled alpha-factor receptor*. *Biochemistry*, 2003. 42(2): p. 293-301.
58. Ding, F.X., et al., *Probing the binding domain of the Saccharomyces cerevisiae alpha-mating factor receptor with fluorescent ligands*. *Biochemistry*, 2001. 40(4): p. 1102-8.
59. Parrish, W., et al., *The cytoplasmic end of transmembrane domain 3 regulates the activity of the Saccharomyces cerevisiae G-protein-coupled alpha-factor receptor*. *Genetics*, 2002. 160(2): p. 429-43.

PART IV

Purification of Cross-linked Receptor Fragments and Mass Spectrometry Analysis

CHAPTER 1

Introduction

Photoaffinity labeling is one of the few direct experimental strategies used to identify ligand-binding sites in biomolecules like GPCRs (see reviews [1-5]). Since the introduction of this technique, researchers have used tagged photoaffinity reagents (mostly radioactively labeled) and purified photolabelled fragments by conventional purification techniques. These fragments are usually further analyzed either by amino acid sequence analysis or fragmentation studies with chemical or enzymatic reagents. Although valuable information may be gained, many of these studies had limited resolution due to the size of the digested photolabelled fragments (in the order of several kDa in most cases) [6-9] or resistance to classical sequencing techniques [2]. Site-directed or random mutagenesis experiments have contributed to the identification of receptor regions that are important in agonist selectivity or affinity, however these studies lack direct structure information about the agonist-receptor complexes.

Mass spectrometry (MS) is becoming the method of choice to overcome problems caused by limited sample yields for labeled peptide fragments produced in small quantities and to obtain better resolution in sequencing. In addition to the development of methods for the identification of post-translational modifications (for example, glycosylation and phosphorylation), electrospray (ES) [10-15] and matrix-assisted laser-desorption ionization (MALDI) MS [16-18] have been used for studies on ligand-

receptor interactions, suicide inhibitors and affinity labels. Recent progress in MS enables detection and sequencing of peptides in sub-picomolar quantities (see reviews [19-22]).

Identification of a cross-linking site generated by photoaffinity labeling often requires the sequencing of the cross-linked fragment. Sequencing could be performed in the conventional fashion by Edman degradation or with exoproteases, however the amount of sample requirement is much greater than that needed for MS (>100 pmol) [23] and neither method is useful for membrane proteins due to low yields in purification and inadequate digestion by proteases [2]. Recently, several MS methods, including post-source-decay MALDI-time of flight (MALDI-TOF) MS [24-26] and tandem MS (MS/MS) [27-30], have been used to analyze the sequence of a peptide fragment.

A few groups have reported successful identification of the specific amino acids labeled in a protein using photoaffinity labeling combined with MALDI-TOF MS, such as the study on NK-1 receptor by Sachon *et al.* [31]. Leite *et al.* [32] used benzophenone based photo-probes and employed on-line liquid chromatography/tandem mass spectrometry (LC-MS/MS) with an ion trap to identify the photolabeled peptides and amino acid residues in the nicotinic acetylcholine receptor. Although the sample amount and handling is minimal with these methods, determination of the primary sequence from the fragmentation pattern of a branched peptide can be quite difficult due to the complexity of the fragmentation process [33, 34]. Frequently, a proteolytic digest of a cross-linked protein includes multiple species: cross-linked peptides, linear peptides, and modified peptides thus making it difficult to identify and analyze the desired labeled fragments at normal instrument resolution. Furthermore presence of complete and incomplete digest fragments increases the number of possible cross-linked peptides in the

complex mixture. While all these cross-linked peptides will not be observed due to chemical preference and proper geometric orientation of the cross-linker and the target residue(s), all possibilities must be considered in interpreting experimentally observed mass/charge (m/z) values. Despite the fact that there are a few computer programs used for the analysis of mass spectra obtained from digested cross-linked proteins[35-38], careful examination of the data manually is often required.

Several methods have been described for distinguishing cross-linked peptides in mass spectra of cross-linked and digested proteins. Some of these methods use isotopically labeled cross-linkers [39, 40] or proteins [41] that yield a distinctive signature in the mass spectrum. These techniques rely on the observation of a characteristic pattern in the mass spectrum or tandem mass spectrum of the analyte mixture. However, if the signal-to-noise ratio of the cross-linked species yielding this pattern is insufficient, the pattern cannot be reliably distinguished.

The few successful examples mentioned above, where mass spectrometry was used to identify photoaffinity labeled residues, revealed that an efficient purification of the cross-linked peptide from a complex mixture is essential prior to MS analyses. Inadequate purification further complicates the collision induced dissociation (CID)-MS, thus making it almost impossible to identify the modified residue. Therefore, a separation method for enriching the cross-linked species from the analyte mixture would be useful for reducing levels of complexity caused by the non-cross-linked peptides. An affinity separation provides such an advantage, as described by Trester-Zedlitz *et al.* [42]. This part of the dissertation mainly describes the use of avidin-biotin interaction to purify the biotinylated α -factor analogs and the cross-linked receptor fragments from a yeast

membrane digest. It has been previously shown that a similar approach aided analysis of biotinylated fragments of avian skeletal muscle troponin C (TnC) from various mixtures of biotinylated TnC, BSA and equine cytochrome *c* following different enzymatic digestions [43].

CHAPTER 2

Materials and Methods

Chemical Reagents:

Immunopure immobilized monomeric avidin and streptavidin beads were purchased from Pierce (Rockford, IL). The acetone, water, and acetonitrile used in all HPLC applications and sample purifications were HPLC grade and obtained from Burdick & Jackson (Muskegon, MI). The 98% formic acid used in these applications was purchased from EM Science (an affiliate of MERCK KgaA, Darmstadt, Germany). Buffer components and salts were from Sigma (St. Louis, MO). Alpha-Cyano-4-hydroxycinnamic acid (CHCA) and Sinapinic acid were purchased from Aldrich (Milwaukee, WI). CHCA was re-crystallized from ethanol before use. Immobilon NC Pure nitrocellulose was obtained from Millipore. Sequencing grade modified trypsin was used as supplied by Roche Diagnostics (Indianapolis, IN). Bovine serum albumin (BSA) and CNBr were from ICN Biomedicals (Aurora, OH). Dialysis tubing was from Spectrapor (Annex, LA). Immobilized-metal affinity chromatography (IMAC) was carried out either with Nitrilotriacetic acid pre-charged with Ni^{2+} (Ni-NTA) from Qiagen (Valencia, CA), or with HiTrap chelating column charged with Cu^{2+} from Amersham Biosciences (Piscataway, NJ).

Photoaffinity cross-linking:

Photoaffinity cross-linking was carried out with various 4-benzoyl-*L*-phenylalanine (Bpa)-containing α -factor analogs as described in Part II and III. Briefly BJS21 pNED membranes (220 μ g/ml of total protein) were incubated with PPBi buffer (total volume 1ml, with 0.1%BSA) in siliconized microfuge tubes for 10 min at ambient temperature. Bpa-scanned biotinylated α -factor analogs (10 to 20 nM) were added, and the reaction was incubated for 30 min at room temperature with gentle mixing. The reaction mixture was aliquoted into 3 wells of a chilled 24 well plastic culture plate pre-blocked with PPBi (0.1% BSA). The samples were held at 4 °C and irradiated without the culture plate lid at 365 nm for 1 hour at a distance of 12 cm in a Stratlinker (Stratagene, La Jolla, CA). Membrane samples were recombined in siliconized microfuge tubes and washed twice by centrifugation (14000g) with PPBi (0.1% BSA). Then membrane pellets were stored at -80 °C for further experiments.

Purification of intact cross-linked Ste2p:

Immobilized-metal affinity chromatography (IMAC), and size exclusion (preparative gel extraction) were used to partially purify the cross-linked Ste2p prior to further analysis. Partial purification before fragmentation and affinity purification helped to increase the yield and decreased the complexity in mass spectrometry analysis. The purification efficiency was tested by western blot analysis of the fractions collected from the columns and total protein in each elution was checked with Silver or Coomassie staining of the protein bands after SDS-PAGE.

a. *Hi-Trap column:*

HiTrap chelating HP from Amersham Biosciences was used for IMAC. This column is composed of highly-cross-linked agarose beads to which iminodiacetic acid (IDA) has been coupled by stable ether groups via a spacer arm. The column is charged with 0.1 M CuSO₄ and used by following the supplier's protocol with the following modifications: The membranes containing Ste2p from BJS21 pNED (cross-linked or not, ~ 1.5 mg/ml total protein) were solubilized in 6M urea (pH = 8.0) for at least 5hr (final volume 1 ml) followed by direct injection to a HiTrap column. The column was then connected to a high performance liquid chromatography (HPLC) instrument (Hewlett Packard, 1100 series). A wash step was then carried out with 50 mM ammonium bicarbonate buffer (pH=8.0), containing 50 mM imidazole and 6M urea. Elution of the bound proteins was achieved by the same buffer with 200 mM imidazole.

b. *Ni-NTA column:*

Ni-NTA agarose from Qiagen was used as an alternative metal-chelating matrix. This column is composed of Ni-NTA coupled to Sepharose[®] CL-6B and offers high binding capacity and minimal nonspecific binding. The protocol was adapted from a previous Ste2p purification study by David *et al.* [44]. Briefly, the membranes (5-10mg/ml total protein) were solubilized in solubilization buffer (1% Dodecyl β Maltoside, 10% glycerol, 150 nM NaCl in 50 mM HEPES, pH=7.5, plus protease inhibitors; final volume 2 ml) and were incubated with 1ml Ni-NTA (pre-equilibrated with equilibration buffer: 10% glycerol, 500 nM NaCl in 50 mM HEPES, pH=7.5, plus protease inhibitors) overnight (o/n) by end-to-end mixing. The flowthrough was collected from the column as the resin packed. The column was washed with 5 column volumes of

equilibration buffer, followed by 10 column volumes of wash buffer (10% glycerol, 150 nM NaCl, 50 mM imidazole in 50 mM HEPES, pH=7.5, plus protease inhibitors).

Column-bound material was then eluted with 5 column volumes of elution buffer (10% glycerol, 150 nM NaCl, 300 mM imidazole in 50 mM HEPES, pH=7.5, plus protease inhibitors). Fractions were concentrated with Microcon[®] YM-30 (Millipore, MW cutoff = 30,000 Da.) before further analysis.

c. Preparative Gel extraction:

BJS21 pNED membranes and cross-linked membranes (~1.5 mg total protein) were dissolved in 400 µl 1x loading buffer (BIO-RAD tricine sample buffer) for at least an hour. The dissolved membranes were then loaded on a preparative 10% SDS gel and resolved for 80 min at 25 mA. After the proteins resolved according to size, a 10 mm wide strip around the 50 kDa marker was cut out of the gel. The strip was then placed in dialysis tubing (MW cutoff = 25,000 Da.) with transfer buffer (25 mM Tris, 0.2 M Glycine and 20% methanol) and electro-eluted for 3 hr at 400 mA in a vertical transfer apparatus (Hoefer Scientific Inst.). Following electro-elution the dialysis tubing (20 ml) was placed in a 4 liter beaker filled with 25 mM ammonium bicarbonate. The buffer was changed every hour for three hours and then kept o/n at 4 °C.

Digestion of cross-linked Ste2p:

Chemical and enzymatic digestions were carried out after the partial purification of the cross-linked samples. The fragmentation was achieved as described in parts II and III. In brief, the concentrated samples (~0.1-0.2 mg/ml) were either re-suspended in 70% formic acid for CNBr digestion or in buffer (100 mM Tris-HCl, pH 8.5) for trypsin

digestion. All digestions were carried out in complete darkness, under nitrogen gas, and at 37 °C for at least 24 hr. All digests were concentrated by vacuum centrifugation (SpeedVac) and analyzed by SDS-PAGE or mass spectrometry.

Test of avidin purification:

Immunopure immobilized monomeric avidin and streptavidin beads were tested for the efficiency of capturing biotinylated peptides from simple and complex mixtures. The compatibility of these beads with MALDI-TOF was analyzed and compared. Ten μl of the biotinylated α -factor analog (Bpa8, 0.1 $\mu\text{g}/\mu\text{l}$) was mixed with an equal volume of beads. The mixture was incubated at room temperature with continuous agitation for an hour. After the incubation the beads were washed with 50 μl PBS (0.1 M sodium phosphate, 0.15 M NaCl, pH = 7.2) 4 times, followed by washing with 50 μl water (5 times). The beads were then left to settle and the supernatant was withdrawn after approximately 15 min.. The pellet was re-suspended in a minimal amount of water (10 μl) and used in a MALDI-TOF experiment.

Capture of biotinylated α -factor analog from a simple and a complex mixture was carried out by applying a similar protocol. Preparation of a simple and a complex mixture of [Bpa⁸] α -factor analog was achieved by mixing with an equal amount of α -factor (0.1 $\mu\text{g}/\mu\text{l}$, 10 μl final volume) or CNBr digested BJS21 pNED membranes (~300 μg total protein), respectively. Ten μl of these mixtures were incubated with the beads as described above. After the wash steps the beads were directly analyzed by MALDI-TOF.

CNBr digested BJS21 pNED membranes cross-linked with various Bpa-scanned biotinylated α -factor analogs were examined under similar conditions.

Purification of cross-linked Ste2p fragments with Monomeric avidin column:

After the fragmentation of the cross-linked membranes (~0.1-0.2 mg/ml) with CNBr or Trypsin, the digests were loaded onto a 1 ml packed monomeric avidin column. The column was washed with at least 5 column volumes of PBS followed by a second wash with 10 column volumes of 10% methanol, 50 mM ammonium bicarbonate. The bound biotinylated fragments were eluted with 5 column volumes of 50% acetonitrile, 0.4% TFA [45]. The elutions were then pooled and concentrated by vacuum centrifugation to a final volume of 100 μ l and analyzed by mass spectrometry.

Mass spectrometry:

All of the mass spectrometry experiments were carried out in collaboration with the Biological Mass Spectrometry group in Oak Ridge National Laboratory (ORNL). Sample preparation and cleanup was done at the University of Tennessee and analysis was accomplished at ORNL. Two main mass spectrometry techniques were applied as described below:

a. Matrix-assisted laser desorption ionization time-of-flight mass spectrometry (MALDI-TOF-MS):

MALDI-TOF experiments were performed on a PerSeptive Biosystems Voyager Elite MALDI-TOF, equipped with a 337 nm nitrogen laser, operating in the positive ion mode (delayed extraction/linear mode). Spectra were obtained in reflector mode, with

+20 kV total acceleration voltage, +18 kV applied to the grid, +10 V applied to the guide wire, and 210 ns acceleration delay. Spectra were averaged from up to 256 individual laser pulses, obtained from several locations on each sample spot. Sample aliquots were applied to a pre-spotted thin-layer matrix. CHCA was prepared by dissolving 40 mg of CHCA in 1 ml of 2-propanol: acetone (50:50, v/v). Nitrocellulose was prepared by dissolving 10 mg in 1 ml 2-propanol: acetone (50:50, v/v). An equal volume of CHCA and nitrocellulose were mixed to give 20 mg/ml CHCA and 5 mg/ml nitrocellulose. A 0.5 μ l aliquot was dispensed onto the MALDI plate and allowed to dry. One-half μ l volume of samples were applied to the thin layer and allowed to dry. Sinapinic acid (SA) was prepared by dissolving 10 mg SA in acetonitrile: 0.1% aqueous TFA (50:50, v/v). Samples were applied as described above. External calibration of the m/z axis was performed using gramicidin S and bovine insulin β -chain. Expected masses were calculated using Protein Prospector [46].

Direct application of the avidin beads to MALDI plate was carried out by the protocol adapted from Li *et al.* [47]. Briefly, a layer of CHCA or SA (dissolved in acetone, 25 mg/ml) was applied to the MALDI plate, forming a dense layer of small crystals to allow adsorption of the beads. One μ l of the bead slurry was then added and allowed to dry partially. An aliquot of a second matrix solution (CHCA or SA dissolved in acetone, >50mg/ml) then was applied to allow solubilization of adsorbed peptides from the beads into the matrix solution. Upon complete drying, the beads were blown off with a stream of dry nitrogen leaving un-adsorbed peptides within the matrix ready for MALDI-TOF analysis. A schematic of the sample preparation procedure is shown in Figure 1.

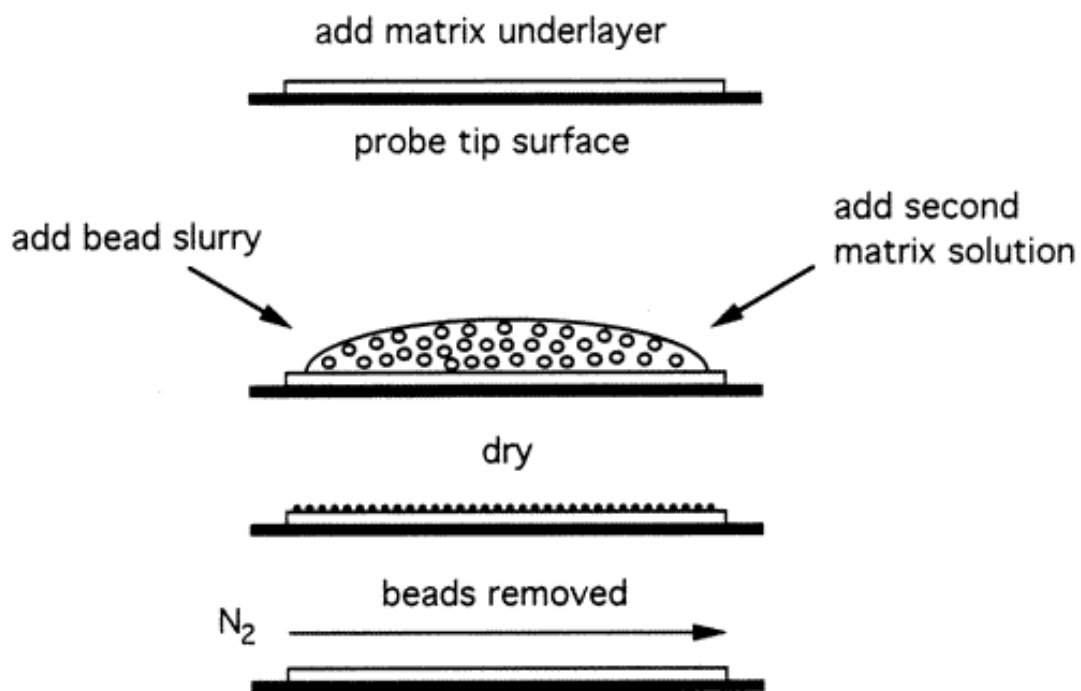


Figure 1: Schematic representation of the MALDI procedure with avidin beads.

Avidin beads were used to capture biotinylated peptides from simple or complex mixtures. Beads were spotted directly on the MALDI matrix for analysis (figure adapted from [47]).

b. Nanospray mass spectrometry (NS-MS):

NS-MS was performed on a LCQ-DECA instrument (Thermo Finnigan) operating in the positive ion mode. Nanospray voltage was set to 2.0kV (Thermo Finnigan nanospray source) and the heated capillary was set at 200°C. A 20µm id fused silica was directly connected to a liquid junction (Thermo Finnigan), which was connected to a 10µm id uncoated fused silica tip (New Objective, Woburn, MA). The MS was operated with 5 microscans averaged for full scans and MS/MS scans, 5 m/z isolation widths for MS/MS isolations and 35% collision energy for collision-induced dissociation. For all experiments, the MS was operated in the data dependent MS/MS mode, where the four most abundant peaks in every full MS scan were subjected to MS/MS analysis. To prevent repetitive analysis of the same intense peptides, dynamic exclusion was enabled with a repeat count of 2. The exclusion duration was set to 1 minute. LC-MS/MS experiments were performed on an integrated Famos/Switchos/Ultimate 1D/2D HPLC system (LC Packings, a division of Dionex, San Francisco, CA) directly coupled to a quadrupole ion trap mass spectrometer (LCQ-DECA Thermo Finnigan, San Jose, CA) outfitted with a Finnigan nanospray (NS) source. The entire system was fully automated and under direct control of the Xcalibur software system (Thermo Finnigan). For all reverse phase separations, gradients were run from 100% Solvent A (95% H₂O/ 5% ACN/ 0.1% formic acid) to 100% Solvent B (30% H₂O/ 70% ACN/ 0.1% formic acid), followed by a wash with 100% Solvent B and a 20 minute equilibration back to Solvent A before the next run (run times dependent upon experiment type). The loading solvent used in the 1D LC-MS/MS experiments was 100% H₂O with 0.1% formic acid. For all nano mode reverse phase separations the flow rate was set at 200nL/min. The reverse

phase separations were carried out by a VYDAC C₁₈ column (Part No. 218MS5.07515; 75µm id x 15cm, 300Å with 5µm particles). All injections were made by an autosampler (Famos) onto a 50µL loop and flushed onto a LC Packings C₁₈ precolumn (300µm id x 5mm, 100Å with PepMap C₁₈ 5µm particles), and eluted after desalting onto the VYDAC C₁₈ column. The outlet from the resolving column was directly connected to the NS source with a short piece of fused silica (20µm id for NS).

The theoretical masses of the fragment ions were calculated by Prowl web site “<http://prowl.rockefeller.edu/>”. This site considers the common modifications to amino acids during fragmentation such as homoserine lactone formation at methionine residues after CNBr digestion (-48 Da)

CHAPTER 3

Results

Purification of intact cross-linked Ste2p:

Membranes obtained from BJS21 strain transformed with pNED (an over expression vector carrying the *STE2* gene) [44] were used in the purification experiments. The α -factor receptor encoded by this plasmid is tagged at its C-terminus with an epitope tag (FLAG) and a 6xHis tag. Two of the methods applied in this study took advantage of the 6xHis affinity tag, which facilitates binding to metal ions. Immobilized-metal affinity chromatography (IMAC), based on this principle, was first used to purify proteins in 1975 by Porath *et al.* [48]. The method was further optimized by other groups to purify a variety of different proteins and peptides [49].

Two different IMAC beads were used to purify the Ste2p (Ste2p.FT.HT) as detailed in Material and Methods. The HiTrap Chelating column from Amersham Biosciences was used by connecting it to a HPLC system. Various concentrations of imidazole (0, 25, 50, and 75 mM) in the wash buffer were tested to optimize the elution of non-specifically bound proteins. Results indicated that most of the protein was washed from the column in the flow-through (Figure 2, fractions 1-10; Figure 3, fractions 2, 4, and 6) and that 50 mM imidazole in the wash buffer effectively removed the proteins that are non-specifically attached to the resin as indicated by the absorbance of fractions 17-30 (Figure 2). Western blot analysis (probed with anti-FLAG antibody) of the fractions showed that elutions with 200 mM imidazole released the bound 6xHis tagged Ste2p in

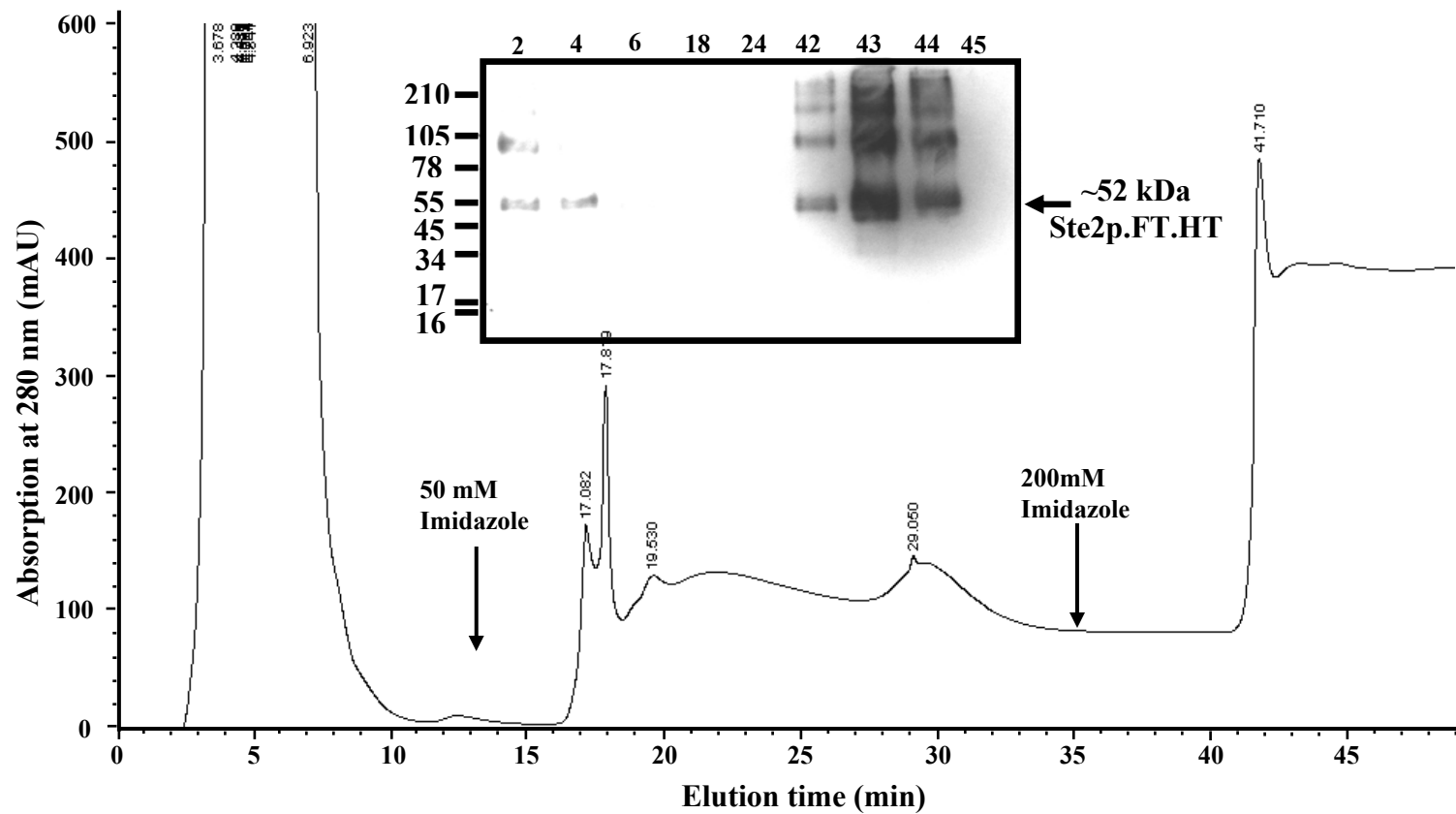


Figure 2: Elution of Ste2p.FT.HT from HiTrap column. HPLC elution profile (Abs. 280nm) of BJS21 pNED membranes from Cu²⁺ charged HiTrap column is plotted. The inset shows the western blot of the selected fractions probed with anti-FLAG antibody. Lanes labeled with the fraction number (indicating the elution time in minutes).

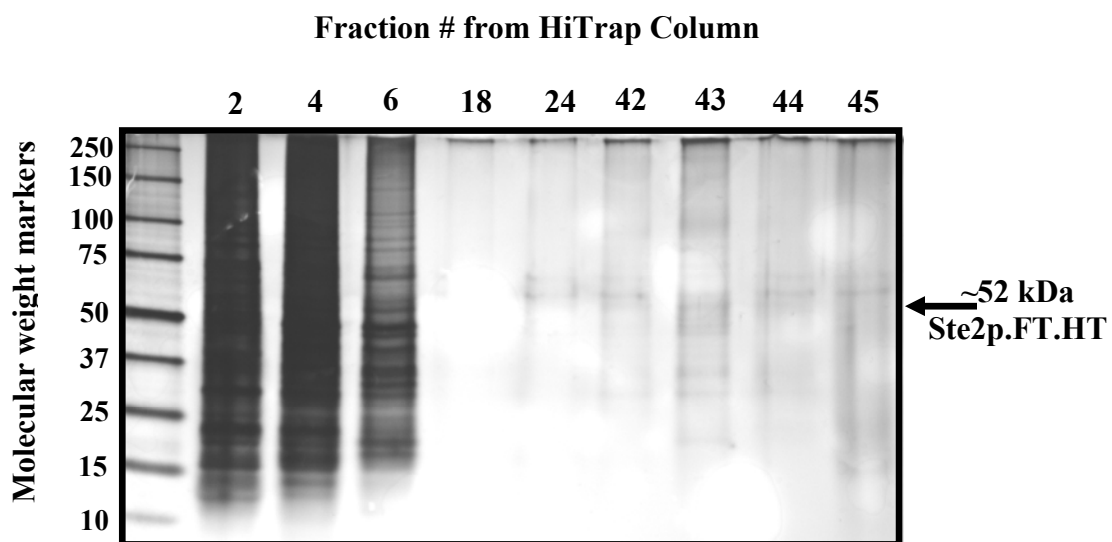


Figure 3: Silver stained SDS-PAGE gel loaded with HiTrap elutions. First lane is the molecular weight markers, other lanes labeled with the fraction number (indicating the elution time in minutes).

fractions 42, 43 and 44. The higher molecular weight bands in fractions 42-44 were due to aggregation of Ste2p in the absence of detergents. The high absorbance observed after fraction 45 was due to the 200 mM imidazole in these fractions.

Similarly proteins solubilized from BJS21 pNED membranes that had been subjected to cross-linking with biotinylated [Bpa¹] α -factor were also partially purified by a HiTrap column. Figure 4 illustrates that cross-linked Ste2p could be eluted with 200 mM imidazole and detected on a blot probed with NA-HRP. Most of the proteins eluted in the flow-through as indicated by the abundance of proteins in the flow-through fractions indicated by high absorbance (Figure 4) and in a silver-stained gel (data not shown). In addition, the lack of bands in the NA-HRP probed blots (Figure 4) indicated that the cross-linked Ste2p was not eluted in these fractions. Washing the column with 50 mM imidazole removed loosely bound proteins leading to a slight increase in absorption. The cross-linked Ste2p was eluted after increasing the imidazole concentration to 200 mM. Both the increase in the absorption and bands detected by the NA-HRP blot indicated that fractions 52-54 contained biotinylated protein. Washing the column with 500 mM imidazole after the elution did not lead to further release of tagged proteins. The overall yield of cross-linked Ste2p (Figure 4) was lower than that obtained from uncross-linked membranes (Figure 2).

The second matrix used for IMAC was Ni-NTA from Qiagen, which is a Ni²⁺-charged Sepharose resin. Fractionation of proteins solubilized from the cross-linked membranes was performed by following the supplier's protocol with the modifications described in Materials and Methods. Elutions from the Ni-NTA column were analyzed after concentrating with vacuum centrifugation. Briefly, proteins were resolved by SDS-

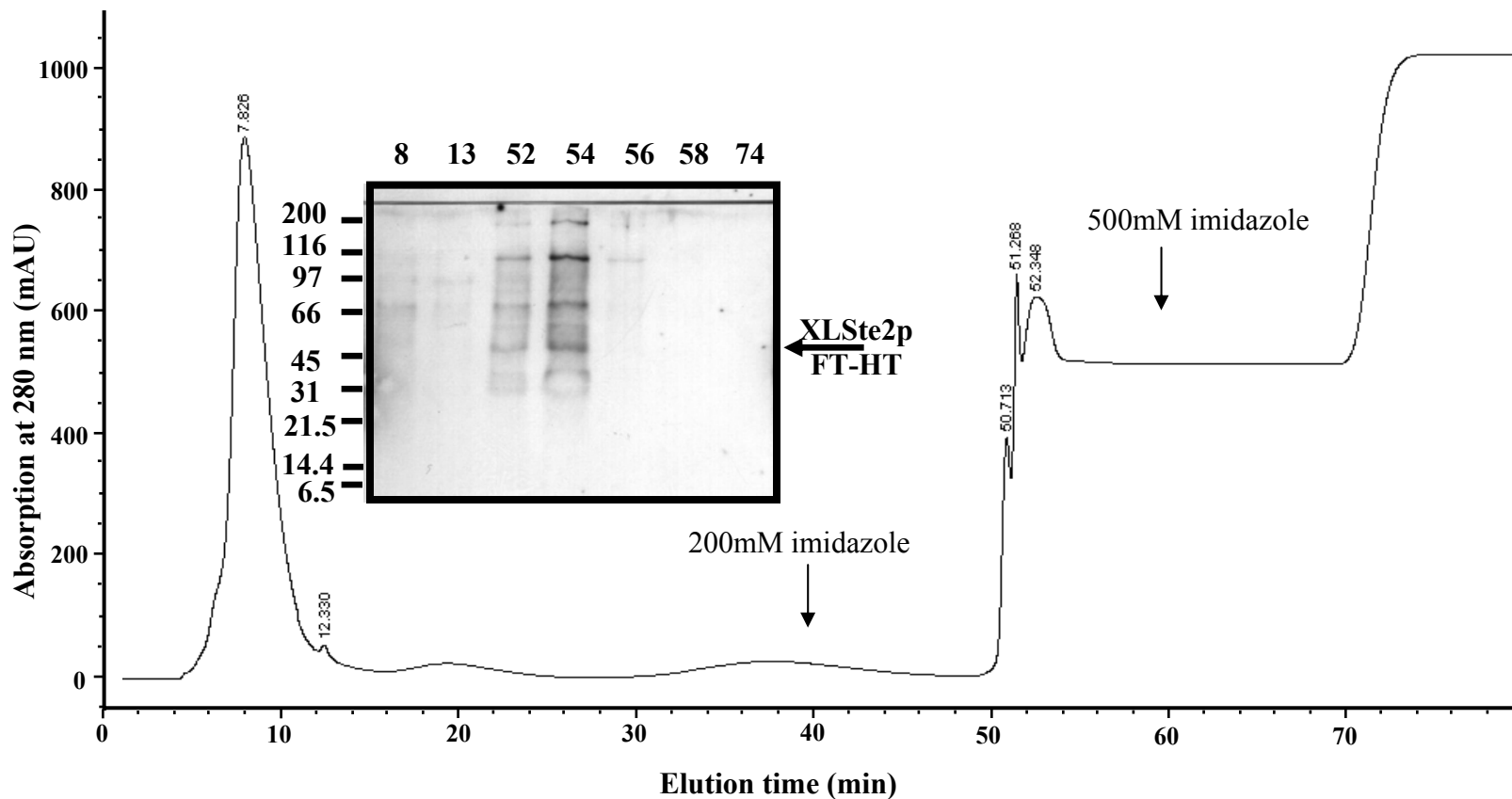


Figure 4: Elution of cross-linked Ste2p.FT.HT from HiTrap column. HPLC elution profile (Abs. 280nm) of cross-linked BJS21 pNED membranes from Cu^{2+} charged HiTrap column is plotted. The inset shows the western blot of the selected fractions probed with NA-HRP. Lanes labeled with the fraction number (indicating the elution time in minutes).

PAGE and transferred to PVDF membrane for western blot analysis. Blots were probed with either Konopka antibody (this antibody was obtained from Prof. James Konopka, SUNY Stony Brook; the antibody reacts specifically to the N-terminal 100 amino acids of Ste2p) or NA-HRP to detect the presence of Ste2p.FT.HT and cross-linked Ste2p.FT.HT, respectively (Figure 5). Analysis of both blots (Figure 5 A and B) showed that elution 2 (E2) contained a protein of approximately 54 kDa that was biotinylated (Figure 5A) and reacted with a specific antibody that recognized Ste2p (Figure 5B). Retention of this protein through the wash steps indicated that it interacted with the column tightly (due to the presence of a 6xHis tag). This blot also showed that a small amount of Ste2p was present in the flow-through and washes 1 (W1) suggesting that either the column was slightly over loaded or there was a small population of Ste2p which lost the 6xHis tag during sample preparation. Detection of these bands with NA-HRP was not observed, probably due to a lower sensitivity of this detection compared to the Konopka antibody. Elutions from the Ni-NTA column were analyzed by silver staining to determine the presence of other proteins that co-eluted with the bound Ste2p (Figure 6). The presence of multiple bands revealed that several other membrane proteins retained on the column after the 50 mM imidazole wash. Comparison of the two IMAC matrices will be detailed in the Discussion part (Chapter 4).

An alternative approach for purification of intact Ste2p was based on size exclusion. This method involved very little sample handling potentially giving higher yield. Briefly, proteins solubilized from cross-linked membranes were dissolved in loading buffer and resolved by 10% SDS-PAGE. After separation of proteins a 10 mm-

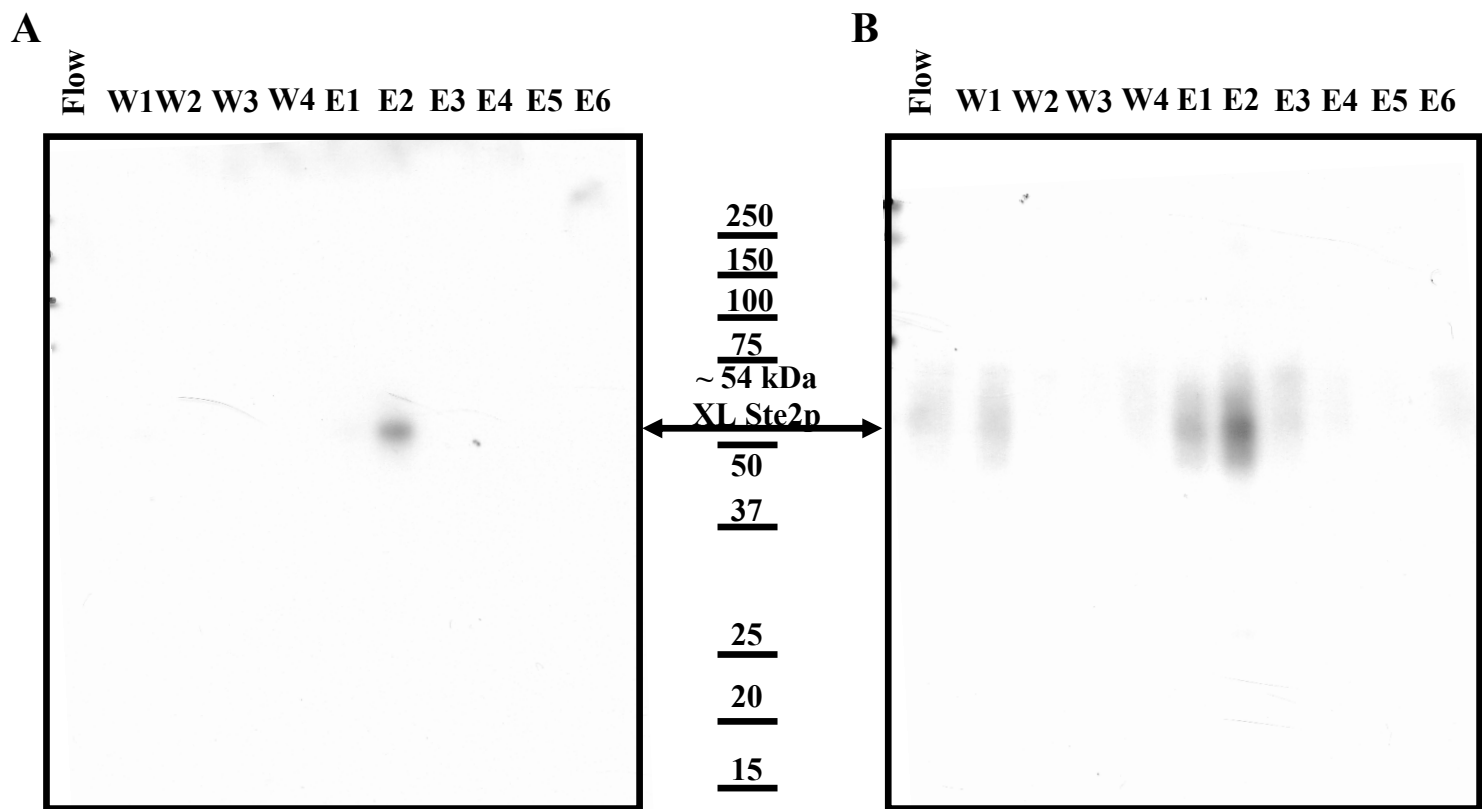


Figure 5: Western blot analysis of the fractions from Ni-NTA column. Fractions collected from a Ni-NTA column loaded with cross-linked BJS21 pNED membranes were concentrated and resolved by 10% SDS-PAGE. After transferred to PVDF membranes blot A) probed with NA-HRP to detect biotin signal, and blot B) probed with Konopka antibody to detect Ste2p.

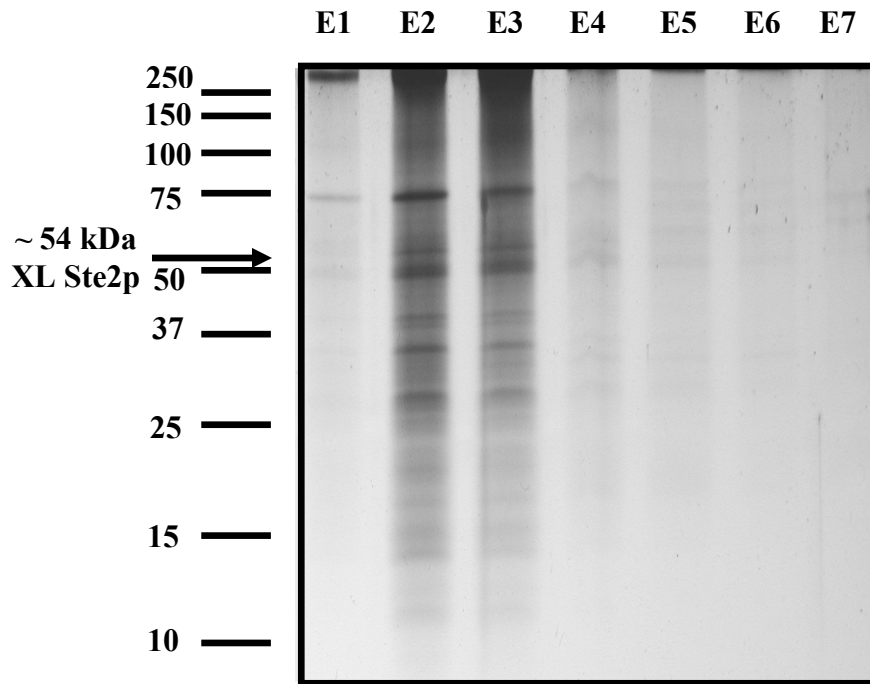


Figure 6: Silver stained SDS-PAGE gel loaded with Ni-NTA column elutions. Cross-linked BJS21 pNED membranes resolved by 10% SDS-PAGE and protein bands detected by silver staining.

wide region of the gel around the 50 kDa band was removed, and proteins were electro-eluted. Following dialysis the samples were concentrated by vacuum centrifugation and assayed with western blot analysis and silver staining (Figure 7). The results showed that there was no other detectable biotinylated protein in the purified sample. Also no aggregation or degradation products were observed. Analysis of the silver stained gels indicated the presence of a few other proteins in the partially purified sample (Figure 7A).

Analysis of partially purified Ste2p with Nanospray-MS (NS-MS):

Following the partial purification of Ste2p the compatibility of the purified sample with tandem mass spectrometry was analyzed. For this assay FLAG-tagged, 6xHis tagged Ste2p was partially purified by a HiTrap column as described above (Figure 2). Following the purification step the concentrated sample (Fractions 42-44, Figure 2) was re-suspended in 70% formic acid and digested with CNBr for 18hr at 37 °C. Digests were then dried by vacuum centrifugation and neutralized with 50 mM ammonium bicarbonate buffer (final volume ~ 100 µl). Analysis of the neutralized sample was carried out with LCQ-DECA (Thermo Finnigan) operating in the positive ion mode. The total ion spectrum obtained from this sample indicated that there were several ion packets throughout the spectrum, indicating the presence of many peptides (Figure 8). Manual analysis of the MS/MS data showed that at least 10% sequence coverage for Ste2p was obtained. Representative spectra of two such fragments are shown in Figure 9. In one spectrum (Figure 9A), a sequence of AAALTLIVM was clearly obtained allowing assignment to the CNBr theoretical peptide FGVRCGAAALTLIVM. However, the

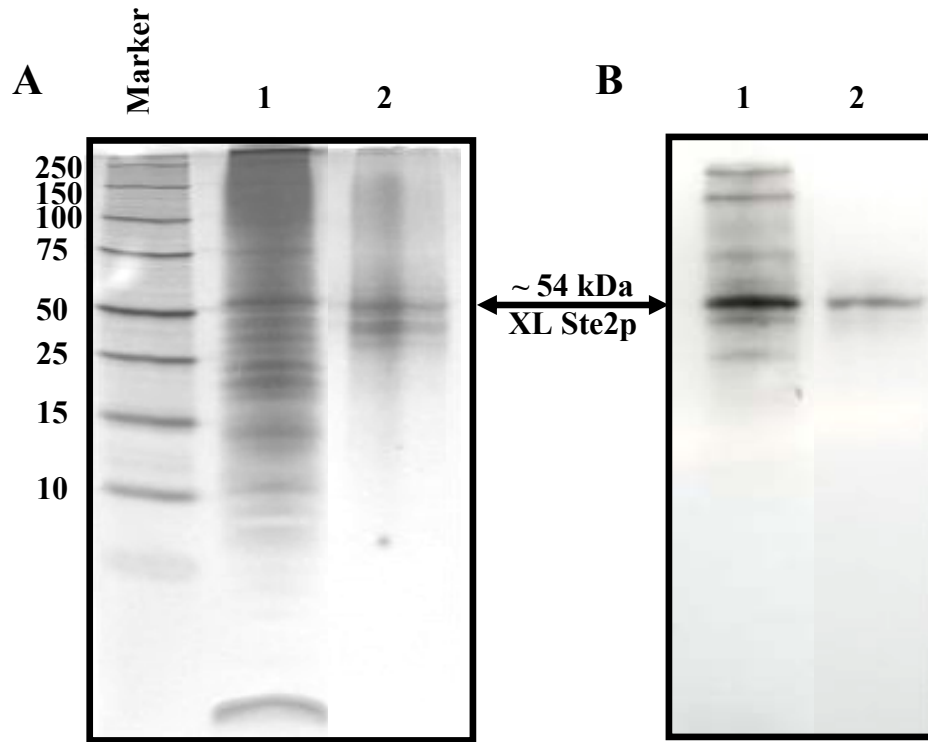


Figure 7: Partial purification of cross-linked Ste2p by gel extraction. A) Silver stained gel to show the total proteins present. Lane one is the unpurified cross-linked BJS21 pNED membranes, lane two is after gel extraction. B) NA-HRP blot of the same samples to detect the biotin tag (from the analog) on Ste2p. Lane 1 is the total membrane and lane 2 is the partially purified sample.

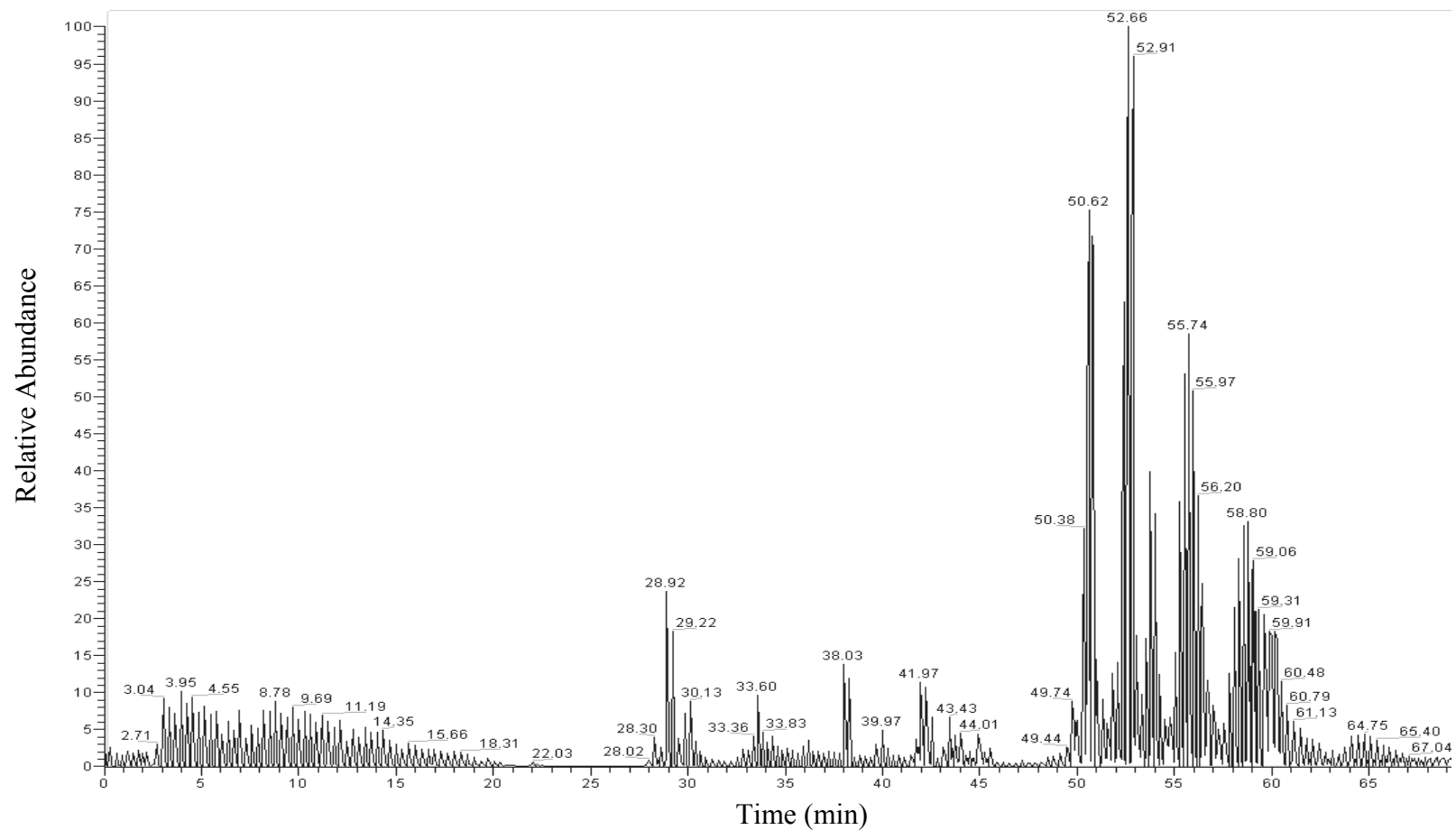


Figure 8: Total ion spectrum of CNBr digested HiTrap elution from LCQ-DECA. Multiple ion packets were observed through out the chromatogram. Most of the peptides start eluting after 25 min.

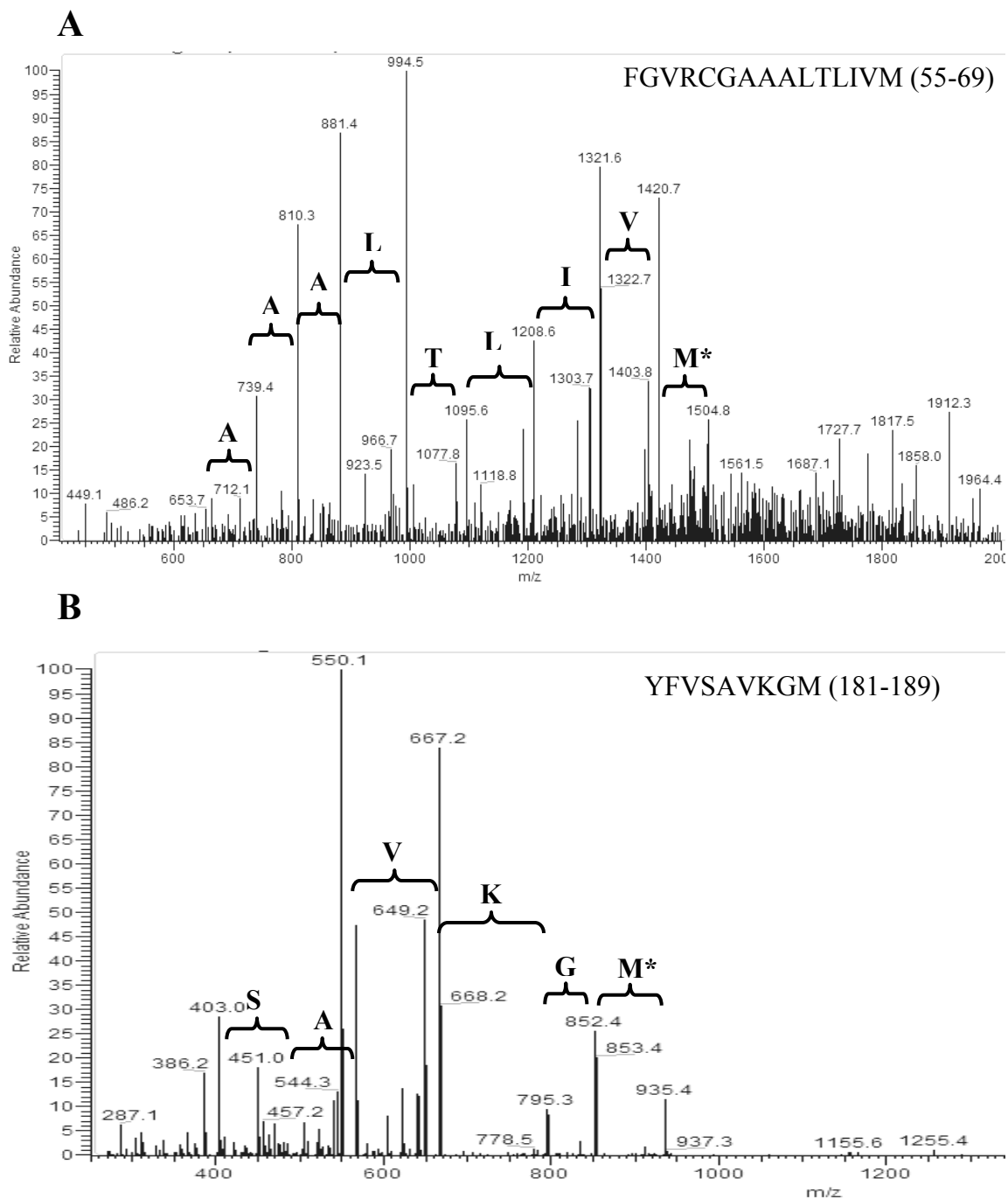


Figure 9: MS/MS spectrums of CNBr digested HiTrap elution from LCQ-DECA.

Two representatives for MS/MS spectrums revealing sequence information of CNBr digested Ste2p fragments A) covering residues 55-69 and B) covering residues 181-189.

* Cleavage at methionine causes loss of 48 Da (formation of homoserine lactone).

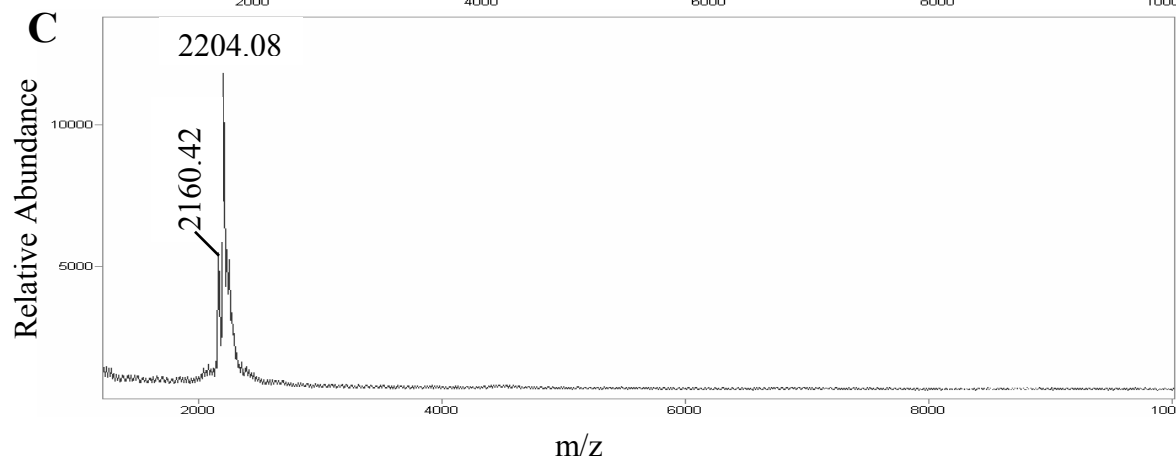
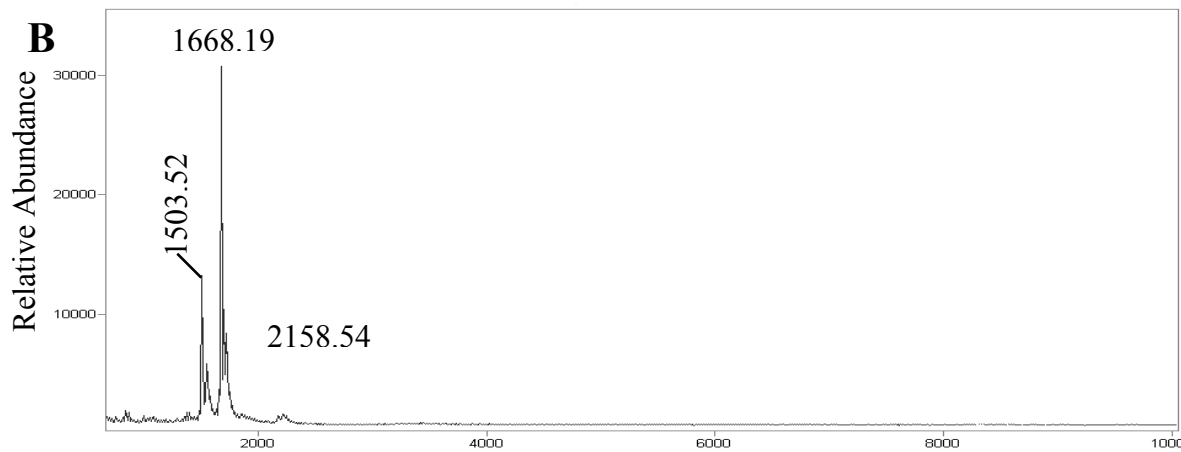
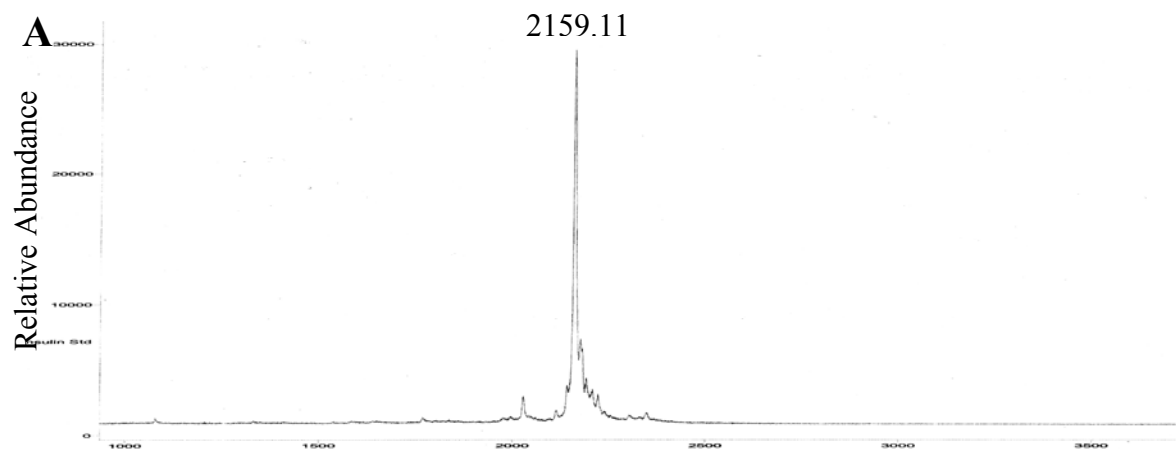
sequence coverage and the presence of many other peptides in the CNBr-digested HiTrap elution necessitated the use of an alternative purification method to enrich cross-linked Ste2p fragment(s).

Optimization of avidin purification and MALDI analysis:

As an alternative purification method, biotinylated samples were enriched by an affinity capture method modified from Li *et al.* [47] and analyzed with MALDI-TOF. This method allowed high sensitivity while minimizing sample handling by taking advantage of the extremely strong interaction between avidin and biotin (having dissociation constant on the order of 10^{-15}) and incorporating this property into mass spectrometry. Two types of immunopure immobilized avidin beads (monomeric avidin and streptavidin from Pierce) were used and compared in this study. Biotinylated [Bpa⁸]α-factor analog was used as the probe throughout the method optimizations, carried out with uncross-linked samples, for mass spectrometry analysis. Capture and detection of the biotinylated ligand from a simple (a 1:1 mixture of the probe with α-factor) and a complex (a 1:300, 1:30, and 1:6 mixture of the probe with CNBr digested BJS21 pNED membranes) mixture was tested.

Analysis of mass spectra from the monomeric avidin beads after incubation with the biotinylated [Bpa⁸]α-factor analog alone indicated that this peptide was captured on the beads, ionized from the matrix during MALDI-TOF analysis, and detected as a 2159.11 m/z ion (theoretical, 2159 Da) (Figure 10). The mixture of α-factor and biotinylated [Bpa⁸]α-factor showed that two peptides were detected in washes, designed

Figure 10: Capture of biotinylated peptides from a simple mixture with monomeric avidin beads. A) Biotinylated [Bpa⁸]α-factor mixed with monomeric avidin beads, B) washes from the monomeric avidin beads after incubation with a mixture of biotinylated [Bpa⁸]α-factor and α-factor (1:1), C) analysis of the washed monomeric avidin beads.



to remove peptides not bound to avidin from the beads (Figure 10B). The detected masses for these two peptides, 1668.19 and 1503.52 Da, matched the theoretical masses for α -factor (1668 Da) and an autolysis product that was missing Tyr¹³ (1504 Da). There were a few minor peaks around 2158 m/z indicating that a very small quantity of the biotinylated probe was eluted in the wash. Spectra from material adsorbed on the washed beads (Figure 10C) had one main peak at 2160 m/z corresponding to biotinylated [Bpa⁸] α -factor (theoretical = 2159 Da) and a neighboring peak possibly due to two sodium (2x22 Da) adduct, observed as 2204.08 Da.

Following the testing of the monomeric avidin beads, streptavidin beads were also tested for the ability to capture biotinylated peptides. The control experiment to confirm the binding to the beads was carried out by incubating the beads with biotinylated [Bpa⁸] α -factor alone. Similar to monomeric avidin beads, analysis of the streptavidin beads resulted in detection of a single peak around 2160 m/z (data not shown). However, analysis of the washes from streptavidin beads showed that these samples contain relatively more biotinylated [Bpa⁸] α -factor as revealed by the detection of peaks at 2159.93 and 2219.19 (a sodium + potassium adduct = +60 Da) m/z (Figure 11A). This result indicated that the streptavidin beads did not bind this ligand as tightly as the monomeric avidin beads. Spectra from washed streptavidin beads (Figure 11B) showed a lower signal at 2161m/z as compared to the signal at this mass obtained from monomeric avidin beads (Figure 10C). In addition, there were other peaks at lower m/z, perhaps due to the presence of residual α -factor. Due to relatively lower binding of the biotinylated peptide to streptavidin beads as compared to monomeric avidin bead, further experiments

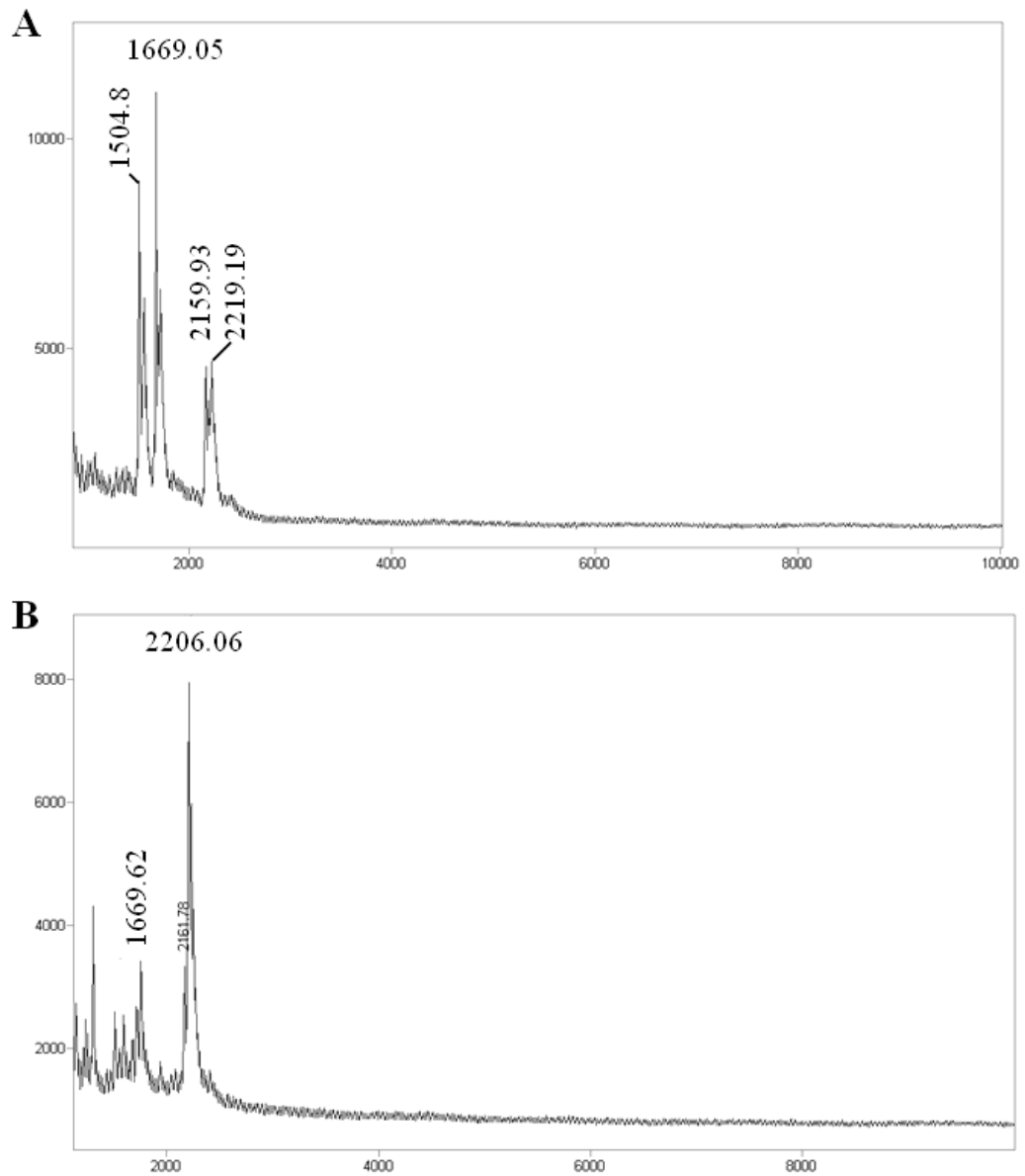


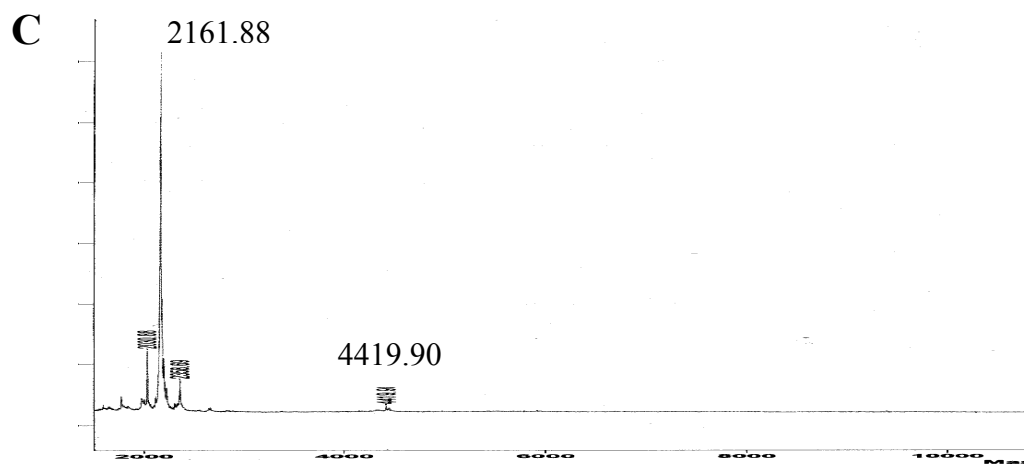
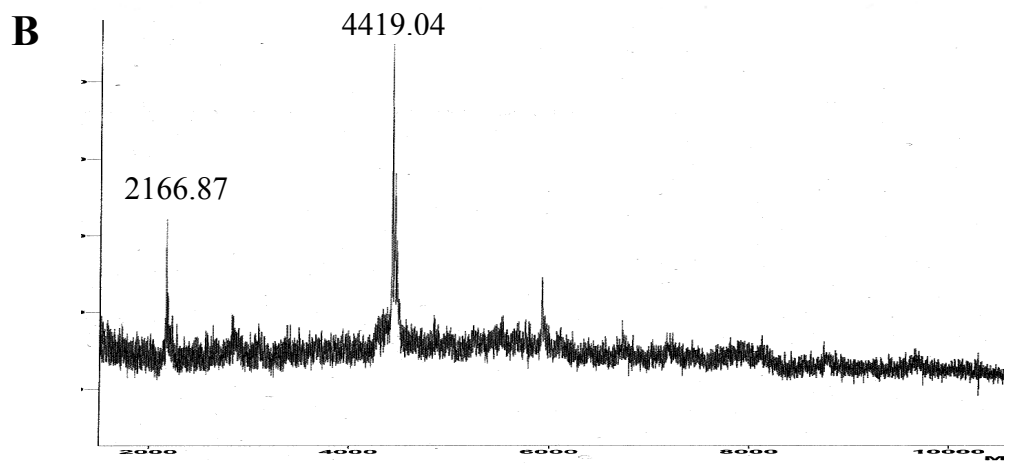
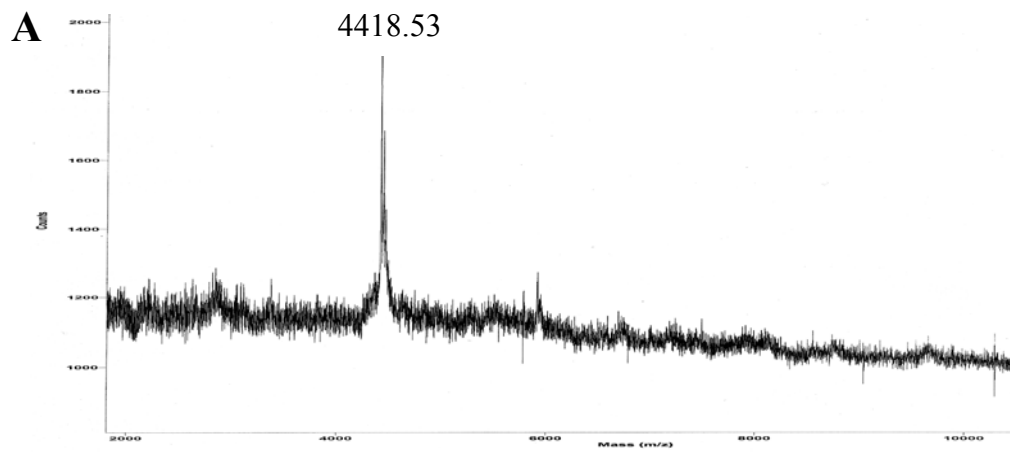
Figure 11: Capture of biotinylated peptides from a simple mixture with streptavidin beads. A) Washes from the streptavidin beads incubated with mixture of biotinylated [Bpa⁸] α -factor and α -factor (1:1), B) analysis of the washed streptavidin beads.

involving purification of biotinylated [Bpa⁸]α-factor from complex mixture was only carried out with monomeric avidin beads.

Analysis of monomeric avidin beads, mixed with CNBr-digested membranes, showed that a major peak at 4418.53 m/z was detected (Figure 12). This peak was likely due to an endogenously biotinylated protein in yeast membranes. Such biotinylated proteins are detected in blots of yeast membranes probed with NA-HRP (See part III of this dissertation). The 4418 m/z peak was detected in all samples (Figure 12 A, B, and C). This mass was excluded from subsequent spectral analyses in this dissertation. Examination of various complex mixtures containing different ratios of biotinylated peptide and membranes digested with CNBr suggested that even at a 1:300 mixture (by weight) the biotinylated [Bpa⁸]α-factor analog (2166 m/z) was captured and identified by MALDI-TOF analysis of monomeric avidin beads (Figure 12B). The 2166 m/z ion detected in this experiment did not coincide exactly with the theoretical 2159 Da peptide. This was attributed to an inaccurate assignment of the m/z ion in a dilute sample with a low signal to noise ratio. A more accurate mass detection was obtained when the mixture had a relatively higher amount of biotinylated probe in the mixture (ratio of biotinylated [Bpa⁸]α-factor to membrane digest approximately 1:30, w/w) (Figure 12C). The discrepancy between the theoretical mass of 2159 Da and the obtained 2161 m/z ion might be due to an inexact calibration of the mass spectrometer.

Following these analyses, CNBr-digested cross-linked membranes were examined under the same conditions. Cross-linking experiments were carried out, as detailed in materials and methods chapter of Part III of this dissertation, with biotinylated [Bpa¹]α-

Figure 12: Capture of biotinylated peptides from a complex mixture with monomeric avidin beads. CNBr-digested membranes were mixed with various amounts of biotinylated [Bpa⁸] α -factor and the beads were analyzed with MALDI-TOF after several washes. A) Beads incubated with CNBr-digested membranes alone, B) beads incubated with [Bpa⁸] α -factor mixed with membrane digest (ratio, 1:300 by weight), C) beads incubated with [Bpa⁸] α -factor with membrane digest (ratio, 1:30 by weight).



factor analog. Analysis of the CNBr-digested membranes prior to cross-linking resulted in detection of a peak at 4417.95 m/z (Figure 13A), the endogenous, biotinylated CNBr fragment in yeast membranes, similar to the fragment found in previous experiments (Figure 12A). The spectrum from the beads that were incubated with CNBr-digested cross-linked membranes had three main peaks, 2071.98, 4413.49, and 6863.9 m/z (Figure 13B). As biotinylated [Bpa¹] α -factor (theoretical mass = 2070 Da) was used in the cross-linking reaction, the 2071.98 ion corresponded to uncross-linked ligand. The peak at 4413.49 was assigned to the endogenously biotinylated peptide and did not match the mass of any cross-linked Ste2p fragments. In addition a peak at 6863.9 m/z was observed. In order to identify a possible cross-linked fragment that could give a signal in this range the theoretical CNBr digestion map of Ste2p was examined. The closest fragment that could generate a signal at this m/z is the region of Ste2p between residues 251 and 294 that gave a mass of 6639 upon cross-linking with biotinylated [Bpa¹] α -factor. The region of Ste2p between residues 251 to 294 was previously identified as the cross-linking region for [Bpa¹] α -factor analogs as described in part II and III of this dissertation. The 6639 theoretical mass was about 224 Da lower than the observed m/z. A literature search on MALDI adducts showed that an adduct of 224 Da from the matrix (SA) used in the MALDI-TOF experiment was observed [50]. If this adduct was indeed associated with the ion found in the experiment (Figure 13), then the experimental mass minus the adduct would match the theoretical mass for biotinylated analog cross-linked to the region of Ste2p covering residues 251 to 294.

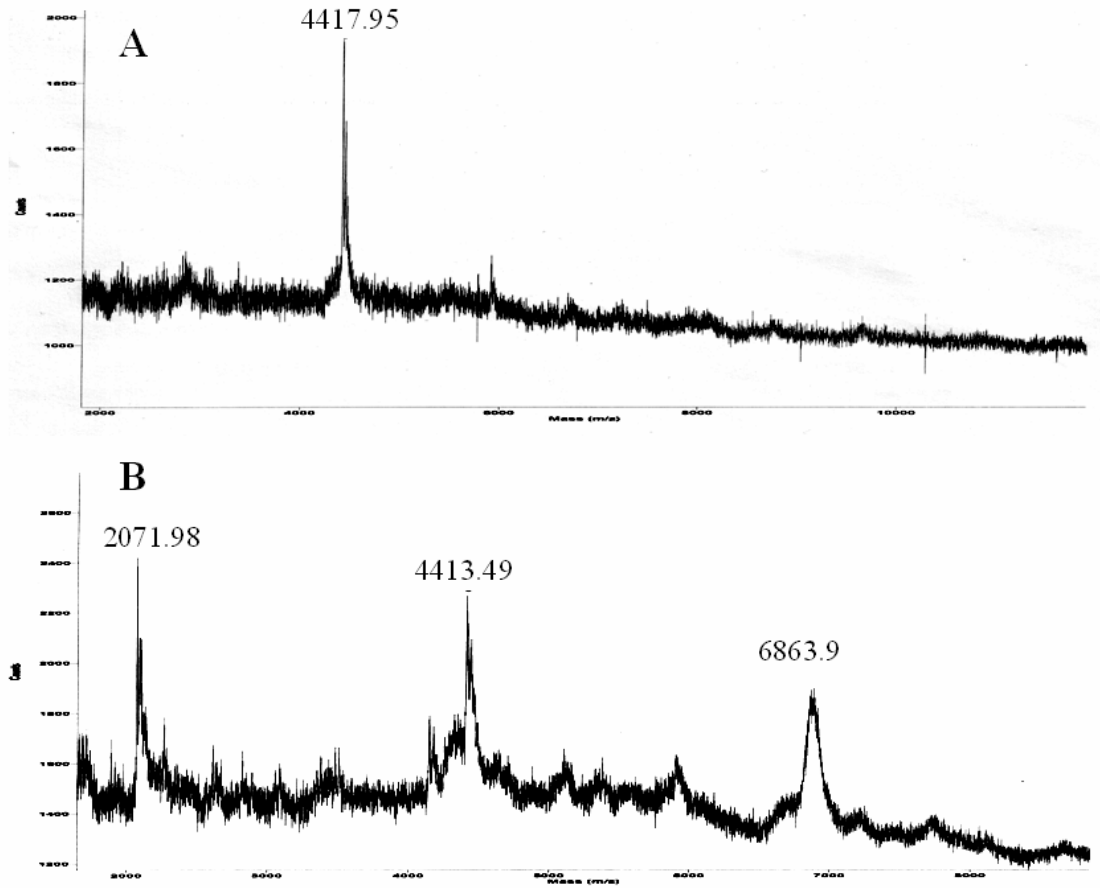


Figure 13: Capture of cross-linked fragments with monomeric avidin beads. A)

CNBr digested yeast membranes were incubated with monomeric avidin beads and

analyzed with MALDI-TOF. B) Membranes cross-linked with biotinylated [Bpa¹] α -

factor analog were digested with CNBr, biotinylated fragments captured by monomeric

avidin beads and analyzed with MALDI-TOF.

Purification and cleanup of biotinylated samples for Nanospray-MS (NS-MS):

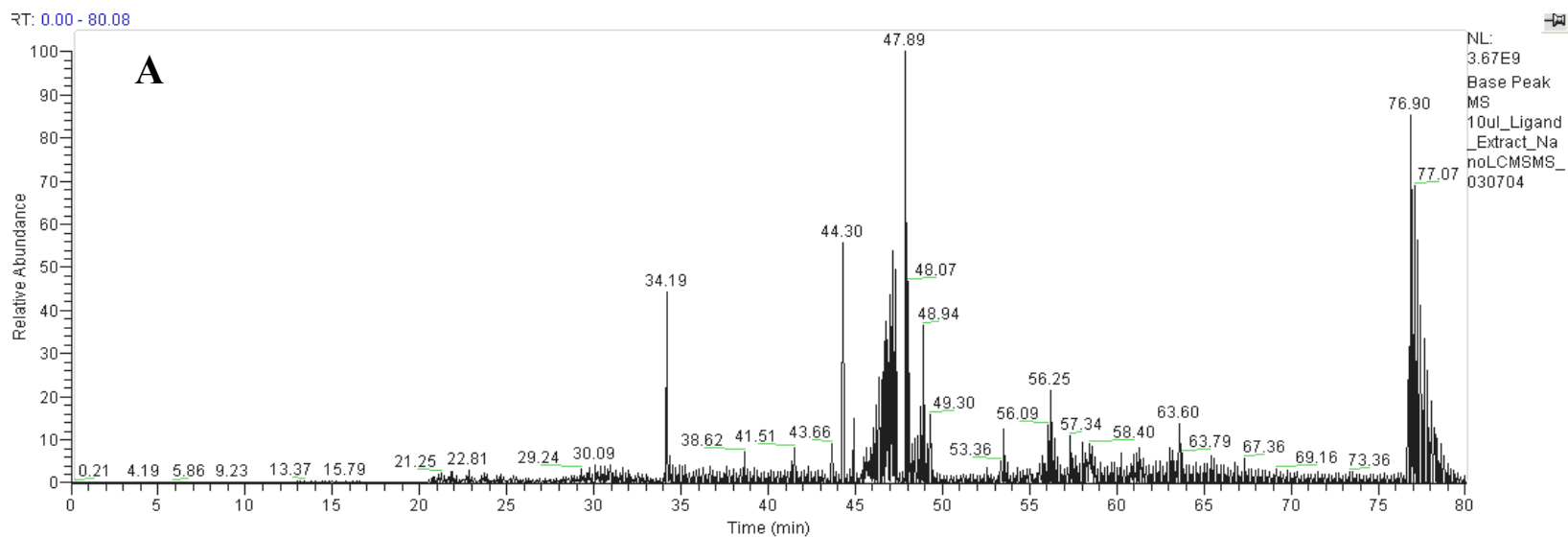
Although the information obtained from MALDI-TOF was much more accurate than calculating peptide masses from SDS-PAGE, sequencing was not possible with this method. In order to identify the Ste2p residue(s) where the cross-linking takes place, sequencing the cross-linked fragments is necessary. Tandem mass spectrometry analyses were carried out, with a LCQ DECA instrument, to obtain sequence information from biotinylated [Bpa⁸] α -factor and cross-linked Ste2p fragments. A column containing monomeric avidin beads was used to purify biotinylated fragments prior to tandem NS-MS analysis. The protocol was first tested with a complex mixture of CNBr-digested yeast membranes and biotinylated [Bpa⁸] α -factor (300:1 mixture, w/w). Elutions from the column were analyzed with the LCQ-DECA instrument. The results (Figure 14) showed that there were relatively few peaks in the total ion spectra in comparison to the HiTrap elutions previously analyzed with the same method (Figure 8).

MS/MS analysis of the main ions at 53 minutes covered almost the complete sequence of biotinylated [Bpa⁸] α -factor (Figure 15). This spectrum also showed that the biotin tag attached to Lys⁷ of the analog can be cleaved during fragmentation inside the ion trap. This experiment showed that a monomeric avidin column could be used to capture biotinylated peptides of sufficient purity for sequence analysis by tandem MS.

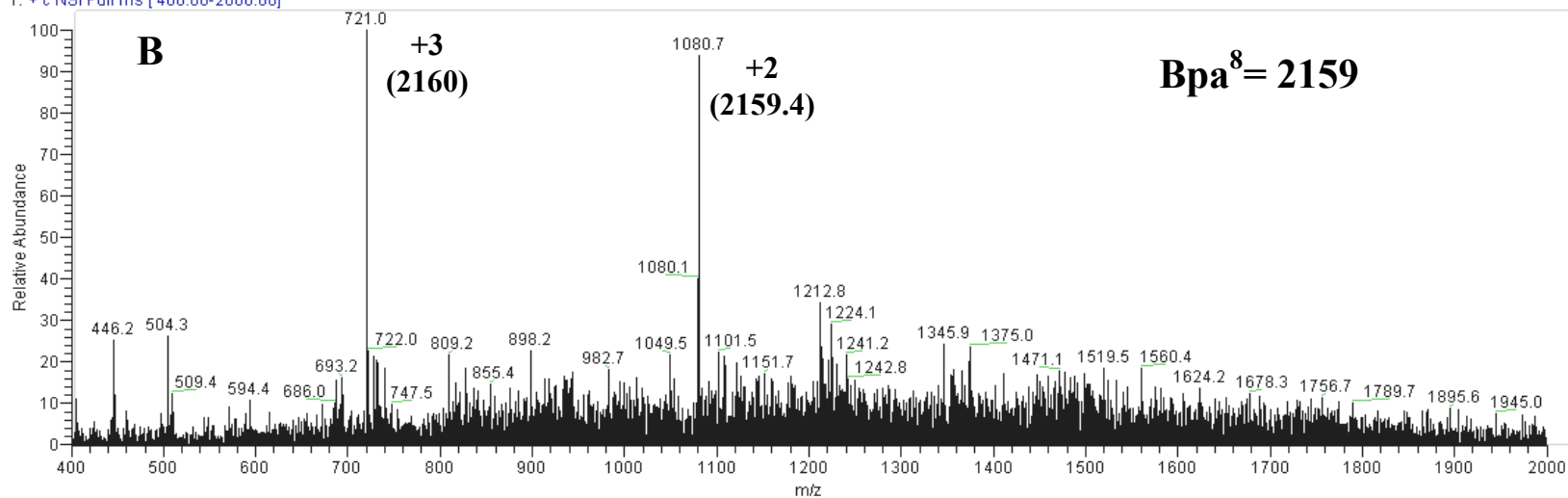
Following these results a similar purification protocol was applied to membranes cross-linked with various biotinylated Bpa-scanned α -factor analogs (Bpa1, Bpa3, Bpa5 and Bpa13). Cross-linked Ste2p was first partially purified with gel extraction from the solubilized membranes. This initial purification was required to get rid of the uncross-

Figure 14: Analysis of elutions from monomeric avidin column with LCQ-DECA.

A) The total ion spectrum of the elutions from monomeric avidin column which was incubated with a complex mixture (CNBr digested yeast membranes + biotinylated [Bpa⁸]α-factor), B) the full MS spectra at 53rd minute indicating detection of a peptide with a mass of ~2160 Da.



10ul_Ligand_Extract_NanoLCMSMS_030704 #1101-1119 RT: 52.96-53.71 AV: 5 NL: 1.74E8
T: + c NSI Full ms [400.00-2000.00]



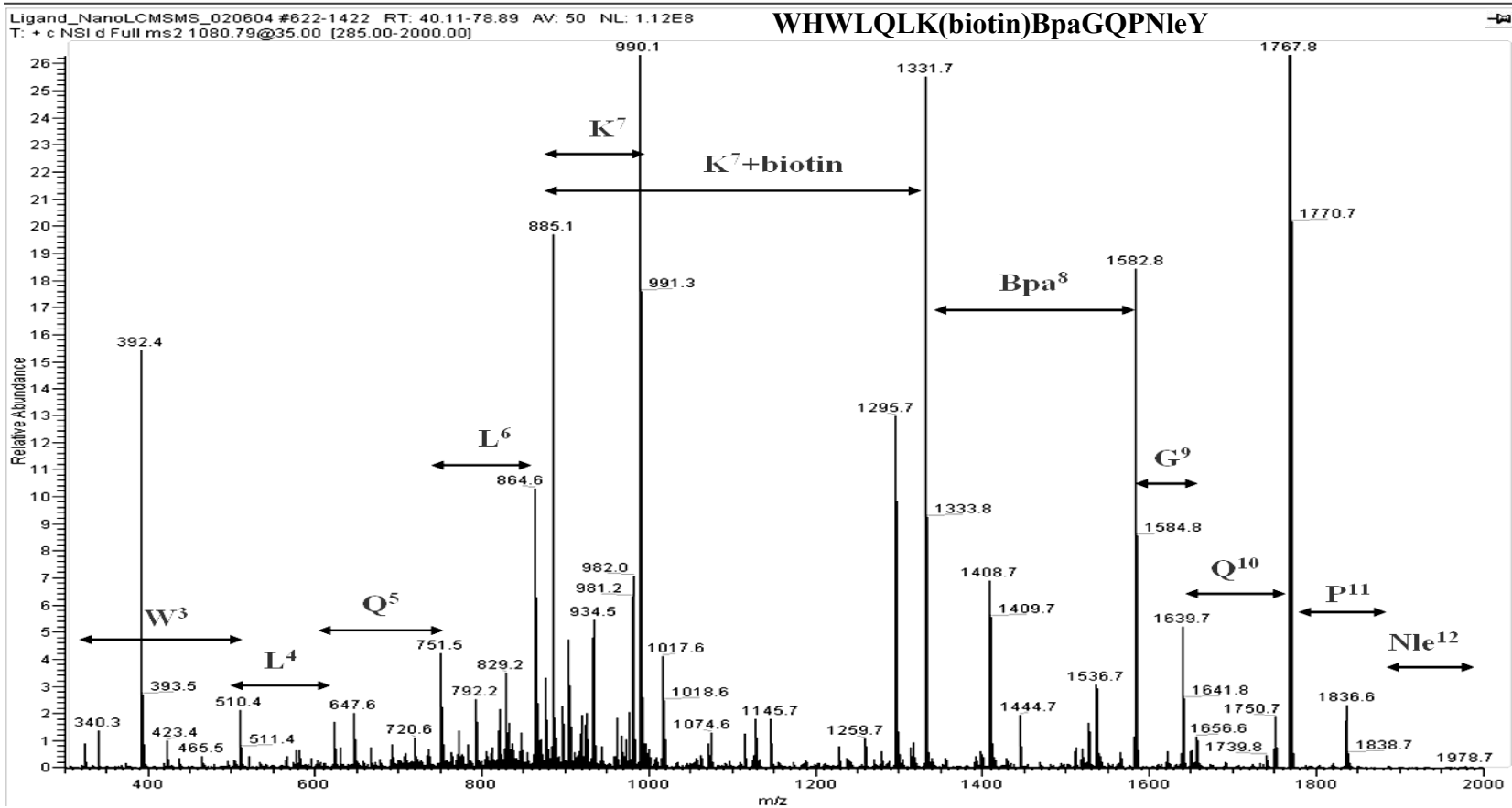
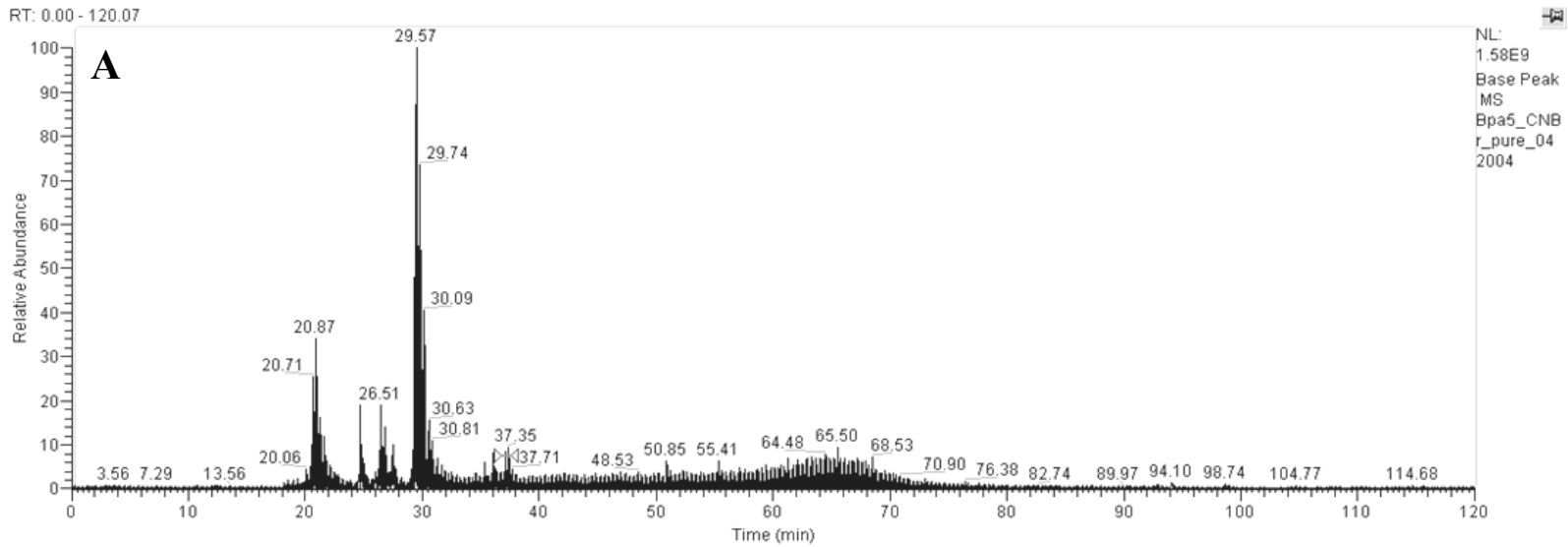


Figure 15: MS/MS analysis of the 1080.79 m/z ion at 53rd minute. The main ion at 53rd min was selected and analyzed after fragmentation by CID.

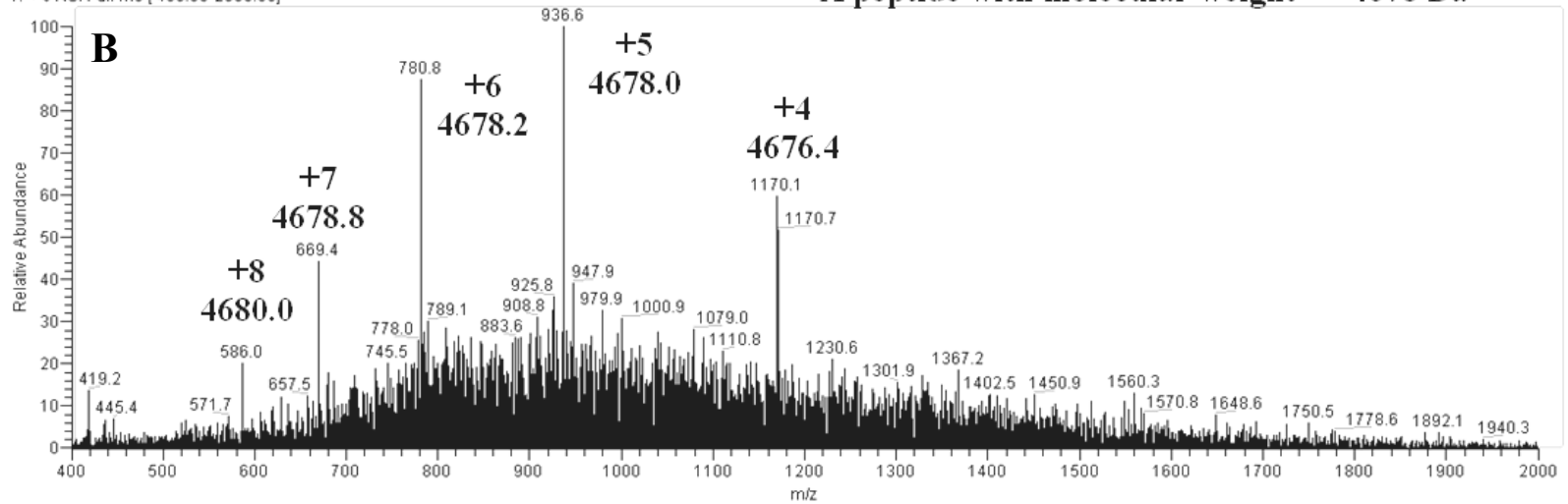
linked ligand that would decrease the purification yield from avidin column. The concentrated electro-elution samples were then re-suspended in 70% formic acid and digested with CNBr. Concentrated digests were neutralized and loaded on a monomeric avidin column to enrich the biotinylated fragments. Analysis of the elutions with LCQ-DECA showed that the total ion spectra contained a few main ion packets as shown in a representative spectrum obtained from biotinylated [Bpa⁵] α -factor cross-linked membrane digests (Figure 16A). Unfortunately, the fragmentation spectra for these ions were too complex to analyze by hand and a proper software was not available to analyze the data automatically. Manual analysis of the total ion spectra obtained from these experiments revealed identification of a few peptide masses. For example the full MS spectrum for biotinylated [Bpa⁵] α -factor cross-linked sample suggested that a 4678 Da peptide was eluted at 37th minute of the MS analysis. The ion packet observed in figure 16B showed that this peptide is highly charged, thus the fragmentation spectrum could contain multiply charged ions. Examination of the theoretical fragments from cross-linked Ste2p illustrated that the CNBr fragment covering residues 166-189 had the closest mass (fragment mass 2488.23 + ligand mass 2128 = 4616.23 Da) to the mass observed. The difference between the theoretical and observed masses was 61 Da, which could be due to a sodium + potassium adduct (60 Da) during the sample preparation. A similar adduct of 60 Da was observed when the biotinylated Bpa⁸ scanned ligand was analyzed by MALDI-TOF (Figure 11A). Although an MS/MS sequence was obtained for the major ions at this time point (data not shown), the sensitivity of the instrument was not great enough to deconvolute the charge states of the fragment ions to identify the sequence. However, the observed mass implied cross-linking of biotinylated [Bpa⁵] α -

Figure 16: Analysis of monomeric avidin column purified CNBr digested cross-linked membranes with LCQ-DECA. A) The total ion spectrum of the elutions from monomeric avidin column loaded with CNBr digested membranes, cross-linked with biotinylated [Bpa⁵] α -factor analog B) the full MS spectra at 37th minute showing the multiple charge states of 4678 Da peptide.



Bpa5_CNBr_pure_042004 #847-865 RT: 36.81-37.53 AV: 5 NL: 9.14E7
T: + c NSI Full ms [400.00-2000.00]

A peptide with molecular weight = ~4678 Da



factor analog to a region of Ste2p covering residues 166-189 (TM4) with the assumption of a 60 Da adduct as discussed above.

CHAPTER 4

Discussion

In order to determine the Ste2p residue where the cross-linking of biotinylated Bpa scanned α -factor analogs takes place, accurate mass detection is crucial. Recent developments in mass spectrometry combined with a proper affinity purification make this technique an invaluable method for detection of peptide masses with very high accuracy and sensitivity [63-65].

Although purification techniques have been previously optimized to purify α -factor pheromone receptor (Ste2p) [44], application of these methods to cross-linked membranes and compatibility of the elutions with mass spectrometry have not been tested. This part of the dissertation outlined the use of different affinity chromatography methods to purify intact Ste2p or biotinylated cross-linked fragments from a complex membrane mixture, and a size exclusion protocol applied to partially purify Ste2p. Also two mass spectrometry techniques were used to identify cross-linked regions on the α -factor pheromone receptor.

Currently, many affinity purification techniques are commonly used to purify various proteins. In this study a 6xHis tagged Ste2p construct was used to take advantage of the immobilized-metal affinity chromatography (IMAC). The FLAG tag present in the same construct was used for detection purposes. After comparing two different metal chelating resins as described in the results, the HiTrap column from Amersham Biosciences was shown to be preferable to the Ni-NTA resin from Qiagen under the

conditions tested. The main difference between the two resins is their interaction with the metal ions. While the HiTrap column uses iminodiacetic acid (IDA) to interact with the metal ions, Ni-NTA resin carries nitrilotriacetic acid (NTA), which provides an additional interaction site for the metal ion (Figure 17A). The supplier of this resin claims that this extra interaction with the metal ion increases the stability of the charged column thus binding to 6xHis tagged proteins would be tighter than IDA matrices. However, occupation of four out of six binding sites of (+2) charged metal ion leaves only two possible sites for the interaction with His from 6xHis tag (Figure 17B). On the other hand IDA matrices could interact with the 6xHis tag at the remaining 3 contact sites potentially yielding higher specificity.

Results from purification with both resins showed that Ste2p.FT.HT could be captured and partially purified from yeast membrane preparations. Elutions from both resins carried a few non-specifically bound proteins detected by silver stain (Figure 3&6). When the specifications of these two resins were compared, the main differences were the ability of the HiTrap column to withstand higher flow-rates and back pressure, thus allowing coupling to a HPLC instrument. Due to this reason and the flexibility in the choice of metal ions that could be used to charge the resin, HiTrap columns were preferred throughout this study for partial purification of Ste2p.FT.HT.

Besides the IMAC, electro-elution from preparative SDS gels was also applied for partial purification of cross-linked Ste2p. Following cross-linking (UV exposure), many proteins in membrane preparations aggregate, causing a decrease in their solubility. Unless treated with denaturants like urea or guanidine-HCl, use of these samples with an

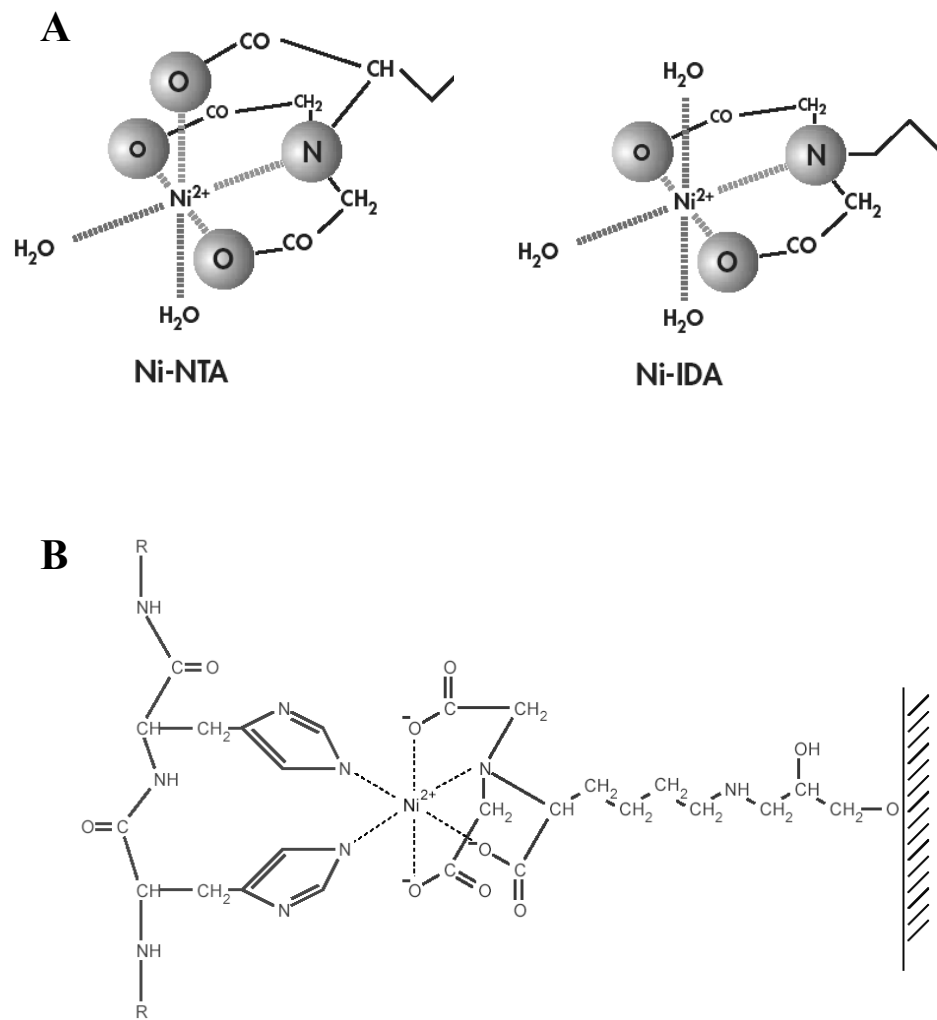


Figure 17: Comparison of the interaction of different metal chelating matrices with nickel ion. A) Shows how the two metal chelating matrices, NTA and IDA, interact with metal ions, B) an illustration of how two His could interact with the NTA bound Ni^{2+} (Figures adapted from “A handbook for high-level expression and purification of 6xHis-tagged proteins” available online at http://www1.qiagen.com/literature/handbooks/PDF/Protein/Expression/QXP_QIAexpressionist/1024473_QXPHB_0603.pdf)

affinity chromatography (like IMAC) is not feasible. Although most of the affinity columns are compatible with many of the denaturants, additional sample cleanup is often necessary, which in most cases could cause low yield. In order to decrease sample handling, a simple and efficient gel extraction method was applied to partially purify cross-linked Ste2p. As detailed in results, this technique was particularly good at removing the aggregates or degradation products that usually co-purified by affinity chromatography (Figure 4 inset). The presence of multiple forms of the cross-linked Ste2p in the purified sample would complicate the fragmentation and the analysis of the fragments afterwards. One disadvantage of gel extraction is the requirement of a dialysis step after the electro-elution to remove the excess detergent and buffer components from the SDS-PAGE. The purity (Figure 7A, lane 2) and the ease of sample handling by gel extraction were comparable to the IMAC method.

The IMAC and gel extraction methods were satisfactory for analysis of cross-linked Ste2p fragments, following chemical or enzymatic digestion, with western blot analysis. On the other hand use of highly sensitive mass spectrometric techniques like MALDI-TOF, or NS-MS requires much purer and enriched samples. For this purpose, during the synthesis of the Bpa-scanned α -factor analogs incorporation of a biotin tag was included to take advantage of the well-studied avidin-biotin chemistry [51, 52]. The extremely strong interaction between the avidin and biotin was useful for both detection and affinity purification [53, 54]. Two different immunopure immobilized avidin beads (monomeric avidin and streptavidin from Pierce) were used and compared in this study.

Streptavidin, immobilized on beaded agarose, is an avidin-like protein that carries four binding sites for biotin, each with a similar binding affinity (dissociation constant ~

10^{-15}). Unlike avidin this protein has a lower pI (5-6) and is not a glycoprotein, therefore it is postulated to be less prone to nonspecific binding [51]. Monomeric avidin, immobilized on beaded agarose, has only one binding site for biotin (dissociation constant $\sim 10^{-8}$). Both beads were incubated with a simple mixture containing a biotinylated α -factor analog and the wild type α -factor pheromone in a 1:1 mixture. Analysis with MALDI-TOF showed that capture of the biotinylated analog from this simple mixture with monomeric avidin beads was more efficient compared to the streptavidin beads. A similar study by Gitlin *et al.* [70] suggested that the biotin binding site of streptavidin could be buried more deeply compared to monomeric avidin [55] requiring a long-chain spacer arm between the analyte and biotin tag for efficient binding. Thus depending on these analyses, monomeric avidin beads were preferred for further experiments.

Following the success in capturing a biotinylated analog from a simple mixture, monomeric avidin beads were tested with a complex mixture that mimics the actual digests containing cross-linked Ste2p fragment(s). Briefly, yeast membranes carrying Ste2p ($\sim 300\mu\text{g}$ total protein) were digested with CNBr and mixed with a biotinylated α -factor analog. Mixtures containing various ratios of ligand to membrane digest were then incubated with monomeric avidin beads and subjected to several washes as described in Materials and Methods. Results showed that biotinylated analog can be captured even from a mixture where the ligand to total membrane digest ratio is 1:300 by weight. There was only one main contamination peak probably originating from an endogenously biotinylated protein. At the lowest ratio tested, peak broadening and adducts were observed. However analysis of higher intensity signals (from 1:30 mixture) revealed an

experimental mass for the biotinylated analog, which was only 2 Da higher than the theoretical weight (Figure 12C).

Although these results suggested that for lower concentration samples, like cross-linked fragments, there could be deviations from mass accuracy, the method was much more sensitive than calculating masses from relative mobility on SDS-PAGE. Therefore the method was applied to a sample where a CNBr digested cross-linked membrane was used (membranes were cross-linked with biotinylated [Bpa1] α -factor). Detection of three main peaks, including a peak at 4417 Da, previously observed in membrane only assay (Figure 12A), was quite promising. Analysis of the masses obtained from these peaks suggested the presence of uncross-linked free ligand (theoretical mass = 2070) and another peptide with observed weight of 6863.9 Da. This observed mass was 224.51 Da higher than the theoretical weight of a possible cross-linked fragment resulting from linking of the biotinylated [Bpa1] α -factor analog (2070 Da) to a region of Ste2p covering residues 251-294 (4569.39 Da) generated by CNBr digestion. Even though this difference is very big considering the mass accuracy of MALDI-TOF, it has been reported that a matrix adduct from sinapinic acid (SA = 224 Da) could be observed in such analyses [47, 50], which will result in such a mass deviation. Testing of a different matrix, α -Cyano-4-hydroxycinnamic acid (CHCA), to solve this problem caused the disappearance of signal at high m/z region from the sample. CHCA matrix is commonly used for small size (2 to 3 kDa) peptides and thus might not be effective in the ionization of bigger fragments observed with SA matrix. These results showed that although the MALDI-TOF-MS is a very sensitive and accurate method to determine masses of peptides, without sequence

information, assignment of these masses to possible cross-linked fragments could not be done unambiguously.

Thus partially purified Ste2p, digested with CNBr, was analyzed with NS-MS to obtain sequence information from receptor fragments. Results indicated that IMAC or gel extraction alone was not enough to obtain sufficient purity for NS-MS. Although a few peptides were detected and sequenced from Ste2p (Figure 9 A and B), the sequence coverage was very low (~10% of the receptor sequence). The presence of several additional peptides from various other proteins complicated the full MS and MS/MS sequences, making it very hard to analyze. Therefore alternative affinity purification methods were tested to obtain purer samples before NS-MS analysis.

A monomeric avidin column was quite successful when tested for purification of biotinylated ligands from CNBr digested yeast membranes. Figure 14 shows that the main ion in the chromatogram belongs to the biotinylated analog, which was mixed with the complex membrane digest. There were only a few other peptides from this mixture observed in the total ion spectrum indicating the sample was relatively pure. In addition, the MS/MS spectrum from this high intensity ion revealed almost the complete sequence for the biotinylated analog (Figure 15). Unfortunately application of this method without any modification to the cross-linked membranes was not as successful. The presence of uncross-linked ligand in these samples competed against the cross-linked fragments from Ste2p during purification with monomeric avidin column. Additionally, the uncross-linked peptides were smaller in size, thus their ionization in the NS-MS experiments was more efficient. The signal from these small peptides masked signal from less abundant peptides like the bulky cross-linked fragments. To overcome these problems, application

of monomeric avidin column following gel extraction and CNBr digestion of cross-linked Ste2p was applied prior to NS-MS analysis. This two-step purification was designed to eliminate the uncross-linked ligand prior to monomeric avidin column resulting in better enrichment of the biotinylated cross-linked fragments.

Preliminary results from these experiments suggested that a few peptides could be enriched and detected by NS-MS. However the MS/MS spectra of these peptides were complicated. Presence of multiple charge states of the fragment ions made it very hard to obtain a series of related ions to determine a sequence tag. Due to the resolution limit of the mass spectrometer used in this study the identification of the charge states of these ions was not possible, thus deconvolution of the sequence information from these MS/MS spectra could not be accomplished. In the absence of sequence information, data obtained from NS-MS studies was only supportive instead of being informative. These problems could be solved with a more sensitive instrument like a Fourier Transform Ion Cyclotron Resonance (FT-ICR) that could do MS/MS analysis, or by the use of isotopically labeled cross-linkers resulting in doublet ions that would aid identification of cross-linked fragments in total ion spectra. The details of these methods are further discussed in Part V, Chapter 2 of this dissertation.

List of References for Part IV

1. Kotzyba-Hibert, F., T. Grutter, and M. Goeldner, *Molecular investigations on the nicotinic acetylcholine receptor: conformational mapping and dynamic exploration using photoaffinity labeling*. Mol Neurobiol, 1999. 20(1): p. 45-59.
2. Brunner, J., *New photolabeling and crosslinking methods*. Annu Rev Biochem, 1993. 62: p. 483-514.
3. Dorman, G. and G.D. Prestwich, *Benzophenone photophores in biochemistry*. Biochemistry, 1994. 33(19): p. 5661-73.
4. Hatanaka Y., N., H., Kanaoka, Y., *Diazirine-based photoaffinity labeling: chemical approach to biological interfaces*. Rev. Heteroatom. Chem, 1996. 14: p. 213-243.
5. Hazum, E., *Photoaffinity labeling of peptide hormone receptors*. Endocr Rev, 1983. 4(4): p. 352-62.
6. Henry, L.K., et al., *Identification of a contact region between the tridecapeptide alpha-factor mating pheromone of Saccharomyces cerevisiae and its G protein-coupled receptor by photoaffinity labeling*. Biochemistry, 2002. 41(19): p. 6128-39.
7. Nakayama, H., et al., *Identification of 1,4-dihydropyridine binding regions within the alpha 1 subunit of skeletal muscle Ca²⁺ channels by photoaffinity labeling with diazpine*. Proc Natl Acad Sci U S A, 1991. 88(20): p. 9203-7.

8. Nakayama, H., et al., *Photolabeled sites with a tetrodotoxin derivative in the domain III and IV of the electroplax sodium channel*. *Biochem Biophys Res Commun*, 1992. 184(2): p. 900-7.
9. Fukayama, S., et al., *New insights into interactions between the human PTH/PTHrP receptor and agonist/antagonist binding*. *Am J Physiol*, 1998. 274(2 Pt 1): p. E297-303.
10. Costello, C.A., et al., *Mechanistic studies on thiaminase I. Overexpression and identification of the active site nucleophile*. *J Biol Chem*, 1996. 271(7): p. 3445-52.
11. Withers, S.G. and R. Aebersold, *Approaches to labeling and identification of active site residues in glycosidases*. *Protein Sci*, 1995. 4(3): p. 361-72.
12. Tull, D., et al., *Identification of derivatized peptides without radiolabels: tandem mass spectrometric localization of the tagged active-site nucleophiles of two cellulases and a beta-glucosidase*. *Anal Biochem*, 1995. 224(2): p. 509-14.
13. Staedtler, P., et al., *Identification of the active-site nucleophile in 6-phospho-beta-galactosidase from Staphylococcus aureus by labelling with synthetic inhibitors*. *Eur J Biochem*, 1995. 232(2): p. 658-63.
14. Salto, R., et al., *In vitro characterization of nonpeptide irreversible inhibitors of HIV proteases*. *J Biol Chem*, 1994. 269(14): p. 10691-8.
15. Caldera, P.S., et al., *Alkylation of a catalytic aspartate group of the SIV protease by an epoxide inhibitor*. *Bioorg Med Chem*, 1997. 5(11): p. 2019-27.

16. Girault, S., et al., *The use of photolabelled peptides to localize the substance-P-binding site in the human neurokinin-1 tachykinin receptor*. Eur J Biochem, 1996. 240(1): p. 215-22.
17. Jespersen, S., et al., *Identification of multiple target sites for a glutathione conjugate on glutathione-S-transferase by matrix-assisted laser desorption/ionization mass spectrometry*. J Mass Spectrom, 1996. 31(1): p. 101-7.
18. Roberts, E.S., et al., *Mechanistic studies of 9-ethynylphenanthrene-inactivated cytochrome P450 2B1*. Arch Biochem Biophys, 1995. 323(2): p. 303-12.
19. Gatlin, C.L., et al., *Protein identification at the low femtomole level from silver-stained gels using a new fritless electrospray interface for liquid chromatography-microspray and nanospray mass spectrometry*. Anal Biochem, 1998. 263(1): p. 93-101.
20. Lim, H., et al., *Identification of 2D-gel proteins: a comparison of MALDI/TOF peptide mass mapping to mu LC-ESI tandem mass spectrometry*. J Am Soc Mass Spectrom, 2003. 14(9): p. 957-70.
21. Jensen, O.N., et al., *Peptide sequencing of 2-DE gel-isolated proteins by nanoelectrospray tandem mass spectrometry*. Methods Mol Biol, 1999. 112: p. 571-88.
22. Chaurand, P., F. Luetzenkirchen, and B. Spengler, *Peptide and protein identification by matrix-assisted laser desorption ionization (MALDI) and MALDI-post-source decay time-of-flight mass spectrometry*. J Am Soc Mass Spectrom, 1999. 10(2): p. 91-103.

23. Smillie, L.B., Carpenter, M.R., *Separation, Analysis, and Conformation*, in *HPLC of Peptides and Proteins*, C.T. Mant, Hodges, R.S., Editor. 1991, CRC Press: Boca Raton, FL. p. 875-894.
24. Wenschuh, H., et al., *Mass spectrometric sequencing of synthetic peptides containing alpha, alpha-dialkylated amino acid residues by MALDI post-source decay analysis*. *Pept Res*, 1996. 9(3): p. 122-6.
25. Van Loo, G., et al., *A matrix-assisted laser desorption ionization post-source decay (MALDI-PSD) analysis of proteins released from isolated liver mitochondria treated with recombinant truncated Bid*. *Cell Death Differ*, 2002. 9(3): p. 301-8.
26. Neubert, H., et al., *MALDI post-source decay and LIFT-TOF/TOF investigation of alpha-cyano-4-hydroxycinnamic acid cluster interferences*. *J Am Soc Mass Spectrom*, 2004. 15(3): p. 336-43.
27. Nesvizhskii, A.I. and R. Aebersold, *Analysis, statistical validation and dissemination of large-scale proteomics datasets generated by tandem MS*. *Drug Discov Today*, 2004. 9(4): p. 173-81.
28. Yates, J.R., 3rd, et al., *Future prospects for the analysis of complex biological systems using micro-column liquid chromatography-electrospray tandem mass spectrometry*. *Analyst*, 1996. 121(7): p. 65R-76R.
29. Wilm, M., *Mass spectrometric analysis of proteins*. *Adv Protein Chem*, 2000. 54: p. 1-30.
30. Wilm, M. and M. Mann, *Analytical properties of the nanoelectrospray ion source*. *Anal Chem*, 1996. 68(1): p. 1-8.

31. Sachon, E., et al., *Met174 side chain is the site of photoinsertion of a substance P competitive peptide antagonist photoreactive in position 8*. FEBS Lett, 2003. 544(1-3): p. 45-9.
32. Leite, J.F., et al., *Conformation-dependent hydrophobic photolabeling of the nicotinic receptor: electrophysiology-coordinated photochemistry and mass spectrometry*. Proc Natl Acad Sci U S A, 2003. 100(22): p. 13054-9.
33. Fournier, I., et al., *Sequencing of a branched peptide using matrix-assisted laser desorption/ionization time-of-flight mass spectrometry*. J Mass Spectrom, 2000. 35(12): p. 1425-33.
34. Vinh, J., et al., *Sequencing branched peptides with CID/PSD MALDI-TOF in the low-picomole range: application to the structural study of the posttranslational polyglycylation of tubulin*. Anal Chem, 1997. 69(19): p. 3979-85.
35. Bayan, N. and H. Therisod, *Photoaffinity cross-linking of acyl carrier protein to Escherichia coli membranes*. Biochim Biophys Acta, 1992. 1123(2): p. 191-7.
36. Rappsilber, J., et al., *A generic strategy to analyze the spatial organization of multi-protein complexes by cross-linking and mass spectrometry*. Anal Chem, 2000. 72(2): p. 267-75.
37. Young, M.M., et al., *High throughput protein fold identification by using experimental constraints derived from intramolecular cross-links and mass spectrometry*. Proc Natl Acad Sci U S A, 2000. 97(11): p. 5802-6.
38. Chen, T., J.D. Jaffe, and G.M. Church, *Algorithms for identifying protein cross-links via tandem mass spectrometry*. J Comput Biol, 2001. 8(6): p. 571-83.

39. Pearson, K.M., L.K. Pannell, and H.M. Fales, *Intramolecular cross-linking experiments on cytochrome c and ribonuclease A using an isotope multiplet method*. Rapid Commun Mass Spectrom, 2002. 16(3): p. 149-59.
40. Muller, D.R., et al., *Isotope-tagged cross-linking reagents. A new tool in mass spectrometric protein interaction analysis*. Anal Chem, 2001. 73(9): p. 1927-34.
41. Taverner, T., et al., *Characterization of an antagonist interleukin-6 dimer by stable isotope labeling, cross-linking, and mass spectrometry*. J Biol Chem, 2002. 277(48): p. 46487-92.
42. Trester-Zedlitz, M., et al., *A modular cross-linking approach for exploring protein interactions*. J Am Chem Soc, 2003. 125(9): p. 2416-25.
43. Schriemer, D.C., T. Yalcin, and L. Li, *MALDI mass spectrometry combined with avidin-biotin chemistry for analysis of protein modifications*. Anal Chem, 1998. 70(8): p. 1569-75.
44. David, N.E., et al., *Expression and purification of the Saccharomyces cerevisiae alpha-factor receptor (Ste2p), a 7-transmembrane-segment G protein-coupled receptor*. J Biol Chem, 1997. 272(24): p. 15553-61.
45. Hurst, G.B., T.K. Lankford, and S.J. Kennel, *Mass spectrometric detection of affinity purified crosslinked peptides*. J Am Soc Mass Spectrom, 2004. 15(6): p. 832-9.
46. Clauser, K.R., P. Baker, and A.L. Burlingame, *Role of accurate mass measurement (+/- 10 ppm) in protein identification strategies employing MS or MS/MS and database searching*. Anal Chem, 1999. 71(14): p. 2871-82.

47. Schriemer, D.C. and L. Li, *Combining avidin-biotin chemistry with matrix-assisted laser desorption/ionization mass spectrometry*. *Anal Chem*, 1996. 68(19): p. 3382-7.
48. Porath, J., et al., *Metal chelate affinity chromatography, a new approach to protein fractionation*. *Nature*, 1975. 258(5536): p. 598-9.
49. Sulkowski, E., *Purification of proteins by IMAC*. *Trends Biotechnol.*, 1985. 3: p. 1-7.
50. Niederkofler, E.E., et al., *Novel mass spectrometric immunoassays for the rapid structural characterization of plasma apolipoproteins*. *J Lipid Res*, 2003. 44(3): p. 630-9.
51. Savage, M.D., Mattson, G., Mielander, G.W., Morgensen, S., Conklin, E.J., *Avidin-Biotin Chemistry: A Handbook*. 1992, Rockford, IL: Pierce.
52. Wilchek, M. and E.A. Bayer, *The avidin-biotin complex in bioanalytical applications*. *Anal Biochem*, 1988. 171(1): p. 1-32.
53. Wilchek, M., Bayer, E.A., *In Protein Recognition of Immobilized Ligands*, T.W. Hutchins, Editor. 1989, Alan R. Liss, Inc.: New York. p. 83-90.
54. Henrikson, K.P., S.H. Allen, and W.L. Maloy, *An avidin monomer affinity column for the purification of biotin-containing enzymes*. *Anal Biochem*, 1979. 94(2): p. 366-70.
55. Gitlin, G., et al., *Studies on the biotin-binding sites of avidin and streptavidin. A chemically induced dynamic nuclear polarization investigation of the status of tyrosine residues*. *Biochem J*, 1989. 259(2): p. 493-8.

PART V

General Conclusions and Future Studies

CHAPTER 1

General Conclusions and Discussion

This dissertation details how Bpa-scanned α -factor analogs have been used to gain insights into structure-function relationships between α -factor, the *Saccharomyces cerevisiae* peptide pheromone, and Ste2p, its G protein-coupled receptor. New detection and purification methods were introduced by the use of biotin as an affinity tag attached to cross-linkable α -factor analogs. The major findings of the studies, contributions to current knowledge of how peptide ligands interact with their GPCRs, and possible future experiments that would provide further details on the mechanism(s) of signal transduction through GPCRs upon ligand binding are summarized in this final part of the dissertation.

Use of Bpa-scanned α -factor Analogs:

It has been shown previously that benzoyl-*L*-phenylalanine (Bpa) can be introduced at positions 1, 3, 5, 7, 8, 12 and 13 replacing the native α -factor residues (Trp, Trp, Gln, Lys, Pro, Met, and Tyr, respectively) to give potential photo-affinity labels with slight decreases in K_i from 4-fold to 45-fold in comparison to α -factor [1]. Based on these observations and our working model for pheromone binding to Ste2p [1, 2], iodlatable α -factor analogs carrying Bpa at position 1, 3, 5, or 13 were synthesized. Studies with these analogs, as detailed in Part II, showed that except for [Bpa¹(I₂)Y³R⁷F¹³] α -factor,

iodinated [Bpa³], [Bpa⁵] and [Bpa¹³] α -factor analogs had poor biological activity and decreased K_s. In addition, chemical iodination of these analogs resulted in multiple iodination at Tyr residue and caused further loss of function. Based on these studies, it was decided to pursue a different mode of tagging the α -factor analog in order to obtain modified analogs with sufficient biological activity and receptor binding to ensure their usage for photo-affinity studies.

Design and syntheses of biotinylated, Bpa-scanned α -factor analogs were achieved (covered in Part III). Analysis of these analogs illustrated that, except for the [Bpa⁸] α -factor analog, the presence of a biotin tag on Lys⁷ had minor effects on biological activity and binding affinity. Photo-activated cross-linking of these analogs to yeast membranes expressing Ste2p resulted in one major band around 54 kDa detected by western blot analysis probed with NA-HRP (NeutraAvidin-Horse Radish Peroxidase conjugate). The NA-HRP detected the biotinyl group which was the tag on α -factor that was cross-linked into Ste2p. The intensity of the bands was reduced by addition of excess α -factor pheromone during the cross-linking reaction. These results indicated that biotinylated [Bpa¹], [Bpa³], [Bpa⁵], and [Bpa¹³] α -factor analogs specifically cross-linked to the Ste2p and could be used in identification of contact sites between α -factor and its GPCR.

Purification of intact Ste2p and enrichment of biotinylated cross-linked fragments:

In order to identify the interaction site(s) between a peptide ligand and its GPCR, fragmentation of the cross-linked receptor followed by analysis of the resulting fragments

is often applied [3, 4](see review [5]). The use of a reporter tag on the peptide ligand, like ^{125}I as mentioned in Part II or biotin as discussed in Part III of this dissertation, aids the identification and analysis of the cross-linked fragments. In the case of the biotin tag, due to the presence of possible endogenously biotinylated proteins in the sample mixture, a partial purification of the cross-linked receptor prior to fragmentation is essential. Two main approaches (IMAC and size exclusion) for partial purification of the intact cross-linked Ste2p were detailed in Part IV. Although a single-step purification was sufficient for western blot analyses, further enrichment of the cross-linked fragments was necessary for the highly sensitive mass spectrometry studies. In order to achieve this goal, following partial purification and fragmentation, the cross-linked fragments were enriched by using monomeric avidin beads, which takes advantage of the strong interaction between biotin and avidin [6, 7]. Results presented in parts III and IV of this dissertation showed that purification methods applied were adequate to obtain samples pure enough to analyze with either western blots or mass spectrometry analyses.

Identification of Ste2p regions cross-linked with Bpa-scanned α -factor analogs:

Following partial purification of the cross-linked Ste2p, chemical and enzymatic fragmentation was carried out to identify the cross-linked region(s). Detection of the cross-linked fragments was achieved by autoradiography or analysis of protein blots by probing with NA-HRP according to the tag attached to the ligand used. Fragmentation of the [Bpa¹, Tyr³(^{125}I), Arg⁷, Phe¹³] α -factor cross-linked Ste2p using CNBr, trypsin, and BNPS-skatole reagent resulted in distinct fragmentation patterns as explained in Part II. Using these analyses and an epitope tagged Ste2p (Ste2p-T7; [8]) the region of cross-

linking was localized to residues 251 to 294 of the receptor. This region corresponds to a portion of Ste2p comprising the sixth and seventh transmembrane domains and the connecting the third extracellular loop.

Similarly, Part III of this dissertation details the use of biotinylated Bpa-scanned α -factor analogs to identify the contact regions between the peptide ligand and Ste2p. Findings from biotinylated [Bpa¹] α -factor were in agreement with the results obtained from studies using [Bpa¹, Tyr³(¹²⁵I), Arg⁷, Phe¹³] α -factor, suggesting an interaction between position one of the α -factor side chain and a region of Ste2p covering residues 251 to 294. In addition, studies with biotinylated [Bpa³] α -factor showed similar fragmentation patterns observed from biotinylated [Bpa¹] α -factor, revealing that position three of α -factor might be interacting with a region of Ste2p covering part of EL2 and an extracellular portion of TM5 or the extracellular portions of TM6 and TM7 including the EL3. Furthermore, results obtained from biotinylated [Bpa¹³] α -factor indicated that the C-terminus of α -factor is in close proximity to the extracellular portion of TM1, covering a region of Ste2p between residues F55 and R58.

Further analysis of the [Bpa13] cross-linked Ste2p region covering residues F55-R58:

After identification of cross-linking regions on Ste2p with various Bpa-scanned α -factor analogs, the next step was to identify contact residues, which will provide a better understanding of agonist-mediated receptor activation. The F55 to R58 residues of Ste2p, identified by cross-linking studies using biotinylated [Bpa¹³] α -factor, were further analyzed by site-directed Ala mutagenesis. Binding analyses carried out with the mutants

generated in these residues indicated that mutations at residue R58 caused a 10- to 50-fold poorer binding of α -factor to the mutant receptor compared to the wild type receptor. Western blot analyses and biological activity assays with these mutants showed that the receptors were expressed on the yeast membranes. Additionally, cross-linking studies done with the mutants using biotinylated [Bpa¹³] α -factor showed that similar biotin signal was detected around 54 kDa from all of the Ala mutants (in the region of Ste2p between residues M54 to R58), except for the R58A mutant. These results suggested that the R58 residue of Ste2p has an important role in ligand binding and that this residue is in close proximity to position 13 of α -factor.

Mass spectrometry analysis and preliminary results:

An alternative approach to site-directed mutagenesis for identification of contact residues between α -factor analogs and Ste2p is the sequencing of the cross-linked fragments. Part IV of this dissertation summarized the use of two mass spectrometry approaches using MALDI-TOF and LCQ DECA instruments to analyze the cross-linked receptor fragments. Although the MALDI-TOF instrument was not used for the sequencing of the cross-linked fragments, valuable information was gained during the optimization of biotinylated peptide enrichment. Results from this instrument showed that a biotinylated peptide ([Bpa⁸] α -factor analog) could be captured and enriched from a complex peptide mixture (CNBr-digested yeast membrane prep.). A protocol adapted from Li *et al.* [9] was used to illustrate the power of an affinity purification combined with MALDI-TOF. Analysis of biotinylated [Bpa¹] α -factor cross-linked membranes after

CNBr digestion with this method revealed the identification of a 6863.9 Da biotinylated peptide. With the assumption of a weight shift due to a matrix adduct from sinapinic acid, this result was in agreement with previous findings suggesting the interaction of position 1 of α -factor with a Ste2p region covering residues 251 to 294 as reported in parts II and III.

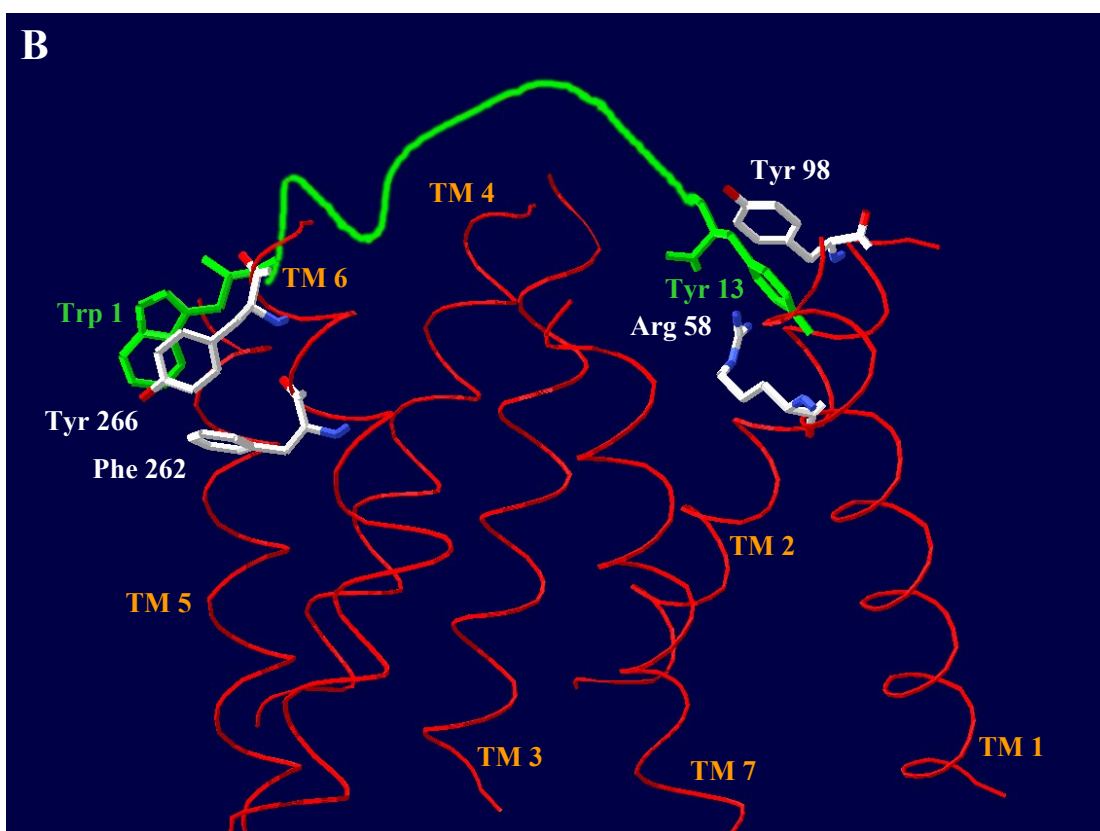
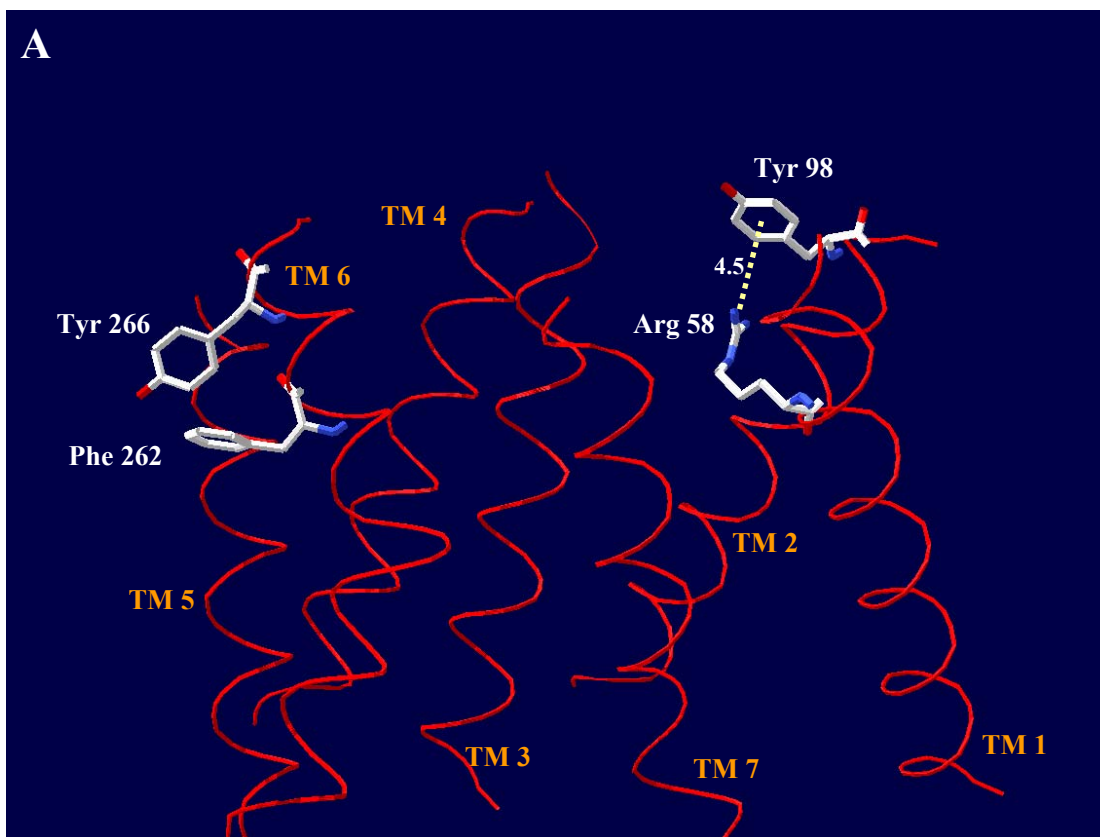
Following the optimization of an affinity purification technique to enrich the biotinylated cross-linked fragments, nanospray mass spectrometry (NS-MS) analysis was carried out by a LCQ DECA instrument. This instrument was preferred due to its capabilities of doing tandem mass spectrometry (MS/MS) analysis. The basic principle behind these experiments was to obtain pure and enriched cross-linked fragments that could be analyzed by NS-MS. Preliminary experiments carried out with biotinylated [Bpa⁸] α -factor in a complex peptide mixture showed that monomeric avidin purification was sufficient to capture and enrich enough peptides for sequencing. Similar analyses, after a two-step purification of CNBr-digested cross-linked membranes, resulted in detection of several clean ion packets representing biotinylated peptide masses. These results showed that the optimized purification methods were compatible with the mass spectrometric analyses. Previous tries of NS-MS analyses with samples prepared by single-step purifications led to a very low signal-to-noise ratio due to the presence of many other peptides, buffer components and detergents. Examination of the MS/MS spectra from the peptides identified were hampered by the insufficient resolution of the instrument used to resolve the charge states of the fragment ions and lack of suitable software to aid the analysis. Manual analysis of these spectra did not reveal more than two consecutive residues during sequencing, which was not enough to identify a contact

residue. Further analysis of the data with specific software would be required to assign cross-linking regions or contact residues.

Working model for pheromone binding to Ste2p and receptor activation:

Although identification of contact residues between the α -factor and its GPCR Ste2p was not accomplished by mass spectrometry, invaluable information was gained from the photoaffinity cross-linking studies. Data obtained from these studies and others including receptor mutagenesis analyses and structure-activity relationships of α -factor analogs allowed the proposal of a binding model for the peptide ligand. The model (Figure 1) suggests a bend in the α -factor around the Pro⁸-Gly⁹ bound [10], with the Lys⁷ side chain facing away from the transmembrane domains and interacting with a binding pocket formed by the extracellular loops [11]. Studies with position one α -factor analogs [12] indicated a strong preference for a large hydrophobic residue at the amino-terminal position of the pheromone. In addition fluorescence analyses with Trp³ indicated that the side chain of this residue is in a hydrophobic cavity (Ding, Becker, and Naider, unpublished results). Based on these studies and cross-linking data presented in this dissertation (parts II and III) it is likely that N-terminus of the pheromone interacts with a pocket consisting of aromatic residues from the extracellular ends of TM5, TM6, and TM7 and the loops EL2 and EL3 attached to these TMs. Depending on the analyses of these regions by site-directed mutagenesis studies [2, 13] our binding model suggests that Trp¹ and Trp³ residues of α -factor could interact with Tyr266 (TM6) and Phe204 (TM5), respectively. Furthermore, the C-terminus of the pheromone interacts with the

Figure 1: Working model for the fitting of α -factor pheromone into the ligand binding site on its GPCR, Ste2p. A) Possible contact residues and their interactions in resting state, B) possible interactions between the α -factor (green) and Ste2p (red)



extracellular tip of TM1, where Gln¹⁰ of α -factor is in close proximity to residues 47 and 48 of Ste2p [2] and position 13 localized between receptor residues Arg58 and Tyr98.

Given the interactions described above, the activity and receptor affinity of truncated pheromones [14], and recent studies with fluorescent α -factor analogs [15] a multi-step binding and activation of Ste2p upon agonist binding is envisaged. According to this hypothesis, first the C-terminus of the pheromone binds to the receptor. Tyr¹³ interacts with Arg58 (TM1) disturbing an interaction between this residue and Tyr98 (TM2), which could destabilize the inactive state of Ste2p. Following this interaction the receptor undergoes a conformational change; the active conformation is stabilized by interactions between the N-terminus of the pheromone and the hydrophobic pocket formed by aromatic residues at the extracellular regions of TM5, TM6 and TM7. Similar stepwise mechanisms have been proposed for other GPCRs, where agonists bind and initiate movements of transmembrane domains of receptor, thus these movements increase the interactions with the various functional groups on the ligand [16-20].

CHAPTER 2

Future Studies

Despite the tremendous progress in understanding the structure of GPCRs over the last few years including the solving of the crystal structure of rhodopsin [21] only partial information is known concerning GPCR binding sites for most molecules including peptides. This dissertation summarizes the first steps accomplished in mapping the α -factor binding site(s) within Ste2p using benzoyl-*L*-phenylalanine (Bpa)-containing analogs of the pheromone. Work to date has determined several interactions between the side chains of α -factor residues and receptor regions as detailed above. However, in order to understand the activation mechanism of GPCRs upon agonist binding, further studies are necessary to reveal additional details of the ligand-bound structure. This final part of the dissertation outlines a few of the methods that could be applied, in our current model system, to elucidate the interactions between the α -factor and its GPCR Ste2p.

Cross-linking studies:

Photoaffinity cross-linking studies using a benzophenone chromophore (Bpa) have been applied successfully throughout this study. Unfortunately, incorporation of the Bpa replacing every single residue of α -factor was not possible, due to loss of biological activity and poor binding. In order to overcome these problems relatively smaller photoactivatable cross-linkers like *p*-azido-phenylalanine or *p*-nitro-*L*-phenylalanine could be used to complete the scan through the whole pheromone. These new cross-

linkers could also be used to confirm the results obtained by Bpa. In cases, when the biological activity and binding of a photoaffinity cross-linker was not optimum, as discussed in Part III of this dissertation, one always can argue the validity of the results. Obtaining similar cross-linking results by using different cross-linkers at the same position and comparing the results could resolve these issues.

Beside new cross-linkers, α -factor analogs that carry two cross-linkers can be designed and synthesized. Such an analog carrying Bpa residues at the first and thirteenth positions could be used to lock the receptor in a certain conformation. After cross-linking, the receptor can be purified and further analyzed to identify the stabilizing interactions. A receptor that is locked in the active conformation would be also very useful for crystallization studies. As there would be relatively less mobility, such a receptor could yield better diffracting crystals.

Alternatively, cross-linking studies could be used to analyze the interactions between TM domains under certain conditions such as agonist or antagonist bound states. Recent studies carried out by Chin *et al.* [22, 23] described the *in vivo* incorporation of photoaffinity cross-linker (Bpa) into any protein sequence (in response to amber codon TAG) by site-directed mutagenesis. These studies made it possible to analyze protein-protein interactions or intra molecular interactions by using photoaffinity cross-linking. Incorporation of Bpa into Ste2p sequence would be very useful to study the proximity of TMs. Following cross-linking the receptor could be digested chemically or enzymatically to further analyze which TM is interacting with the residue modified by the cross-linker. Also this approach can be used to cross-link the receptor back to the ligand to identify the important residues on the receptor that are likely to interact with the α -factor.

Combination of results from such cross-linking studies with the results discussed in this dissertation could reveal contact residues between the pheromone and Ste2p.

Site-directed mutagenesis:

Another way to identify the contact residues between the α -factor and its receptor is to carry out site-directed mutagenesis. The regions of Ste2p identified by cross-linking studies could be analyzed by site-directed mutagenesis as described in Part III of this dissertation. Binding and biological activity assays with these mutants could aid the identification of the ligand interacting site(s). However, mutagenesis studies carried out by methionine instead of classical alanine mutagenesis would be useful. Insertion of a methionine in these regions could be used in combination with further CNBr digestion to decrease the size of the region identified by cross-linking. In addition a recent approach reported by Rihakova *et al.* [24] could be used, which takes advantage of a modified Bpa analog (NO₂Bpa), to determine contact residues. This modified Bpa analog has an increased selectivity for methionine and does not cross-link unless a methionine residue is in proper distance and orientation. Use of such a cross-linker and a methionine scanned receptor will help the identification of contact residues.

Mass Spectrometry:

Part IV of this dissertation details the use of mass spectrometry in the analysis of cross-linked receptor fragments. However, the data analyses from these studies were limited due to relatively low sensitivity of the instruments used, lack of proper algorithms to analyze complex fragmentation patterns, natural losses common in peptide ion

fragmentation, and unusual and difficult-to-interpret fragmentation of branched peptides. In addition, the low signal-to-noise ratio observed in the MS/MS spectra further complicated the analysis and determination of sequence information from cross-linked peptides.

Recent developments in instrument design and computational analyses could help to overcome most of these problems. Studies with new instruments, using a combination of quadrupolar ion trap and a fourier transform ion cyclotron resonance cell, showed that it is possible to obtain very high mass accuracy (below 2 ppm) and do MS/MS analysis at the same time [25, 26]. This new strategy suggested that determination of the amino acid composition of the peptide prior to sequencing would aid the subsequent peptide sequencing which could be performed by a permutation-based scoring algorithm. Analysis of the cross-linked fragments by such a powerful instrument and proper algorithms could help identification of the contact residues between the α -factor and Ste2p.

Besides the complexity of the fragmentation spectra and the sensitivity of the mass spectrometer used, identification of the cross-linked fragment ions in a total ion spectrum was challenging. Specific labeling of the cross-linked fragments by the use of α -factor analogs that are identical except from the overall mass would result in twin peaks in relative abundance vs. time spectrum (Figure 2). This property could be used to identify parent ions from cross-linked fragments in complex mixtures. The idea is based on the principle of identifying target peptides by the use of stable-isotope labeling named as the isotope coded affinity tag (ICAT)-based protein profiling [27, 28]. Such α -factor

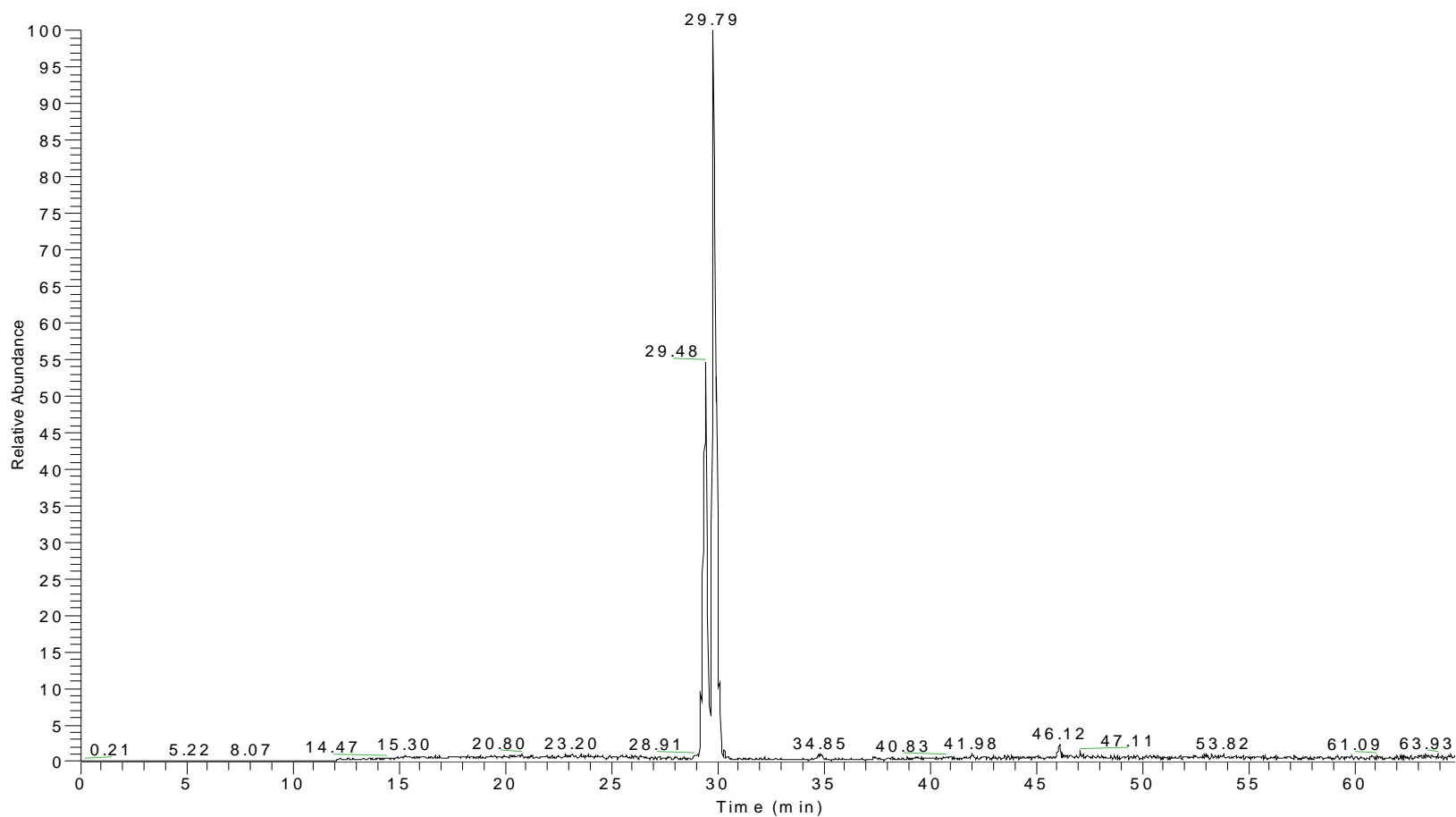


Figure 2: Total ion spectrum of two [Bpa¹] α -factor analogs, obtained by LCQ DECA. Two analogs containing Bpa at position one and had a mass difference of 42 Da were mixed and analyzed by NS-MS. Twin peaks were observed at about 30 min of the elution from a C₁₈ column.

analogues that carry the cross-linker at the same position and differ by only several Da in mass could be designed and used for identification of cross-linked fragments in mass spectrometry analysis. Currently in our lab, studies with such peptides that have Bpa at position 1 and carry a mass difference of 42 Da (due to different length linkers between the biotinyl group and the epsilon amine of lysine at position seven in α -factor) are being used to optimize conditions to identify cross-linked fragments (Figure 2). After fragmentation, Ste2p cross-linked with analogues that only differ by mass will generate cross-linked fragments that are 42 Da apart with the assumption that they cross-link to the same fragment. Detection and analysis of twin peaks generated by this method will simplify the data analysis, thus increase accuracy.

List of References for Part V

1. Henry, L.K., et al., *Identification of a contact region between the tridecapeptide alpha-factor mating pheromone of Saccharomyces cerevisiae and its G protein-coupled receptor by photoaffinity labeling*. *Biochemistry*, 2002. 41(19): p. 6128-39.
2. Lee, B.K., et al., *Identification of residues of the Saccharomyces cerevisiae G protein-coupled receptor contributing to alpha-factor pheromone binding*. *J Biol Chem*, 2001. 276(41): p. 37950-61.
3. Bitan, G., et al., *Mapping the integrin alpha V beta 3-ligand interface by photoaffinity cross-linking*. *Biochemistry*, 1999. 38(11): p. 3414-20.
4. Mouledous, L., et al., *Direct identification of a peptide binding region in the opioid receptor-like 1 receptor by photoaffinity labeling with [Bpa(10),Tyr(14)]nociceptin*. *J Biol Chem*, 2000. 275(38): p. 29268-74.
5. Chorev, M., *Parathyroid hormone 1 receptor: insights into structure and function*. *Receptors Channels*, 2002. 8(3-4): p. 219-42.
6. Henrikson, K.P., S.H. Allen, and W.L. Maloy, *An avidin monomer affinity column for the purification of biotin-containing enzymes*. *Anal Biochem*, 1979. 94(2): p. 366-70.
7. Wilchek, M., Bayer, E.A., *In Protein Recognition of Immobilized Ligands*, T.W. Hutchins, Editor. 1989, Alan R. Liss, Inc.: New York. p. 83-90.

8. Dube, P., A. DeCostanzo, and J.B. Konopka, *Interaction between transmembrane domains five and six of the alpha -factor receptor*. J Biol Chem, 2000. 275(34): p. 26492-9.
9. Schriemer, D.C. and L. Li, *Combining avidin-biotin chemistry with matrix-assisted laser desorption/ionization mass spectrometry*. Anal Chem, 1996. 68(19): p. 3382-7.
10. Zhang, Y.L., et al., *Synthesis, biological activity, and conformational analysis of peptidomimetic analogues of the Saccharomyces cerevisiae alpha-factor tridecapeptide*. Biochemistry, 1998. 37(36): p. 12465-76.
11. Ding, F.X., et al., *Probing the binding domain of the Saccharomyces cerevisiae alpha-mating factor receptor with rluorescent ligands*. Biochemistry, 2001. 40(4): p. 1102-8.
12. Zhang, Y.L., et al., *Position one analogs of the Saccharomyces cerevisiae tridecapeptide pheromone*. J Pept Res, 1997. 50(5): p. 319-28.
13. Lin, J.C., et al., *Aromatic residues at the extracellular ends of transmembrane domains 5 and 6 promote ligand activation of the G protein-coupled alpha-factor receptor*. Biochemistry, 2003. 42(2): p. 293-301.
14. Eriotou-Bargiota, E., et al., *Antagonistic and synergistic peptide analogues of the tridecapeptide mating pheromone of Saccharomyces cerevisiae*. Biochemistry, 1992. 31(2): p. 551-7.
15. Bajaj, A., Celic, A., Ding, F.X., Naider, F., Becker, J.M., Dumont, M.E., A *Fluorescent alpha factor analog exhibits multible steps on binding to its G protein coupled receptor in yeast*. Biochemistry, 2004. Submitted.

16. Hoare, S.R., T.J. Gardella, and T.B. Usdin, *Evaluating the signal transduction mechanism of the parathyroid hormone 1 receptor. Effect of receptor-G-protein interaction on the ligand binding mechanism and receptor conformation.* J Biol Chem, 2001. 276(11): p. 7741-53.
17. Jarnagin, K., et al., *Mutations in the B2 bradykinin receptor reveal a different pattern of contacts for peptidic agonists and peptidic antagonists.* J Biol Chem, 1996. 271(45): p. 28277-86.
18. Turner, P.R., et al., *Transmembrane residues together with the amino terminus limit the response of the parathyroid hormone (PTH) 2 receptor to PTH-related peptide.* J Biol Chem, 1998. 273(7): p. 3830-7.
19. Kobilka, B., *Agonist binding: a multistep process.* Mol Pharmacol, 2004. 65(5): p. 1060-2.
20. Liapakis, G., et al., *Synergistic contributions of the functional groups of epinephrine to its affinity and efficacy at the beta2 adrenergic receptor.* Mol Pharmacol, 2004. 65(5): p. 1181-90.
21. Palczewski, K., et al., *Crystal structure of rhodopsin: A G protein-coupled receptor.* Science, 2000. 289(5480): p. 739-45.
22. Chin, J.W., et al., *An expanded eukaryotic genetic code.* Science, 2003. 301(5635): p. 964-7.
23. Chin, J.W., et al., *Addition of a photocrosslinking amino acid to the genetic code of Escherichiacoli.* Proc Natl Acad Sci U S A, 2002. 99(17): p. 11020-4.

24. Rihakova, L., et al., *Methionine proximity assay, a novel method for exploring peptide ligand-receptor interaction*. J Recept Signal Transduct Res, 2002. 22(1-4): p. 297-313.
25. Spengler, B., *De novo sequencing, peptide composition analysis, and composition-based sequencing: a new strategy employing accurate mass determination by fourier transform ion cyclotron resonance mass spectrometry*. J Am Soc Mass Spectrom, 2004. 15(5): p. 703-14.
26. John E. P. Syka, J.A.M., Dina L. Bai, Stevan Horning, Michael W. Senko,, B.U. Jae C. Schwartz, Benjamin Garcia, Scott Busby, Tara Muratore,, and a.D.F.H. Jeffrey Shabanowitz, *Novel Linear Quadrupole Ion Trap/FT Mass Spectrometer: Performance Characterization and Use in the Comparative Analysis of Histone H3 Post-translational Modifications*. Journal of Proteome Research, 2004. 3: p. 621-626.
27. Gygi, S.P., et al., *Quantitative analysis of complex protein mixtures using isotope-coded affinity tags*. Nat Biotechnol, 1999. 17(10): p. 994-9.
28. Ranish, J.A., et al., *The study of macromolecular complexes by quantitative proteomics*. Nat Genet, 2003. 33(3): p. 349-55.

VITA

Cagdas D. Son was born in Ankara, Turkey on January 10th, 1975. He graduated from TED Ankara collage in August 1993. After the getting a high score in the placement exam he entered the Middle East Technical University. During his undergraduate years he made a minor in organic chemistry, and learned software and hardware management for computers. In August 1997 he received his Bachelor of Sciences degree in molecular biology. He started working for his Master of Science degree in September 1997 in the same university. He received his degree in August 1999, during these two years he worked in dean's office as a computer administrator. He was accepted to the Ph.D. program in Biochemistry, Cellular and Molecular Biology (BCMB) department at the University of Tennessee, Knoxville in August 1999. He started his graduate work in Dr. Jeffrey M. Becker's laboratory. Throughout the course of his time in this program, he served as a Graduate Teaching Assistant (1999-2003) and become an assistant for several courses. He officially received a Doctor of Philosophy degree in BCMB in December 2004.

He continues to work in Dr. Jeffrey M. Becker's laboratory, while waiting for his wife's graduation and searching for a postdoctoral position.